

**Evaluation of Skeletal Muscle Satellite Cell
Activity in Rodent Models Depicting Muscle
Hypertrophy and Atrophy**

Dr. Idris L. Sidique BSc (Hons) PhD



**The University of
Nottingham**

UNITED KINGDOM • CHINA • MALAYSIA

School of Biomedical Sciences

University of Nottingham

Medical School, Queen's Medical Centre

Nottingham

United Kingdom

Thesis submitted to the University of Nottingham for the
Degree of Doctor of Philosophy

May 2012

ABSTRACT

Satellite cells are muscle-specific progenitor cells involved in the routine maintenance of skeletal muscle homeostasis, growth and regeneration. They are activated by various stimuli (myotrauma, growth factors etc), undergo rounds of proliferation as skeletal muscle myoblasts, to differentiate and fuse with each other to generate new myotubes or onto existing myofibres to augment growth or repair damaged fibres. Satellite cells contribute to hypertrophy by facilitating nuclear addition, which maintains contractile protein synthetic capacity. Conversely, during atrophy the dysregulation of satellite cells (e.g., via myogenic suppression), causes an opposing deficit in nuclear supplementation/contractile protein synthesis. The 'activity status' of satellite cells, an important determinant of muscle regenerative capacity is not routinely addressed in studies characterising mechanisms of muscle hypertrophy and atrophy. Therefore, the investigations described within this thesis examined the satellite cell specific signalling events that contribute to muscle loss or gain, in rodent models experiencing non-mechanically-induced muscle hypertrophy or atrophy.

Chronic administration of an anabolic agent (BRL-47672, the pro-drug of clenbuterol) increased the expression of early components of satellite cell myogenesis (pax7, ki-67, myoD) but caused no alteration in myogenin expression, relative to control in rat soleus muscle. Pro-drug administration increased myostatin expression, with no concomitant change in follistatin mRNA; this is likely a compensatory mechanism to check excessive muscle growth. These results provided evidence of increase satellite cell activity in hypertrophying muscle. In a lipopolysaccharide (LPS)-infusion model of muscle atrophy, satellite cells were inhibited in an inflammatory-dependent manner. LPS infusion caused early (<2hr) elevations inflammatory cytokines TNF- α , IL-6 and NF- κ B. LPS-induced elevation in cytokine transcript levels paralleled increased myostatin and decreased pax7 and myoD mRNA and protein expression. The differential increase in cytokines also paralleled the reduction in the number of pax7⁺ and myoD⁺ satellite cells. These results suggest that alterations in satellite cell activity may contribute to the progression of muscle atrophy, due to the suppression of muscle compensatory mechanisms, which include satellite cell activation, differentiation and fusion for nuclear supplementation. Co-infusion with an anti-inflammatory agent, dexamethasone (Dex), blunted LPS-induced increase in inflammatory cytokines but had an additive effect on myogenic suppression. Dex+LPS infusion prevented LPS-induced increase in myogenin and resulted in an additional suppression of pax7 and myoD, greater than that elicited by either substance alone. Negative regulation of satellite cells by glucocorticoids could impede their efficacy in the treatment of inflammatory muscle disorders.

The research within this thesis emphasise satellites are important for maintenance of muscle homeostasis and their activation/inhibition, may determine the magnitude of muscle loss or gain. This was demonstrated by the pattern of pax7 and myoD expression in hypertrophying muscle, where both markers were up-regulated and in atrophying muscle, where they were down-regulated. Down-regulation of these markers in atrophy could have implications for muscle regenerative capacity, especially myoD, whose expression was continuously inhibited across all time-points sampled in septic muscles. Satellite cells are a major source of compensatory action in skeletal muscle, their activation and subsequent myogenesis represents an auxiliary mechanism by which muscle responds to damaging stimuli; therefore their dysregulation (through the alteration of key myogenic markers) results in an alteration of normal function. Such dysregulation, as frequently reported in cases of progressive muscle degeneration and sarcopenia, limits the efficacy of muscle compensatory processes (i.e. satellite cell activation/proliferative or differentiation potential), thereby contributing to the progression of muscle atrophy and myopathy

TABLE OF CONTENTS

ABSTRACT	i
TABLE OF CONTENTS	ii
ACKNOWLEDGEMENTS	vi
ABBREVIATIONS	viii
DECLARATION	xiii
CHAPTER 1: General Introduction	1
1.1 Introduction and aims	2
1.2 Satellite cell biology	6
1.2.1 Overview of skeletal muscle and satellite cell structure	6
1.2.2 Developmental origins of satellite cells	10
1.2.3 Satellite cell identification	12
1.2.4. Satellite cell markers	14
1.2.4.1 Quiescence	14
1.2.4.2 Activation and proliferation	17
1.2.4.3 Differentiation and fusion	21
1.2.4.4 Negative regulatory markers	22
1.2.5 Sequential events regulating satellite cell myogenesis	24
1.2.6 Satellite cell self-renewal	27
1.2.5 Mechanisms modulating satellite cell activation and regulation	28
1.3 Satellite cell response to skeletal muscle hypertrophy	30
1.3.1 Definition of muscle hypertrophy	30
1.3.2 Satellite cells and muscle hypertrophy	31
1.3.3 Summary of satellite cell activity in non-mechanically induced hypertrophy models	32
1.4 Satellite cells during muscle atrophy	34
1.4.1 Overview of muscle atrophy	34
1.4.2 Satellite cell response to atrophic stimuli	35
1.5 Summary and hypotheses	36
CHAPTER 2: General Methods	37
2.1 <i>In vivo</i> techniques	38

2.1.1 Ethics statement.....	38
2.1.2 β_2 -agonist pro-drug BRL-47672 study.....	38
2.1.1.1 Background.....	38
2.1.1.2 Animals and tissue collection	40
2.1.2 Lipopolysaccharide (LPS) study	41
2.1.2.1 Background.....	41
2.1.2.2 Animals and surgical preparation	41
2.1.2.3 Lipopolysaccharide administration and tissue collection	42
2.1.3 Dexamethasone (Dex) study	43
2.1.3.1 Background.....	43
2.1.3.2 Animals and tissue collection	43
2.2 Molecular biology techniques	45
2.2.1 Analysis of mRNA expression.....	45
Quantitative real-time polymerase chain reaction (qRT-PCR).....	45
2.2.2 Total RNA extraction	54
2.2.2.1 Formaldehyde gel electrophoresis	55
2.2.3 cDNA synthesis.....	57
2.2.4 Taqman analysis.....	57
2.2.4.1 DNA electrophoresis	58
2.2.5 Analysis of protein expression (Western blotting).....	61
2.2.5.1 Muscle protein extraction	61
2.2.5.2 Muscle protein quantification (Lowry assay).....	62
2.2.5.3 Sodium dodecyl sulphate polyacrylamide gel electrophoresis (SDS-PAGE).....	63
2.2.5.4 Western blotting.....	65
2.2.6 Histological analyses.....	67
2.2.6.1 Immunohistochemistry	67
2.2.6.2 Immunofluorescence.....	69
2.2.6.3 Duolink [®] Bright-field Proximity Ligation Assay (PLA).....	70
2.2.6.4 Muscle Fibre Diameter Determination	73
2.2.6.4.1 <i>Image acquisition and analyses</i>	73
2.2.6.5 Stereology	78
 CHAPTER 3: Chronic administration of the clenbuterol pro-drug BRL- 4767 increases satellite cell activity	 81
3.1 Summary	82
3.2 Introduction	84

3.3 Methods	90
3.3.1 Animals and tissue collection.....	90
3.3.2 Analysis of muscle fibre hypertrophy	90
3.3.3 mRNA Measurements (Real Time PCR)	90
3.3.4 Protein measurements (Western blotting)	92
3.3.5 Statistical Analyses.....	96
3.4 Results	97
3.4.1 Analysis of muscle fibre diameter.....	97
3.4.2 mRNA and protein expression of muscle specific markers	97
3.4.2 Myostatin Protein Expression	103
3.5 Discussion	109
CHAPTER 4: Continuous lipopolysaccharide infusion suppresses components of the satellite cell myogenic program	117
4.1 Summary	118
4.2 Introduction	120
4.3 Methods	128
4.3.1 Animals and tissue collection.....	128
4.3.2 mRNA measurements (real-time PCR).....	129
4.3.3 Protein measurements (Western Blotting)	131
4.3.4 Histology	131
4.3.4.1 Immunohistochemistry	131
4.3.4.2 Immunofluorescence.....	133
4.3.4.3 Duolink [®] Bright-field Proximity Ligation Assay (PLA).....	134
4.3.4.4 Stereology	135
4.3.5 Statistical analyses.....	137
4.4 Results	138
4.4.1 Inflammatory Cytokines.....	138
4.4.2 Macrophage Infiltration.....	147
4.4.3 TNF- α /macrophage co-localisation	154
4.4.4 Myogenic Regulatory Factors (MRFs).....	158
4.4.5. Myostatin.....	169
4.5 Discussion	175
CHAPTER 5: Co-infusion of low dose dexamethasone is additive to lipopolysaccharide-induced myogenic suppression	185

5.1 Summary	186
5.2 Introduction	188
5.3 Methods	191
5.3.1 Animals and tissue collection.....	191
5.3.2 mRNA measurements (real-time PCR).....	192
5.3.3 Protein Measurements (Western Blotting).....	192
5.3.4 Statistical Analyses.....	195
5.4 Results	196
5.4.1 Cytokines.....	196
5.4.2 Myogenic Regulatory Factors (MRFs).....	203
5.4.3 Myostatin.....	208
5.5 Discussion	210
CHAPTER 6: General Discussion	220
6.1 Overview of thesis	221
6.2 Conclusions	224
6.3 Limitations and future directions	226
METHOD DEVELOPMENT APPENDICES	230
Appendix I	231
1. Rationale.....	232
2. Methods	233
2.1 Myostatin competitive blocking studies	233
2.2 Minimum myostatin protein concentration for western blotting...	234
3. Observations and conclusions	234
Appendix II	240
1. Summary	241
2. Background	243
3. Methods	246
4. Results	248
5. Discussion	251
REFERENCES	257

ACKNOWLEDGEMENTS

Firstly, I would like to thank my supervisors, Dr Rudi Billeter-Clark and Professor Paul Greenhaff for their guidance and support during my PhD. I'd especially like to thank Rudi for all his time, effort and guidance over the last four years. I could not have wished for a better primary supervisor, his expertise, enthusiasm for the project, and willingness to help have had an immeasurable influence on my scientific development.

I'd also like to thank Dr Rob Layfield and the members of lab D45, for the use of his lab facilities, the occasional pinching of reagents and helpful advice on protein biochemistry. I am grateful to Dr Peter Wigmore, not only for his kind donation of Ki-67 antibodies but also for his helpful assessments of my annual reports. I would also like to thank Professor Terry Mayhew for his useful advice of stereology. I must also thank Drs Andy Bennett (for the kind donation of a thermal cycler) and Lynn Bedford, and the members of their labs, for allowing me free use of their equipment and facilities. I owe a huge debt of gratitude to Dr Emma King and the members of the AMU (Denise Christie, Marie Smith and Ian Ward), whose friendship, support and advice has been of tremendous value to me during the course of my PhD.

Secondly, I'd like to thank all the people in and around Nottingham who helped me not only with my research, but have also been a social outlet during the years; particularly the lunch bunch (Barry Shaw, Alice Goode, Ryan Atkins, Laura Lyons, Katherine Bridge, Dan Foxler, Vicky James, Donna Bentley – I am sorry if I've omitted anyone) and the D83 office crew (Ricardo Samms, Chris Shannon, Chris Gaffney and Kevin Bailey). I'd also like to thank Sarah Skirrow for her friendship, the proof reading service (I liked the smiley faces) and interesting office conversations. I am eternally indebted to Jo Strachan, I am not sure the last four years would have gone as smoothly without her influence. As well as being a brilliant work colleague, her friendship has been of tremendous value to me – thanks so much for letting me bend your ear a few times (well, a lot actually!), stay at your place so often and just generally being a social relief from 'thesisness'.

Thirdly, for their support and camaraderie, I'd like to thank all my friends in Nottingham, especially Chris McHugh, James Henstock, Alex Hulse, Benjamin Whitehead, Jonathan Alldis, John Boden and Gary Patmore, who ensured I took occasional breaks from my studies. I realise this is probably unprecedented but must also thank my haematologist, Dr Marie Donohue and the members of staff at the Centre for Clinical Haematology, particularly, Maxine, Emma, Fay, Cath, Kay and 'the two Anges' – thank you so much for putting up with my veins and for making the Day Unit feel like a second home over the last seven years.

My special and genuine thanks to Marion Adair, who always ensured I was fed, watered and generally well-looked after during the writing of this thesis. I'd also like to thank my family for all their support during the course of my education, especially my sister Aminata, who has been a rock during these last three years. Lastly, but certainly not the least, I'd like to dedicate this thesis to Kevin T. Adair, without whom, the last four and a half years would have simply been impossible – thank you for putting up with me, especially during the production of this thesis.

ABBREVIATIONS

ABC	Avidin biotin complex
ACTH	Adrenocorticotrophic hormone
ADAM12	A disintegrin and metalloproteinase-domain-containing protein 12
ADAM17	A disintegrin and metalloproteinase-domain-containing protein 17
ALK-4/5	Activin receptor-like kinase-4/5
ANOVA	Analysis of variance
APS	Ammonium persulphate
ATP	Adenosine triphosphate
bHLH	basic helix-loop-helix
BMP	Bone morphogenic protein
BSA	Bovine serum albumin
cAMP	Cyclic adenosine monophosphate
CD14	Monocyte differentiation antigen CD14
CD34	hematopoietic progenitor cell antigen CD34
CD45	Receptor-type tyrosine-protein phosphatase C
cDNA	complementary DNA
CLP	Caecal ligation and puncture
c-met	Hepatocyte growth factor receptor
c-Myc	Myc proto-oncogene protein
COX	Cytochrome-c oxidase
C _t	Cycle threshold
DAB	3, 3'-diaminobenzidine
DAPI	4',6-diamidino-2-phenylindole
dATP	deoxyadenosine tri-phosphate
dCTP	deoxycytidine tri-phosphate
Dex	Dexamethason
dGTP	deoxyguanosine tri-phosphate

DMD	Duchenne muscular dystrophy
DNA	Deoxyribonucleic acid
DTT	Dithiothreitol
dTTP	deoxythymidine tri-phosphate
dUTP	deoxyuridine tri-phosphate
E3	Ubiquitin ligase
ECL	Enhanced Chemiluminescence
EGF	Endothelial-derived growth factor
EDL	Extensor digitorum longus
EDTA	Ethylenediaminetetraacetic acid
EGTA	Ethylene glycol tetraacetic acid
eIF	Eukaryotic initiation factor
eIF2B	Eukaryotic initiation factor 2B
ERK	Extracellular regulated kinase
FAM	6-carboxyl-fluorescein
FGF	Fibroblast growth factor
flk	Vascular endothelial growth factor receptor 2
FRET	Fluorescent resonance energy transfer
GAB	Gel application buffer
GDF8	Growth and differentiation factor 8 (myostatin)
GFP	Green fluorescent protein
GILZ	Glucocorticoid-induced leucine zipper
GRE	Glucocorticoid response element
GSEA	Gene Set Enrichment Analysis
GSK3	Glycogen synthase kinase 3
GTG	Genetic technology grade
HEPES	4-(2-hydroxyethyl)-1-piperazineethanesulfonic acid
HGF	Hepatocyte growth factor
HLH	Helix-loop-helix

HMBS	Hydroxymethylbilane synthase
HRP	Hydrogen peroxide
HPA	Hypothalamic-pituitary-adrenal axis
i.p.	intraperitoneal
i.v.	intravenous
Iba-1	Ionised calcium binding adaptor molecule-1
IHC	Immunohistochemistry
IGF-I/II	Insulin-like growth factor –I/II
IκB	Inhibitory proteins of κB family
IKK	IκB kinase
IL-1	Interleukin-1
IL-6	Interleukin-6
IL-10	Interleukin-10
IL-10R	Interleukin-10 receptor
IRAK	IL-1 receptor-associated kinase
Ki-67	antigen identified by monoclonal antibody Ki-67
LAP	Latency associated peptide
LIF	Leukaemia inhibitory factor
LPS	Lipopolysaccharide
MAFbx	Muscle atrophy F-box
MAPK	Mitogen-activated protein kinase
MD2	Myeloid differentiation protein-2
MEF2	Myocyte enhancer factor 2
MGB	Minor groove binder
MHC	Myosin heavy chain
MMLV	Maloney murine leukaemia virus
MOPS	3-(N-morpholino) propanesulfonic acid
mRNA	messenger RNA
mTOR	mammalian target of rapamycin

MuRF1	Muscle RING-finger 1
MyD88	Myeloid differentiation primary gene 88
Myf5	Myogenic factor 5
MyoD	Myogenic determination factor 1
NCAM	Neural cell adhesion molecule
NF- κ B	Nuclear factor kappa B
NFQ	Non-fluorescent quencher
NLS	Nuclear localisation signal
NO	Nitric oxide
NOS	Nitric oxide synthase
NSAID	Non-steroidal anti-inflammatory drug
OCT	Optimal cutting temperature
p38 MAPK	p38 mitogen-activated protein kinase
Pax3	Paired box 3 transcription factor
Pax7	Paired box 7 transcription factor
PBGB	Porphobilinogen deaminase
PBS	Phosphate-buffered saline
PCR	Polymerase chain reaction
PDGF	Platelet-derived growth factor
PFA	Paraformaldehyde
PI3K	Phosphatidylinositol 3-kinase
PKA	Protein kinase A
PLA	Proximity ligation assay
qRT-PCR	Quantitative real-time PCR
RHD	Rel homology domain
RNA	Ribonucleic acid
ROS	Reactive oxygen species
RT	Reverse transcriptase
s.c.	subcutaneous

sca-1	Putative surface cell antigen sca1
SDS	Sodium Dodecyl Sulphate
SDS	Sequence detection system
SDS-PAGE	Sodium Dodecyl Sulphate polyacrylamide gel electrophoresis
SEM	Standard error of the mean
siRNA	Short-interfering ribonucleic acid
SMAD	Mothers against decapentaplegic homolog
STAT3	Signal transducer and activator of transcription 3
TA	Tibialis anterior
TBE	Tris-Borate-EDTA
TBS	Tris-Buffered-Saline
TEMED	Tetramethylethylenediamine
TGF- β	Transforming growth factor beta
TLR4	Toll-like receptor 4
TNF- α	Tumour necrosis factor alpha
TRAF6	TNF-receptor associated factor 6
TUNEL	Terminal deoxynucleotidyl transferase dUTP nick end labelling
UV	Ultraviolet
VCAM-1	Vascular cell adhesion molecule 1

DECLARATION

I hereby confirm the work contained within this thesis was the result of experimental work done by me, with a few exceptions noted below:

Chapter 3 – Animal work and tissue collection was carried out by David Baker and Simon Jones.

Chapters 4 and 5 – Animal work and tissue collection was conducted by Julie March and Phillip Kemp.

In chapter 5, cDNA synthesis and protein extraction was carried out by Hannah Crossland

CHAPTER 1

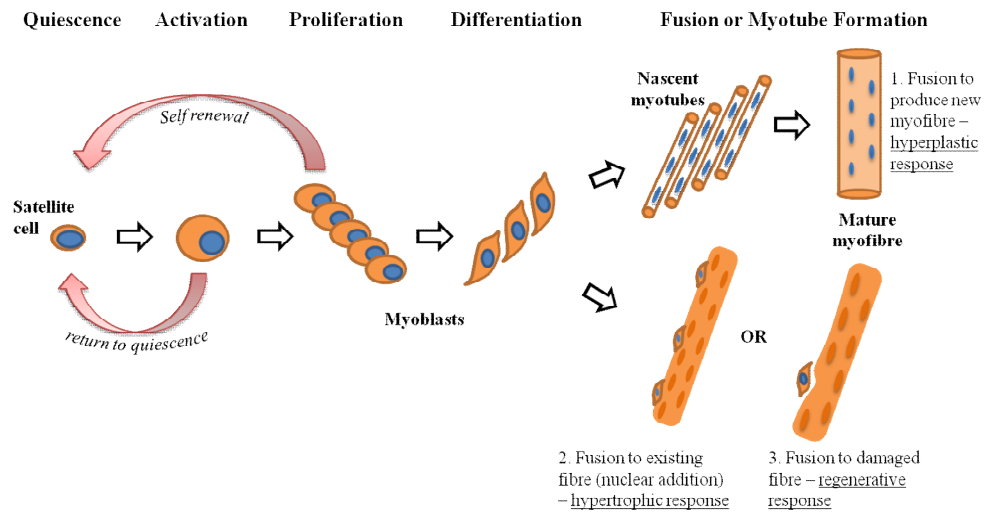
General Introduction

1.1 INTRODUCTION AND AIMS

Satellite cells are muscle-specific progenitor cells found in adult skeletal muscle fibres between the basal lamina and the sarcolemma. They are activated by various stimuli (exercise, myotrauma, or trophic factors, e.g. HGF) to undergo rounds of proliferation and may commit to myogenic lineage. This usually includes differentiation into skeletal muscle myoblasts, and the lining up and fusion of these myoblasts to form myotubes; these eventually mature into myofibres (summarised in figure 1.1). Myoblasts can also fuse into existing muscle fibres, to support growth or fuse to damaged muscle fibres to facilitate repair following injury.

Skeletal muscle is the most abundant tissue in mammals with the capacity to adapt to physiological demands such as postnatal growth, training or injury. However, adult skeletal muscle fibres are terminally differentiated cellular entities, with each fibre nucleus serving a limited cytoplasmic domain and thus providing limited synthetic capacity. Therefore, a muscle's remarkable ability for self-repair and physiological adaptation is dependent on its satellite cells, as a source of new nuclei. Adult skeletal muscle homeostasis is precisely adjusted between (contractile) protein synthesis and degradation, their balance is deterministic for muscle hypertrophy or atrophy. Activation, proliferation, differentiation and fusion of satellite cells may ultimately be required for muscle hypertrophy – via reducing nuclear domain size and increasing synthetic capacity. Conversely, the opposing phenomenon is the loss of nuclei (e.g. by apoptosis of myonuclei and satellite cells during muscle atrophy),

Figure 1.1: Schematic representation of Skeletal Muscle Satellite Cell Myogenesis. Mitotically quiescent satellite cells in adult muscle express the canonical specification marker pax7; activated satellite cells are denoted by cytoplasmic expansion and increased expression of myoD and myogenin is up-regulated during differentiation.



which causes an increase in the nuclear domain size and a reduction in protein synthetic capacity. The activity status of satellite cells, denoted by expression of certain myogenic markers (e.g., myogenic determination factor 1, (myoD) for activation), is a major determinant of skeletal muscle regenerative capacity and growth. Therefore an impairment or inhibition of satellite cell activity/function (e.g., via alteration of key myogenic regulatory factors, MRFs) could result in attenuation of muscle growth or lead to a reduction in muscle regenerative potential, which could contribute to progressive muscle degeneration.

The mechanisms of satellite cell regulation are not fully understood; activated satellite cells do not always commit to differentiation, but can return to a quiescent, undifferentiated state. For example, satellite cells activated during mild exercise soon return to quiescence upon cessation of training. It is thought this ability of some activated satellite cells to return to quiescence is likely a mechanism for self renewal; however it is still undetermined what dictates which satellite cells undergo self-renewal and which ones ultimately differentiate. The process of activation or maintenance of quiescence is complex, it appears linked to a balance between intrinsic (e.g. myogenic regulatory factors) and extrinsic factors (stretch, trauma, growth factors, etc), whose activity and/ or frequency provides impetus for satellite cell myogenesis. Given the crucial role of satellite cells in the maintenance of muscle homeostasis, a more comprehensive understanding of satellite cell activity in rodent models characterised by muscle hypertrophy and atrophy should further illuminate our knowledge of muscle biology, which could

facilitate the development of novel techniques and therapies for affected muscles.

The experiments described within this thesis aim to elucidate satellite cell specific signalling events in rodent models associated with muscle hypertrophy and atrophy. More specifically, the aims of the present investigations are;

- i) To examine myogenic signalling events in hypertrophying muscle induced by chronic administration of an anabolic agent; the clenbuterol pro-drug BRL-47672.
- ii) To examine the temporal aspects of inflammatory cytokine signalling during endotoxaemia (by continuous infusion of lipopolysaccharide) and the impact on components of the satellite cell myogenic program, in order to determine factors that contribute to progressive inflammation-induced muscle wasting.
- iii) To determine whether a strategy aimed at reducing excessive lipopolysaccharide-induced muscle inflammation (i.e., administration of an anti-inflammatory agent dexamethasone) alters satellite cell activity towards improvement of inflammation-induced muscle wasting.

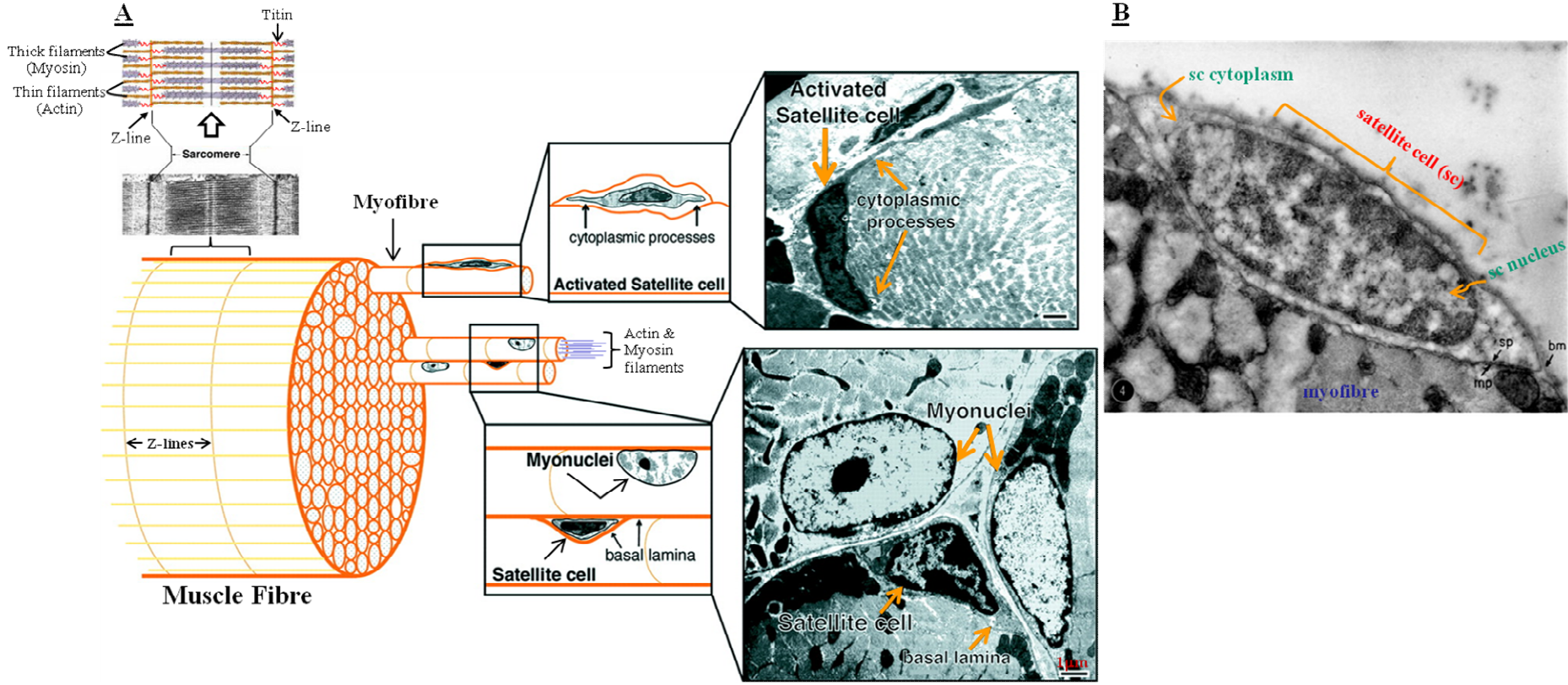
1.2 SATELLITE CELL BIOLOGY

1.2.1 Overview of skeletal muscle and satellite cell structure

Skeletal muscle accounts for just over a third of adult body mass (reviewed by Janssen *et al.* 2000); it is composed of bundles of repeated contractile units of post-mitotic multi-nucleated muscle fibres. Individual myofibres are surrounded by a basal lamina (called the basement membrane in light microscopy), beneath which a population of muscle progenitor cells (satellite cells) are located. These myofibres are syncytial cells stacked with an array of myofibrils consisting of thick (myosin) and thin (actin) filaments organised into contractile units called sarcomeres (summarised in figure 1.2). Sliding of the two contractile filaments actin and myosin, in a ratchet-style motion whilst utilising adenosine tri-phosphate (ATP) reduces the distance of opposing ends of the sarcomere (Z-lines; consisting of α -actinin and titin, by which actin and myosin filaments are attached to the Z-line), thus shortening the sarcomeres and causing muscle contraction (reviewed by Jarosch 2000).

The contractile and metabolic properties vary between muscle fibres and are categorised into two groups: slow-twitch (type 1 – prevalent in rat soleus) muscle fibres, which utilise mitochondrial respiration and fast-twitch muscle fibres (prevalent in e.g. rat extensor digitorum longus). Fast-twitch muscle fibres are further sub-divided into three main groups; type 2A, type 2B and type 2X fibres, all of which favour glycolytic cellular metabolism and have a faster contraction time and a more rapid relaxation compared to slow-twitch fibres. In rodents, the proportion of satellite cells associated with type I fibres is higher than those in contact with type II fibres

Figure 1.2: Summary of Skeletal Muscle and Satellite Cell Structure. **A**; Skeletal muscle is composed of repeating units of sarcomeres, myofibrils, myofibres, and muscle fibre bundles. Satellite cells reside in a sub-laminar indentation between myofibres surrounded by the basal lamina. Satellite cells are also distinguishable from myonuclei by their cytoplasmic processes and more abundant heterochromatin (Adapted from Hawke and Garry 2001). **B**; High magnification electron micrograph showing the close association between a satellite cell and the basal lamina (bm), which surrounds it completely, and the apposing plasma membranes of the myofibre (mp) and the satellite cell (sp) (Adapted from Mauro 1961).

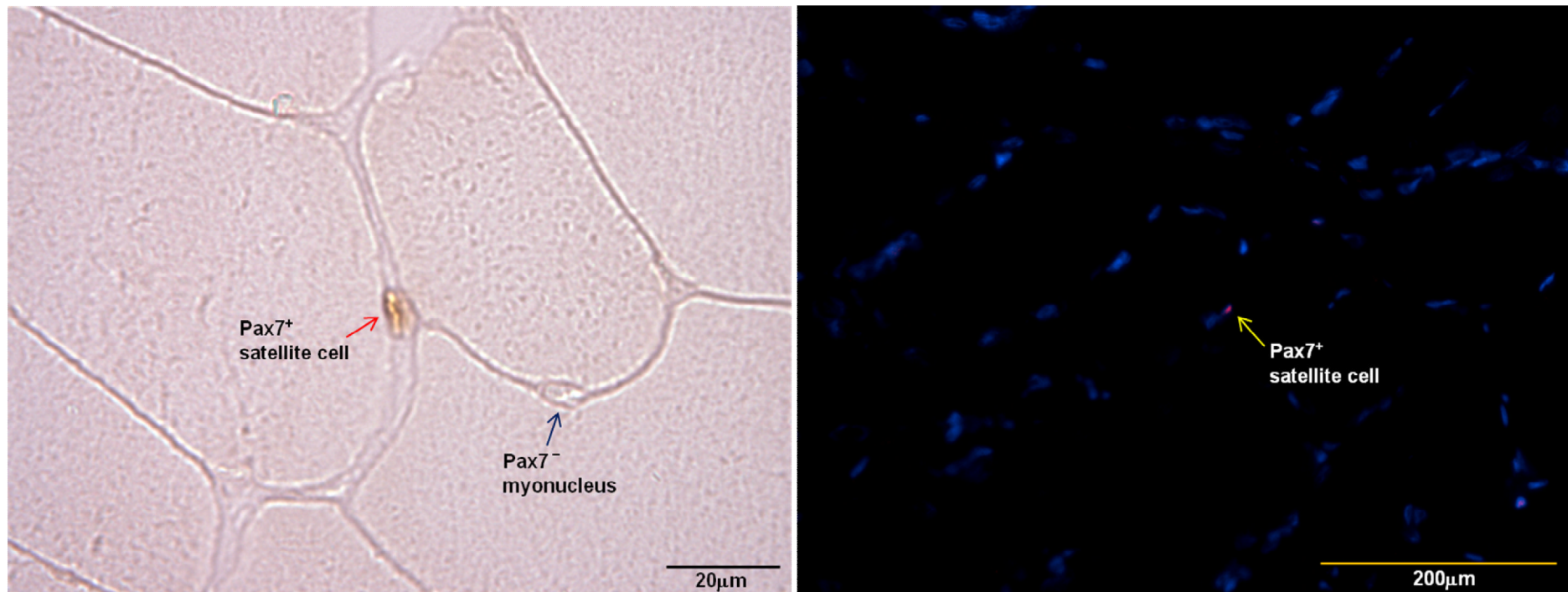


(Schmalbruch and Hellhammer 1977; Gibson and Schultz 1982). The satellite cell content of predominantly oxidative (type I) muscles tends to be 5-6 times greater in rats than that of predominantly glycolytic (type II) muscles; it is thought the increased satellite cell content is due to a combination of increased capillarity and motor-neuron density in slow oxidative muscles, compared to fast glycolytic ones. Increased satellite cell density is found with the proximity of capillaries and at motor-end plates (Wokke *et al.* 1989). It has also been suggested that since slow fibres are the first and most frequently recruited for muscle activity (e.g. the soleus muscle experiences a constant pull in maintaining standing posture), they perhaps require a larger satellite cell pool to parallel the daily micro-injuries occurred as a result (Schultz 1989).

Satellite cells have been the point of much discussion since their initial description by two papers in 1961 (Katz 1961; Mauro 1961). They are so named due to their anatomical position underneath the basal lamina and they occupy an identical anatomical position in most vertebrates. This close association with the basal lamina enables a sense of immediacy between satellite cells and myofibres and may function as a sensor for muscle fibre mechanical, structural and functional integrity. For decades, electron microscopy was the only definitive method for identifying and studying satellite cells until the discovery of satellite cell-specific molecular markers, most notably the satellite cell specification marker paired box transcription factor 7 (*pax7*) (Seale *et al.* 2000) – thus making their identification and characterisation more accessible by light microscopy (see figure 1.3).

Immunohistochemical techniques using specific molecular markers are very useful for deciphering the activity status of satellite cells but ultrastructural

Figure 1.3: Light and fluorescence micrographs of pax7 positive satellite cells on untreated rat soleus muscle cross-sections. Note satellite cells are a sparse population of cells, as denoted by the proportion of satellite cells to myonuclei in the fluorescence photomicrograph



techniques have enhanced our understanding of satellite cell structure and morphology. Satellite cells were described by Muir *et al.* (1965) as flattened, spindle-shaped structures that align in parallel to the axis of myofibres in intact adult muscle (see figure 1.2b). Schmalbruch (1978) noted that virtually all satellite cells exhibit cytoplasmic process that extend from the poles of the cells, and activation of satellite cells by myotrauma or denervation causes a significant increase in branching. This branching nature of cytoplasmic processes is thought to aid the fusion process or migratory activity on myofibres to sites of trauma (Schultz 1976; Watt *et al.* 1987). The physical and morphological characteristics of quiescent satellite cells include a small nuclear size relative to myonuclei (Watkins and Cullen 1988), high nuclear –to– cytoplasmic ratio, with few organelles and large amounts of heterochromatin compared to myonuclei (reviewed by Schultz and McCormick 1994). These findings support the idea that satellite cells in adult muscle are predominantly quiescent and transcriptionally less active. Activated satellite cells tend have a higher number of organelles compared to quiescent cells, a high number of caveolae (invaginations of plasma membrane observed in most cell types) and reduced heterochromatin (reviewed by Champion 1984). Activated satellite cells are also more easily identified as they appear as swellings on the myofibre as a result of cytoplasmic extension and increased mitotic activity.

1.2.2 Developmental origins of satellite cells.

In the early stages of embryonic development of mammals and birds, the mesoderm germ layer (from which skeletal muscle is derived), differentiates

into transitory structures on either side of the neural tube, collectively known as the somite (Armand *et al.* 1983). Satellite cells are thought to be derivatives of the somite; fate-mapping and chimeric interspecies grafting experiments in avian embryos demonstrated that transplanted embryonic somatic cells with distinguishing morphological characteristics to those of the host embryo migrated from the somite and contributed to the development of the limb musculature and the postnatal skeletal muscle satellite cell population (Le Douarin and Barq 1969; Christ *et al.* 1974). The head, trunk and limb muscles all develop from the somites but as separate lineages. The somites are further subdivided into two domains; the epaxial (gives rise to muscles of the back) and the hypaxial (develops into intercostal, abdominal and limb musculature) (Ordahl and Le Douarin 1992; Ben-Yair *et al.* 2003).

Intriguingly, De Angelis *et al.* (1999) proposed that satellite cells may also be derived from a non-somitic origin; cells isolated from the embryonic dorsal aorta had similar morphological characteristics and gene expression profiles to somite-derived satellite cells, and their transplantation into newborn mice contributed to postnatal muscle growth. Furthermore, Tzahor *et al.* (2003) provided evidence of non-somitic satellite cells, exemplified by some head muscles, which are derived from the prechordal mesoderm rather than the somites. It is possible satellite cells derived from either source may not be mutually exclusive and both lineages could contribute to the postnatal satellite cell population. Future fate-mapping experiments will have to delineate the derivation of all satellite cells resident in adult skeletal muscle.

During somitogenesis, it is thought cross-talk between growth factors such as Wnt proteins, Notch, sonic hedge hog, bone morphogenetic proteins (BMPs)

and myogenic transcription factors (myogenic factor 5 (*myf5*), *myoD*, *pax3/7*, etc) between the developing somite and anatomically adjacent structures such as the ectoderm generates temporally and spatially distinct lineages of myogenic cells that ultimately lead to the formation of skeletal muscles (reviewed by Miller *et al.* 1999). Avian satellite cells are first detected during the latter stages of embryonic development (around embryonic day 18), upon formation of the basement membranes and myofibres (Hartley *et al.* 1992). In rodents, satellite cells are present in the limbs of mid-gestational mouse embryos (around embryonic day 15-16) (Cossu *et al.* 1987). Satellite cell numbers drop during maturation; they account for approximately 30% of muscle nuclei in the perinatal hindlimb skeletal muscle but reduce to about 10% by postnatal day 28 and plateau to approximately 2-7% of total muscle nuclei in adult muscle (Allbrook *et al.* 1971; Schultz 1974; Halevy *et al.* 2004). During the neonatal growth phase, as muscles enlarge, satellite cells are proliferative and add nuclei to growing myofibres but they are typically quiescent in mature adult muscle unless activated by various factors for maintenance and repair.

1.2.3 Satellite cell identification

As mentioned above, satellite cell identification has historically relied on the use of ultrastructural techniques (electron microscopy) and by definition constitutes all single nuclei cells located beneath the basal lamina and just above the plasmalemma of a myofibre regardless of the function or gene expression profile. In practice however, the use of immunohistochemical

techniques based on the expression of a range of specific markers that can be detected by immunostaining represents a more efficient means of satellite cell identification in their native position. A limiting factor in this field is the fact that the gene expression profiles of quiescent and activated satellite cells are largely unknown. Recently, the use of genetically modified reporter mice has enabled direct detection of satellite cells, based on the specific expression of a fluorophore (e.g. green fluorescent protein; GFP) or via a reporter dye system such as β -galactosidase. For example, in nestin-GFP transgenic mice (Mignone *et al.* 2004), GFP expression is driven by regulatory elements of the intermediate filament, nestin, which labels progenitor cells and enables detection of quiescent satellite cells in isolated myofibres (Day *et al.* 2007). Similarly, the Myf5^{nLacZ/+} transgenic mouse (Tajbakhsh *et al.* 1996), in which one of the Myf5 alleles is modified to drive lacZ expression, results in the presence of β -galactosidase protein in the nuclei of satellite cells, thus allowing detection of satellite cells in the presence of X-gal by a distinctive blue stain (Beauchamp *et al.* 2000). Another transgenic strain frequently used to label satellite cells is the MLC3F-nLacZ transgenic mice (Kelly *et al.* 1995), in which the regulatory elements of myosin light chain (MLC) direct LacZ expression in myonuclei but not satellite cells, thus providing a means of distinguishing between satellite cells and myonuclei (Beauchamp *et al.* 2000). Crosses of nestin-GFP and Myf5^{nLacZ/+} or MLC3F-nLacZ transgenic mice enable detection of satellite cells by direct fluorescence and X-gal staining. For example, the double nestin-GFP/MLC3F-nLacZ transgenic mouse shows clear distinction between satellite cells (GFP⁺/X-gal⁻¹) and myonuclei (GFP⁻/X-gal⁺) (Day *et al.* 2010).

1.2.4. Satellite cell markers

1.2.4.1 Quiescence

Many regard satellite cell quiescence as a state characterised by decreased cell size and metabolic activity; however the work of Yusuf and Fruman (2003) on quiescent lymphocytes discovered quiescence is not merely an inactive basal state but one that is under active transcriptional control. The study of satellite cell quiescence is often fraught with difficulty since they are a relatively small population of cells *in vivo* and their isolation often results in activation. The location of satellite cells beneath the basal lamina means that disturbance to the satellite cell microenvironment increases the probability of activation, which may alter the gene expression profile. The close association between the myofiber and the satellite cells suggests active communication between the two and may be essential for maintaining quiescence. Furthermore, quiescent satellite cells have also been shown to express syndecan-3, syndecan-4 and c-met, the hepatocyte growth factor (HGF) receptor, the latter of which is also expressed by activated satellite cells. All are involved in signal transduction pathways essential for early activation and proliferation of quiescent satellite cells and may be responsible for maintaining a 'state of readiness' for activation (Tatsumi *et al.* 1998).

Pax7 is the most useful genetic marker for identifying quiescent and activated satellite cells (see figure 1.3); it has been implicated in satellite cell specification, as the survival of mice lacking the pax7 gene was compromised (Seale *et al.* 2000). The pax7 gene is a member of the paired box containing gene family, involved in the development of skeletal muscle, organogenesis

and maintenance of pluripotent stem cell populations (reviewed by Chi and Epstein 2002). It is commonly expressed in satellite cells but it is down-regulated upon myogenic differentiation, thus marking pax7 an important marker for quiescent and activated/proliferating satellite cells. Intriguingly, the skeletal muscles of pax7^{-/-} mice lack satellite cells and myoblasts are unable to undergo myogenesis when cultured. Pax7 null mice appear normal at birth but fail to grow postnatally, lose approximately 50% of their body weight by 7 days compared with wild type litter-mates and usually perish within 2 weeks after birth (Mansouri *et al.* 1996). This suggests pax7 is vital for muscle function and it is indisputably, required for satellite cell development. Recent evidence suggests pax7 is able to maintain satellite cell quiescence by inducing inhibitory helix-loop-helix (HLH) proteins – inhibitors of differentiation (Id) proteins (Id2 and Id3), which block the DNA binding activity of myogenic regulatory factors (Kumar *et al.* 2009).

Several other markers of quiescent satellite cells have been described including the muscle specific cell adhesion molecule M-Cadherin, CD34 (a cell surface cell-cell adhesion glycoprotein also localised to cells of the haematopoietic and endothelial cell lineages) and myocyte nuclear factor (MNF) (reviewed in Hawke and Garry 2001; Wozniak *et al.* 2005; Zammit *et al.* 2006). M-Cadherin is usually expressed in quiescent satellite cells but its expression has been shown to be up-regulated in upon activation; especially in response to denervation or traumatic injury (Irintchev *et al.* 1994; Cornelison and Wold 1997). Other recent markers discovered in quiescent satellite cells include lysenin (Nagata *et al.* 2006) and caveolin-1, a membrane protein that forms oligomers and associates with sphingolipids and cholesterol to give rise to

caveolae (Volonte *et al.* 2004). Neural cell adhesion molecule (NCAM) and vascular adhesion molecule-1 (VCAM-1) are also potential markers of quiescent satellite cells.

The molecular signature of quiescent satellite cells in adult skeletal muscle retains the cell's proliferative and differentiative potential throughout their lifetime and as such, an increase in expression of some genes such as myostatin is observed. Lines of evidence suggest myostatin, a negative regulator of muscle mass (McPherron *et al.* 1997) is expressed in quiescent satellite cells and myostatin null mice have an increased percentage of actively proliferating satellite cells compared to wild type littermates (McCroskery *et al.* 2003).

Myostatin induces a potent cyclin-dependent kinase inhibitor, p21, which inhibits cell cycle progression and maintains quiescence (Fukada *et al.* 2007).

There is also increasing evidence for the role of myoD (a prominent marker of activation) suppression in the maintenance of satellite cell quiescent/proliferative state. Pax7 overexpression results in a decrease in myoD protein and promotes activated satellite cells to reacquire a quiescent, undifferentiated state (Olguin and Olwin 2004). Similarly, the overexpression of metalloprotease disintegrin ADAM12 protein in proliferating C2C12 myoblasts has been shown to suppress myoD protein and lead to the up-regulation of quiescence makers p130 and p27, cell cycle arrest and a quiescence-like phenotype that does not stimulate differentiation (Cao *et al.* 2003). Gene Set Enrichment Analysis (GSEA) of quiescent satellite cells observed an up-regulation of gene sets involved in cell-cell adhesion, extra-cellular matrix maintenance, growth, lipid transport and copper, iron and calcium homeostasis, most notably an up-regulation of the calcitonin receptor

and calcitonin, which have been implicated in the attenuation of satellite cell activation (Fukada *et al.* 2007).

1.2.4.2 Activation and proliferation

Satellite cell activation is a multi-step process involving the transition from G₀-G₁ stage of the cell cycle. It is marked by cell cytoplasmic extension, expansion of organelles and a lower chromatin density. Satellite activation is dependent on the availability of extrinsic (e.g., HGF) and intrinsic signals (e.g., an up-regulation of myoD and a down-regulation of pax7) to drive the process forward. Once entered into the first cell cycle, satellite cells may enter a highly proliferative intermediate progenitor stage as myoblasts capable of myogenic differentiation and fusion (reviewed by Dhawan and Rando 2005). Activated satellite cells continue to proliferate as myoblasts and express muscle regulatory genes such as myogenic factor 5 (myf5) and myoD, both members of the bHLH family of MRF. Myf5 has been identified in activated and proliferating satellite cells. It is probably expressed in quiescent satellite cells, but at a lower level than in proliferating cells (Beauchamp *et al.* 2000). Myf5 gene expression declines when myoblasts enter differentiation whereas myoD persists well into the differentiation stage.

MyoD induces the cyclin-dependent kinase inhibitor p21, cyclin D3, retinoblastoma protein (pRb) and myogenin, all of which couple the attenuation of satellite cell proliferation with cell cycle exit and the induction of myogenic differentiation (Kitzmann *et al.* 1999). Its DNA binding activity is inhibited by Id proteins, with which it forms non-functional heterodimers

incapable of trans-activating the regulatory regions of many muscle specific genes such as myosin heavy and light chains, desmin, creatine kinase and others (reviewed by Legerlotz and Smith 2008). Interestingly, myoD-null mice contain functioning satellite cells although delayed muscle regeneration is noted; cultured myoblasts from such animals fail to fuse *in vitro*. In single myofibre extracts, satellite cells demonstrated a 90% reduction in differentiation efficiency (Sabourin *et al.* 1999; Cornelison *et al.* 2000). Committed myoblast expressing myoD will continue to proliferate until the balance of protein expression, including the accumulation of myoD, pushes cells toward differentiation (reviewed in Yablonka-Reuveni 2011).

The Notch signalling pathway has also been implicated in satellite cell activation; the Notch receptor (Notch-1) is expressed on activated satellite cells and its antagonism (demonstrated, for e.g. via overexpression of its inhibitor, Numb) has been shown to prevent satellite cell activation and proliferation (Conboy and Rando 2002). The pathway is often found up-regulated in response to muscle injury, through increased expression of the Notch-1 ligand, Delta-1, which activates the Notch-1 receptor expressed on satellite cells and promotes cell proliferation. However, uncontrolled Notch-mediated induction of satellite cell proliferation has been shown to have consequences for differentiation. For example, excessive activation of Notch-1 by overexpression of Delta also delays differentiation by suppressing myoD and myogenin (Nofziger *et al.* 1999; Delfini *et al.* 2000). Taken together, these findings suggest that Notch-mediated satellite cell proliferation and differentiation must be intricately balanced between activation and inhibition of the Notch-1 receptor to appropriately control myogenesis.

The work of Tatsumi *et al.*(1998) showed that HGF is capable of satellite cell activation *in vivo* and *in vitro*. It is released during muscle crush injury to stimulate satellite cell activation. Furthermore, injection of HGF directly into the tibialis anterior of adult mice resulted in activation of quiescent satellite cells in the absence of myotrauma. The authors also found that administration of HGF neutralising antibody during crush injury attenuated satellite cell activation (Tatsumi *et al.* 1998).

HGF-mediated activation of satellite cells may be regulated by nitric oxide (NO), also a potent activator of satellite cells, usually released in injured muscle (Anderson 2000). Mice deficient in NO production (via nitric oxide synthase-1 (NOS-1) mutation or pharmacological NOS inhibition) experience delayed satellite cell activation and muscle regeneration following injury. Interestingly, the work of Wehling *et al.* (2001) and Anderson and Vargas (2003) noted NO promoted muscle regeneration in injured muscle by fulfilling an anti-inflammatory function. Also, normalisation of aberrant NOS signalling in mdx mice alleviated the muscle dystrophy phenotype. Intriguingly, inhibition of NOS reduces the amount of HGF released following myotrauma. It is therefore likely NO is involved in the release of HGF from the extracellular matrix and, although the interplay between the HGF and NO/NOS signals is still unclear, it is probable that both are involved in myotrauma-induced satellite cell activation (reviewed by Holterman and Rudnicki 2005).

Satellite cell are already activated by relatively mild exercise (reviewed by Kadi *et al.* 2005). Exercise-induced activation is triggered by localised ultra-structural or segmental muscle fibre damage, which in turn initiates the release of inflammatory substances and growth factors (Roth *et al.* 2001). The highest

frequency of fibres with ultra-structural damage should also contain the highest proportion of active satellite cells. Rupture of the basal lamina in response to myotrauma causes migration of satellite cells to adjacent myofibers by using tissue bridges, to participate in the repair process (reviewed by Hawke and Garry 2001). Exercise-induced myotrauma initiates an immune response to attract macrophages to the damaged region, which consecutively secrete various cytokines and growth factors that regulate the satellite cell pool and modulate the repair process (reviewed by Nathan 1987). Such growth factors/or cytokines include interleukin-6 (IL-6), fibroblast growth factors (FGF), insulin-like growth factors (IGF-I, IGF-II, which are specifically up-regulated in response to hypertrophic signals, e.g., resistance exercise), HGF and members of the transforming growth factor- β (TGF- β) family. These factors have pleiotropic actions on satellite cell activity depending on the combination and concentration of inducing factors. For example, IGFs specifically increase satellite cell proliferation and differentiation, FGFs have been observed to attenuate satellite cell differentiation and members of the TGF- β family, which includes bone morphogenetic protein (BMP) and myostatin, inhibit satellite cell proliferation and differentiation (e.g., via suppressing myoD) (reviewed in Hawke and Garry 2001). Macrophages are also an important component of the repair process following muscle trauma; for example, there is a lack of muscle regeneration in the absence of macrophages and an increase in satellite cell proliferation and differentiation is noted when macrophage numbers are enhanced (Lescaudron *et al.* 1999).

Several other markers of activation have been proposed; for example, flk, sca-1, CD45, jagged-1, caveolin-1 etc (Dreyfus *et al.* 2004; Seale *et al.* 2004;

Volonte et al. 2004; Gnocchi *et al.* 2009). Although not specific to satellite cells, they are routinely used in single myofibre analyses for mapping the molecular signature of satellite cells in various stages of activity.

1.2.4.3 Differentiation and fusion

The onset of myogenic differentiation is marked by the expression of myogenin and MRF4 (also known as Myf6). It elicits a process whereby proliferating myoblast withdraw from the cell cycle and either fuse to existing fibres (e.g. to aid in the repair of damaged segments) or with each other to form nascent myotubes, which mature to replace damaged fibres. Early differentiation is also often measured by an increase in creatine kinase activity (reviewed by Florini and Magri 1989) or the subsequent shift in expression of contractile protein isoforms from developmental to adult. The up-regulation of myogenin coincides with the expression of various genes encoding structural proteins such as myosin heavy chains (Andres and Walsh 1996). Gross defects in embryonic muscle development of myogenin-null mice have impeded further study of its role in satellite cell myogenesis. Mouse mutants of myogenin die at birth and loss of myogenin in postnatal mice (via myogenin deletion after embryonic development) resulted in animals that were 30% smaller than control. It appears that myogenin is absolutely required for embryonic muscle development; myogenin-null mice exhibit severe muscle deficiencies and unlike single knock-out studies of other MRFs, myogenin has no redundant or compensatory mechanisms to replace its function (Knapp *et al.* 2006).

Markers that have been implicated in the myoblast fusion process include M-cadherin, M-calpain and desmin amongst others (reviewed by Charge and Rudnicki 2004). Cadherins are trans-membrane proteins involved in calcium-dependent cell-cell interactions. As mentioned above, M-cadherin is detected in quiescent satellite cells but it is markedly induced upon muscle injury, suggesting it is important for the repair process, which includes fusion of myoblasts. Interestingly, satellite cells from *myoD*^{-/-} mice (which fail to fuse when cultured) demonstrated reduced expression of M-cadherin in response to injury-induced activation (Sabourin et al. 1999; Cornelison et al. 2000). On the other hand, M-calpain activity is increased during myoblast fusion, an action subsequently blocked by calpastatin, an inhibitor of M-calpain. Myoblasts have also been noted to fuse earlier and faster after injection of M-calpain (Temmgrove *et al.* 1999).

1.2.4.4 Negative regulatory markers

As discussed earlier, myostatin is considered a negative regulator of satellite cell function. It is a member of the TGF- β family of secreted regulatory factors; myostatin knock-out mice displayed a 30% increase in body weight, largely as a result of increased skeletal muscle mass (McPherron et al. 1997). Additionally, myostatin mutations have been linked to the substantial increase in muscle mass observed in Belgian Blue and Piedmontese cattle breeds (Grobet *et al.* 1997; Kambadur *et al.* 1997). Recently, the discovery of a homozygote loss of function myostatin mutation in a German boy presented with pronounced muscle development at birth has supported the idea that myostatin specifically controls muscle growth (For a review, see Kocamis and

Killefer 2002). The exact mechanisms by which myostatin inhibits muscle growth are largely unknown, however, myostatin mRNA and protein is frequently found elevated in various pathological conditions such as human immuno deficiency syndrome (Gonzalez-Cadavid *et al.* 1998), hind-limb unloading (Carlson *et al.* 1999), thermal injury (Lang *et al.* 2001), cachexia (Zimmers *et al.* 2002), space-flight (Lalani *et al.* 2000), in age and denervation-induced muscle atrophy (Baumann *et al.* 2003).

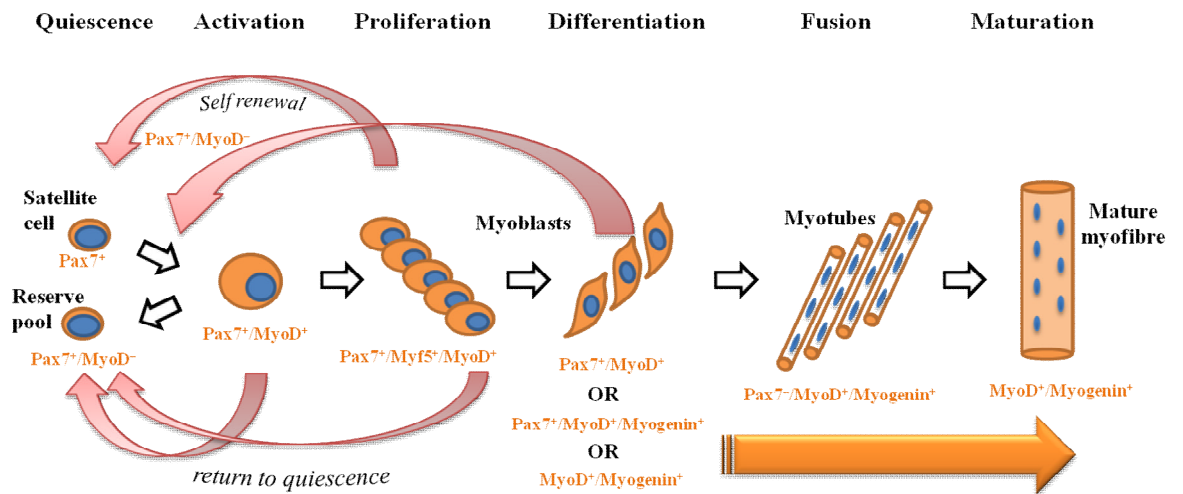
Studies done by McCroskery *et al.* (2003) show that myostatin negatively regulates satellite cell myogenesis. It is produced in increasing amounts as satellite cells progress through activation, myoblast proliferation and differentiation. Myostatin signals through the activin receptor IIB-ALK4/5 (activin receptor-like kinase) heterodimer, expressed on satellite cells, to activate multiple intracellular signalling cascades including SMAD and MAPK pathways. Activation of these pathways results in the induction of p21/Rb (to promote G1-S cell cycle arrest via inhibition of cyclin dependent kinases, e.g., cdk2) and nuclear translocation of smad4, which blocks myoD transcription. This results in the inhibition of satellite cell activation and cell cycling in proliferating myoblasts, which consequently slows down further myogenesis (reviewed by Joulia-Ekaza and Cabello 2006; Bradley *et al.* 2008). These findings are further supported by the work of McCroskery *et al.* (2005), who noted higher numbers of activated satellite cells in muscle fibres of myostatin-null mice relative to wild-type animals.

1.2.5 Sequential events regulating satellite cell myogenesis

The sequential expression of MRFs is an important regulatory mechanism for controlling satellite cell myogenesis. The induction of myogenic factors which drive differentiation and myotube formation will also suppress proliferation and quiescence markers. For example, *pax7* is expressed in quiescent satellite cells but its expression is reduced in those cells undergoing differentiation. Likewise, myogenin is reduced in proliferating satellite cells. It appears that a balance between feed-forward and feed-back mechanisms controls satellite cell myogenesis, whereby sufficient induction of a certain myogenic factor (e.g. myoD) stimulates trans-activation of other factors to drive the myogenic program forward (e.g. myogenin), whilst inhibiting factors are responsible for maintaining quiescence (e.g. *pax7*). Studies carried out by Halevy *et al.* (2004) in chicken showed increased myogenin expression was concomitant with a reduction in *pax7*. Quiescent avian satellite cells expressed *pax7* but reduced MyoD and expressed no myogenin, whilst proliferating satellite cells co-expressed *pax7* and myoD but not myogenin. It is thought those satellite cells positive for myogenin but negative for *pax7* ($pax7^-/myogenin^+$) may represent satellite cells that are committed to terminal differentiation. In addition, suppression of Pax7 whilst maintaining myoD was observed in differentiating myoblasts. It is thought satellite cells positive for *pax7* but negative for myoD ($pax7^+/myoD^-$) may represent the reserve pool of satellite cells, those that return to quiescence after activation (summarised in figure 1.4). Some myoblasts were shown to maintain *pax7* expression, down-regulate myoD expression and eventually stop proliferating but enter a state quite similar to

Fig1.4: Summary of sequential regulation of Satellite Cell Myogenesis.

Quiescent cells express pax7 only, proliferating cells express both pax7 and MyoD, which then either undergo a stochastic on/off gene switch or asymmetric division, leading to differentiation or a return to the cell reserve pool respectively. Myogenin expression induces a decision to undergo differentiation. Cells expressing all genes are probably at the turning point of differentiation



quiescence where they can be rapidly activated again (Halevy et al. 2004; reviewed by Zammit et al. 2004).

1.2.6 Satellite cell self-renewal

Satellite cells numbers in adult muscle remain relatively constant through repeated bouts of injury and regeneration. It is assumed this is as a result of their ability to self-renew. Activated satellite cells assume divergent fates - not all cells progress toward myogenic differentiation and some return to quiescence. It is thought asymmetric division is the chief method by which satellite cells maintain their baseline cell numbers throughout adult life (Moss and Leblond 1971). During proliferation, one daughter cell is committed as the progenitor cell, which returns to a quiescent state (see figure 1.3), whilst the other commits to differentiation and fusion. It is postulated that after several cell divisions, $pax7^+/myoD^+$ cells may undergo asymmetric division and/or are subject to a stochastic, non-deterministic process whereby differential accumulation of one protein or the other, causes some gene(s) to be switched on/or off. This stochastic on/off process could determine whether a cell differentiates or returns to the reserve pool (reviewed by Paldi 2003).

This concept of asymmetric division was also proposed by Conboy and Rando, (2002), who directly implicated Notch-1 and its antagonist Numb in satellite cell activation and self-renewal. A reduction in Notch-1 signalling due to increasing Numb expression led to the expression of $pax7$ and desmin, which likely indicates a commitment to myogenic lineage. Numb was found to localise asymmetrically in actively dividing cells, whereby those cells accumulating Numb show a commitment to myoblast fate. This suggests that daughter cells produced by satellite cell activation and proliferation assume divergent cell fates based on the accumulation of Notch and its antagonist in

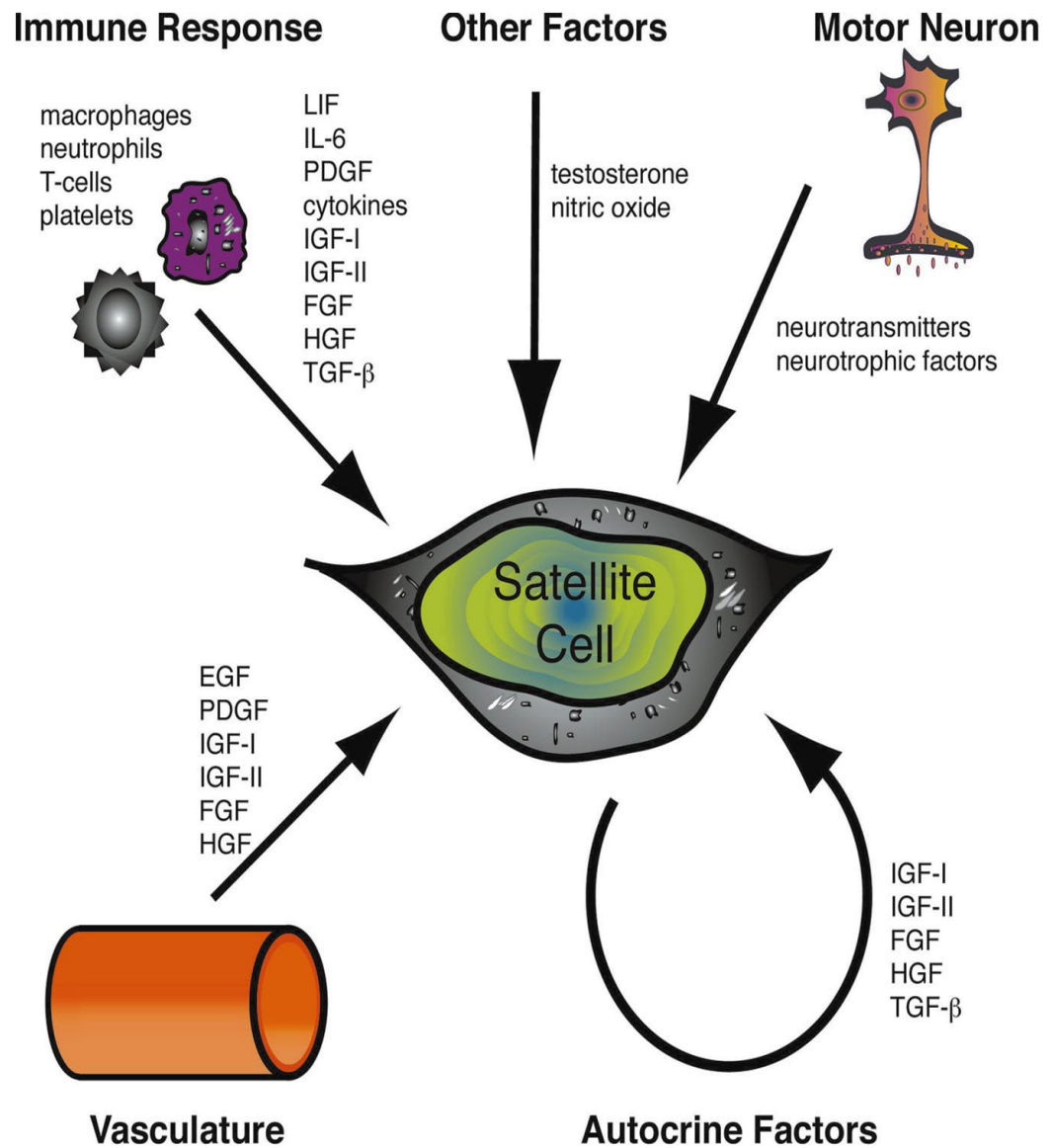
actively dividing cells. Taken together, these reports suggest that a combination of on/off switches of several genes, the differential accumulation of specific myogenic proteins, coupled with extrinsic cell signals, ultimately push satellite cells toward a path for self-renewal or myogenic differentiation.

1.2.5 Mechanisms modulating satellite cell activation and regulation

As highlighted above, the gene expression profiles of satellite cells at different stages of activity paints a complex and intricate picture of satellite cell regulation. The exchange of signals between different tissues/cells and satellite cells and vice versa, all form part of the satellite cell micro-environment.

Figure 1.5 below highlights some of the factors that influence satellite cell activity. These signals are believed to change significantly in various stages of satellite cell quiescence and activity. Myogenic regeneration responses, which mediate satellite cell activation, ensue from injury, exercise, muscle loading, denervation, etc. The nature of the satellite cell microenvironment and its role in regulating the quiescent and active states of satellite cells or mechanisms of self-renewal is largely unknown. For example, exercise in humans can induce activation of satellite cells without proliferation (Appell *et al.* 1988). As mentioned above, satellite cells are activated by relatively mild exercise and the satellite cell pool can increase as early as 4 days following a single bout of exercise and can be maintained at a higher level following weeks of training (Kadi *et al.* 2005). A gradual decrease in the previously enhanced satellite cell pool is observed upon cessation of training.

Figure 1.5: Summary of factors influencing satellite cell activity. The process of muscle regeneration involves growth factors released from a number of tissues that act either alone or in combination to influence satellite cell activity, which may include activation, chemotaxis, proliferation, differentiation and/or fusion. From (Hawke and Garry 2001).



1.3 SATELLITE CELL RESPONSE TO SKELETAL MUSCLE HYPERTROPHY

1.3.1 Definition of muscle hypertrophy

Skeletal muscle is highly adaptive and has a remarkable ability to increase its size to parallel demand; for example during resistance exercise (Kadi, 2004) or in response to anabolic stimuli such as growth hormones during puberty.

Skeletal muscle hypertrophy is characterised by an increase in muscle fibre cross sectional area or an increase in the number of muscle fibres. Hypertrophy could also be classed into two categories; sarcoplasmic hypertrophy – an increase in sarcoplasmic volume without concomitant increase in strength (typical of body-builder muscles) and myofibrillar hypertrophy – an increase in myofibre number, which is accompanied by an increase muscle strength and size (for a review, see Schoenfeld 2010).

Muscle hypertrophy is considered to occur when muscle protein synthesis exceeds protein breakdown and since skeletal muscle is a postmitotic tissue, it does not undergo significant cell replacement throughout life. Loss of nuclei (for e.g. due to apoptosis) reduces the synthetic capacity of myofibres by increasing the domain size (the cytoplasmic volume served by a single myonucleus). An efficient method of repair is therefore required to counteract loss of nuclei and maintain the regenerative capacity of myofibres throughout the organism's lifetime. This is achieved by the injection of satellite cells, which add new nuclei to myofibres to preserve domain size and hence synthetic capacity. Additionally, activated satellite cells express various MRFs that aid muscle repair and growth.

1.3.2 Satellite cells and muscle hypertrophy

The concept of a myonuclear domain proposes that a single myonucleus provides RNA for a limited sarcoplasmic volume and that increases in fibre size must be accompanied by proportional increases in myonuclei. Hypertrophy is thought to occur by an increase in the number of domains (via an increase in myonuclear number) as well as an increase in the size of existing domains (reviewed by Toigo and Boutellier 2006); both mechanisms involve significant contribution from satellite cells, which donate extra nuclei to myofibres, thus increasing their capacity to synthesise new contractile proteins (Moss and Leblond 1971; Barton-Davis *et al.* 1999).

Various physiological stimuli such as resistance exercise, chronic stretch, muscle overload (e.g. by agonist ablation or tenotomy) promote hypertrophic responses in many human and animal models by activating satellite cells among other systems. It is thought such responses and satellite cell activation occur because of the induction of various hormones and cytokines such as IGF-1, HGF and IL-6, which act as upstream of regulators of anabolic processes (reviewed in section 1.2.4.2 and figure 1.4 above). Among these, IGF-1 appears to be one of the most important factors linking hypertrophy and satellite cells (Barton-Davis *et al.* 1999). IGF-1 supplementation via localised transgene expression is known to prevent age-related muscle wasting (Musaro *et al.* 2001). Furthermore, satellite cells isolated from IGF-1 overexpressing mice show increased regenerative potential compared to non-transgenic animals; IGF-1 also increased the DNA content per myofibre and the expression of different myosin isoforms (Fiorotto *et al.* 2003).

In summary, it appears the primary role of satellite cells during hypertrophy is the addition of nuclei to growing myofibres in order to produce bigger muscles with a greater capacity for peak force generation. Although a number of questions still remain, it is clear that satellite cell activity is required for full compensatory muscle hypertrophy. This was demonstrated in studies done by Rosenblatt *et al.* (1992; 1993; 1994), where load-induced hypertrophy of EDL muscle, by synergistic removal of the tibialis anterior in rats, was prevented when satellite cells were ablated by gamma radiation sterilisation.

1.3.3 Summary of satellite cell activity in non-mechanically induced hypertrophy models

The role of satellite cells in hypertrophy induced by non-mechanical intervention such as drugs (e.g. β -agonists), anabolic steroids and nutritional supplementation is still being elucidated. Numerous studies have shown that administration of β -agonists induces hypertrophy in many species (reviewed by Lynch and Ryall 2008) by increasing the rate of contractile muscle protein synthesis and decreasing the rate of muscle protein breakdown. Whether nuclear addition from satellite cells is implicated in β -agonist-induced muscle growth has not been clarified and this will be the purpose of the investigations outlined in chapter 3.

Androgenic anabolic steroids are synthetic derivatives of the male hormone testosterone, which have been found to increase muscle strength and mass. Use of anabolic steroids boosts muscle hypertrophy beyond inherent limits by

increasing the transcription rate of myofibrillar proteins (for a review, see Aagaard 2004; Bhasin *et al.* 2006). A rapid increase in activated satellite cells and myogenesis in response to androgen treatment has been observed *in vitro* and *in vivo* (Joubert and Tobin 1995; Sinha-Hikim *et al.* 2003; Sinha-Hikim *et al.* 2004). The androgen receptor is expressed on satellite cells and it is thought the accelerated activation of satellite cells is as a result of direct androgen action, all of which help maintain an optimal nuclear-to-cytoplasmic ratio of growing myofibres during steroid-induced muscle hypertrophy.

Nutritional supplementation (e.g. timed protein intake in combination with ergogenic supplements such as creatine) has been shown to enhance muscle hypertrophy; especially when used in combination with training. Precisely timed protein supplementation after resistance exercise is thought to increase the availability of intracellular amino acids, which promote an acute increase in net protein balance that is utilised by growing myofibres (for a review, see Gibala 2000). Creatine supplementation augments the muscle hypertrophy response by eliciting larger increases in fibre cross-sectional area compared to training alone; chiefly by enhancing satellite cell activity and the production of MRFs (Dangott *et al.* 2000; Olsen *et al.* 2006).

1.4 SATELLITE CELLS DURING MUSCLE ATROPHY

1.4.1 Overview of muscle atrophy

Muscle atrophy is defined as a reduction in muscle mass occurring through a reduction in fibre size (hypotrophy) or number (hypoplasia). Changes in the size are thought to arise from an alteration in nuclear number, nuclear domain size or a combination of both (reviewed by Allen *et al.* 1999). As with muscle hypertrophy, atrophy may arise from a down-regulation of contractile protein synthetic pathways, an up-regulation of protein degradative pathways or a combination of both. Muscle atrophy is often a consequence of catabolic diseases such as cancer, acquired immune deficiency syndrome (AIDS), sepsis, thermal injury and chronic obstructive pulmonary disease (COPD); in all of them, it contributes to patient morbidity and mortality, due to the associated muscle weakness, reduced muscle function, and chronic frailty (reviewed in Vinciguerra *et al.* 2010).

Muscle atrophy may also be triggered by disuse (e.g. unloading during limb immobilisation/unloading, prolonged bed-rest or space-flight), denervation (e.g. spinal cord injury or sciatic nerve transaction in the rat), fasting and ageing (for reviews, see Marimuthu *et al.* 2011; and Narici and de Boer 2011). Age-related muscle loss (termed sarcopenia) is thought to occur via different mechanisms relative to other types of atrophy, predominantly involving a combination of myonuclei loss due to apoptosis, loss of motor units and reduced regenerative capacity of satellite cells (reviewed by Marzetti *et al.* 2010). Additionally, muscle atrophy can also be initiated by increased levels of circulating cytokines and catabolic hormones such as glucocorticoids

(reviewed by Hasselgren *et al.* 2005). This is frequently observed in cases of sepsis, in which the mechanisms of muscle loss and the role of satellite cells are largely unknown. The latter will be the purpose of the investigations described in chapters 4 and 5.

1.4.2 Satellite cell response to atrophic stimuli

The behaviour of satellite cells in models of atrophy tends to be quite varied and dependent on the atrophic stimulus; however a consistent finding appears to be a loss of myonuclei, which leads to an increase in domain size and thus reduced synthetic capacity. This is exacerbated by reduced satellite cell activation and inadequate nuclear replacement (Brack *et al.* 2005).

Furthermore, hindlimb unloading of juvenile rats resulted in reduced muscle size after 9 weeks but satellite cell content and proliferative capacity was reduced within 3 days in soleus and EDL muscles (Darr and Schultz 1989; Mozdziak *et al.* 2000).

In a similar model of hindlimb immobilisation utilised by Wanek and Snow (2000), a ~50% reduction in satellite cell number was noted in the soleus muscles of casted animals after 10 weeks of immobilisation. Disuse atrophy from prolonged denervation also produces a similar decline in the satellite cell population and it is hypothesised this is as a result of satellite cell apoptosis and lack of neurotrophic input, which negatively impacts satellite cell function due to reduced induction of growth factors (Viguie *et al.* 1997). Satellite cells from denervated muscle show distinctive phenotypic alterations such as proliferative

resistance, separation from associated fibres and basal lamina disruption (Lu *et al.* 1997; Kuschel *et al.* 1999).

1.5 SUMMARY AND HYPOTHESES

Taken together, the findings in this review highlight the importance of satellite cells in the maintenance of muscle homeostasis; we hypothesise their up-regulation in response to hypertrophic stimuli (such as in our clenbuterol pro-drug model of muscle hypertrophy) and their dysregulation in response to atrophic stimuli (in the sepsis model of muscle atrophy), which will contribute the severity of muscle loss or gain. The evidence reviewed above suggests that effective satellite recruitment predominantly contributes to muscle hypertrophy by nuclear addition; further understanding of the mechanistic events regulating satellite cell activity in pharmacological models of hypertrophy and atrophy in the rat should provide interesting avenues of therapeutic intervention aimed at combating muscle wasting. Furthermore, there is some evidence of satellite cell aberration during muscle atrophy which may account for the failure, delay or resistance of atrophied muscle to full regeneration, due in part to the reduction in the restorative capacity of satellite cells, especially in ageing muscle.

CHAPTER 2

General Methods

2.1 *IN VIVO* TECHNIQUES

2.1.1 Ethics statement

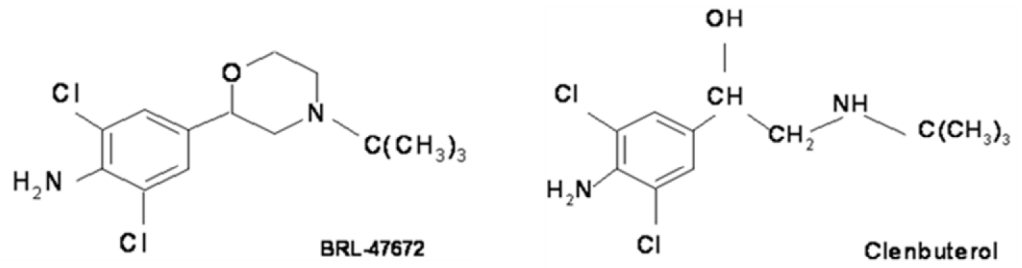
All procedures involving live animals detailed below were approved by the University of Nottingham Ethics Review Committee and carried out under UK Home Office Project and Personal License authority. All animals were obtained from Charles River Laboratories (Sandwich, UK) and housed in the Biomedical Services Unit, School of Biomedical Sciences for at least 10 days after delivery; the holding room temperature was maintained at $21\pm 2^{\circ}\text{C}$ with a 12hr light/dark cycle (6am-6pm) and standard rat chow (Beekay Foods, Hull, UK) and tap water was provided *ad libitum*. The human tissues used in these studies were obtained for general research purposes from the University of Bern, Switzerland, with the permission of the Canton of Bern Medical Ethics Commission.

2.1.2 β_2 -agonist pro-drug BRL-47672 study

2.1.1.1 Background

The morpholine compound BRL-47672 has a chemical structure similar to the β_2 -agonist clenbuterol (see figure 2.1 below); it causes similar anabolic effects in rats but with reduced haemodynamic effects compared to clenbuterol (Sillence *et al.* 1995). It is thought to be metabolised *in vivo* to the biologically active clenbuterol and the work of Sillence *et al.* (1995) noted that BRL-47672 has very little or no direct effect on β_2 -adrenoreceptors, as daily injection of the selective β_2 -antagonist, ICI-118551 showed no effect on the BRL-47672-

Figure 2.1: Chemical properties of BRL-47672 and Clenbuterol. Adapted from Sillence *et al.* (1995)



induced anabolic responses but these effects were blunted when ICI-118551 was administered in the diet. Similarly, administration of a selective β_1 -antagonist also failed to reduce the anabolic effects of BRL-47672, which lead to the conclusion that BRL-47672 is the pro-drug of clenbuterol and it is rapidly metabolised *in vivo* to a potent β_2 -agonist, thus having less impact on blood flow and pressure relative to active clenbuterol. This was validated by our group in the work of Jones *et al.* (2004) using an *in vivo* model of haemodynamics in conscious rats (Gardiner and Bennett 1988). In these preliminary studies, single bolus doses of clenbuterol or BRL-47672 (250 - 900 μ g/kg) were administered to conscious rats surgically implanted with Doppler flow probes. BRL-47672 caused significant reductions in heart rate, mean arterial pressure, and hindquarters vascular conductance compared to clenbuterol over a forty minute measuring period. The pro-drug is therefore more suitable for chronic administration due to its reduced haemodynamic response compared to clenbuterol.

2.1.1.2 Animals and tissue collection

Male Wistar rats (150-160g) were randomly assigned to one of two groups and received daily subcutaneous (s.c.) injections of β_2 -agonist pro-drug BRL-47672 (900 μ g/kg body mass, dissolved in 0.9% sterile saline, n=7) or an equal volume of 0.9% sterile saline (n=6) for 8 weeks. The dose of 900 mg/kg body mass of BRL-47672 was used because it demonstrated the greatest effect on muscle metabolism and function (Baker 2004). Twenty-four hours following final injections, rats were terminally anaesthetised intraperitoneally (i.p.) with

120mg/kg of thiobutabarbital sodium (Inactin; Sigma-Aldrich, St. Louis, USA) and the soleus muscles were excised, snap frozen in liquid nitrogen, and stored at -80°C for subsequent analysis.

2.1.2 Lipopolysaccharide (LPS) study

2.1.2.1 Background

The administration of LPS is one of the most widely used methods for studying animal models of Gram-negative sepsis. While some would consider this to be an inaccurate reflection of the human sepsis syndrome, it nevertheless produces a hyperdynamic circulatory response similar to human sepsis syndrome (Gardiner et al, 1995; Parillo, 1993). In addition, LPS is a relatively stable compound, allows accurate dosing and is associated with a high degree of reproducibility. This is reviewed further in chapter 4, section 4.2.

2.1.2.2 Animals and surgical preparation

Animals were housed in groups of 3-5 per cage before surgery, but were kept separate following intravenous catheter implantation. Male Sprague-Dawley rats (380-480g; Charles River) were anaesthetised with each of fentanyl citrate (300µg/kg; i.p., Janssen-Cilag, High Wycombe, UK) and medetomidine (300µg/kg; i.p., Domitor, Pfizer, Sandwich, UK), prior to intravenous (i.v.) catheter implantation in the jugular vein for administration of substances, as previously described by Murton (2007). Animals assigned to the 24 hr LPS treatment group were also implanted with arterial catheters for measurement of mean arterial pressure and heart rate. All catheters were flushed with sterile

heparinised (15 U/ml) saline (Monoparin; CP Pharmaceuticals Ltd, Wrexham, UK) and sealed with metal spigots. Whilst under anaesthesia, animals were fitted with a harness connected to a counter-balanced spring to carry the catheter, which allowed unrestricted movement within the cage and continuous administration of substances. Anaesthesia was reversed and analgesia provided with atipamezole (1mg/kg; s.c., Antisedan, Pfizer, Sandwich, UK) and buprenorphine (0.03mg/kg; s.c., Vetergesic; Alstoe Animal Health, York, UK), respectively. Animals were left to recover for 24 hr in individual home cages (26 x 30 x 38cm) with open access to food and water. Catheters were connected to an infusion pump via a fluid filled swivel, which maintained a continuous i.v. infusion of sterile heparinised saline (15 U/ml) at 0.4ml/hr. Animals were allowed to recover overnight and administration of substances commenced the following morning.

2.1.2.3 Lipopolysaccharide administration and tissue collection

Prepared rats were divided into six groups; three groups received a continuous infusion of sterile isotonic saline (0.4 ml/hr) for either 2hr (n=4), 6hr (n=4) or 24hr (n=6) as control. The remaining three groups received a continuous infusion of LPS (*E. coli*, serotype 0127:B8; 15µg/kg/hr - dissolved in sterile isotonic saline, Sigma, Poole, UK) for either 2hr (n=4), 6hr (n=4) or 24hr (n=6). After the specified time, animals were terminally anaesthetised with thiobutabarbital sodium (Inactin; 80mg/kg, i.v., Sigma-Aldrich, St. Louis, USA). The EDL and gastrocnemius muscles from both limbs were removed as previously described by Murton (2007), immediately snap frozen and stored in

liquid nitrogen for subsequent analyses. Muscle tissues were freeze clamped *in situ* with the use of aluminium tongs cooled in liquid nitrogen before removal.

2.1.3 Dexamethasone (Dex) study

2.1.3.1 Background

Administration of low doses of glucocorticoids such as dexamethasone (Dex) is thought to be beneficial for reducing the symptoms of sepsis and septic shock by preventing excessive production of pro-inflammatory cytokines and thus reduce mortality associated with sepsis. Therefore, dexamethasone was co-administered with LPS to determine if it blunted signalling events associated with LPS- mediated sepsis. This is reviewed further in chapter 5, section 5.2.

2.1.3.2 Animals and tissue collection

Male Sprague-Dawley rats (350-450g; Charles River) were implanted with an intravenous catheter in the jugular vein, under anaesthesia as described above in section 2.1.2.2. Following surgery, animals were allowed to recover for 24hr in individual home cages with open access to food and water. A continuous infusion of sterile heparinised saline (15 U/ml, 0.4ml/hr; i.v.) was administered via a fluid filled swivel to maintain catheter patency. Following catheterization, prepared rats were assigned to one of four groups (n=7-8 per group) and received a continuous intravenous infusions of sterile isotonic saline (0.4ml/hr) as control, LPS (15µg/kg/hr), Dex (12.5µg/kg/hr; Sigma Aldrich, Poole, UK) or both. In the Dex+LPS group, dexamethasone was administered for 1hr

before the commencement of and during the 24hr infusion of LPS. After 24 hr, animals were terminally anaesthetised as described above and the EDL muscle from both limbs was freeze clamped and removed. Muscles were immediately snap-frozen and stored in liquid nitrogen for subsequent analyses.

2.2 MOLECULAR BIOLOGY TECHNIQUES

2.2.1 Analysis of mRNA expression

Quantitative real-time polymerase chain reaction (qRT-PCR)

qRT-PCR is a widely used method for the rapid and accurate determination of specific mRNA transcripts. Unlike the traditional end-point PCR, which is often associated with errors and the need for optimisation (reviewed by Stanton 2001), qRT-PCR enables the quantification of specific mRNA transcripts after each thermal cycle without interfering with the reaction. In summary, RT-PCR involves the reverse transcription of total mRNA into cDNA and the cDNA template of interest (the amplicon) is specifically amplified. To achieve this, two synthetic DNA oligonucleotides (primers) are designed to be complementary in sequence to opposite ends of template of interest. Successive heating (to allow strand separation) and cooling (to allow annealing of primers to DNA template) of the reaction mixture in the presence of DNA polymerase and deoxyribonucleoside triphosphates (dATP, dCTP, dGTP, dTTP) allows synthesis of DNA from the two primers in a 5' – 3' direction, resulting in the exponential amplification of the amplicon.

Each step of the reaction can be monitored in real-time PCR by the use of a third shorter fluorescently-labelled DNA oligonucleotide (the probe) designed to hybridise to the template upstream /downstream of the primers. A variety of different probes with different chemistries are available. Here, the Taqman[®] probes were used, which consists of a short oligonucleotide, covalently linked at opposite ends with a 5' reporter dye (6-carboxyl-fluorescein; FAM[™]) and a

3' minor groove binder (MGB) non-fluorescent quencher (NFQ). When the probe is intact, the proximity of the quencher reduces the fluorescence emitted by the reporter dye via Fluorescent Resonance Energy Transfer (FRET). The 5' exonuclease activity of DNA polymerase cleaves the probe to remove the annealed nucleotides and proceed with polymerisation, thus releasing the quencher and reporter dyes (figure 2.2). This separation of reporter from its quencher increases the reporter dye signal, allowing the spectrophotometric detection of reporter dye emissions when excited by a light source (e.g. 488nm). The fluorescence intensity detected with each PCR cycle increases as more reporter dye molecules are cleaved and separated from the quencher with each cycle. Thus, the kinetics of the PCR can be monitored in real time based on the intensity of fluorescence emissions after each thermal cycle.

The kinetics of the reaction during amplification can be categorised into three phases; an exponential, linear and plateau phase (see figure 2.3). The fluorescence intensity is initially below the threshold of detection but gradually increases with cycle number until it is roughly proportional to amplicon quantity, such as during the exponential phase, where assuming 100% PCR efficiency, the amplicon product is doubling after every cycle. It is at this stage that transcripts are compared since the log of fluorescence detected is theoretically proportional to the quantity of cDNA sample. An arbitrary threshold of fluorescence is set in the exponential phase of the reaction by the Sequence Detection System (SDS; Applied Biosystems, Foster City, USA), which represents the cycle number at which this threshold of fluorescence is

Figure 2.2: Schematic representation of the Taqman[®] Polymerase Chain Reaction (PCR). Diagrammatically describes the steps detailing the principles behind Taqman probes and Fluorescent Resonance Energy Transfer (FRET) in one complete cycle of real time PCR reaction.

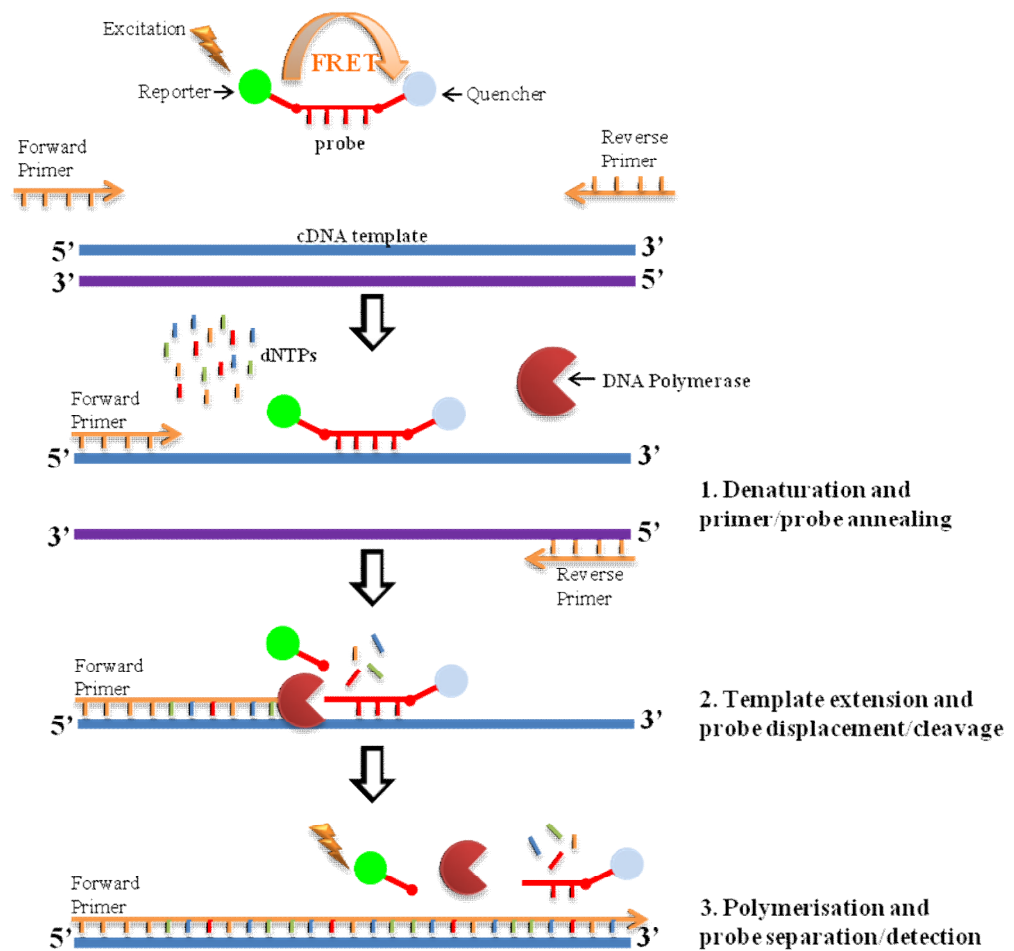
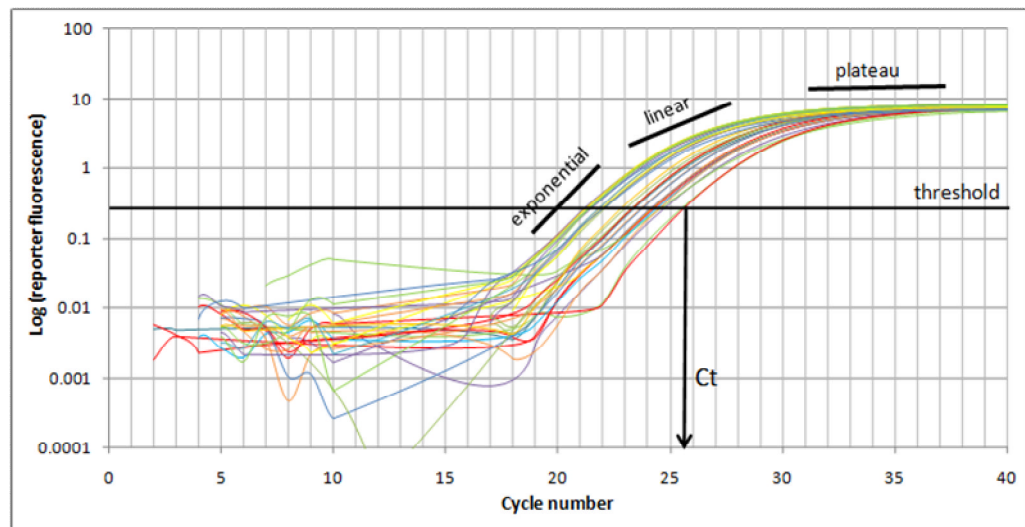


Figure 2.3: Schematic representation of the kinetics of Taqman[®] Polymerase Chain Reaction showing the three main phases of the reaction; an exponential, linear and plateau phase. A threshold of reporter emission is set in the exponential phase of the reaction by the Sequence Detection System (SDS) software and the cycle number at which the reporter emission of a sample reaches this threshold is logged as the cycle threshold (C_t) value.



achieved, i.e. the cycle threshold (C_t) value. The threshold value of fluorescence (C_t value) is reached sooner or later depending on the initial quantity of cDNA at the start of the reaction. Relative quantification of mRNA is calculated from the acquired C_t values using either a standard curve or comparative C_t method (User Bulletin No.2 for ABI Prism 7700 SDS (Part No. 430859); Applied Biosystems).

The standard curve method involves the use of serially diluted standards on each plate examined and mRNA expression is expressed as fold change relative to an undiluted standard. Absolute mRNA quantification is also possible using this method if the concentrations of the standards are known. This is a useful method for mRNA quantification but requires precise pipetting and accurate determination of standard concentration. On the other hand, the comparative C_t method uses an endogenous reference to quantify mRNA expression based on alterations in the steady state mRNA levels of the target gene relative to the levels of a housekeeping gene. The relative amount of mRNA between two groups can be calculated thus:

$$\text{Relative amount of target mRNA} = 2^{-\Delta\Delta C_t}$$

$$\text{Where: } \Delta\Delta C_t = \Delta C_{t[\text{treatment group}]} - \Delta C_{t[\text{control group}]}$$

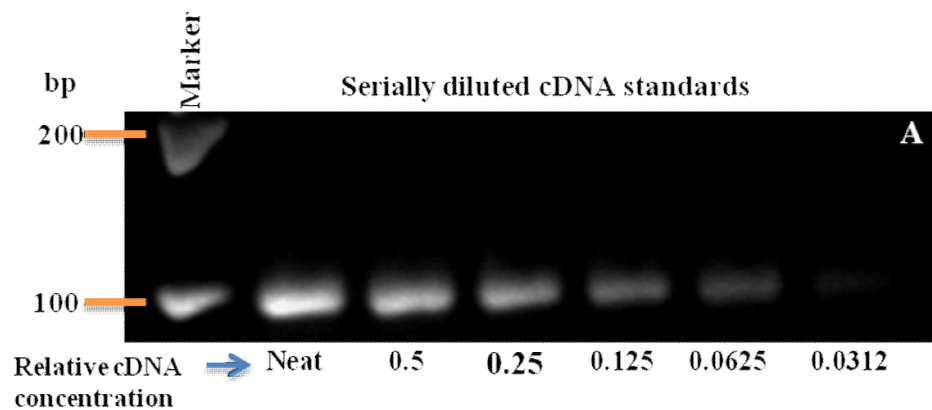
$$\text{and: } \Delta C_t = C_{t[\text{target gene}]} - C_{t[\text{endogenous reference}]}$$

The ΔC_t is the difference between the cycle threshold of the transcript of interest and the endogenous control; the ΔC_t of the treated group is normalised to the mean of ΔC_t of the control group. With the comparative C_t method, there is a need for optimisation, as the amplification efficiency of the target gene and the endogenous reference need to be roughly equal. Efficiency is determined

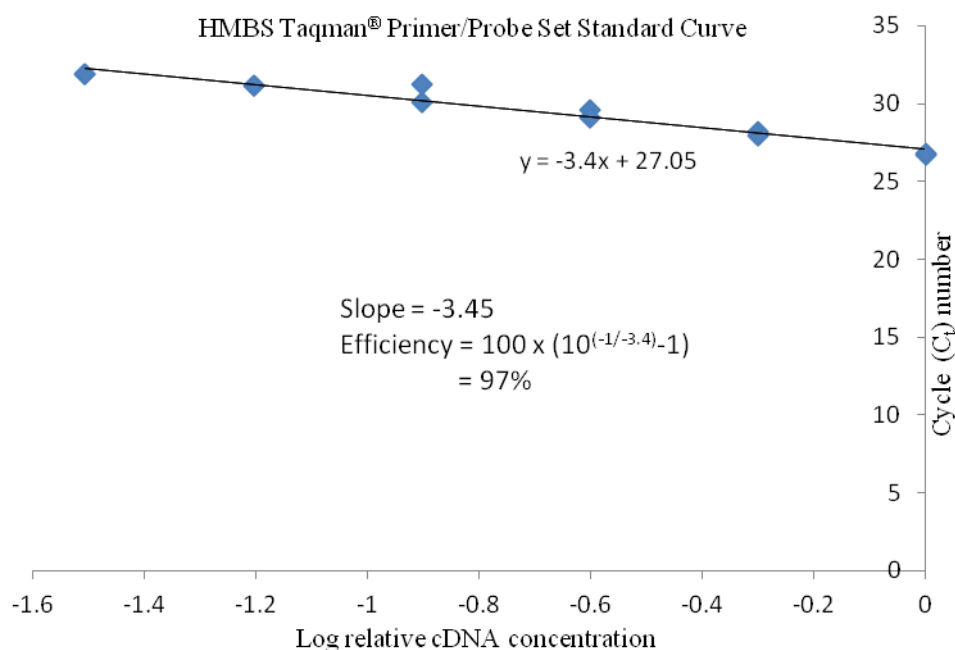
from the slope of a standard curve plot of log cDNA concentration versus cycle number of serially diluted standards, for both the target gene and endogenous reference primer/probe sets (see figure 2.4). All primer/probe sets amplified cDNA with similar efficiency (two examples are shown in figure 2.4 – the endogenous reference, HMBS and a target gene, myostatin). An advantage of the comparative C_t method is that once optimised, a standard curve for every plate analysed is not necessary and sample-to-sample variations in RT-PCR efficiency or pipetting errors are corrected for by the use of an endogenous reference. In addition to the efficiency of primer/probe sets, choosing an appropriate housekeeping gene chosen as an endogenous reference is essential for reliable results. The housekeeping gene hydroxymethylbilane synthase (HMBS), also known as porphobilinogen deaminase (PBGD) has been used extensively by our group and was used here to maintain consistency of results (Alamdari *et al.* 2008; Crossland *et al.* 2008; Murton *et al.* 2009; Crossland *et al.* 2010). HMBS exists in two isoforms; one is expressed in erythrocytes where it is involved in haem biosynthesis (Chretien *et al.* 1988). The other is ubiquitously expressed and has been suggested as a reliable endogenous reference for use in RT-PCR (Fink *et al.* 1999). HMBS expression is unaffected by LPS treatment in skeletal muscle and myocardium (Murton *et al.* 2009) and we confirmed this in the present studies (figure 2.5) to further demonstrate HMBS is a suitable reference for mRNA quantification.

Figure 2.4: Validation of the efficiency of Taqman primer/probe sets. RT-PCR was performed on a series of duplicate 2-fold dilutions of untreated gastrocnemius cDNA to obtain a standard curve of log relative cDNA concentration against C_t number. (A) In the example shown, the correct HMBS amplicon was amplified at intensity relative to cDNA concentration. (B) RT-PCR efficiency was calculated according to Applied Biosystems User Bulletin No.2, from the slope of the curve using the formula: $100 \times (10^{(-1/\text{slope})}-1)$, thus for HMBS, PCR efficiency was approximately 97%. (C) RT-PCR standard curve and efficiency for myostatin.

A. HMBS amplicon length and relative intensity



B. HMBS primer/probe set standard curve



C. *Myostatin primer/probe set standard curve*

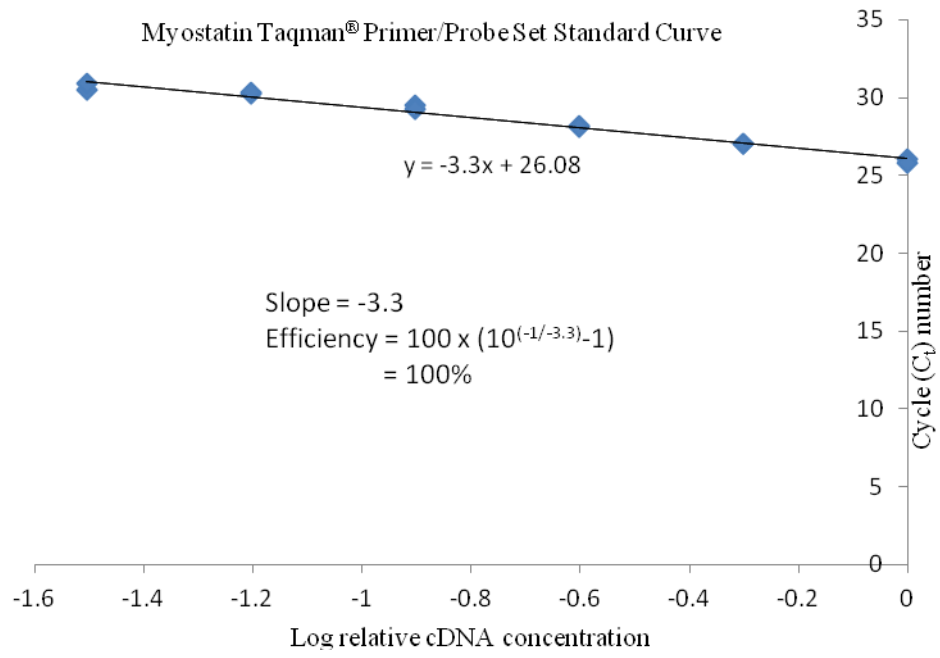
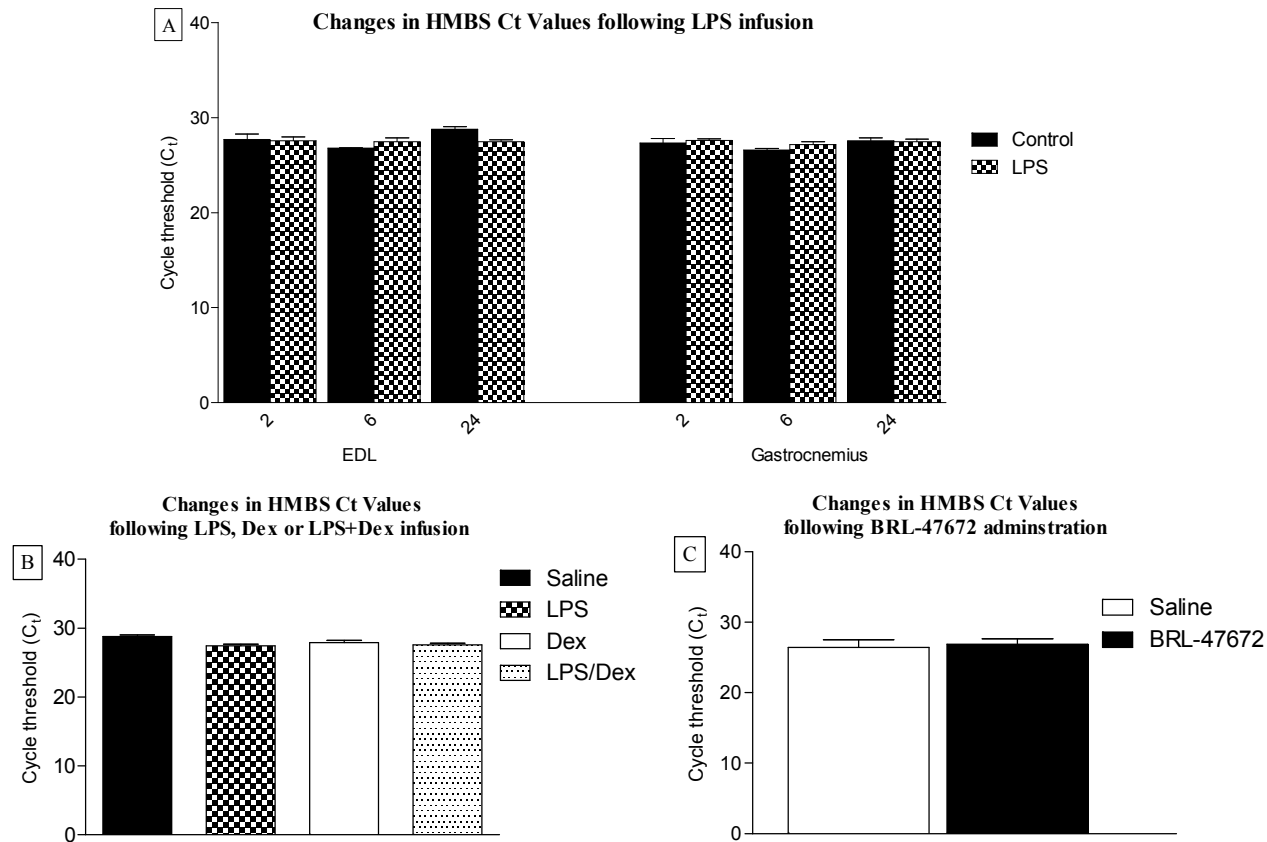


Figure 2.5: Analysis of Cycle threshold (Ct) values of Hydroxymethylbilane synthase (HMBS) in different muscle tissues following various interventions (A, B, C; see chapters 4, 5 and 3 respectively). No significant differences were detected control and treated groups. Data represented as mean \pm S.E.M (n=4-8 per group)



2.2.2 Total RNA extraction

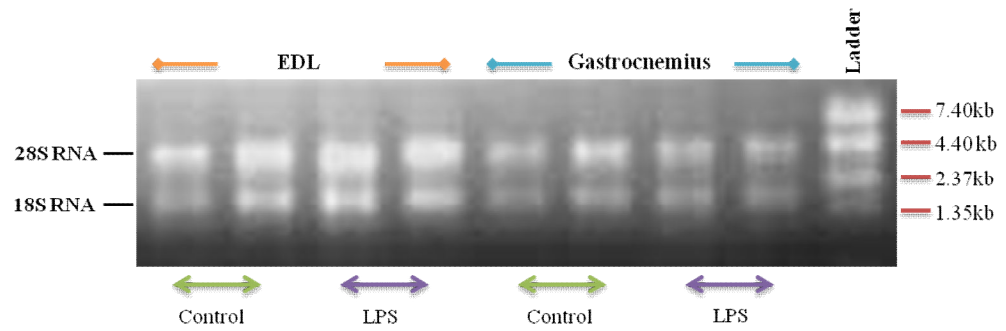
Total RNA was extracted from approximately 20-25mg of frozen wet muscle by homogenising in 800µl ice cold TRIzol[®] (Invitrogen, Paisley, UK) supplemented with glycogen (10µg/µl; Roche, Burgess Hill, UK) as a carrier. Samples were homogenised over ice for approximately 30 seconds using a polytron hand-held homogeniser. The homogenates was incubated at room temperature for 5 minutes prior to the addition of 160µl chloroform:iso-amyl alcohol (Sigma) at a ratio of 49:1 respectively. Samples were vortexed briefly before additional incubation at room temperature for 3 minutes. Homogenates were then centrifuged for 15 minutes at 12,000g, 4°C and the top clear RNA-containing aqueous phase was transferred to clean eppendorfs and precipitated with an equal volume (1:1 ratio) of ice-cold iso-propanol (Sigma). Samples were left overnight at -20°C to precipitate RNA and subsequently pelleted by centrifugation at 12,000g for 15 minutes at 4°C.

The pellets were air-dried at room temperature for 5 minutes, washed with 800µl of 75% ethanol and spun at 10,000g for 10 minutes. The ethanol was discarded and pellets were once more air dried to remove excess ethanol before re-suspending in 35µl RNase-free water. The quantity of RNA was assessed spectrophotometrically (ND-100 spectrophotometer, NanoDrop[®] Technologies Inc, Wilmington, USA) by measuring the absorbance at 260nm and 280nm and quality of RNA was determined by the 260:280 ratios. RNA yields were in the range of 250 - 350ng/µl.

2.2.2.1 Formaldehyde gel electrophoresis

RNA quality was also assessed qualitatively by visually assessing the ratio of 18:28S ribosomal RNA on a 1% formaldehyde gel (1% agarose, 1x MOPS, 0.7% formaldehyde). Briefly, 0.4g of low melting point Nusieve[®] GTG[®] agarose (Bio-Rad Laboratories, UK) was dissolved in 35.3ml double distilled water by heating and allowed to cool slightly before addition of 4ml 10x MOPS buffer (400mM MOPS, 100mM sodium acetate, 10mM EDTA; Eppendorf, Cambridge, UK) and 0.7ml deionised 37% formaldehyde (Sigma). The gel solution was poured into a prepared plate and comb mould and allowed to set at 4°C. The gel was run at 130mA for 20 minutes in gel buffer (1x MOPS, 0.7% formaldehyde) and RNA samples (1µl) were heated for 15 minutes at 55°C in RNA buffer (0.25µg/µl ethidium bromide, 1x MOPS, 50 % (v/v) deionised formamide, 6% deionised formaldehyde). Samples were mixed with a loading buffer (43.5% (v/v) glycerol, 2mM EDTA, 0.02% (w/v) bromophenol blue) and loaded along with a 0.24 – 9.5 kb RNA ladder (Invitrogen). RNA was visualised using a UV transilluminator (Syngene, Cambridge, UK) and images were acquired with Gene Tools software (Syngene,). See example in figure 2.6.

Figure 2.6: Qualitative assessment of total RNA extracted. In the example displayed, 1µl of extracted RNA was resolved on a 1% formaldehyde gel and the two bands present in each sample correspond to ribosomal 28S and 18S RNA. The minimal smearing and the approximate 2:1 ratio of 28S:18S RNA are both indicators of good quality RNA.



2.2.3 cDNA synthesis

First strand cDNA synthesis was carried out by reverse transcription using 1 µg of total RNA. RNA samples were incubated with 1 µl of random hexamer primers (0.5 µg/µl; Promega, Madison, USA) at 70°C for 5 minutes in a thermocycler to denature RNA secondary structure and then immediately placed on ice. To each sample was added 1 µl of Maloney murine leukaemia virus (MMLV) reverse transcriptase (200 U/µl; Promega), 5 µl MMLV reverse transcriptase buffer (Promega), 0.5 µl RNase inhibitor (40 U/µl; Promega) and 1.25 µl of a nucleotide mix containing dATP, dCTP, dGTP and dUTP (10mM each; Qiagen, Crawley, UK) up to a final volume of 30 µl with RNase-free water. An extra sample, which excluded the reverse transcriptase and had 1 µl of RNase-free water instead, was created to use as a reverse transcription minus (RT-) control in RT-PCR analyses. All samples were incubated at room temperature for 10 minutes, then 40°C for 1 hr followed by 15 minutes incubation at 70°C in a thermocycler to inactivate the reverse transcriptase.

2.2.4 Taqman analysis

All Taqman primer/probe sets were obtained from Applied Biosystems (ABI, Foster City, CA, USA); the primer and probe sequences are unavailable due to protection of intellectual property rights. However, primers were designed to span across exon/exon boundaries, thus ensuring genomic DNA was not amplified. Each primer/probe set was validated in accordance with Applied

Biosystems User Bulletin No.2 by running a series of RT-PCRs using serially diluted 2-fold cDNA templates to obtain standard curves of C_t number versus log relative concentration (see figure 2.4). All probe/primer sets amplified cDNA with similar efficiencies (reviewed in section 2.2.1), thus allowing use of the comparative C_t method for relative quantification of gene expression. Amplicon lengths were verified by resolution on a 4% agarose Tris-borate-EDTA (TBE) gel (see figure 2.7)

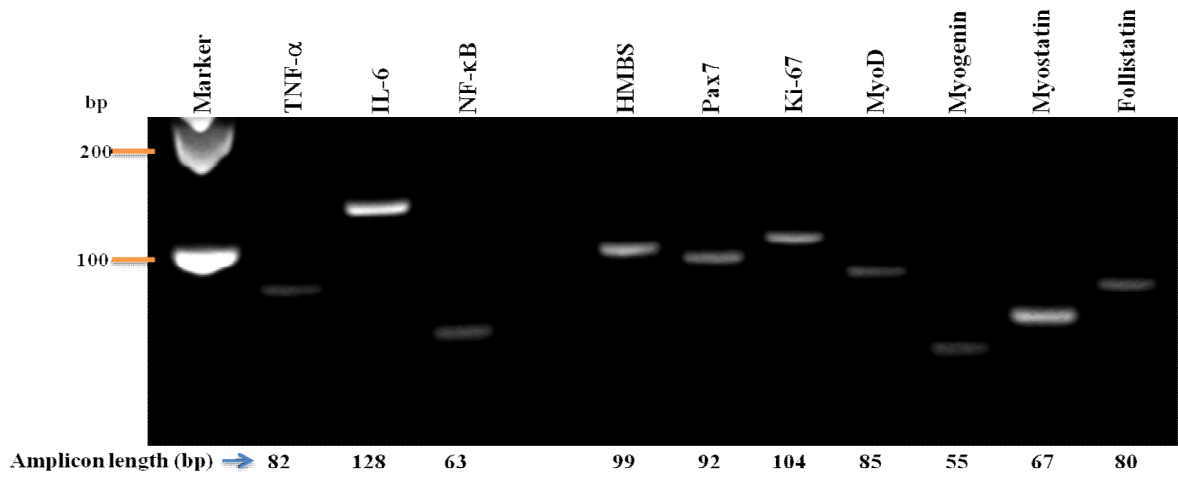
All real-time PCR reactions (including non-template and RT- controls) were carried out in duplicate using the ABI Prism 7700 Sequence Detection System (Applied Biosystems) in MicroAmp 96-well reaction plates (Geneflow, Fradley, UK). Each well contained 12.5 μ l of Taqman universal master mix (catalogue no.4369514; Applied Biosystems), 1.25 μ l primer/probe mix (final concentrations were: primers – 900nM each and probe – 250nM), 2 μ l cDNA template (or no-template control or RT- sample), in a 25 μ l final reaction volume with RNase-free water. Cycling parameters were 50°C for 2 minutes, 95°C for 10 minutes followed by 40 cycles of 95°C for 15 seconds, and 60°C for 1 minute. The C_t value for each duplicate was averaged and data from the treated group was normalised to the control group as described in section 2.2.1. The control group was given a value of 1 and fold changes in mRNA expression of the treated group are relative to the control group.

2.2.4.1 DNA electrophoresis

The specificity of RT-PCR was verified by resolving PCR products on an agarose gel alongside a DNA ladder to determine if fragments of the correct molecular weight were amplified. A 4% agarose gel was used for the resolution

of small PCR products (see figure 2.7). Briefly, Nusieve[®] GTG[®] agarose (Bio-Rad) was dissolved in 0.5x Tris-borate-EDTA (TBE; 45mM Tris base, 45mM boric acid, 1mM EDTA, pH 8) and distilled water by heating. The solution was allowed to cool slightly, ethidium bromide (0.07µg/ml) was added before the gel was cast and allowed to set at room temperature. Loading buffer (43.5% (v/v) glycerol, 2mM EDTA, 0.02% (w/v) bromophenol blue) was added to DNA samples at a ratio of 1:1.6 respectively; samples and DNA ladder (100bp direct load DNA ladder, Sigma) were loaded and the gel was run in 0.5x TBE running buffer at 200Volts for 20 minutes. RNA was visualised using a UV illuminator (Syngene) and images were acquired with Gene Tools software (Syngene).

Figure 2.7: Verification of correct amplicon lengths for all primer/probe sets used. RT-PCR using specific primer/probe sets amplified targeted sequences and produced amplicons of the correct molecular weight when resolved on a 4% (w/v) agarose gel by electrophoresis.



2.2.5 Analysis of protein expression (Western blotting)

Western blotting is routinely used for the analysis of protein expression by using specific antibodies to identify protein targets separated by sodium dodecyl sulphate polyacrylamide gel electrophoresis (SDS-PAGE). Proteins separated according to molecular weight are first transferred electrophoretically to a membrane support such as nitrocellulose followed by a blocking step to reduce non-specific antibody interaction and subsequent incubations with primary and secondary antibodies. Secondary antibodies are usually conjugated to haptens such as biotin or horse radish peroxidase (HRP) to facilitate visualisation of protein bands. These blotting steps are preceded by protein extraction and quantification in order to normalise protein load. Relative protein expression can be determined by densitometry; comparing the intensity of protein bands between control and treated groups after normalisation to an endogenous control, such as β -actin.

2.2.5.1 Muscle protein extraction

Cytosolic and nuclear proteins were extracted from muscle using a modification of the method by Blough *et al.*(1999). Approximately 30mg of frozen muscle was homogenised in 600 μ l homogenisation buffer (50mM Tris-HCl, 1mM EDTA, 1mM EGTA, 1% (v/v) NP-40, 0.1%(v/v) 2-mercaptoethanol, pH7.5) supplemented with mammalian protease inhibitor cocktail (10 μ l/ml, Sigma-Alrich, Poole, UK). Muscle lysates were incubated on ice for 10 minutes before centrifugation (13,000g, 10minutes at 4°C); the supernatant was used as crude cytosolic protein fraction and stored at -80°C.

The remaining pellets were resuspended in 500µl of an ice-cold high salt lysis buffer (20mM HEPES, 25% (v/v) glycerol, 500mM NaCl, 1.5mM MgCl₂, 0.2mM EDTA, pH7.9) supplemented with more protease inhibitor cocktail (10µl/ml) and incubated on ice for 30 minutes with intermittent mixing. Samples were spun (3,000g, 5min at 4°C) and the supernatant was collected as nuclear protein fraction. The insoluble pellet containing collagen and fibrous connective tissue was discarded and the soluble nuclear fraction was stored at -80°C.

2.2.5.2 Muscle protein quantification (Lowry assay)

Extracted proteins were quantified using the Lowry assay (Lowry *et al.* 1951). Briefly, 1µl of each protein sample was submitted for quantification alongside bovine serum albumin (BSA; 1mg/ml diluted in 0.1M sodium hydroxide (NaOH)) standards in duplicate. BSA standards were in the range of 0 – 80µg total protein in a final volume of 100µl in 0.1M NaOH. Protein samples and blanks (NaOH, homogenisation buffer and water) were also in a final volume of 100µl in 0.1M NaOH. All standards/blanks/samples were pipetted onto a 96 well microtitre plate and 50µl of the Lowry reagent (2% (w/v) sodium carbonate, 2% (w/v) sodium potassium tartate and 1% (w/v) copper sulphate solutions at a ratio of 10:1:1 (v/v)) was added to each well and incubated at room temperature for 10 minutes with gentle rocking. Subsequently, 50µl of Folin reagent (Folin and Ciocalteu's phenol reagent (Fisher Scientific, Loughborough, UK) 10% (v/v) in 0.1M NaOH) was added to each well and incubated for 30 minutes at room temperature with gentle rocking to encourage

colour development. The plate was read in a plate reader (DYNEX technologies, Worthing, UK) at 650nm. Protein concentration was determined based on the absorbance of protein samples (after blank subtraction) relative to the BSA protein standard curve.

2.2.5.3 Sodium dodecyl sulphate polyacrylamide gel electrophoresis (SDS-PAGE)

SDS-PAGE separates proteins according to molecular weight and protein samples are diluted in a reducing buffer containing urea, dithiothreitol (DTT), 2-mercaptoethanol and SDS to denature and solubilise proteins. SDS is an anionic agent which binds to polypeptide chains in a mass ratio of 1.4:1 to confer negative charge on the peptides such that their migration speed within the gel is roughly proportional to their mass, when an electric field is applied to the gel. Polyacrylamide gels are a chemically inert hydrophilic network of hydrocarbons cross-linked by bisacrylamide groups. The pore size is determined by the ratio of polyacrylamide-to-bisacrylamide cross-linker, which ultimately determines the degree of protein fractionation. The acrylamide concentration can be varied between 5-20% for various purposes; lower percentage gels are used for resolving high molecular weight proteins whilst higher percentage gels resolve smaller proteins. Gradient gels, which are used within this thesis, resolve both high and low molecular weight proteins and are useful for achieving a much greater separation. With gradient gels, the pore size varies uniformly (typically 5% at the top to 20% at the bottom of the gel) 5-20% polyacrylamide resolving gels were poured using a gradient mixer. Firstly, 5 and 20% resolving gel mixtures were prepared and made up to a

10ml final volume with deionised water. The 5% solution contained 1.67ml of 30% (w/v) acrylamide (acrylamide to bisacrylamide 37.5:1; Severn Biotech, Kidderminster, UK), 3.33ml of buffer B (1.1M Tris, 0.1% (w/v) SDS, pH 8.8) and 100µl of 0.1% (w/v) SDS. The 20% solution contained 6.67ml acrylamide, 3.33ml of buffer A (1.1M Tris, 0.1% (w/v) SDS, 30% (v/v) glycerol pH 8.8), and 100µl of 0.1% (w/v) SDS. Just before pouring, 100µl of 10% (w/v) ammonium persulphate (APS) and 10µl of undiluted tetramethylethylenediamine (TEMED; Sigma Aldrich) were added to each solution and mixed to catalyse polymerisation. The gel was layered at the top with a thin film of water-saturated butanol, which removed air bubbles and prevented dehydration, then allowed to set at room temperature.

A 5% stacking gel (0.12M Tris, 0.1% (w/v) SDS, pH 6.8) was similarly prepared and polymerised using APS and TEMED as above. The stacking gel (the purpose of which is to concentrate protein samples into sharp bands before they enter the main separating gel and trap proteins of molecular weights above ~250kDa) is poured on top of the resolving gradient gel and wells are formed into this for protein loading. Protein samples were diluted with double distilled water to required concentration before the addition of a Laemmli type SDS buffer (gel application buffer (GAB); 0.15M Tris, 8M urea, 2.5% (w/v) SDS, 20% (v/v) glycerol, 10% (w/v) 2-mercaptoethanol, 3% (w/v) DTT, 0.1% w/v bromophenol blue, pH6.8) at a ratio of 2.5:1. For example, 20µl of diluted protein sample to 8µl of GAB. Samples (containing ~2.5µg/µl of protein) were heated at 95°C for 5mins prior to loading, along with protein ladders (BIO-RAD All Blue Precision Plus Protein™ Standards, Hercules, CA, USA). The gel was run at 40mA (E-C Apparatus Corporation, Milford, MA,

USA), until the advancing dye front just starts to run out into the surrounding electrode buffer (0.025M Tris, 0.19M glycine, 0.1% (w/v) SDS).

2.2.5.4 Western blotting

Following electrophoresis, the negatively charged proteins in the gel are transferred electrophoretically onto nitrocellulose membrane (Amersham, Hybond™-C Extra, GE Healthcare, Little Chalfont, UK). The gel and nitrocellulose membrane are soaked in Western transfer buffer (0.025M Tris, 0.192M glycine, 20% (v/v) methanol) prior to contact. The membrane was placed next to the gel (taking into account the direction of protein migration) and sandwiched between absorbent materials and clamped between solid supports to maintain tight contact between the gel and the membrane. Proteins were transferred onto nitrocellulose membrane in transfer buffer overnight at 40mA (Fisher Electrophoresis unit) at room temperature. Confirmation of protein transfer was achieved by staining membrane with Ponceau S solution (0.1% (w/v) Ponceau S, 10% (v/v) glacial acetic acid) until protein bands were visible and membranes were subsequently de-stained with TBS-T (tris-buffered-saline with tween; 10mM Tris, 150mM NaCl, 0.05% (v/v) tween-20, pH 7.5)

Membranes were blocked with 5% non-fat milk in TBS-T for 1hr at room temperature and then incubated with primary antibody overnight at 4°C. For specific antibody information, including dilutions and manufacturer, see individual chapters. Membranes were washed for 3 x 5 minutes in TBS-T to remove excess/unbound primary antibody before incubating in HRP-conjugated secondary antibody for 1hr at room temperature. After washes in

TBS-T (3 x 5 minutes), membranes were immersed in Enhanced Chemiluminescence solution (ECL; Western Lightning Plus, Perkin Elmer, Waltham, MA, USA) for 1-2 minutes according to manufacturer's instructions. Briefly, reagents A and B were mixed at a 1:1 ratio and added to membranes, which were blotted briefly to remove excess ECL solution before exposure to hyperfilm (Amersham Hyperfilm ECL, GE Healthcare) for 1 to 30 minutes. HRP conjugated to the secondary antibody reacts with the chemiluminescence substrate, which produces light as a by product detected on hyperfilm. The amount of light produced (signal intensity) is relative to amount of bound antibodies and therefore the amount of a specific protein on the membrane.

Following exposure, films were developed (developing solution diluted 1:10 with distilled water; Calumet Photographic Ltd, Milton Keynes, UK), fixed (fixing solution diluted 1:5; Calumet Photographic Ltd), rinsed in water and air-dried. Films were scanned to produce digital copies and bands were quantified using densitometry and Gene Tools Software (Syngene, Cambridge, UK), which produces arbitrary intensity values correlated to the protein band intensity. These values were adjusted by subtracting the background and normalising to respective endogenous controls; actin for cytosolic proteins and lamin A/C for nuclear proteins. Cross-contamination between cytosolic and nuclear fractions was assessed using these two antibodies; blots of cytosolic protein fractions showed no bands for lamin after long exposure (>30 minutes). Similarly, blots containing nuclear protein fractions did not show actin bands after exposure for over 30 minutes.

2.2.6 Histological analyses

2.2.6.1 Immunohistochemistry

To localise and in some cases quantify protein expression in skeletal muscle, 10µm frozen serial cross sections were cut (Leica Microtome, Leica Microsystems, Wetzlar, Germany) and mounted onto Superfrost[®] Plus slides (ThermoFisher Scientific, Loughborough, UK). Frozen muscles were first secured onto a chuck using optimal cutting temperature (OCT) mounting medium (Tissue-TEK, Sakura, Thatcham, UK); the cryostat chamber temperature was between -18°C and -24°C and the chuck temperature was in the range of -16°C to -20°C depending on the optimal cutting parameters of the tissue being cryo-sectioned. Unless otherwise specified, sections were fixed in 4% Paraformaldehyde/Phosphate-Buffered-Saline (PFA/PBS: 4% (w/v) PFA, 137mM NaCl, 2.7mM KCl, 4.3mM KH₂PO₄ 5mM MgCl₂, pH 7.4) for 10 minutes, washed for 3x5 minutes in TBS (0.05M Tris, 0.15M NaCl, pH 7.4) and the reaction area for each section on the slide was delimited using a liquid blocker/pap-pen (Sigma-Aldrich).

Sections were then blocked for 1hr at room temperature with 5% normal serum (Vector Laboratories, Burlingame, CA, USA) diluted with TBS. For all incubation steps, slides were incubated in a moist chamber (tissue paper saturated with TBS) to prevent dehydration. The blocking serum employed was from the species in which the secondary antibody was raised (e.g. horse). Sections were briefly aspirated to remove blocker before incubating with primary antibody diluted in blocking solution; for specific antibody information including manufacturer details, dilution, and incubation

temperature/duration, see chapter 4, section 4.3.4. Negative control sections were incubated in blocker only. Slides were washed for 3 x 30 minutes in TBS prior to the addition of a labelled secondary antibody (e.g. biotin) and incubation at room temperature for 1 hr. Following secondary antibody incubation, slides were washed for 3 x 5 minutes in TBS. Antibody binding was visualised with the Vectastain[®] ABC Kit (Vector Labs). The “ABC” (Avidin: Biotin enzyme Complex) technique employs avidin, which has very high affinity for biotin and binds biotin essentially irreversibly at four different sites. The ABC kit contains reagent A (streptavidin) and reagent B (biotinylated HRP) and these were mixed in 5ml TBS at a 1:1 ratio and incubated for a minimum of 1 hr at room temperature, before applying to sections. This enables the formation of the ABC complex whereby streptavidin cross-links biotinylated HRP in a three-dimensional array with few exposed/unbound biotin molecules but with at least one remaining biotin binding site, to which the biotinylated secondary antibody binds. Secondary antibodies are conjugated with several molecules of biotin, which increases the sensitivity and specificity of the reaction. Sections were incubated with ABC reagent for 30 minutes at room temperature followed by 3 x 5 minute washes in TBS.

The antigen of interest is visualised by incubating sections with a substrate for the biotinylated enzyme; in this case, the 3, 3'-diaminobenzidine (DAB) peroxidase substrate kit (Vector Labs) was used according to the manufacturer's instructions. Briefly, 1 drop of buffer stock solution (pH 7.5), 2 drops of DAB stock solution and 1 drop of hydrogen peroxide solution were added to 2.5ml of distilled water with intermittent mixing in-between. The

DAB solution was added to sections and colour development was controlled visually under a light microscope. The optimal duration for colour development was replicated for the remaining slides. DAB is oxidised by HRP and leaves a brown precipitate at the site of antigen recognition. To stop the DAB reaction, slides were rinsed for 3 x 5 minutes in distilled water. As DAB is a carcinogen, excess solution and that aspirated from slides was neutralised in equal volumes of 3% (w/v) potassium permanganate and 2% (w/v) sodium carbonate. Slides were rinsed, air dried and mounted in glycerol gelatine (Merck, Darmstadt, Germany) for microscopy (DM4000B light microscope, Leica). Images were acquired using a Micropublisher 3.3 RTV digital camera (Q-Imaging, British Columbia, Canada) with OpenLab software (Perkin Elmer)

2.2.6.2 Immunofluorescence

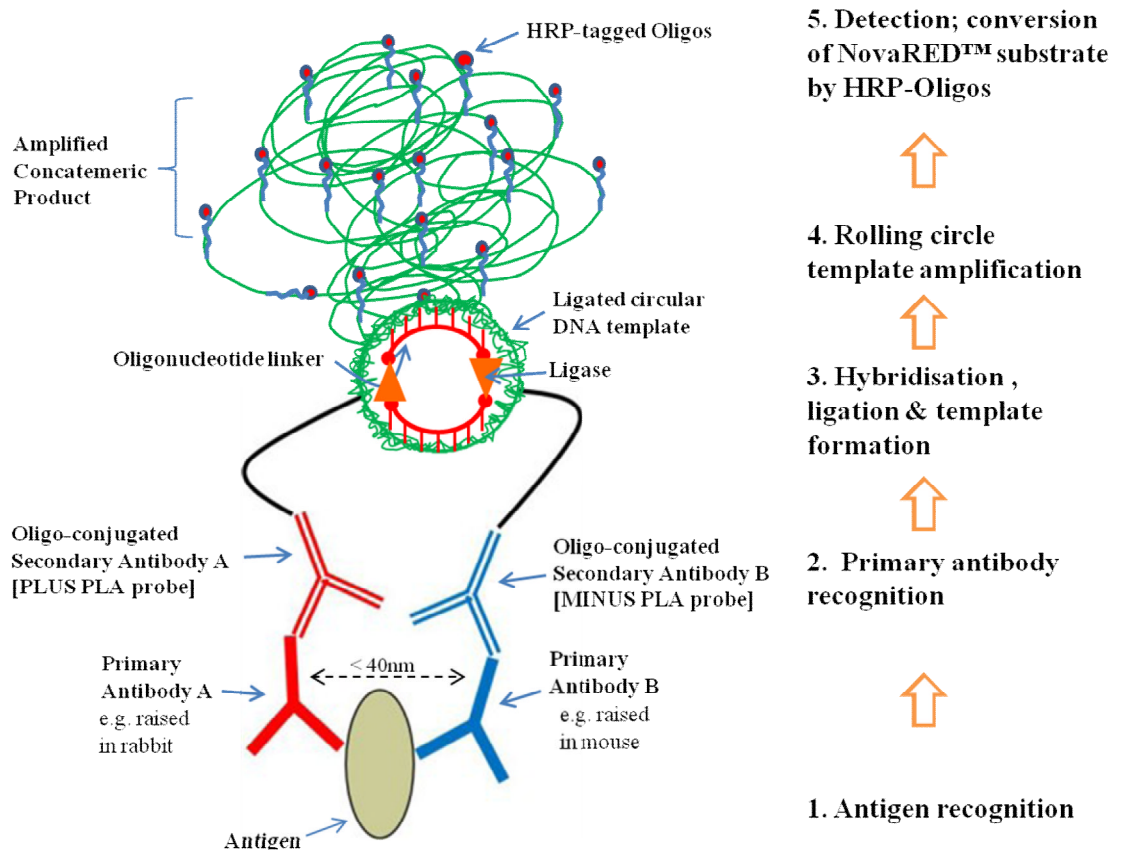
Protein expression was also analysed by immunofluorescence to confirm the co-localisation of protein targets of interest. Tissue samples were cryo-sectioned as described above in section 2.2.6.1. Formaldehyde vapour fixation was used to localise secreted protein targets such as TNF- α . This method of fixation methylates protein lysine groups thereby denaturing and partially cross-linking proteins. Using vapour fixation minimises the loss of soluble antibody targets in solution compared to PFA fixation; soluble proteins are cross-linked in a frozen state, keeping them as close to *in vivo* structure as possible. Briefly, tissue paper was saturated with 37% formaldehyde and placed in a sealed chamber at -20°C, to which slides were immediately added and fixed in formaldehyde vapour for 30 minutes. After fixing, sections were washed for 3 x 5 minutes in TBS and the reaction area delimited as above.

Sections were blocked with 5% normal serum for 1 hr at room temperature and incubated with primary antibodies (see chapter 4, section 4.3.4.2 for specific antibody information and conditions). Negative, technical control sections were incubated with blocker only. Slides were washed for 3 x 5 minutes in TBS before incubation with fluorescently-labelled secondary antibody or antibodies (for double detection). The fluorescent secondary antibodies were purchased from Invitrogen (Paisley, UK) and were used at 1:200, diluted in blocker. The excitation/emission of the fluorophores conjugated to the secondary antibodies was carefully considered to prevent antibody species cross-reactivity and spectral cross over, e.g. rabbit vs mouse – alexa 488 vs 568. Sections were incubated with the respective secondary antibody (or a combination) in a dark moist chamber for 1hr at room temperature. Slides were then rinsed for 5 x 5minutes in TBS, air dried and mounted in ProLong Anti-fade Gold with DAPI (Invitrogen). Visualisation and image acquisition were carried out using a DMIRB fluorescence microscope with an attached digital camera (Leica) and OpenLab software (Perkin Elmer).

2.2.6.3 Duolink[®] Bright-field Proximity Ligation Assay (PLA)

The Duolink[®] PLA enables *in-situ* detection and visualisation of proteins or protein complexes in tissue samples prepared for microscopy. Specificity for a single protein target is enhanced by using two different primary antibodies raised in two different species. Oligonucleotide-conjugated secondary antibodies (PLUS and MINUS PLA probes), bind to the two different F_c fragments when in close proximity and combine to form a circular DNA

Figure 2.8: Schematic representation of Bright-field Proximity Ligation Assay (PLA) to detect and quantify a single protein target with high specificity. The use of two primary antibodies directed against different non competing epitopes on the same antigen increases the specificity of the assay; this is useful for conditions where the use of either antibody independently yields unsatisfactory results. The oligonucleotides on the PLA probes when within less than 40nm of each other are hybridised via linker oligonucleotides to form a circular DNA template, which is subsequently ligated and amplified by rolling circle DNA replication. Complementary HRP-tagged oligonucleotides hybridise to amplified product and addition of a HRP substrate (NovaRED™) results in its enzymatic conversion to produce a visible red/brown precipitate at the site of antigen detection.



template that is subsequently amplified by rolling cycle amplification (see figure 2.8 for a summary of the method). HRP-tagged oligonucleotides specifically hybridise with amplified DNA and the signal from each detected pair of primary antibody is visualised as a quantifiable individual spot by microscopy

Briefly, cross sections were prepared and fixed in 4% PFA as described in section 2.2.6.1 above. Cross sections were blocked in 5% normal serum for 1hr at room temperature. Primary antibodies were added either individually (as an additional technical negative control) or in combination and negative control sections were incubated in blocking solution only. See chapter 4 for specific antibody dilutions and manufacturer information. All were incubated at 4°C overnight. Sections were washed for 3 x 30 minutes in TBS. The oligonucleotide-conjugated Minus and Plus PLA probes were used at a dilution of 1:5 in blocking solution and incubated with respective sections for 2hr at 37°C in a humid chamber. Slides were then incubated in the following solutions between washes in TBS-T: hybridisation (diluted 1:5 with high purity distilled water, 15min at 37°C), ligation (ligase was 1U/μl, 15min at 37°C) amplification (polymerase was 10 U/μl, 90min at 37°C) and HRP detection solutions (diluted 1:5, 30min at room temperature).

Slides were incubated in Duolink[®] substrate solution (containing the HRP substrate NovaRED[™]) for 10 minutes at room temperature, washed and nuclear stained (Mayers Haematoxylin) for 2 minutes. Slides were left under running tap water for 10 minutes to allow stain development. Prior to mounting in non-aqueous medium (Canada Balsam with xyelene, Merck, Darmstadt, Germany) for light microscopy, slides were dehydrated and cleared in

increasing concentration of ethanol (96%, 99.7% for 2 x 2 minutes each) then two changes with xylene for 10 minutes. Images acquisition using light microscopy was performed as described above.

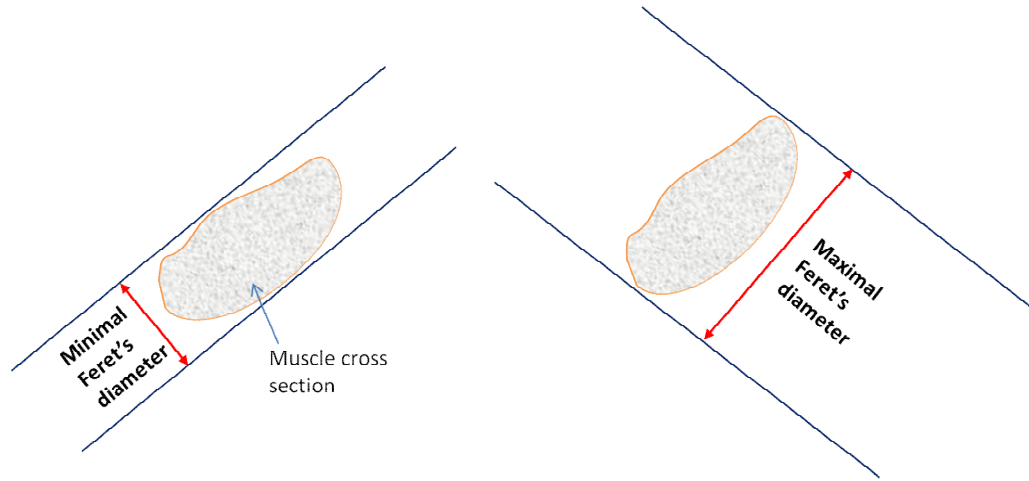
2.2.6.4 Muscle Fibre Diameter Determination

To establish whether BRL-47672 treated muscle exhibited muscle hypertrophy, muscle fibre diameter in control and treated muscle cross sections were determined using a quantitative method developed by Briguet *et al.* (2004). This method reliably measures the size of muscle fibres based on the minimal Feret's diameter of muscle fibre cross sections; this is easily done using ImageJ (Rasband, W.S., ImageJ, National Institutes of Health, Bethesda, Maryland, USA; ImageJ 1.40g, <http://rsb.info.nih.gov/ij>) with the ImageJ plug-ins MosaicJ (Thevenaz and Unser 2007) and TurboReg (Thevenaz, P., Biomedical Imaging group, Swiss Federal Institute of Technology Lausanne). ImageJ defines the maximal Feret's diameter as the longest distance between any two points along the selection boundary. This is also known as the 'maximum calliper' distance (ImageJ User Guide, IJ 1.40g; <http://rsb.info.nih.gov/ij/docs>), whereas the minimal Feret's diameter is the 'minimal calliper' distance (see figure 2.9). The minimal Feret's diameter is least affected by changes in the cutting plane in which muscles are sectioned (Briguet *et al.* 2004) and was therefore deemed suitable for comparing muscle fibre size in control and treated rat muscle.

2.2.6.4.1 Image acquisition and analyses

Soleus muscles from saline or BRL-47672-treated rats were processed for histochemical analysis as described in section 2.2.6.1. Briefly, sections were

Figure 2.9: Schematic representation of the minimal and maximal Feret's diameter.



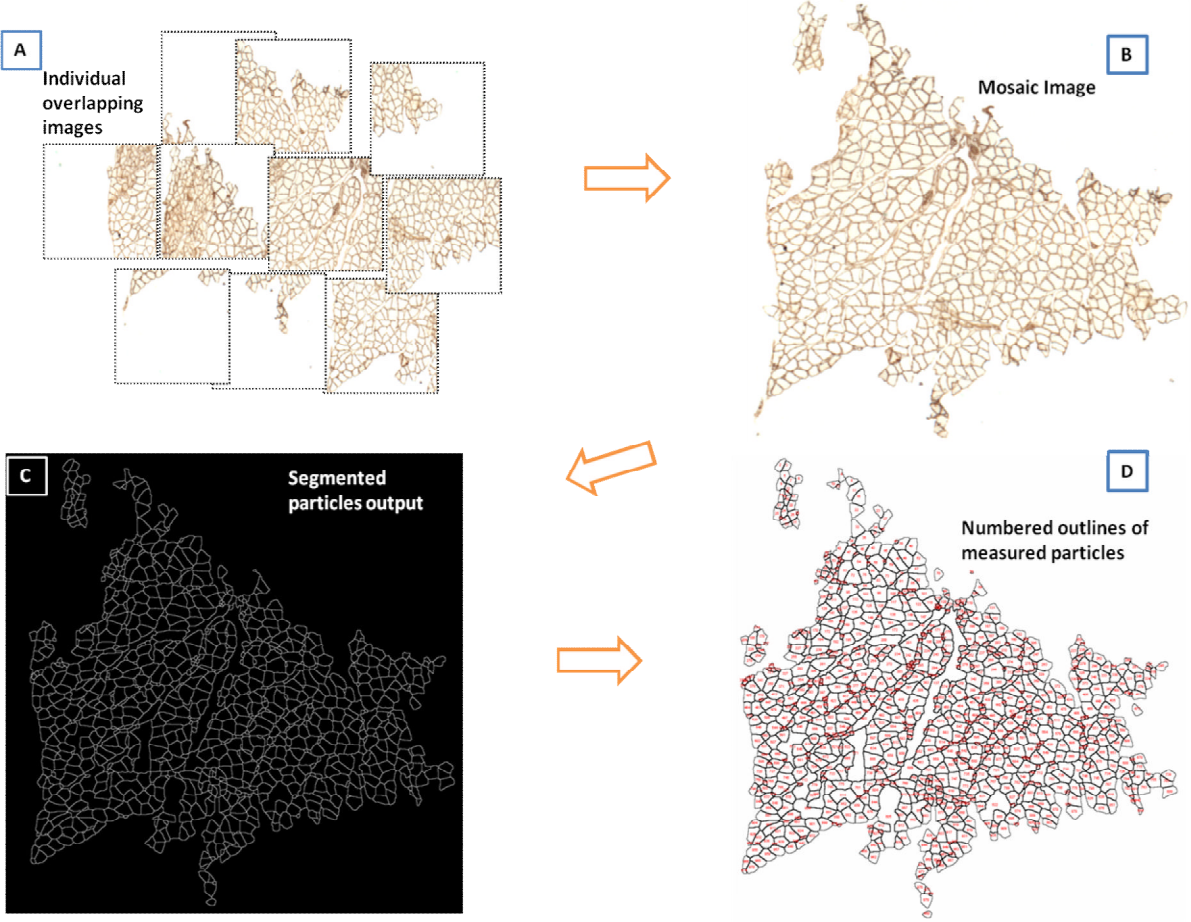
fixed in 4% PFA, blocked in 5% normal goat sera and stained with rabbit anti-laminin polyclonal antibody (diluted 1:300; Sigma) for 1 hr at room temperature. Primary antibody localisation was visualised using the ABC systems and DAB as outlined above; this localised laminin to the sarcolemma and created defined borders representing muscle fibres and enabled particle recognition for fibre diameter measurement using ImageJ software (see figure 2.10). The staining with DAB was controlled visually and allowed to develop to a strength which was sufficient for the production of definitive borders for particle recognition.

Images were acquired by light microscopy (Axioplan/Tessover, Carl Zeiss Ltd, Oberkochen, Germany) using a 1.25x objective lens and OpenLab software (Perkin Elmer). Three to four sections of each muscle sample was photographed by acquiring overlapping images which were subsequently stitched into a single cross-sectional image using MosaicJ. Additionally, an image of a light microscope stage graticule ruler (Leica) was taken as a reference for scale calibration using ImageJ. Minimal Feret's diameter analyses of stained muscle fibres were carried out by firstly selecting the area to be analysed on the mosaic image, thus excluding folded areas, large artefacts or areas where staining was too deemed too light for maxima detection.

Firstly, using the ImageJ command 'Process => Find Maxima => Output type => Segmented particles produced an 8-bit binary image output from your selected image, displaying segmented particles, each of which represents detected local maxima, the defined borders of muscle fibres. These segmented particles were analysed by setting measurements to include the Feret's

diameter (Analyze => Set Measurements => Check Feret's Diameter box) then by using the ImageJ command Analyze => Analyze Particles => Show Outlines and checking the 'Display results' box. This counted and measured particles in the selected area by scanning the image to find the edge of the particles, then outlining and measuring each particle. This generated another 8-bit image containing numbered outlines of measured particles (ie, muscle fibres – see figure 2.10) and a results table displaying the minimal Feret's diameter among other measurements for each particles. The average minimal Feret's diameter for each cross section was taken after exclusion of the minimal Feret's diameter data for small particles such as capillaries and really large particles representing two or more merged muscle fibres or large arteries and veins.

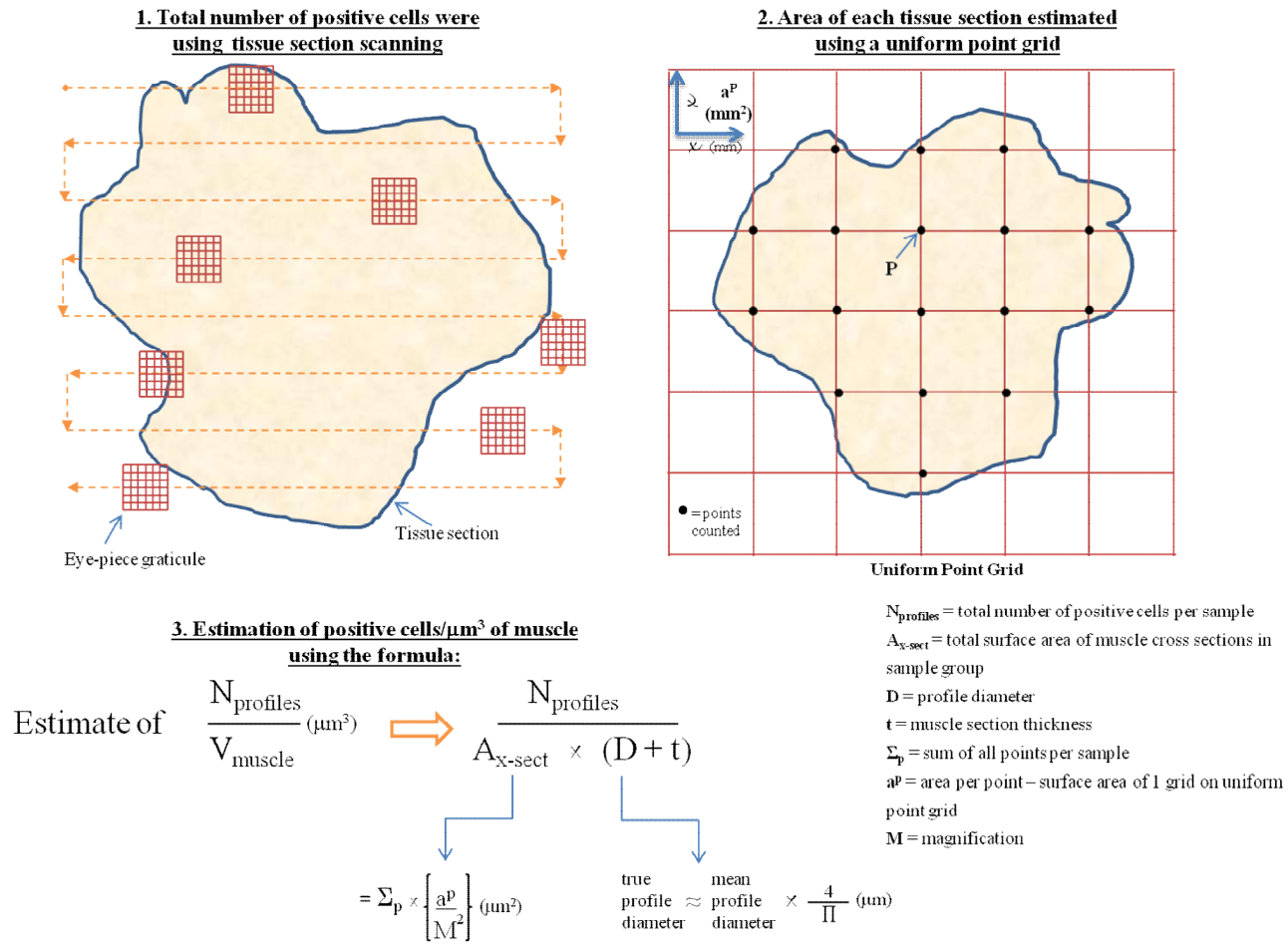
Figure 2.10: Schematic summary of Feret's diameter methodology



2.2.6.5 Stereology

Stereological methods in histology obtain quantitative information about three-dimensional (3D) features of tissues from two-dimensional physical sections. 10µm muscle cross sections were prepared from control and treated animals randomly sampled from the proximal, distal or mid-belly regions of EDL and gastrocnemius muscles as described above. The total numbers of profiles (i.e. positive cells) for each section were counted with the aid of an eye-piece graticule and section scanning (see figure 2.9). The profiles counted were Iba-1⁺, Pax7⁺, MyoD⁺ cells and Ki-67 PLA spots (see chapter 4). A minimum of 3 and a maximum of 5 sections were counted per sample, which were approximately 100µm apart (that is roughly every 10th section was taken). The surface area of each muscle section ($A_{x\text{-sect}}$) was estimated using a systematic uniform point grid of known area (a^p - e.g. 1mm² per point) randomly superimposed over a low magnification image of the section. Points (represented by the crossing of horizontal and vertical lines over the muscle section) were counted and an estimate of the surface area of each cross section is given by the formula: $A_{x\text{-sect}} (\mu\text{m}^2) = \Sigma \text{ points} \times (a^p/M^2)$ where M is the magnification used. Using a modification of the method by Mayhew *et al.*(1997), an estimate of the number of profiles (N_{prof}) per volume of muscle (V_{musc}) was calculated using the formula presented in figure 2.9. The mean diameter of each profile of interest (immuno-positive cells or Ki-67⁺ nuclei)

Figure 2.11: Summary of stereological methodology for the quantification of positive cells in muscle cross sections prepared by immunocytochemistry.



was estimated from approximately 50 positive profiles using Open Lab software and integrated into the equation below. The equation assumes the profiles are roughly spherical ($4/\pi$) and takes into account the three dimensional aspects of cells stained via immunohistochemistry (section thickness/surface area and cell or nuclear diameter) to estimate the number per volume of muscle. For a review, see Muhlfeld *et al.* (2009).

CHAPTER 3

Results (I)

Chronic administration of the clenbuterol pro-drug BRL-47672 increases skeletal muscle satellite cell activity

3.1 SUMMARY

High doses of β_2 -agonists such as clenbuterol have demonstrable anabolic actions on muscle metabolism and growth, the latter of which is thought to occur via stimulation of muscle protein synthesis and suppression of protein degradation. However, the effects on satellite cell activity *in vivo* are less documented. The use of clenbuterol to prevent or reverse muscle wasting accompanied by many disease states (e.g. cancer cachexia, AIDS, etc) has so far been limited due to deleterious cardiovascular effects. In the present study, the β_2 -agonists pro-drug, BRL-47672 was used; it replicates the anabolic actions of clenbuterol with reduced cardiovascular consequences.

Male Wistar rats were injected with BRL-47672 (900 μ g/kg; s.c., n=7) or an equal volume of saline (n=6) daily for 8 weeks. 24 hrs following final injections, rats were terminally anaesthetised (Inatin; 120mg/kg; i.p) and the soleus muscles were removed and analysed for mRNA transcript and protein expression of muscle and satellite cell specific markers, pax7, ki-67, myoD, myogenin, myostatin and follistatin.

BRL-47272 caused a slight increase in muscle fibre diameter and is indicative of muscle fibre hypertrophy. It also caused a significant increases in mRNA expression of pax7, ki-67, myoD and myostatin relative to saline control ($p < 0.05$). No significant changes were noted in the mRNA expression of myogenin and follistatin. The protein expression of pax7 and myoD were tendentially increased by pro-drug treatment ($p \sim 0.12$ and $p \sim 0.09$, respectively). Protein expression of the myostatin precursor protein was also significantly increased by BRL-47672 administration ($p < 0.05$).

Taken together these results suggest the pro-drug increases muscle growth and thus satellite cell activity (activation/proliferation; denoted by increased pax7, ki-67 and myoD expression), which is compatible with maintaining myoblasts in an actively proliferating 'state of readiness', available for subsequent incorporation by growing myofibres. However, the transient effects of chronic β -agonist administration may have resulted in skeletal muscle acclimatisation, which could include the stimulation of compensatory pathways, such as myostatin up-regulation. This could have limited myoblast differentiation (denoted by reduced/unchanged myogenin) and ensured further muscle growth was limited but not entirely ablated. Intermittent β -agonist administration coupled with myostatin suppression (for e.g., via an inhibitory transgene expression such as follistatin) may represent an effective method of preventing β -receptor desensitization in order to maintain exponential muscle growth and prevent or reverse severe muscle atrophy.

3.2 INTRODUCTION

Endogenous beta agonists such as noradrenaline, adrenaline and isoprenaline are produced by the sympathetic nervous system and adrenal medulla to stimulate β -adrenoreceptors in peripheral tissues. These activate downstream signalling pathways controlling heart rate and contractility, vasoconstriction (gut and skin), or vasodilatation in skeletal muscle (reviewed in Lynch and Ryall 2008).

Synthetic β -agonists, which are structurally similar and can elicit similar responses in peripheral tissues, were primarily used to treat asthma and other chronic obstructive diseases until it became apparent doses higher than those used therapeutically could increase muscle growth.

Consequently, the anabolic actions of β -agonists on skeletal muscle have been extensively studied as a means to prevent or reverse muscle wasting in numerous disease states such as cachexia, sepsis, sarcopenia and muscular dystrophies. The main mechanisms by which β -agonists elicit anabolic responses in skeletal muscle are traditionally believed to occur by stimulating protein synthesis, suppressing protein degradation or a combination of both (Emery *et al.* 1984; Benson *et al.* 1991). Canonical β -agonists signalling is well described; its downstream effects include the activation of protein kinase A (PKA) via heterotrimeric G-protein ($G\alpha_s$ subunit) and cyclic AMP, and the activation of phosphoinositol 3-kinase (PI3K)-protein kinase B (AKT) via the $G\beta\gamma$ subunit, all of which are regulators of both protein synthesis and degradation (for a review, see Ryall and Lynch 2008)

In addition to anabolic alterations in skeletal muscle, several studies have implicated β -agonists in the transition of muscle fibre type phenotype from a slow-oxidative to faster oxidative-glycolytic fibres (Zeman *et al.* 1988; Criswell *et al.* 1996; Rajab *et al.* 2000; Jones *et al.* 2004). Postnatal fibre type transitions are initiated to meet physiological demand (reviewed in Sieck and Regnier 2001); for instance inactivity results in a general shift in myosin heavy chain (MHC) isoform expression and metabolic properties from type I to II and endurance training promotes a shift in the opposite direction. Similar fibre type transitions have been reported in response to hormonal imbalances, electrical stimulation and in human skeletal muscle during ageing, whereby a decrease in the number and size of fast fibre types has been associated with impaired muscle function in the elderly (Termin and Pette 1992; Larsson *et al.* 1994; Dutta *et al.* 1997; Balagopal *et al.* 2001).

Whilst the mechanisms underlying changes in fibre type toward a slower phenotype have been extensively characterised (Hughes 2004; Oh *et al.* 2005; Handschin *et al.* 2007; Kim *et al.* 2008), the pathways regulating the establishment and maintenance of fast fibre type phenotypes have remained largely unknown (Grifone *et al.* 2004). One hypothesis is that they are thought to occur by the transient modulation of myoD-myogenin expression (reviewed in Talmadge 2000). Adult slow muscles contain a high myogenin:myoD ratio whereas the reverse is seen in fast muscles (low myogenin, high myoD) and β -agonist-induced fast fibre type transitions are concomitant with altered expression of myogenin and myoD (high myoD, low myogenin). However, this appears to be dependent on the activity status of the muscle; Mozdziak *et al.* (1998) showed that clenbuterol did not induce fibre type transitions in

overloaded soleus muscle. Likewise, clenbuterol fed to rats in a hindlimb immobilisation study led to an increase in myogenin but no change in myoD (Delday and Maltin 1997). These fibre type transitions are not without consequences for muscle function; although largely dose-dependent, a dramatic shift from a slow to fast MHC phenotype can alter muscle contractile properties (Ryall *et al.* 2004) and increase muscle fatigability (Dodd *et al.* 1996).

A major drawback of β -agonists which has limited their use in a clinical setting is their potentially deleterious effects on the cardiovascular system. Clenbuterol administration causes substantial haemodynamic changes in rats; it increases heart rate and vascular conductance in the hindquarters, whilst reducing mean arterial blood pressure (Rothwell *et al.* 1987; Jones *et al.* 2004). These changes increase the risk of ischemia, congestive heart failure, arrhythmias and even sudden death. Therefore, in the present study, the pro-drug of clenbuterol, BRL-47672 (Sillence *et al.* 1995) was administered. It is thought to be metabolised to a potent β_2 -agonist *in vivo*. The work of Jones *et al.* (2004) demonstrated BRL-47672 minimised the cardiovascular and haemodynamic effects compared to clenbuterol without compromising anabolic and fibre type changes.

The effects of chronic β_2 -adrenergic stimulation on satellite cell activation are less documented. There have been numerous demonstrations of the growth promoting effects of β -agonists on skeletal muscle; however, the link between satellite cell activation and myogenesis and β -agonist-induced muscle growth remains elusive. Studies on β_2 -agonist treated satellite cell cultures either found a lack of effect (Young *et al.* 1990; McMillan *et al.* 1992) or an increase in proliferation but no apparent change in differentiation or fusion (Grant *et al.*

1990). Consistent with these studies was a time and dose-dependent increase in protein and DNA content, which was attributed to satellite cell activation. *In vivo*, clenbuterol stimulated earlier activation and proliferation of satellite cells in transplant studies (Roberts and McGeachie 1992). Maltin and Delday (1992) found evidence of satellite cell activation and some division in denervated and innervated muscles of clenbuterol treated rats. Whether β_2 -agonists act directly to stimulate satellite cell activation or indirectly as a result of increased blood flow and delivery of blood-borne mitogens remain undetermined.

Two prominent markers of satellite cell activation (myoD) and differentiation (myogenin) are implicated in β_2 -agonist-induced modulation of MHC phenotype but as far as we are aware, no studies have correlated these fibre type transitions or the growth promoting effects of β_2 -agonists with a comprehensive picture of satellite cell activity. Lines of evidence suggest that the mRNA and protein expression of these two MRFs accumulate preferentially in activated satellite cells, proliferating myoblasts and newly formed myotubes, especially following trauma (Cooper *et al.* 1999). It is also possible changes in the level of myoD and myogenin expression could occur in the nuclei of mature muscle fibres or activated satellite cells but it is still unclear which has the predominant source of myoD and myogenin in normal adult muscle (Dedkov *et al.* 2003). In the present study, we examine the effects of long term BRL-47672 pro-drug treatment on the expression of well characterised satellite cell markers. Discovery of the role of satellite cells in changes in muscle mass and postnatal fibre type transitions could illuminate how skeletal muscle adaptations occur in disease states that lead to muscle dysfunction.

In addition, myostatin, a negative regulator of muscle mass, is examined to determine its role in the anabolic actions of β_2 -agonists. Lack of myostatin leads to increased skeletal muscle mass (McPherron *et al.* 1997), while conversely, systemic administration of myostatin leads to muscle wasting in rodents (Zimmers *et al.* 2002). Therefore it is tempting to speculate that the anabolic actions of β -agonist probably occur by down-regulating myostatin. Myostatin shares structural and regulatory similarities with members of the TGF- β superfamily; these include an N-terminus which functions as a secretory signal and a proteolytic processing site (RSRR) in the C-terminus. It is synthesised as high molecular weight precursor protein that migrates on SDS-PAGE at ~52-55kDa; this is higher than that predicted from myostatin's 375 amino acid sequence, and has been attributed to differential glycosylation of the uncleaved protein. This is subsequently cleaved by furin, a calcium-dependent serine protease to release the biologically active ~12.5kDa C-terminal mature protein (Lee and McPherron 2001). A ~40kDa N-terminal Latency Associated Peptide (LAP), which lacks the signal peptide and a ~26kDa protein suspected to represent a dimeric form of the mature 12.5kDa protein have also been reported. Further analyses of the molecular forms of myostatin are described in appendix I. The bioavailability of the 12.5kDa C-terminal peptide is tightly regulated through post-translational modifications and sequestration of its precursors (reviewed in Bradley *et al.* 2008; Huang *et al.* 2011). Myostatin is also reviewed in chapter 1, section 1.2.4.4.

In summary, the aims of the present study are to examine the effects of long term BRL-47672 pro-drug administration on the expression of well characterised satellite cell markers pax7, myoD and myogenin. We hypothesise

that pro-drug treatment should increase muscle growth and activate these factors since satellite cell activation could be a primary mechanism by which muscle hypertrophy occur. Secondly, we hypothesise that stimulation of these factors is synonymous with a suppression of negative markers of satellite cell activity, such as myostatin. Therefore, we aim to examine the expression of myostatin and its antagonist follistatin to determine whether stimulation of satellite cell activity in hypertrophying muscle is achieved via myostatin suppression or follistatin stimulation.

3.3 METHODS

3.3.1 Animals and tissue collection

Male Wistar rats (150-160g; Charles River, Margate, UK) were randomly assigned to one of two groups and received daily injections of β_2 -agonist pro-drug BRL-47672 (900 μ g/kg; s.c., n=7) or an equal volume of Saline (n=6) for 8 weeks. Twenty-four hours following final injections, rats were terminally anaesthetised with Inactin (120mg/kg; i.p., Sigma-Aldrich, UK) and the soleus muscles were excised, snap frozen in liquid nitrogen, and stored at -80°C for subsequent analysis.

3.3.2 Analysis of muscle fibre hypertrophy

Evidence of muscle fibre hypertrophy was assessed using the minimal Feret's diameter method as described in chapter 2, section 2.2.6.4. This quantitative analysis outlines individual muscle fibres via histological staining using laminin antibody.

3.3.3 mRNA Measurements (Real Time PCR)

Total RNA was extracted from approximately 20mg of frozen wet muscle using TRIzol[®] (Invitrogen, Paisley, UK) according to the manufacturer's protocol. The quality and quantity of RNA was assessed spectrophotometrically by measuring the absorbance at 260nm and 280nm. First strand cDNA synthesis was carried out using 1 μ g of total RNA as described in chapter 2 section 2.2.3. Taqman

Table 3.1: Catalogue and Unigene Numbers for Taqman Primer/Probes sets

Gene	Catalogue Number	Unigene Number
HMBS	Rn00565886_m1	Rn.11080
Pax7	Rn00834076_m1	Rn.226327
MKi-67	Rn01451446_m1	Rn.73551
MyoD1	Rn00598571_m1	Rn.9493
Myogenin	Rn00567418_m1	Rn.9465
Myostatin	Rn00569683_m1	Rn.44460
Follistatin	Rn00561225_m1	Rn.162557

primer/probe sets (Table 3.1) were obtained from Applied Biosystems (ABI, Foster City, CA, USA) and real-time PCR was performed using Taqman gene expression master mix (Applied Biosystems) in a MicroAmp 96-well reaction plate (Geneflow, Fradley, UK). Reactions were carried out in an ABI Prism 7000 sequence detection system in duplicate; each well contained 2µl cDNA template, 12.5µl PCR master mix and 1.25µl primer/probe mix in a 25µl reaction volume.

Relative quantification of gene expression between control and treated groups was calculated using the $2^{-\Delta\Delta C_t}$ method. Briefly, duplicate cycle threshold (C_t) values for each control or treated sample were averaged and the ΔC_t calculated by subtraction of the corresponding mean C_t of an endogenous control (HMBS). $\Delta\Delta C_t$ was calculated by subtracting the ΔC_t of prodrug treated samples from the mean ΔC_t of corresponding time-matched saline controls and the relative amount of target mRNA was determined by $2^{-\Delta\Delta C_t}$. The saline control groups were given a value of 1 and fold changes in mRNA expression of LPS treated groups were calculated relative to their corresponding control group. Thus values >1 or <1 indicate an increase or decrease in mRNA expression from control, respectively.

3.3.4 Protein measurements (Western blotting)

Protein extractions and western blotting was carried out as described in chapter 2, section 2.2.5, to determine the protein expression of the targets listed in table 3.2. Briefly, cytosolic and nuclear proteins were extracted using a modification of the method by Blough *et al.* (1999), for the extraction of proteins from striated muscle. Approximately 30mg of frozen muscle was homogenised in

Table 3.2: Primary and secondary antibodies used in the Western blotting protocol.

Primary Antibodies	Supplier	Dilution
Mouse Anti-Pax7 mAb	DSHB Iowa City, IA, USA	1:500
Rabbit Anti-MyoD (C-20) pAb	Santa Cruz Biotechnology Santa Cruz, CA, USA	1:500
Mouse Anti-Myogenin mAb	DSHB Iowa City, IA, USA	1:500
Rabbit Anti-Myostatin, Near C-terminus pAb	Millipore Billerica, MA, USA	1:250
Mouse Anti-β-Actin, mAb	Sigma Aldrich Poole, UK	1:25000
Secondary Antibodies		
Swine Anti-Rabbit Immunoglobulins/HRP	Dako Glostrup, Denmark	1:2000
Rabbit Anti-Mouse Immunoglobulins/HRP	Dako Glostrup, Denmark	1:2000

,

0.6ml homogenisation buffer (50mM Tris-HCl, 1mM EDTA, 1mM EGTA, 1% (v/v) NP-40, 0.1% (v/v) 2-mercaptoethanol, pH7.5). Mammalian protease inhibitor cocktail was added homogenisation buffer (0.01% (v/v); Sigma-Aldrich, Poole, UK) before use. Muscle lysates were centrifuged (13,000g, 10 min at 4°C) and the supernatant was used as crude cytosolic protein fraction. The remaining pellets were resuspended in 500µl of an ice-cold buffer (20mM HEPES, 25% (v/v) glycerol, 500mM NaCl, 1.5mM MgCl₂, 0.2mM EDTA pH7.9) supplemented with protease inhibitor cocktail (0.01% (v/v)) and incubated on ice for 30 minutes with intermittent mixing. Samples were spun down (3,000g, 5min at 4°C) and the supernatant collected as nuclear protein fraction. Extracted proteins were quantified using the Lowry assay (Lowry *et al.* 1951) and diluted to required concentration before the addition of a Laemmli type SDS buffer (gel application buffer (GAB); 0.15M Tris, 8M urea, 2.5% (w/v) SDS, 20% (v/v) glycerol, 10% (w/v) 2-mercaptoethanol, 3% (w/v) DTT, 0.1% w/v bromophenol blue, pH6.8) at a ratio of 2.5:1. For example, 20µl of diluted protein sample to 8µl of GAB. Samples were heated at 95°C for 5mins prior to loading.

Unless otherwise stated, 50µg of total protein from samples were loaded onto 5-20% SDS-PAGE gel and separated by molecular weight then transferred overnight onto nitrocellulose membranes (GE Healthcare, Little Chalfont, UK). Equal loading of samples was confirmed by Ponceau S staining of membranes. Membranes were blocked for 1hr with 5% (w/v) non-fat milk in Tris-buffered-saline-tween (TBS-T; 10mM Tris, 150mM NaCl, 0.05% (v/v) tween-20, pH 7) at room temperature followed by an overnight incubation at 4°C in primary antibody and for 1hr in the appropriate HRP-conjugated secondary antibody at

room temperature (Table 3.2). Protein bands were visualised by enhanced chemiluminescence plus (Perkin Elmer, MA, USA) and quantified by densitometry using GeneTools software (Syngene, Cambridge, UK) after background subtraction and normalising to actin or lamin control.

3.3.5 Statistical Analyses

The raw data from each experiment was tested for normality using GraphPad Prism v6. Data were tested for the tendency to assume a Gaussian distribution using the Kolmogorov-Smirnov and the D'Agostino-Pearson omnibus tests and were found to be consistent with a Gaussian distribution. All data are represented as the mean \pm standard error of the mean (S.E.M) and comparisons between the control and treated groups were performed using unpaired t-tests and statistical significance was accepted at $p < 0.05$.

3.4 RESULTS

3.4.1 Analysis of muscle fibre diameter

Although several lines of evidence suggest muscle does undergo muscle fiber hypertrophy in response to clenbuterol and similar agonists (reviewed in section 3.2), we firstly wanted to determine whether the tissues analysed exhibited signs of muscle hypertrophy. This was done using the Feret's diameter method; a quantitative method developed by Briguet *et al.* (2004) for measuring the size of muscle fibres using the minimal Feret's diameter of a muscle fibre cross section (described in detail in chapter 2, section 2.2.6.4). Based on this analysis, there was a slight but statistically significant increase in the muscle fibre diameter of treated samples, which suggests BRL-47672 elicited muscle growth (see figure 3.1)

3.4.2 mRNA and protein expression of muscle specific markers

Currently, it is unclear how satellite cells are implicated in β -agonist mediated changes in muscle growth and fibre type composition. The effects of 8 weeks pro-drug treatment on the mRNA and protein expression of early, late and negative satellite cell markers were measured by real-time PCR (figures 3.2 and 3.3).

Pro-drug treatment elicited significant increases in the mRNA expression of early markers pax7 and ki-67 relative to saline control ($p < 0.05$). MyoD mRNA expression was also significantly increased relative to control ($p < 0.05$) and the

protein expression of both pax7 and myoD showed a similar tendency (p~0.12 and p~0.09, respectively).

There was no significant change in the mRNA and protein expression of the late marker of myogenin. Interestingly, there was a significant ~5.5 fold increase in myostatin mRNA expression relative to saline control. There was no change in follistatin mRNA expression, which lends credibility to the increased expression of myostatin observed since the two are thought to act antagonistically against each other (Lee and McPherron 2001; Gilson *et al.* 2009).

Figure 3.1: Muscle fibre diameter of rat soleus muscle following 8 weeks of Saline or β 2-agonist BRL-47672 administration. Values are means \pm S.E.M, $n=3-4$. Significantly different from corresponding saline control via Student's unpaired *t*-test: ** $p<0.005$

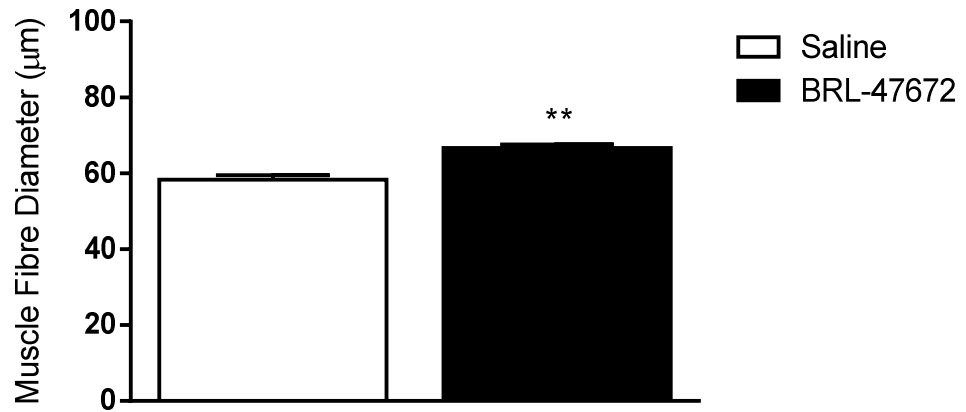


Figure 3.2: mRNA expression of transcripts involved in satellite cell function and muscle growth in rat soleus muscle following 8 weeks of Saline or β 2-agonist BRL-47672 administration. Relative mRNA expression of saline controls was set at 1. Values are means \pm S.E.M, $n=6-7$. Significantly different from corresponding saline control via Student's unpaired t -test: * $p<0.05$.

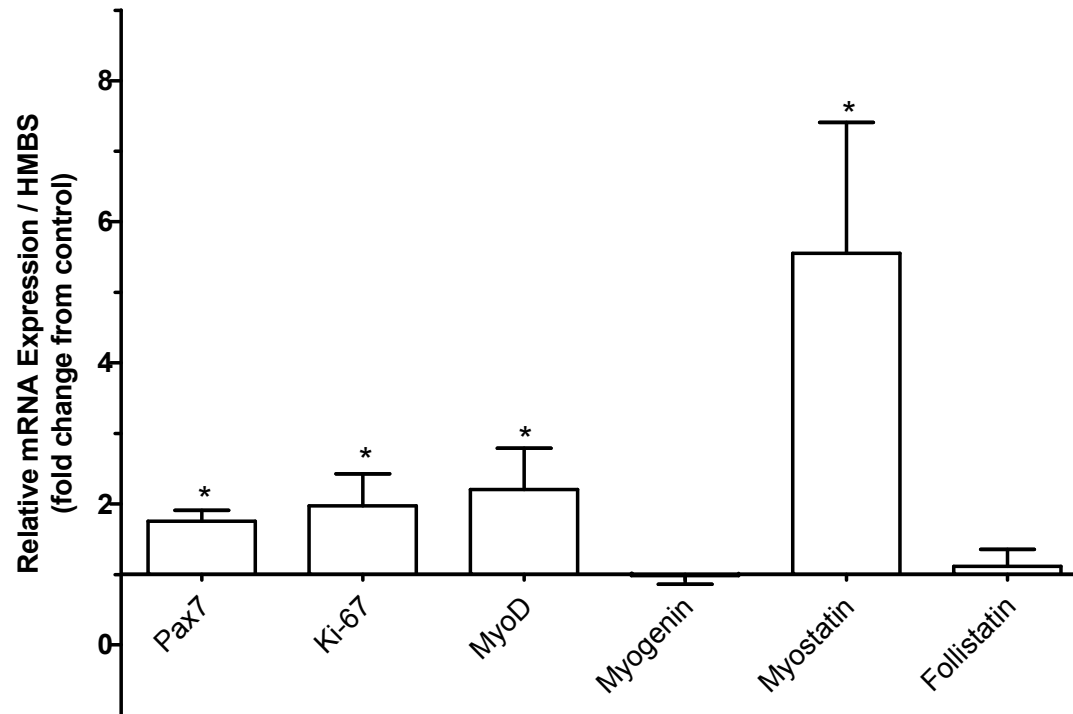
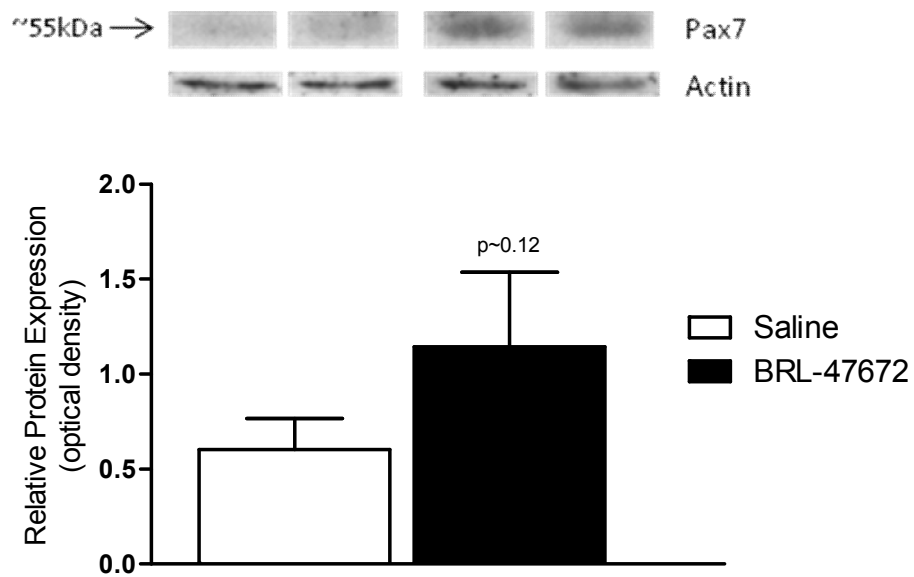
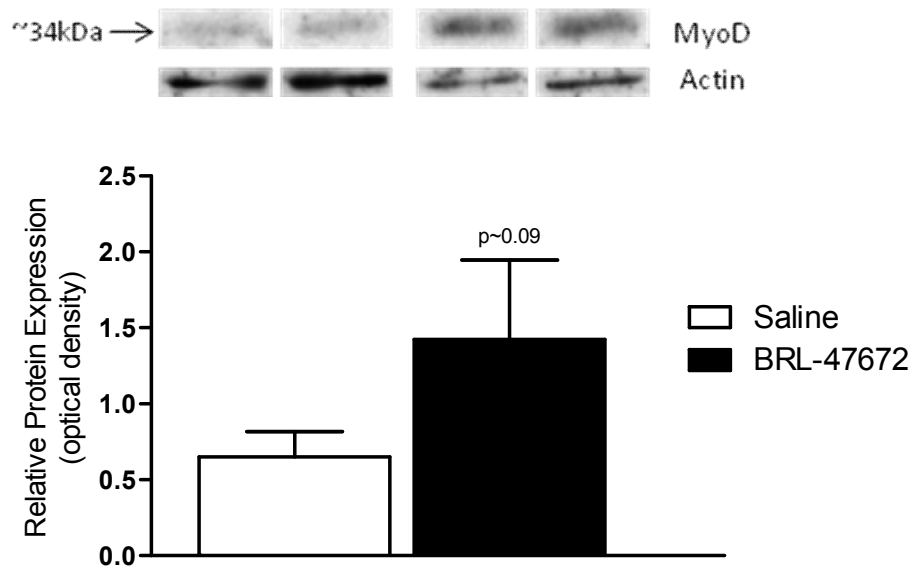


Figure 3.3: Protein expression of satellite cell specific markers in rat soleus muscle following 8 weeks of saline or β_2 -agonist BRL-47672 administration. Values are means \pm S.E.M. The densities of immunoreactive bands were measured by western blotting and representative bands for each treatment group are shown above their corresponding bar in duplicate. $n=6-7$ per group. Significantly different from Saline group: * $p<0.05$ using a Student's unpaired *t*-test.

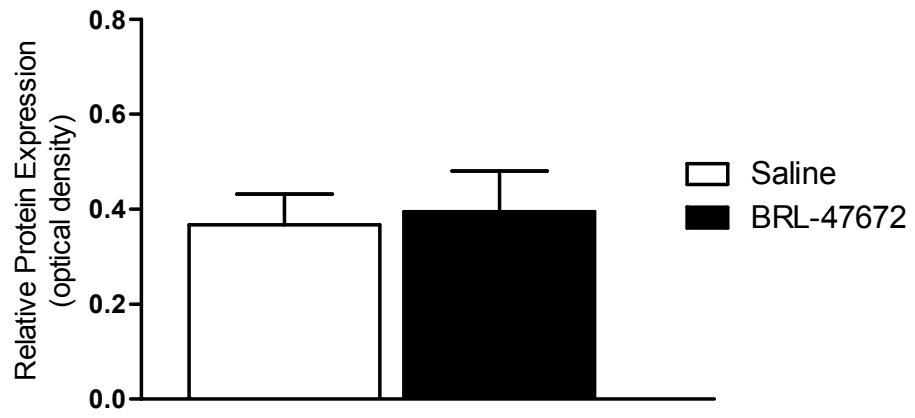
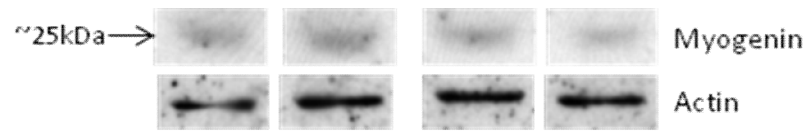
a) *Pax7* protein expression



b) *MyoD* protein expression



c) *Myogenin protein expression*



3.4.2 Myostatin Protein Expression

The protein expression of myostatin followed a similar trend with its total mRNA expression. There was a statistically significant increase ($p < 0.05$) in pro-myostatin protein expression but no change was detected in the protein expression of the latency form of the peptide relative to saline controls (figure 3.4). The former was detected as a ~55kDa migrating immuno-reactive band in cytosolic fractions by western blotting, representing the unprocessed form of the protein. This increase in total myostatin mRNA and pro-myostatin protein expression suggests myostatin synthesis was enhanced in response to pro-drug administration but its further processing was limited as the latency form was unchanged relative to control.

When probed for myostatin protein, nuclear fractions of control and treated samples showed no obvious myostatin bands although the same blots were positive for the endogenous control lamin A/C bands (figure 3.5). Figure 3 in appendix I show that myostatin protein could be detected in nuclear fractions if the concentration of protein loaded is very high. In 200 μ g of total protein load, the active dimeric myostatin was detected in the nuclear extracts from four different muscle types. We deduced that since myostatin is a rare protein, it is probably below the limit of detection in the nuclear protein fractions.

Thus we sought to determine the minimum concentration of active myostatin protein that can be detected by western blotting (figure 3.6). Decreasing concentrations of the recombinant myostatin peptide were loaded and blotted for myostatin. Muscle homogenate from EDL and gastrocnemius muscles were

Figure 3.4: Myostatin protein expression in Rat Soleus muscle following 8 weeks of Saline or β_2 -agonist BRL-47672 administration. Values are means \pm S.E.M. The densities of immunoreactive bands were measured by western blotting and representative bands for each treatment group are shown above their corresponding bar in duplicate. n=7-8 per group. Significantly different from Saline group: *p<0.05 using a Student's unpaired *t*-test.

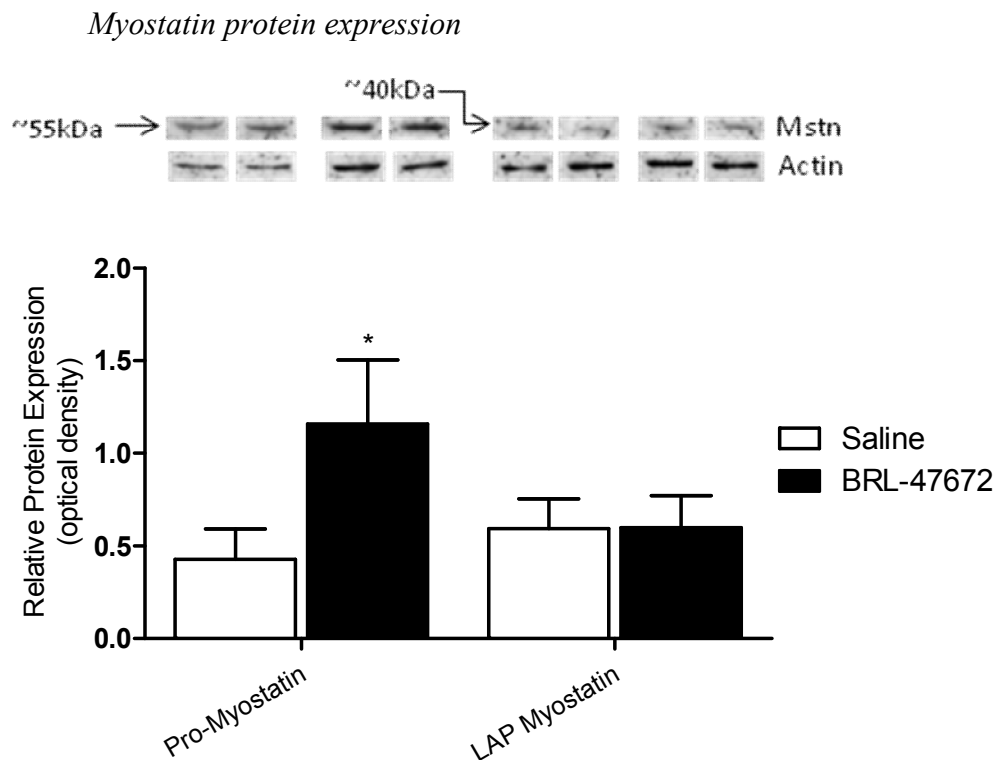


Figure 3.5: Myostatin protein was below threshold of detection in nuclear protein samples of Control and treated Rat Soleus muscles by western blotting. (**A**) Representative immunoblot showing bands for endogenous Lamin A/C. (**B**) The same blot was negative for myostatin protein bands when blotted below 70kDa marker. 50 μ g of protein sample was loaded per lane. Blots were developed with ECL for 2 minutes and **A** was exposed to photographic film for 5 and **B** for 10 minutes, which is usually sufficient to pick up any rare species of myostatin.

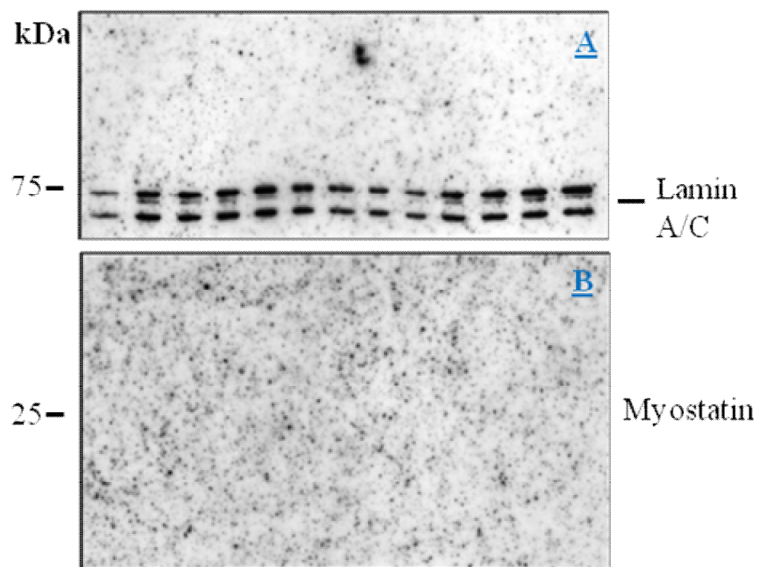
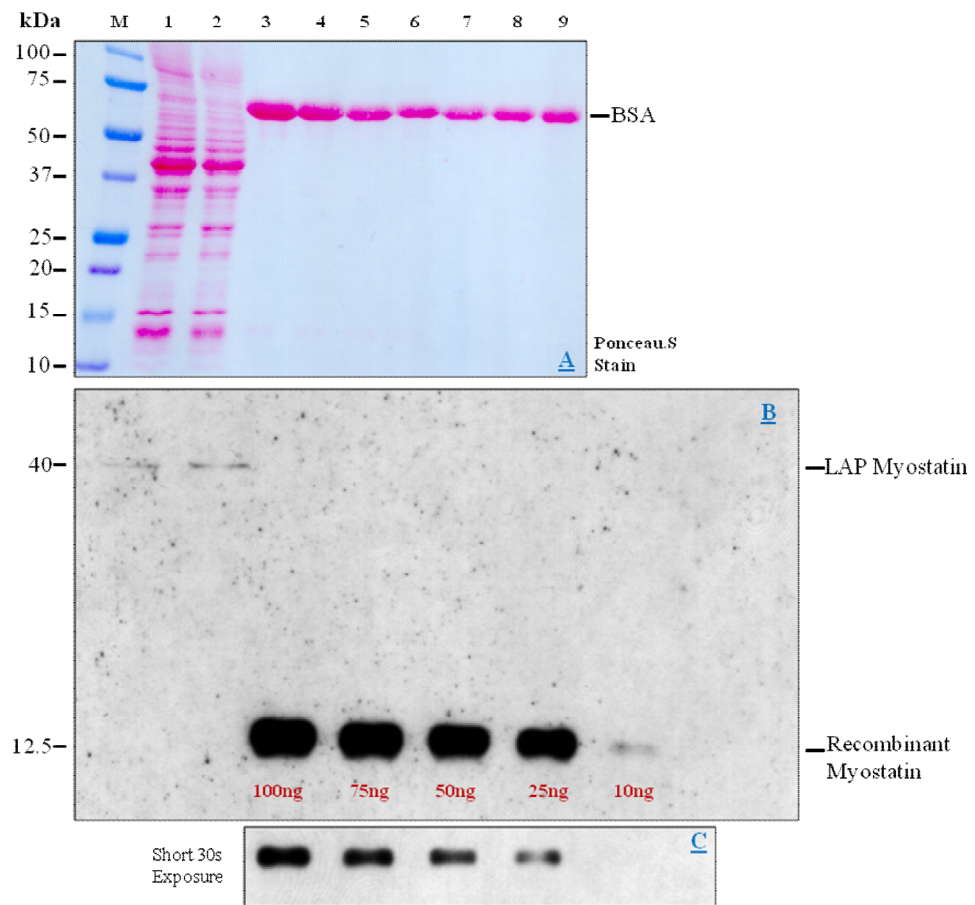


Figure 3.6: The minimum concentration of recombinant myostatin protein detectable by western blotting. (A) Ponceau stain to confirm protein transfer. (B) Immunoblot of myostatin protein bands in untreated adult skeletal muscle extract and recombinant myostatin peptide mix. Blot was exposed to hyperfilm for 5 minutes to enable detection of rare species of myostatin. (C) Short 30 seconds exposure of B. Loading order: 1-EDL cytosolic fraction, 2- Gastrocnemius cytosolic fraction, 3- 100ng/ μ l, 4- 75ng/ μ l, 5- 50ng/ μ l, 6 - 25ng/ μ l, 7 -10ng/ μ l, 8 -5ng/ μ l, 9 -1ng/ μ l.



also loaded as positive controls. The minimum concentration of peptide detected was 10ng/μl; bands containing a lower concentration were not detected after long exposure (>30 minutes)

The work by Gonzalez-Cadavid (1998) showed that 7ng/μl of a myostatin peptide, which was composed of c-terminal fragments (the epitope used to raise the antibody) was sufficient to block antibody activity. Therefore it is tempting to speculate this is similar to the minimum amount of the mature myostatin peptide that may be required for detection via western blotting in our samples. Our results show the minimum concentration detectable is 10ng/μl, thus we can surmise the nuclear fractions contained very little myostatin (<7ng) and so below threshold of detection. When put within the context of muscle mass, the 50μg of total nuclear protein loaded represented 0.38mg of the 30mg (roughly 1.3%) wet muscle initially homogenised. This was calculated from the volume of homogenate loaded per lane (6.4μl on average) and the volume of total homogenate extracted (500μl); thus $(6.4/500\mu\text{l}) \times 30\text{mg} = 0.38\text{mg}$. The total volume of diluted protein sample loaded per lane was 20μl, therefore the final concentration of protein per sample was $50\mu\text{g}/20\mu\text{l} = 2.5\mu\text{g}/\mu\text{l}$ on average. Given the minimum concentration of myostatin detectable was 10ng/μl and the final concentration of nuclear protein loaded being $\sim 2.5\mu\text{g}/\mu\text{l}$, this represents a factor of 250.

Therefore, we could speculate that the final concentration of the loaded nuclear protein fraction would need to be 250 times higher in order to detect myostatin, which would have to be at a concentration of 10ng/μl or greater. The equivalent protein concentration per sample would have to be $\sim 625\mu\text{g}/\mu\text{l}$ ($2.5 \times$

250), 12500 μ g total nuclear protein, or roughly 95mg (0.38 x 250) of muscle will be required. These assumptions do not take into account antibody sensitivity and western blotting variability or the pool of endogenous myostatin (i.e. cytosolic or secreted myostatin), which is likely variable. It is representative of enriched nuclear myostatin..

3.5 DISCUSSION

Daily *i.p.* injections of BRL-47672 for 8 weeks significantly increased ($p < 0.05$) the mRNA (and tendentially, protein) expression of the satellite cell specific marker pax7. Pax7 is a well established marker for tracing cells of the myogenic lineage; it is expressed exclusively in satellite cells (Seale *et al.* 2000) and studies on ageing in mice have shown that loss of Pax7 expression leads to a loss of the stem cell phenotype, allowing satellite cells to differentiate into fibroblasts thus contributing to increased fibrosis during ageing (Brack *et al.* 2007). Hence, pax7 is a good measure of the muscle satellite cell population. The increase in pax7 expression in response to chronic β -agonist treatment is an indication for an increase in satellite cell number. This is the first such report to link β -agonist mediated muscle hypertrophy with increased pax7 expression in adult muscle.

These observations are directly correlated with the increased mRNA expression of ki-67, a well known marker of proliferation. Although not exclusively expressed in satellite cells, it is increasingly used as a marker for assessing the proliferative potential of satellite cells (Mackey *et al.* 2009). Ki-67 was chosen because it has a distinct proliferative role; for example, it is not involved in DNA repair unlike other markers of proliferation such as PCNA (proliferating cell nuclear antigen). Ki-67 is also present in cell nuclei through G₁-S and G₂ phases of the cell cycle, thus offering a larger window/opportunity for detection. It is likely this increase in ki-67 mRNA expression is due to satellite cell proliferation. β_2 sympathomimetics such as clenbuterol increase muscle blood flow by relaxing the smooth muscle of blood vessels, thus

increasing the availability of blood-borne mitogens and cytokines that activate satellite cells (Roberts and McGeachie 1992). Our study highlights the possibility that the increased protein and DNA content observed in animals administered β -agonist is due to increased satellite cell activation and proliferation. Whether initial recruitment of satellite cells is required for muscle hypertrophy or satellite cells are recruited as myofibres enlarge remains to be determined. Rats fed clenbuterol showed increased muscle mass prior to any significant increase in DNA content (Reeds *et al.* 1988). However, Jones *et al.* (2004) saw an increase in myoD protein expression 1 day after *i.p.* injection of BRL-47672. It appears the dose and method of administration may play an important part in the degree of satellite cell activity elicited.

Additional evidence for increased satellite cell activation and proliferation is demonstrated by a significant ($p < 0.05$) in myoD mRNA and a similar tendency in protein expression. Satellite cell myogenic potential relies on the sequential expression or repression of pax7 and MRF genes (myoD, myf5, myogenin, MRF4). Increased expression of pax7 and myoD is associated with actively proliferating satellite cells with a potential for differentiation (Halevy *et al.* 2004; Zammit *et al.* 2004). It is likely the pro-drug increases the differentiation potential of activated satellite cells to improve availability for recruitment into growing myofibres. An increase in pax7 and myoD could also be indicative of an increase in the satellite cell population due to β -agonist-induced proliferation of satellite cells (denoted by increased ki-67 expression).

Interestingly, the mRNA and protein expression of myogenin in treated samples showed no change relative to control. It is possible that although BRL-47672 stimulated satellite cell activation and proliferation, it may have no

effect on terminal differentiation of myoblasts. This stage of myogenesis is thought to be regulated through independent mechanisms in adult muscle. Myogenin is not involved in satellite cell development or maintenance but its induction is necessary and sufficient for the formation of myotubes or fusion to fibres (Knapp *et al.* 2006). MyoD and Myogenin are thought to be regulated through independent mechanisms in adult muscle (Delday and Maltin 1997). The study by Delday and Maltin (1997) reported that myoD was decreased whilst myogenin was increased in immobilised clenbuterol fed rats, so the up-regulation of either may be dependent on atrophy elicited or lack thereof. It is interesting to note that myogenin is a known activator of ubiquitin ligases during muscle atrophy (Moresi *et al.* 2010), thus unaltered levels of myogenin expression observed are perhaps a function of the reduced protein degradation pathways, frequently observed in β -agonist treated animals.

MyoD and myogenin are expressed at high levels during development but expression is reduced in adult muscle. They are believed to be involved in establishing and maintaining adult muscle phenotype, as myoD is expressed at higher levels than myogenin in fast muscle (Hughes *et al.* 1993b; Voytik *et al.* 1993). Myogenin is associated with the expression of the slow type I myosin heavy chain isoform and the fast type IIA heavy chain isoform. The fast type IIA heavy chain isoform has the slowest contraction speed compared to type IIB and IIX heavy chain isoforms, with which myoD expression is associated (Hughes *et al.* 1997). These results support a previously published report by our group, that high myoD and low myogenin expression in chronically treated rats are associated with changes in MHC composition from a slow type I phenotype to a fast type II phenotype (Jones *et al.* 2004).

However, some investigators have suggested myoD and myogenin may not simply have a casual relationship to fibre type in mature muscle, but rather that the relative ratios of all MRFs regulate myosin heavy chain isoform distribution than are changes in a single MRF (Jacobs-Ei *et al.* 1995; Hu *et al.* 1997). It is unlikely that the up-regulation myoD protein expression after a single injection of BRL-47672 reported by Jones *et al.*(2004) is merely a pre-requisite for fibre-type “switching”, but rather a result of increased satellite cell activation and myogenesis, for their subsequent recruitment onto muscle fibres to decrease the nuclear domain size. Furthermore, if myoD is the primary positive regulator of the fast MHC isoform expression, myoD knockout should result in reduced numbers of fast fibres. However, the EDL muscle of myoD knockout mice contained normal levels of fast (type IIb) fibres. Conversely, the soleus contained reduced proportions of slow type I fibres, elevated numbers of fast type IIx fibres and no type IIb fibres (Hughes *et al.* 1993a). Indeed, mice over-expressing myogenin show no alterations in MHC-based fibre types compared to wild type in the EDL, TA and soleus muscles (Hughes *et al.* 1999). It is possible BRL-47672 elicits growth promoting effects via satellite cell activation and maintaining increased myoD protein levels in a “state of readiness” essential for the subsequent recruitment of myoblasts into fibres to decrease the nuclear domain and thus increase myofibre synthetic capacity to allow fibre hypertrophy.

The increase in myostatin total mRNA and pro-myostatin protein in treated animals is indicative of increased myostatin synthesis that is not compatible with increased precursor processing. Given its key role in muscle homeostasis, it is not surprising that the availability of bioactive myostatin is tightly

regulated (e.g. through cleaving of precursor and sequestration in LAP) and that the mature c-terminal peptide is not always detectable in adult muscle (see figure 3.3 above). Additionally, there were no alterations in the LAP myostatin. This labile form of the protein usually plays an inhibitory role in the negative auto-regulatory feedback mechanism of pro-myostatin. However, the work of McMahon *et al.* (2003) postulates that LAP myostatin probably represents a stable pool of myostatin; it was unaffected by mass physiological changes in rat hindlimb suspension studies. Since the low molecular weight forms of mature myostatin were not detected after long exposure, we hypothesise that myostatin protein was synthesised in response to its increased mRNA transcript but further processing was low. These results are consistent with myostatin being a negative regulator of muscle mass despite muscle hypertrophy.

Increased myostatin is not always associated with muscle atrophy (Carlson *et al.* 1999). Whilst several reports show increased myostatin in skeletal muscle during atrophy (Gonzalez-Cadavid *et al.* 1998; Sakuma *et al.* 2000), studies showing a lack of association between myostatin expression and atrophy have also been found. For example, Wehling *et al.* (2000) showed that myostatin levels in rat hindlimb muscles were elevated during atrophy from hindlimb unloading, but myostatin still remained elevated when muscles were subsequently loaded with daily exercise.

Interestingly, increased myostatin expression has been linked to activation of satellite cells in controlling excessive myogenesis and muscle growth.

Myostatin has a negative effect on satellite cell differentiation in culture (Langley *et al.* 2002). *In vivo*, the increased myogenesis observed in the absence of myostatin (McMahon *et al.* 2003) is an additional demonstration of

myostatin's ability to suppress terminal myogenic differentiation. This suggests that under normal physiological conditions, myostatin up-regulation is a negative feedback mechanism to inhibit satellite cell differentiation and further limit muscle fibre hypertrophy and hyperplasia. This is further evidenced in another myostatin knockout mouse model, in which skeletal muscle hypertrophy and hyperplasia is prevented if satellite cell myogenesis is blocked by gamma irradiation (Rosenblatt and Parry 1992). This suggests that with the absence of myostatin, muscle still doesn't grow if satellite cells are prevented from functioning.

Furthermore, the anabolic effects of β -agonists are transient; it is believed growth characteristics disappear with prolonged treatment (McElligott *et al.* 1989; Maltin and Delday 1992; Kissel *et al.* 2001) due to adreno-receptor desensitization (by internalisation) (Kim *et al.* 1992) or lack of downstream effectors (reviewed in Lohse 1993). Indeed, Rothwell *et al.* (1987), found a 50% reduction in β -receptor density when rats were chronically treated with clenbuterol for 18 days. The same phenomenon is seen with satellite cell myogenesis *in vitro*; when C2C12 cells are treated with the β -agonist ractopamine, a clear increase in proliferation is observed, with no discernable change in rate of differentiation (Shappell *et al.* 2000)). There is also an increase in cell number, protein and DNA content of myoblasts but not myotubes after 48hr and no increase in cell number, protein or DNA content at later passage (Grant *et al.* 1990), suggesting older satellite cells are less functional or responsive to the growth promoting effects of β -agonists. A reduction in drug effect is also seen *in vivo*; a study by Reeds *et al.* (1986) showed that the growth promoting effects of clenbuterol were evident after 4

days of administration but these effects became less with time and were blunted by day 21.

The BRL-47672 pro-drug also displays evidence of a transient effect. In the study by Jones *et al.* (2004) the highest magnitude of change for myoD protein was 1 day after treatment but then did not change significantly between 4-8 weeks. This reduction in drug effect could represent an eventual limitation of skeletal muscle growth imposed by reduced synthetic capacity due to reduced satellite cell recruitment. This could explain the increased synthesis of myostatin when the pro-drug is administered chronically. The half life of agonist probably plays a significant role in the temporal effects of β -agonist administration; although the half-life of BRL-47672 is unknown, we can infer this to be similar to analogous compounds such as salbutamol and clenbuterol, which have half lives of approximately 3-4 hours and 12 hours respectively.

It is uncertain if myostatin up-regulation due to chronic β -agonist treatment has a role in maintaining the fibre type transition. Welle *et al.* (2009) found myostatin knockout did not down-regulate genes encoding slow myosin isoforms, whereas myostatin knockout resulted in a switch from slow to fast myosin fibre types, in studies done by Steelman *et al.* (2006) and Girgenrath *et al.* (2005). Previous research has also shown that myostatin is preferentially expressed in fast-twitch muscles in mice (Carlson *et al.* 1999), therefore it is tempting to speculate increased myostatin expression is a result of an increased percentage of fast type II fibres in treated animals, previously reported by our group in Jone *et al.* (2004).

We can surmise from our study that the transient effect of β -agonist treatment elicits satellite cell activity, which is controlled by myostatin up-regulation. This influences satellite cell differentiation (low myogenin expression) but not activation/proliferation (increased pax7/ki-67/myoD) such that further muscle growth is checked but not entirely ablated. Chronic administration of β_2 -agonists eventually leads to acclimatisation of skeletal muscle and stimulation of compensatory pathways, in which myostatin may be involved. Intermittent administration of the pro-drug may represent a more effective means of preventing β_2 -receptor desensitisation, similarly to intraperitoneal injection of β -agonists, which is more effective for muscle hypertrophy than its administration via drinking water (Moore *et al.* 1994). A combination of intermittent β_2 -agonist stimulation and myostatin suppression (for example, myostatin suppression by transgenic overexpression of its inhibitory pro-domain (Kim *et al.* 2011)) may present a more effective means of preventing or reversing muscle atrophy.

CHAPTER 4

Results (II)

**Continuous lipopolysaccharide infusion
transiently suppresses components of the satellite
cell myogenic program.**

4.1 SUMMARY

Sepsis is a complex and potentially fatal condition arising from an exacerbated inflammatory response to an infection. The rapid and debilitating loss of skeletal muscle mass is a major cause of mortality in critically ill patients. Loss of skeletal muscle mass is thought to be the result of increased suppression of myofibrillar protein synthesis and stimulation of muscle protein degradation. The effects of sepsis on the pathways regulating muscle mass, especially the influence on satellite cells, are poorly understood. The present study utilises a rodent model of sepsis to examine the effects of lipopolysaccharide (LPS)-induced endotoxaemia, to examine the mRNA and protein expression of select components of the inflammatory response and the satellite cell myogenesis.

Male Sprague-Dawley rats were continuously infused with saline (0.4ml/hr, i.v.) or LPS (15 µg/kg/hr, i.v.) for either 2hr (n=4), 6hr (n=4) or 24hr (n=6). After the specified times, animals were terminal anaesthetised (Inactin; 80 mg/kg, i.v.) and the extensor digitorum longus (EDL) and gastrocnemius muscles were removed, snap-frozen and stored in liquid nitrogen for subsequent analyses.

LPS infusion caused significant, early (<2hr) elevations in the expression of inflammatory cytokines TNF- α , IL-6 and NF- κ B relative to control, which were subsequently, slightly attenuated after 24hr. The increase in local muscle cytokine expression was attributed to increased muscle macrophage infiltration and activation. Additionally, TNF- α protein was localised to the macrophages in treated muscles. The differential increase in cytokines paralleled the suppression of the satellite cell specific markers pax7 and myoD, which were

concomitant with a reduction in pax7⁺ and myoD⁺ satellite cells in the gastrocnemius muscle. Pax7 mRNA, protein and pax7⁺ satellite cells showed a tendency to a return to basal levels of expression/numbers, whilst myoD mRNA, protein and myoD⁺ satellite cells remained reduced relative to control, after 24 hr of LPS. LPS also caused an early (<2hr) increase in myostatin mRNA and protein, which was subsequently reduced relative to control after 24hr in both muscles.

These results indicate that LPS increases the levels of inflammatory cytokines in skeletal muscle, in a temporally-dependent manner that is concomitant with a time-dependent, cytokine concentration-dependent effect on satellite cell activity. Early elevations in cytokine expression produced a greater magnitude of pax7 and myoD suppression. Such alteration of satellite cell activity may contribute to the progression of muscle atrophy, due to the suppression of muscle compensatory mechanisms, which include satellite cell activation, differentiation and fusion for nuclear supplementation. This LPS-induced reduction in satellite cell readiness could have consequences for muscle regeneration following atrophy. LPS-induced impairment of satellite cell function could lead to less effective muscle homeostasis, which could have consequences for muscle regeneration following atrophy.

4.2 INTRODUCTION

Sepsis is a severely debilitating condition, the clinical manifestations of which include marked muscle loss, hypotension and multiple organ failure resulting in high levels of morbidity and mortality (reviewed in Bone *et al.* 1992). It arises from an excessive systemic inflammatory response to an infection, initiated through an inflammatory cascade via the innate immune response. Infection can be caused by a range of circulating microbial antigens such as fungi, parasites viruses and Gram-negative bacteria (e.g. *Escherichia coli*), which accounts for 35% of septic cases (Alberti *et al.* 2002).

Lipopolysaccharide (LPS) is a bacterial outer membrane component largely responsible for the endotoxic properties of Gram-negative bacteria. It is an essential component of bacterial viability and has a highly conserved structure that is recognised by the innate immune system (reviewed in Cohen 2002).

LPS activates the innate immune response by eliciting the production of monocyte/macrophage derived inflammatory mediators such as Tumour Necrosis Factor Alpha (TNF- α), Interleukin-6 (IL-6) and Nuclear Factor - kappa B (NF- κ B), which in turn mediate the release of more TNF- α and IL-6 (reviewed in Lu *et al.* 2008). A signal cascade follows from the recognition of LPS by the soluble shuttle protein LPS-binding protein (LPB), which facilitates the association of LPS to a cell surface protein complex including the membrane-bound monocyte differentiation antigen CD14, the trans-membrane Toll-like receptor-4 (TLR4) and its adaptor protein MD2 (myeloid differentiation protein-2). The formation of this complex elicits a subsequent downstream intracellular signalling cascade through adaptor proteins such as

myeloid differentiation protein (MyD88) and various kinases (e.g. IL-1 receptor associated kinase (IRAK), TNF receptor associated factor (TRAF6), etc); this ultimately leads to the activation and nuclear translocation of NF- κ B and the production of pro-inflammatory cytokines such as TNF- α and IL-6 (reviewed in Guha and Mackman 2001).

Activation of the innate immune system in response to infection is normally a protective phenomenon; however, during sepsis the host response is exacerbated. Macrophages and neutrophils release cytokines such as TNF- α and IL-6, which in turn activate surrounding monocytes and endothelial cells to secrete more cytokines and chemokines. The result is a positive feedback loop where, if unchecked, causes continuous release of pro-inflammatory mediators that trigger repeated cycles of inflammation, potentially resulting in systemic inflammation and multiple organ damage. Increased levels of circulating cytokines at the onset of sepsis have been implicated in the impairment of the normal function of most organs (reviewed in Jacobi 2002) including skeletal muscle, where a profound loss of muscle mass in septic patients increases the recovery times and reduces the quality of life due to chronic frailty and muscle weakness.

The exact mechanisms underlying sepsis induced muscle loss are still poorly understood but inflammatory cytokines such as TNF- α , IL-6 and NF- κ B are frequently implicated. It is important to note that cytokines often act in synergy (Paludan 2000) and the effects often attributed to the action of one may actually be due to the coordinated action of several cytokines. Therefore a comprehensive review of the role of cytokines in sepsis induced muscle loss is

beyond the scope of this chapter. The production and early release of TNF- α by immune cells appears to be a major step that mediates cachectic muscle wasting (reviewed in Tracey and Cerami 1993). The catabolic actions of TNF- α were first demonstrated in tumour bearing nude mice, where marked muscle loss was noted (Tracey *et al.* 1990). Secondly, administration of TNF- α to rodents altered several protein synthetic, protein degradative and apoptotic pathways and resulted in hindlimb muscle atrophy after eight days (Llovera *et al.* 1993). Exposure to LPS or increased production of TNF- α activates NF- κ B, which is controlled by the phosphorylation and subsequent degradation of I κ B, which sequesters NF- κ B in the cytosol, preventing nuclear translocation and transcription (reviewed in Baldwin 1996). NF- κ B belongs to a family of pleiotropic transcription factors, of which there are five members in mammals: p50/p105, p52/p100, RelA (p65), c-Rel and RelB. They form homo- or heterodimers in different combinations to mediate gene transcription of various inflammatory cytokines (including TNF- α and IL-6) immune-regulatory molecules, acute-phase stress response proteins and several enzymes, including those involved in protein degradation by the ubiquitin proteasome system, such as the E3 ubiquitin ligase Muscle Ring Finger 1 (MuRF1) (reviewed in Li *et al.* 2008). The role of IL-6 in muscle atrophy may be multifunctional; although plasma levels are elevated during infection, elevations in response to exercise are also common and are thought to play an anti-inflammatory role by inhibiting the production of TNF- α (reviewed in Pedersen *et al.* 2003). IL-6-deficient mice display impaired inflammatory response and are more resistant to muscle damage (Scuderi *et al.* 2006). Conversely, IL-6 transgenic mice

experience significant muscle loss, which is attenuated by administration of anti-mouse IL-6 receptor antibody (Tsujioka *et al.* 1996).

In short, several studies suggest the concerted action of these cytokines may mediate many of the conditions that initiate the rapid loss of muscle mass during sepsis; by coordinating a reduction in muscle protein synthesis and an up-regulation of protein degradation (Vary and Kimball 1992; Lang *et al.* 2007). Furthermore, derangements in translational efficiency (via repression of translation initiation and suppression of the guanine exchange factor eIF2B) (Vary *et al.* 1994; Murton *et al.* 2009), enhanced protein degradation (via up regulation of the ubiquitin proteasome, calpain and lysosome-dependent proteolytic pathways) (Voisin *et al.* 1996; Lecker *et al.* 1999) carbohydrate oxidation (Alamdari *et al.* 2008) and in the development of insulin resistance (Lang *et al.* 1990) have been noted. For a review, see Hasselgren *et al.* (2005).

Under normal physiological conditions, muscle protein synthesis and degradation is precisely adjusted to maintain appropriate muscle mass. An imbalance in signalling among the regulatory pathways (e.g. IGF-1, AKT/PI3K, GSK3/mTOR, MAFbx/MurF1 etc) in numerous disease states, characterised by systemic inflammation such as cancer, AIDS, and sepsis are widely considered to initiate muscle atrophy. For a review, see Glass (2005).

The multifactorial nature of sepsis has made it difficult to fully understand the molecular mechanisms underlying its pathogenesis, development of effective therapeutic strategies. Treatment in a clinical setting is often reactive rather than proactive and prevention of muscle wasting is often a secondary consideration in critical care. Animal models have proven an effective means of studying the pathophysiology of sepsis, especially within the context of

muscle atrophy. Current research employs a variant of three methods for the induction of Gram-negative sepsis; administration of live bacterial, surgical induction of peritonitis via caecal ligation and puncture (CLP) or the administration of bacterial toxin such as LPS. Each method has its benefits and limitations; for example the CLP procedure delivers a variable microbial dose and the distance of caecum ligated and the size of puncture is major determinant of the degree of sepsis elicited. Although the infusion of live bacteria represents an effective way to investigate extreme cases of sepsis often seen in a clinical setting such as meningococemia pneumococcal bacteraemia, the severity and reproducibility of the septic response is dependent on the dose, species and viability of bacteria as well as the route of administration. Also, certain strains of bacteria used in such models, whilst able to elicit an infection in rodents, have no effects on humans or are not commonly reported in critically ill patients. For a review, see Poli-de-Figueiredo *et al*, (2008).

The rat model of LPS induced endotoxaemia described here-in was developed and optimised within our research group; it produces a hyperdynamic circulatory response that mimics the cardiovascular changes seen in the early stages of human clinical sepsis (Parrillo 1993; Gardiner *et al*. 1995). This experimental model, which involves a continuous infusion of a non-lethal dose of LPS in conscious chronically instrumented rats, produces a high degree of reproducibility and allows accurate dosing. Since increased serum LPS in critically ill patients is associated with severity and mortality rate of sepsis (Casey *et al*. 1993), it is beneficial to be able to calibrate the dose of toxin administered in order to appropriately measure responses. Previous work on this model by our research group has focussed on the metabolic consequences

of sepsis including the changes in carbohydrate metabolism (Alamdari *et al.* 2008; Crossland *et al.* 2008), alterations in protein synthesis (Murton *et al.* 2009) and the molecular events characterising the up-regulation of components of the ubiquitin proteasome system (Strachan 2012); ultimately, to elucidate the pathways dysregulated in sepsis mediated muscle atrophy. In this chapter we describe the expression profiles of satellite cell myogenic regulatory factors (MRFs) during the early stages of endotoxaemia, which when impaired, may limit muscle regeneration after atrophy

Little is reported of satellite cell specific responses to LPS *in vivo* but a few studies have explored the behaviour of satellite cells in inflammatory milieu *in vitro* (Gallucci *et al.* 1998; Li and Schwartz 2001; Doyle *et al.* 2011). Cultured myoblasts respond to inflammatory stimuli and have been shown to express TLR4. This suggests satellite cells participate in infection control and may not be inconsequential to the inflammatory response (reviewed by Lightfoot *et al.* 2009). Furthermore, C2C12 myotubes treated with LPS experienced a dose-dependent loss of myosin heavy chain (MHC) myofibrillar protein and a reduction in myotube diameter after 48h (Doyle *et al.* 2011). Myotube atrophy was due to a coordinated stimulation of the ubiquitin-proteasome and autophagy-lysosomal pathways. Likewise, highly purified human myoblasts, when stimulated with pro-inflammatory agents such as TNF- α or LPS, selectively express and secrete IL-6, which activate myofibrillar cachectic proteolysis (Ebisui *et al.* 1995; Gallucci *et al.* 1998) or myoblast proliferation (Austin and Burgess 1991; Cantini *et al.* 1995), although the choice of action may be time/dose dependent. There is also evidence of muscle fibres and myocytes responding to LPS stimulation via TLR4 *in vivo*; studies by Frost *et*

al. (2004; 2006) noted LPS administration failed to elicit nitric oxide synthase (NOS) expression in myocytes of C3H/HeJ mice harbouring a mutation in the LPS receptor. Additionally, LPS-induced NOS was found to co-immunoprecipitate with the muscle specific caveolin-3 protein.

A review by Degens (2009) highlights the importance of the *in vivo* satellite cell microenvironment during systemic inflammation; circulating systemic factors affect the regenerative capacity of satellite cells, which may contribute to the slow progressive loss of muscle mass over time. This is supported by the impaired regeneration of young rat muscle when transplanted into an old rat (Carlson and Faulkner 1989), where chronic low grade systemic inflammation is thought to be the main cause of impairment (Bruunsgaard *et al.* 2001; Degens 2007) and the rejuvenation of old satellite cells exposed to serum from young animals (Conboy *et al.* 2005). It is speculated the increased levels of circulating inflammatory cytokines during sepsis impairs satellite cell function by altering the expression of MRFs. This could likely explain why satellite cells exposed to TNF- α *in vitro* or inflammatory milieu *in vivo* are able to proliferate but not differentiate (Foulstone *et al.* 2004; Langen *et al.* 2006). Likewise, mice over-expressing or injected with TNF- α exhibited reduced MyoD protein levels (Langen *et al.* 2004) that were concomitant with impaired muscle regeneration. In the present study, we describe the expression profile of the inflammatory cytokines TNF- α , IL-6 and NF- κ B and their influence of on components of satellite cell myogenesis during the early stages of endotoxaemia.

In summary, the aims of the present study are to examine the regulation of satellite cell activity in a pharmacological model of atrophy (via continuous LPS administration) in the rat. More specifically, to measure the expression of inflammatory markers in order to determine what impact they have on satellite activity. We hypothesise that increased expression of inflammatory cytokines in response to continuous LPS infusion should have a negative effect on components of the satellite cell myogenic program, thus contributing to progressive inflammation-mediated muscle wasting.

4.3 METHODS

4.3.1 Animals and tissue collection

Animal work was carried out as described in chapter 2, section 2.1.2.2. Briefly, male Sprague-Dawley rats (380-480g; Charles River, Sandwich, UK) were anaesthetised with fetanyl citrate (300µg/kg; i.p., Janssen-Cilag, High Wycombe, UK) and medetomidine (300µg/kg; i.p., Domitor, Pfizer, Sandwich, UK) prior to catheter implantation in the jugular vein for administration of substances. Under anaesthesia, animals were fitted with a harness to carry the catheter and allowed unrestricted movement. Anaesthesia was reversed with atipamezole (1mg/kg; s.c., Antisedan, Pfizer, Sandwich, UK), analgesia was provided (buprenorphine; 0.03 mg/kg, s.c., Vetergesic; Alstoe Animal Health, York, UK) and animals were left to recover for 24 hours with open access to food and water. The venous line was connected to an infusion pump via a fluid filled swivel, which maintained a continuous i.v. infusion of sterile heparinised saline (15U/ml) at 0.4ml/hr to maintain catheter patency.

Prepared rats were divided into six groups; three groups received a continuous infusion sterile isotonic saline (0.4ml/hr) for either 2h (n=4), 6h (n=4) or 24h (n=6) and the remaining three groups received a continuous infusion of LPS (*E. coli*, serotype 0127:B8; 15 µg/kg/hr i.v., Sigma, Poole, UK: dissolved in sterile isotonic saline;) for either 2h (n=4), 6h (n=4) or 24h (n=6). After the specified times, animals were terminally anaesthetised with sodium pentobarbital (Inactin; 80 mg/kg, i.v., Sigma-Aldrich, St. Louis, USA). The

extensor digitorum longus (EDL) and gastrocnemius muscles from both limbs were removed and immediately snap frozen and stored in liquid nitrogen.

4.3.2 mRNA measurements (real-time PCR)

Total RNA was extracted from approximately 25mg of frozen wet muscle using TRIzol[®] (Invitrogen, Paisley, UK) according to the manufacturer's instructions. The quality and quantity of RNA was assessed spectrophotometrically (by measuring the absorbance at 260nm and 280nm) and qualitatively by visually assessing the ratio of 18:28S ribosomal RNA on a 1% formaldehyde gel. First strand cDNA synthesis was carried out using 1µg of total RNA, as described in chapter 2, section 2.2.3. Taqman[®] primer/probe sets (Table 4.1) were obtained from Applied Biosystems (ABI, Foster City, CA, USA). Real-time PCR was performed using Taqman gene expression master mix (Applied Biosystems) in a MicroAmp 96-well reaction plate (Geneflow, Fradley, UK). Reactions were carried out in an ABI Prism 7000 sequence detection system in duplicate; each well contained 2µl cDNA template, 12.5µl PCR master mix and 1.25µl primer/probe mix in a 25µl reaction volume (See Chapter 2, section 2.2.4)

Relative quantification of gene expression between time matched control and LPS-treated groups was calculated using the $2^{-\Delta\Delta C_t}$ method. Briefly, duplicate cycle threshold (C_t) values for each control or treated sample were averaged and the ΔC_t was calculated by subtraction of the corresponding mean C_t of an endogenous control (HMBS). $\Delta\Delta C_t$ was calculated by subtracting the ΔC_t of

Table 4.1: Catalogue and Unigene Numbers for Taqman primer/probes sets

Gene	Catalogue Number	Unigene Number
HMBS	Rn00565886_m1	Rn.11080
TNF-a	Rn00562055_m1	Rn.2275
IL-6	Rn00561420_m1	Rn.9873
NFkB1	Rn01399583_m1	Rn.2411
Pax7	Rn00834076_m1	Rn.226327
MKi-67	Rn01451446_m1	Rn.73551
MyoD1	Rn00598571_m1	Rn.9493
Myogenin	Rn00567418_m1	Rn.9465
Myostatin	Rn00569683_m1	Rn.44460

LPS treated samples from the mean ΔC_t of corresponding time-matched saline controls and the relative amount of target mRNA was determined by $2^{-\Delta\Delta C_t}$. The saline control groups were given a value of 1 and fold changes in mRNA expression of LPS treated groups were calculated relative to their corresponding control group. Thus values >1 or <1 indicate an increase or decrease in mRNA expression from control, respectively.

4.3.3 Protein measurements (Western Blotting)

Protein extractions and western blotting was carried out using approximately 30mg of muscle, as described in chapter 2, section 2.2.5 and chapter 3 section 3.3.3, to determine protein expression of the targets listed in table 4.2.

4.3.4 Histology

4.3.4.1 Immunohistochemistry

To localise and quantify (see section.4.3.6 below) macrophage infiltration of skeletal muscle in response to LPS infusion, 10 μ m frozen serial cross sections were cut (Leica Microtome, Leica Microsystems, Wetzlar, Germany) and mounted onto Superfrost[®] Plus slides (ThermoFisher Scientific, Loughborough, UK) as described in chapter 2, section 2.2.6. Cross sections of normal adult brain tissue were used as a positive control for the antibody because brain tissue is specific for microglia. Sections were fixed in 4% Paraformaldehyde/Phosphate-Buffered-Saline (PFA/PBS: 4% (w/v) PFA,

Table 4.2: Primary and secondary antibodies used in the Western blotting protocol.

Primary Antibody	Supplier	Dilution
Goat Anti-TNFα pAb	R&D Systems Mineapolis, USA	1:500
Goat Anti-IL-6 pAb	R&D Systems Mineapolis, USA	1:500
Rabbit Anti-NFκB p105/p50 [E381] mAb	Abcam Cambridge UK	1:2500
Rabbit Anti-Iba1 pAb	Wako Osaka, Japan	1:500
Mouse Anti-Pax7 mAb	DSHB Iowa City, IA, USA	1:500
Rabbit Anti-MyoD (C-20) pAb	Santa Cruz Biotechnology Santa Cruz, CA, USA	1:500
Mouse Anti-Myogenin mAb	DSHB Iowa City, IA, USA	1:500
Rabbit Anti-Myostatin, Near C-terminus pAb	Millipore Billerica, MA, USA	1:250

Secondary Antibody	Supplier	Dilution
Rabbit Anti-Goat Immunoglobulins/HRP pAb	Dako Glostrup, Denmark	1:2000
Swine Anti-Rabbit Immunoglobuline/HRP pAb	Dako Glostrup, Denmark	1:2000
Rabbit Anti-Mouse Immunoglobulins/HRP pAb	Dako Glostrup, Denmark	1:2000

137mM NaCl, 2.7mM KCl, 4.3mM KH₂PO₄ pH 7.4) for 10 minutes, washed for 3x5 minutes in Tris-Buffered-Saline (TBS: 0.05M Tris, 0.15M NaCl, pH 7.4) and blocked for 1hr with at room temperature with 5% normal horse serum (Vector Laboratories, Burlingame, CA, USA). Sections were incubated with rabbit anti-Iba-1 polyclonal antibody (Wako, Osaka, Japan), diluted 1:1000 in blocking solution at 4°C for 72 hr. Control sections were incubated in blocker only. Primary antibody was visualised with vectastain anti-mouse kit (Vector Labs) as described in chapter 2, section 2.2.6.1. Slides were rinsed, air dried and mounted in glycerol gelatine (Merck, Darmstadt, Germany) for microscopy (DM4000B light microscope, Leica). Iba-1⁺ macrophages were counted and expressed per volume of muscle, as outlined in chapter 2, section 2.2.6.4.

4.3.4.2 Immunofluorescence

Iba-1 and TNF- α were co-localised by immunofluorescence to determine the major source of cytokine production. Muscle samples from representative animals showing high TNF- α and Iba-1 expression were cryo-sectioned and fixed in formaldehyde vapour for 30 minutes at -20°C as described in chapter 2, section 2.2.6.2. This method of fixation methylates protein lysine groups thereby denaturing and partially cross-linking proteins. Using vapour fixation minimises the loss of soluble antibody targets in solution compared to PFA fixation; soluble proteins are tagged in a frozen state, keeping them as close to natural as possible. Sections from normal adult brain tissue were used as a positive control for both antibodies. Sections were blocked with 5% normal horse serum for 1hr at room temperature. Antibody dilutions were: goat anti-

TNF- α (1:100) and rabbit anti-Iba-1 (1:1000). Technical control sections were incubated with blocker only and all sections were incubated for 72hr at 4°C. Secondary antibodies were donkey anti-rabbit Alexa488 and donkey anti-goat Alexa594, diluted 1:200 each (Invitrogen, Paisley, UK). Sections were incubated with the respective secondary antibody or a combination of both in for 1hr at room temperature, rinsed and mounted with ProLong anti-fade gold with DAPI (Invitrogen).

4.3.4.3 Duolink[®] Bright-field Proximity Ligation Assay (PLA)

The Duolink[®] PLA enables *in-situ* detection and visualisation of individual proteins or protein complexes in tissue samples prepared for microscopy. Specificity for a single protein target is enhanced by using two different primary and oligonucleotide-conjugated secondary antibodies (PLUS and MINUS PLA probes), which when in close proximity (within 40nm) combine to form a circular DNA template that is subsequently amplified by rolling cycle amplification. HRP-tagged oligonucleotides specifically hybridise with amplified DNA and the signal from each detected pair of primary antibody is visualised as a quantifiable individual spot by microscopy (see chapter 2, section 2.2.6.3 for a detailed description).

Preliminary optimisation experiments using two commercially available antibodies for ki-67 (rabbit polyclonal and mouse monoclonal anti-ki-67, Vector Labs) determined that when used individually by immunohistochemistry, the polyclonal antibody gave a good signal but with high background whilst the monoclonal antibody produced a low background with poor signal. Duolink[®] PLA was therefore an ideal candidate to amplify the

signal detected without compromising signal-to-noise ratio. Briefly, muscle cross sections from randomly assigned 2hr and 24hr treated animals were prepared and fixed in 4% PFA as described above. Cross sections from human embryonic tissue were used as a positive control and all were blocked in 5% normal horse serum for 1hr at room temperature.

Antibodies were added at a dilution of 1:100 in blocking solution either individually (as an additional technical negative control) or in combination and control sections were incubated in blocking solution only. All were incubated at 4°C overnight. The oligonucleotide conjugated anti-mouse (MINUS) and rabbit (PLUS) PLA probes were incubated with respective sections for 2 hours at 37°C. Sections were then incubated in the following solutions in-between washes in TBS-T: hybridisation (15min at 37°C), ligation (15min at 37°C) amplification (polymerase 90min at 37°C) and HRP detection solutions (30min at room temperature). Slides were incubated in Duolink[®] substrate solution (containing the HRP substrate NovaRED[™]) for 10 minutes at room temperature, washed and nuclear stained for 2 minutes. Prior to mounting in non-aqueous medium (Canada Balsam with xyelene, Merck, Darmstadt, Germany) for light microscopy, slides were dehydrated and cleared in increasing concentration of ethanol then xylene.

4.3.4.4 Stereology

Stereological methods in histology obtain quantitative information about three-dimensional (3D) features of tissues from two-dimensional physical sections.

Using a modification of the method by Mayhew *et al.* (1997), 10µm muscle

cross sections were prepared from control and treated animals randomly sampled from the proximal, distal or mid-belly regions of EDL and gastrocnemius muscles as described in section 2.2.6.4. The total numbers of profiles (i.e. Iba-1⁺, pax7⁺, myoD⁺ cells or ki-67⁺ PLA spots) for each section were counted with the aid of an eye-piece graticule using a section scanning technique (see figure 2.9). The surface area of muscle cross-sections ($A_{x\text{-sect}}$) was estimated using a systematic uniform point grid of known area. Points (represented by the crossing of horizontal and vertical lines over the muscle section) were counted and an estimate of the surface area of each cross section is given by the formula below, which estimates the number of profiles (N_{prof}) per volume of muscle (V_{muscle}).

$$\text{Estimate of } \frac{N_{\text{profiles}}}{V_{\text{muscle}}} (\mu\text{m}^3) \Rightarrow \frac{N_{\text{profiles}}}{A_{x\text{-sect}} \times (D + t)}$$

$$= \Sigma_p \times \left[\frac{a^p}{M^2} \right] (\mu\text{m}^2) \quad \begin{array}{l} \text{true} \\ \text{profile} \\ \text{diameter} \end{array} \approx \begin{array}{l} \text{mean} \\ \text{profile} \\ \text{diameter} \end{array} \times \frac{4}{\Pi} (\mu\text{m})$$

N_{profiles} = total number of positive cells per sample

$A_{x\text{-sect}}$ = total surface area of muscle cross sections in sample group (μm^2)

D = profile diameter (μm)

t = muscle section thickness (μm)

Σ_p = sum of all points per sample

a^p = area per point – surface area of 1 grid on uniform point grid

M = magnification

4.3.5 Statistical analyses

Some of the data obtained were inconsistent with a Gaussian distribution and tests for normality (such as the Kolmogorov-Smirnov and the D'Agostino-Pearson omnibus tests used by Prism) and plots of frequency distribution could not definitively prove the data were sampled from a Gaussian distribution (D'Agostino and Stephens 1986). With smaller data sets (where $n=4$), normality tests and frequency distributions did not have enough power to detect modest deviations from the Gaussian ideal; therefore comparisons between control and treated groups, between different sampling points (e.g., 2hr vs 6hr) were performed using the Kruskal-Wallis one-way analysis of variance (ANOVA), a non-parametric test. The Dunn's multiple comparison *post-hoc* test was used to highlight significant difference between treated groups and sampling points (e.g., 2hr LPS vs 24hr LPS groups). Significance was accepted at $p<0.05$.

4.4 RESULTS

4.4.1 Inflammatory Cytokines

Sepsis induced alterations in skeletal muscle metabolism and growth are thought to be fibre-type and tissue specific (Vary and Kimball 1992; Murton *et al.* 2009). The study by Tiao *et al.* (1997) also suggested that the EDL (a primarily fast muscle) is more susceptible to atrophy than the slow-twitch soleus muscle. Therefore, we measured the mRNA transcripts and protein expression of the inflammatory cytokines TNF- α , IL-6 and NF- κ B in the EDL and gastrocnemius (a muscle of mixed fibre type composition) to determine whether a muscle of intermediate characteristics, such as the gastrocnemius, relative to the soleus and EDL, would display intermediate responses to endotoxin relative to the other two muscles.

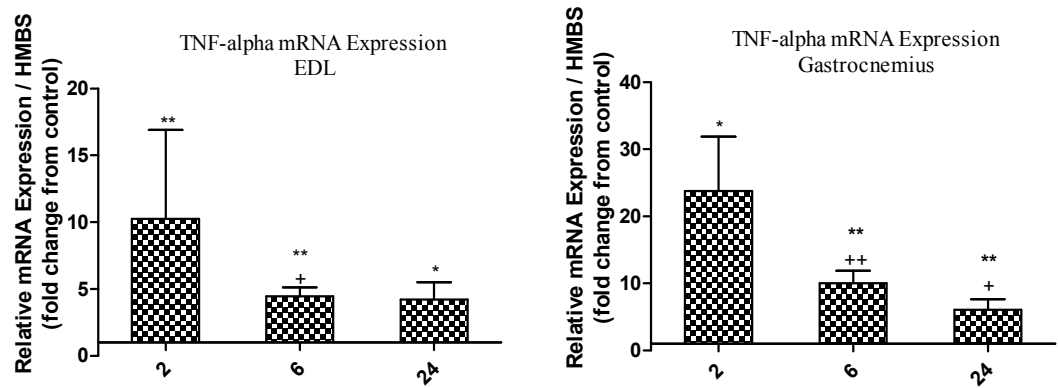
There were substantial transient increases in the mRNA expression of TNF- α and IL-6 across all time points, in both the EDL and gastrocnemius muscles. The highest mRNA expression was after 2hr LPS infusion and the lowest was after 24hr compared to their corresponding time-matched saline controls. These expression profiles were synonymous with the respective protein expression, which were also highest after 2hr of LPS (figures 4.1 - 4.3). TNF- α protein expression after 24hr of LPS was lower relative to saline control, whilst its mRNA was increased in both EDL and gastrocnemius muscles at this sampling point (~3 fold and ~5 fold respectively). We do not believe this represents divergent fates of TNF- α mRNA and protein expression but likely denotes increased proteolytic processing of the ~26kDa membrane-bound TNF-

α (Kriegler *et al.* 1988), by a family of ‘TNF-Alpha-Converting-Enzyme’ (TACE) such as ‘A-Disintegrin-and-Metalloproteinase-domain-containing’ protein 17 (ADAM17), which cleaves the membrane bound precursor of TNF- α to its mature soluble form (reviewed in Black 2002). The protein expression of IL-6 in gastrocnemius muscle was not measured due to time constraints but based on its similar mRNA expression profile to the EDL muscle; we surmised its protein expression following LPS is also similar to that of the EDL.

Interestingly, the magnitude of mRNA expression of both cytokines was considerably higher in the gastrocnemius compared to the EDL, especially after 2hr of LPS (TNF- α : 22 vs. 10 fold and IL-6: 660 vs. 135 fold). Tiao *et al.* (1997) reported that the fast twitch EDL was more susceptible to atrophy than the slow twitch soleus muscle due to differential activation of the energy-ubiquitin-dependent proteolytic pathway. It is likely the increased sensitivity of the gastrocnemius muscle to LPS reported here highlights a fibre type specific response to LPS that may be independent of the degree of potential atrophy elicited.

Figure 4.1: Expression of TNF- α a) mRNA and b) protein in EDL and gastrocnemius muscle following 2, 6 or 24hr continuous LPS or saline infusion. a) Relative mRNA expression of saline controls was set at 1; bars denote fold change in mRNA expression from corresponding time matched control with values >1 = increased mRNA expression and <1 = decreased mRNA expression. Values are means \pm S.E.M. b) The densities of \sim 26kDa TNF- α immunoreactive bands (Kriegler *et al.* 1988) were measured by western blotting and representative bands for each group are shown above their corresponding bar. n=4 (2, 6hr) n=6 (24hr). By Kruskal-Wallis 1-way ANOVA: significantly different from corresponding time matched control group: * $p<0.05$, ** $p<0.005$. Significantly different from 2hr LPS treated group: $^+p<0.05$, $^{++}p<0.005$. Significantly different from 6hr LPS treated group: $^{\#}p<0.05$

a) *TNF- α mRNA expression*



b) *TNF- α protein expression*

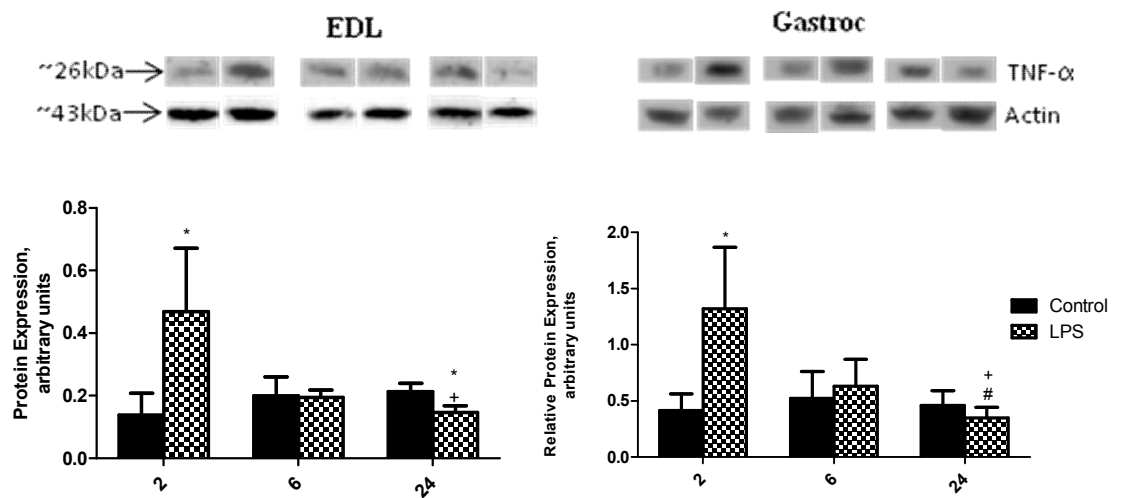
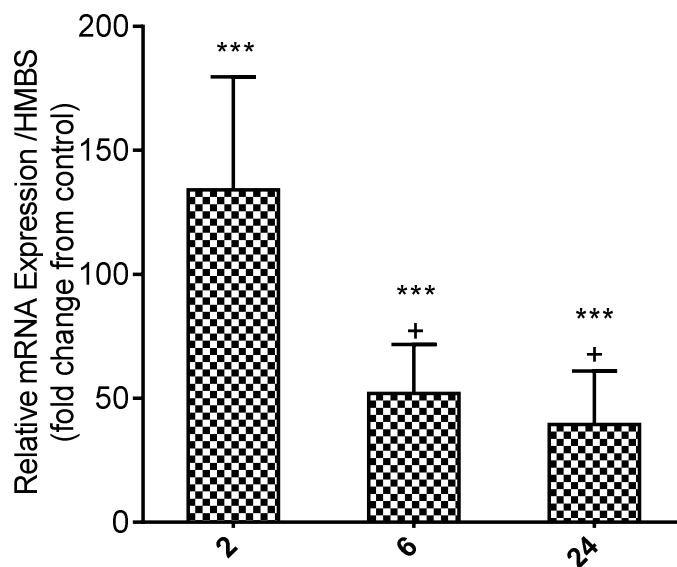


Figure 4.2: Expression of IL-6 a) mRNA and b) protein in EDL muscle following 2, 6 or 24hr continuous LPS or saline infusion. a) Relative mRNA expression of saline controls was set at 1; bars denote fold change in mRNA expression from corresponding time matched control with values >1 = increased mRNA expression and <1 = decreased mRNA expression. Values are means \pm S.E.M. **b)** The densities of ~24kDa IL-6 immunoreactive bands were measured by western blotting and representative bands for each group are shown above their corresponding bar. n=4 (2, 6hr) n=6 (24hr). By Kruskal-Wallis 1-way ANOVA: significantly different from corresponding time matched control group: *** p<0.0005. Significantly different from 2hr LPS treated group: + p<0.05.

a) *IL-6 mRNA expression – EDL*



b) *IL-6 protein expression – EDL*

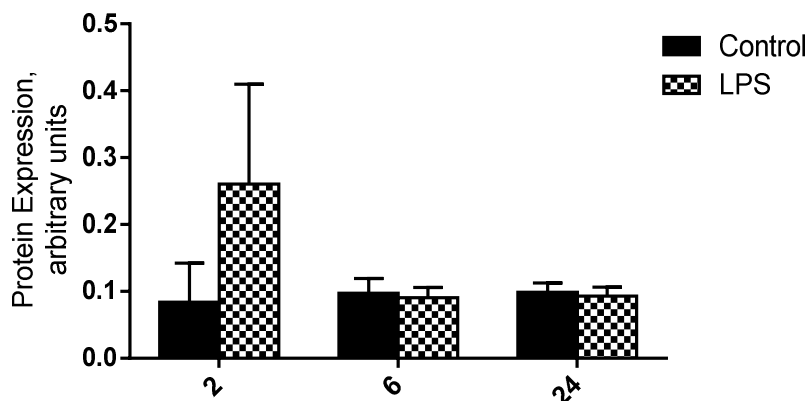
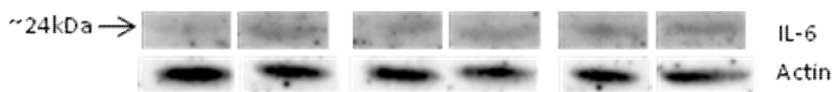
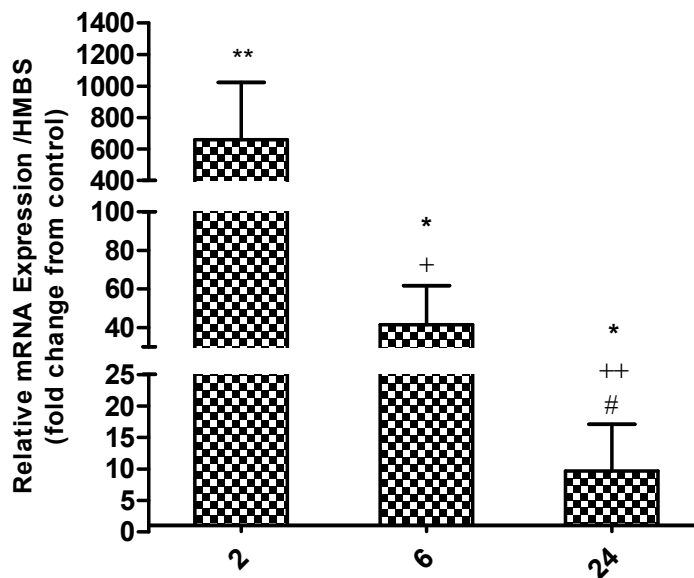


Figure 4.3: Fold changes in IL-6 mRNA expression in gastrocnemius muscle following 2, 6 or 24hr continuous LPS or saline infusion. Relative mRNA expression of saline controls was set at 1; bars denote fold change in mRNA expression from corresponding time matched control with values >1 = increased mRNA expression and <1 = decreased mRNA expression. Values are means \pm S.E.M. n=4 (2, 6hr) n=6 (24hr). By Kruskal-Wallis 1-way ANOVA: significantly different from corresponding time matched control group: * p<0.05, ** p<0.005. Significantly different from 2hr LPS treated group: + p<0.05, ++ p<0.005. Significantly different from 6hr LPS treated group: # p<0.05.

IL-6 mRNA expression - gastrocnemius



The transient up-regulation of pro-inflammatory cytokines such as TNF- α and IL-6 is mediated in part by NF- κ B signalling (Muller *et al.* 1993), therefore we measured NF- κ B mRNA and protein expression in the EDL to compare its expression profile to that of TNF- α and IL-6. NF- κ B mRNA was significantly ~3 fold higher in the EDL after 2 and 6hr but was only ~1.6 fold higher than control after 24hr (figure 4.4a). As described in section 4.1, NF- κ B belongs to a family of pleiotropic transcription factors, which form homo- or hetero-dimers in different combinations to mediate gene transcription. There are five members in mammals: RelA(p65), RelB and c-Rel are categorised as one group. They are synthesised as mature proteins containing an N-terminal Rel Homology Domain (RHD), which is essential for dimerization and DNA binding, and a C-terminal containing the transcriptional activation domain. The latter group consists of NF- κ B1 p50/p105 and NF- κ B2 p52/p100 proteins; these are synthesised as large precursors (p105 and p100 respectively) and proteolytic processing at the C-terminal gives rise to the RHD-containing p50 or p52, both of which lack the C-terminal trans-activation domain and thus hetero-dimerization is required for gene transcription. NF- κ B dimers are retained in the cytoplasm by specific inhibitors (I κ Bs) and the precursor proteins p105 and p100. These mask their nuclear localisation signal (NLS) and prevent nuclear translocation, thus maintaining NF- κ B in an inactive state in the cytoplasmic compartment (reviewed in Li *et al.* 2008).

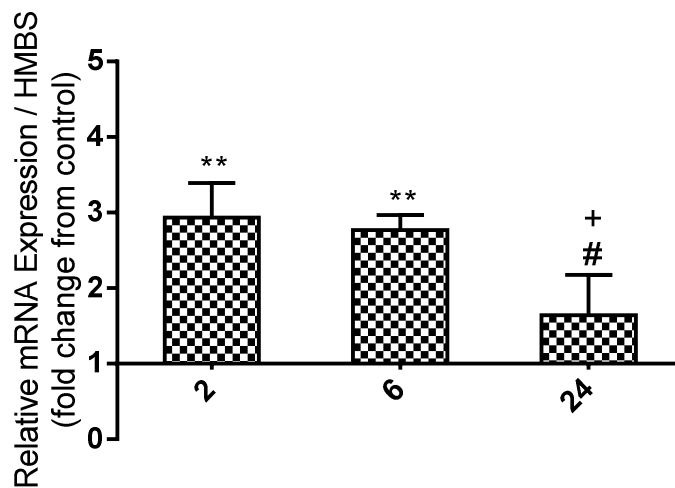
The inhibitory p105 and the processed, active p50 subunits of NF- κ B were measured by western blotting. Both subunits were significantly higher in LPS treated muscle after 2hr and showed a tendency to be higher after 6hr (p~0.07

and $p \sim 0.2$ respectively). No significant change was detected after 24h of LPS for either subunit (figure 4.4b).

The protein expression of NF- κ B in gastrocnemius muscle was not measured; we speculate, from the mRNA data (figure 4.5) that the expression profiles of both cytokines were likely similar in both muscles.

Figure 4.4: Expression of NF- κ B a) mRNA and b) protein in EDL muscle following 2, 6 or 24hr continuous LPS or saline infusion. a) Relative mRNA expression of saline controls was set at 1; bars denote fold change in mRNA expression from corresponding time matched control with values >1 = increased mRNA expression and <1 = decreased mRNA expression. Values are means \pm S.E.M. b) The densities of ~ 105 kDa and ~ 50 kDa immunoreactive bands, corresponding to the p105 and p50 subunits of NF κ B, were measured by western blotting and representative bands for each group are shown above their corresponding bar. n=4 (2, 6hr) n=6 (24hr). By Kruskal-Wallis 1-way ANOVA: significantly different from corresponding time matched control group: * $p<0.05$, ** $p<0.005$. Significantly different from 2hr LPS treated group: + $p<0.05$, ++ $p<0.005$. Significantly different from 6hr LPS treated group: # $p<0.05$.

a) *NF κ B mRNA expression – EDL*



b) *NF κ B protein expression - EDL*

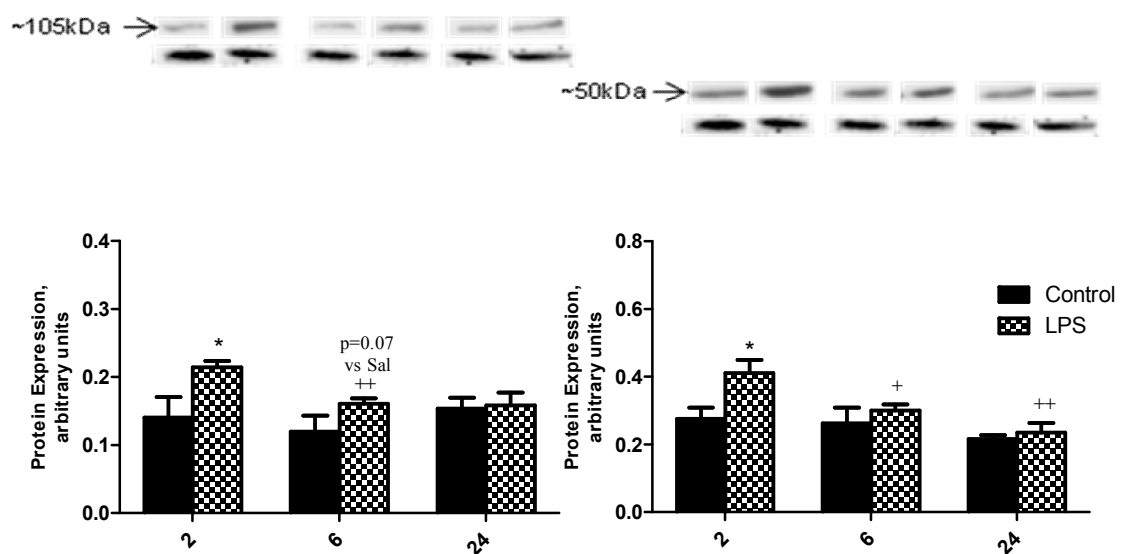
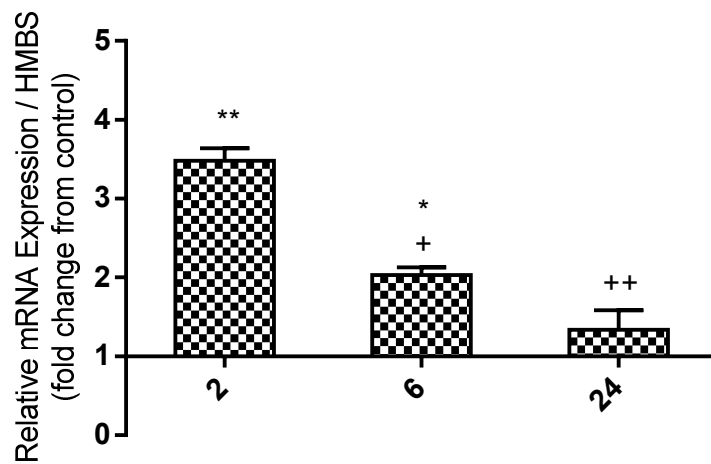


Figure 4.5: Fold changes in NF- κ B mRNA expression in gastrocnemius muscle following 2, 6 or 24hr continuous LPS or saline infusion. Relative mRNA expression of saline controls was set at 1; bars denote fold change in mRNA expression from corresponding time matched control with values >1 = increased mRNA expression and <1 = decreased mRNA expression. Values are means \pm S.E.M. n=4 (2, 6hr) n=6 (24hr). By Kruskal-wallis 1-way ANOVA: significantly different from corresponding time matched control group: * $p<0.05$, *** $p<0.0005$. Significantly different from 2hr LPS treated group: + $p<0.05$, +++ $p<0.0005$.

NF κ B mRNA expression – Gastrocnemius



4.4.2 Macrophage Infiltration

Macrophages play an important role in cytokine production. In fact TNF- α is one of the most abundantly synthesised products of activated macrophages and accounts for about 5% of their total secretory content (Beutler *et al.* 1985a).

The degree of macrophage infiltration in skeletal muscle in response to LPS was measured using ionised calcium binding adaptor molecule 1 (Iba1), a well characterised macrophage/microglia marker specific for quiescent and activated macrophages (Imai *et al.* 1996). Iba1 is a 17kDa EF-hand calcium binding protein implicated in macrophage membrane ruffling, motility and phagocytosis of infectious particles (Ohsawa *et al.* 2000).

Iba1⁺ cells were detected on cross sections of untreated adult rat brain tissue (microglia) and gastrocnemius muscle (macrophages) by immunohistochemistry (figure 4.6). A first impression indicated that the frequency of Iba1⁺ cells was distinctly higher in LPS treated muscle; thus the total number of distinct positive cells per area of muscle were counted on sections from saline and LPS treated gastrocnemius and EDL muscle as described in section 4.3.4.4. The total number of macrophages in muscle increased after LPS administration across all time points in both muscles (figure 4.7). Interestingly, the numbers of macrophages were higher in the gastrocnemius than the EDL, which corresponds to the higher cytokine mRNA expression observed for gastrocnemius muscle (see figures 4.1a, 4.2a and 4.3a).

Figure 4.6: Representative photomicrographs of Iba1⁺ microglia/macrophages on 10µm cross sections of rat brain (A-B) and gastrocnemius muscle (C-F). A and C are no primary antibody controls; C and D are cross sections from normal adult rat muscle, whilst E and F are from Saline and Lipopolysaccharide infused animals. Arrowed; Iba⁺ cells, Scale bars; A, C, D = 50µm B, E, F = 25µm

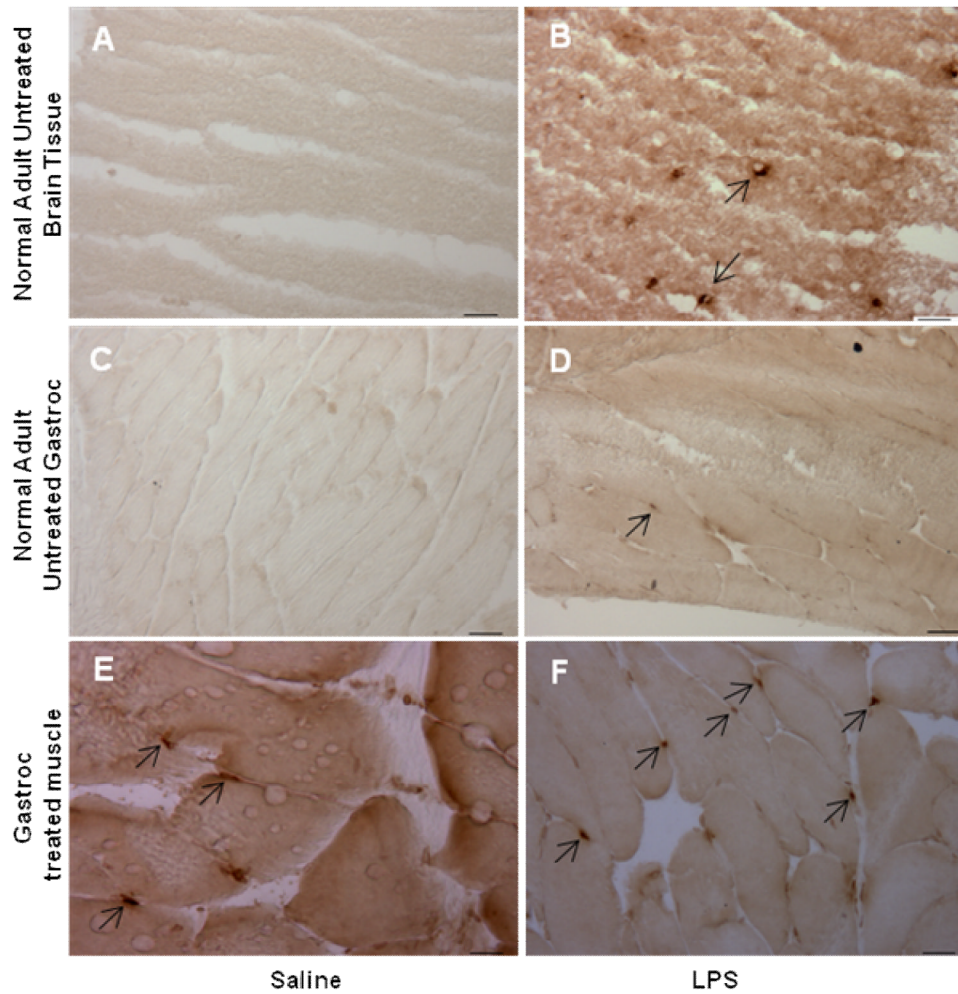
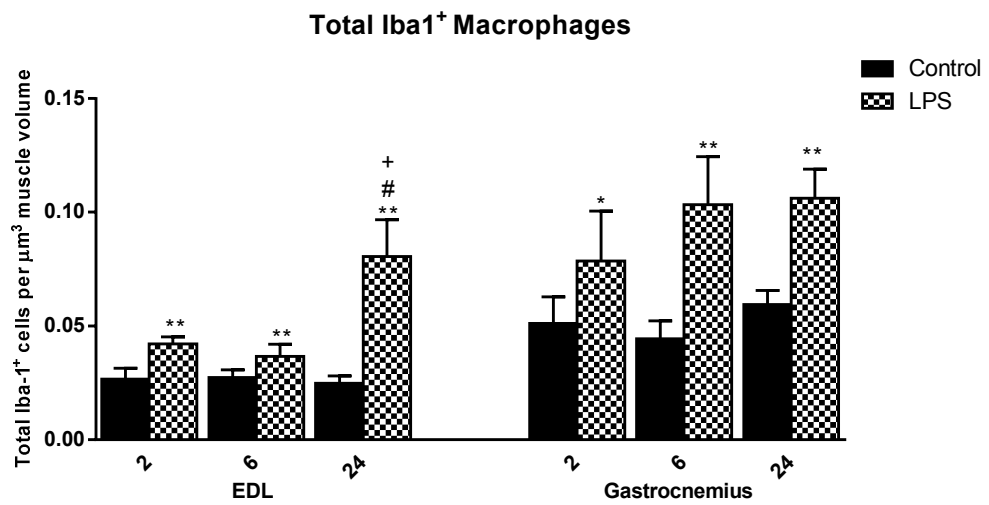


Figure 4.7: The total number of Iba1⁺ macrophages in rat gastrocnemius and EDL muscle following 2, 6 or 24hr LPS or saline continuous intravenous infusion. 10 μ m cryosections were stained against Iba1 via immunocytochemistry and positive cells counted by light microscopy. Values \pm S.E.M. n=3 (2, 6hr) n=5 (24hr). By Kruskal-Wallis 1-way ANOVA: significantly different from corresponding time matched control: * p<0.05, ** p<0.005. Significantly different from 2hr LPS treated muscle: ⁺ p<0.05. Significantly different from 6hr LPS treated muscle: [#] p<0.05.



To verify the increased presence of macrophages in LPS treated muscle, we also measured Iba1 protein expression by western blotting. Iba1 was higher in LPS treated gastrocnemius muscle after 2hr and 24hr (figure 4.8). The EDL muscle also showed a tendency toward higher levels of Iba1 protein after 2 and 24hr of LPS. Although the quantitative immunohistochemistry results are more striking compared to Western blotting results, both methods provide sufficient evidence for increased muscle macrophage infiltration.

The appearance of macrophages was also studied by immunohistochemistry and immunofluorescence to examine morphological changes (if any) after LPS administration (figure 4.9 and 4.10). Qualitatively, macrophages were larger and expressed more Iba1 after 24hr continuous LPS infusion; these had a distinct cytoplasm and were indicative of activated macrophages, which tend to be larger due to cytoplasmic expansion (Wirenfeldt *et al.* 2009). From counting macrophages, we also had the impression saline treated sections showed more quiescent macrophages, which were smaller in diameter, contained more prominent thin branching processes and expressed less Iba1 (Finnie *et al.* 2010).

Figure 4.8: Expression of Iba1 protein in gastrocnemius and EDL muscle following 2, 6 or 24hr continuous LPS or saline infusion. Values are means \pm S.E.M. The densities of \sim 17kDa immunoreactive bands were measured by western blotting and representative bands for each group are shown above their corresponding bar. n=4 (2, 6hr) n=6 (24hr). Significantly different from corresponding time matched control group: * p<0.05, ** p<0.005. Significantly different from 2hr LPS treated group: ⁺p<0.05 by 1-way ANOVA

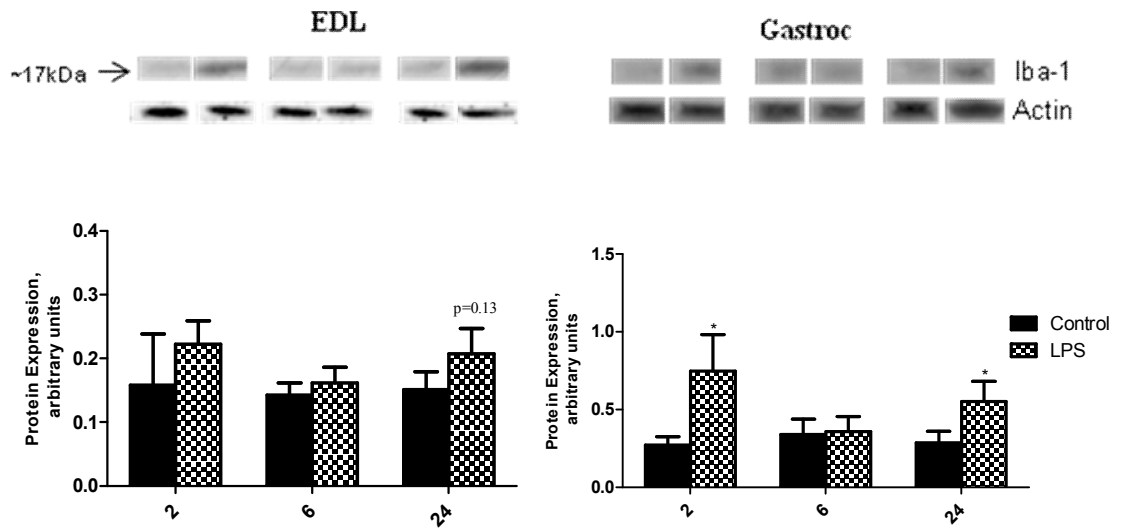


Figure 4.9: Representative photomicrographs of Iba1⁺ cells on 10µm cross sections of rat brain (A), Saline (B,D) and LPS-treated (C,E) gastrocnemius muscle. A, shows Iba1⁺ microglia in untreated adult brain; B-C are 2hr treated muscle, whilst D-E are from 24hr Saline and LPS infused animals. Scale bars; 10µm

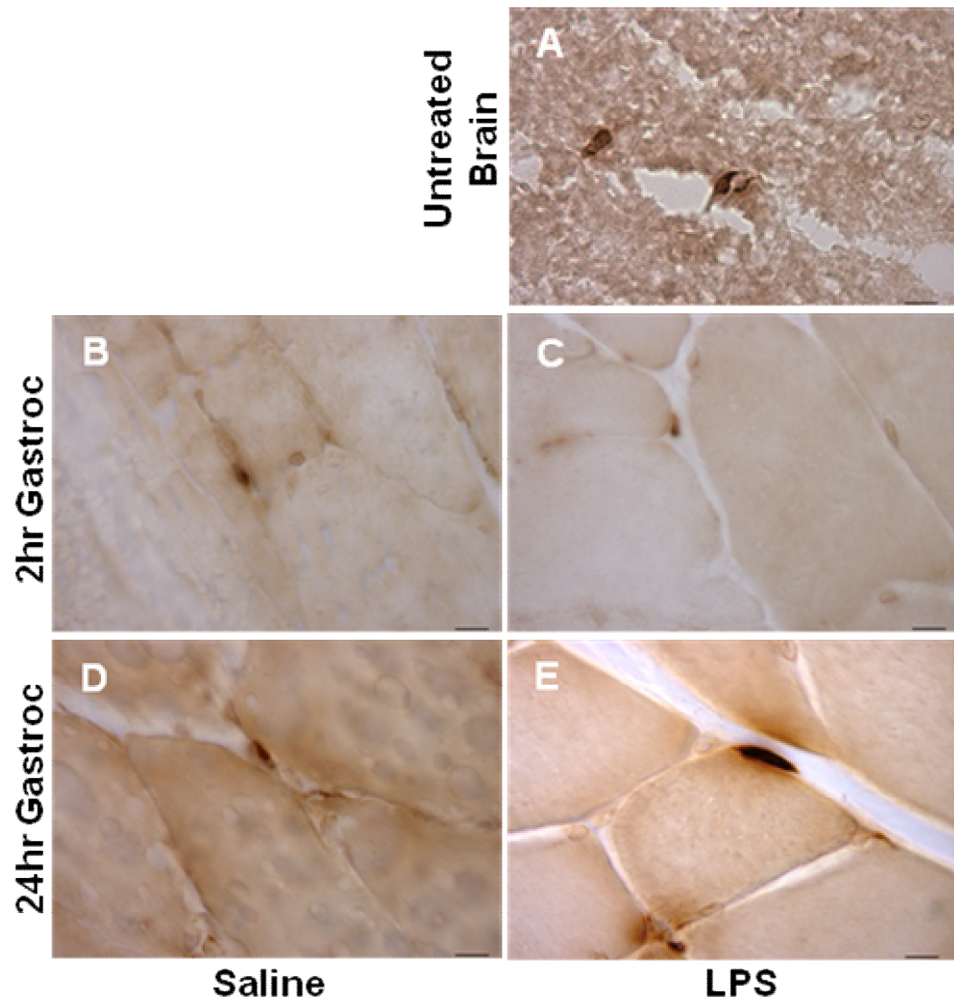
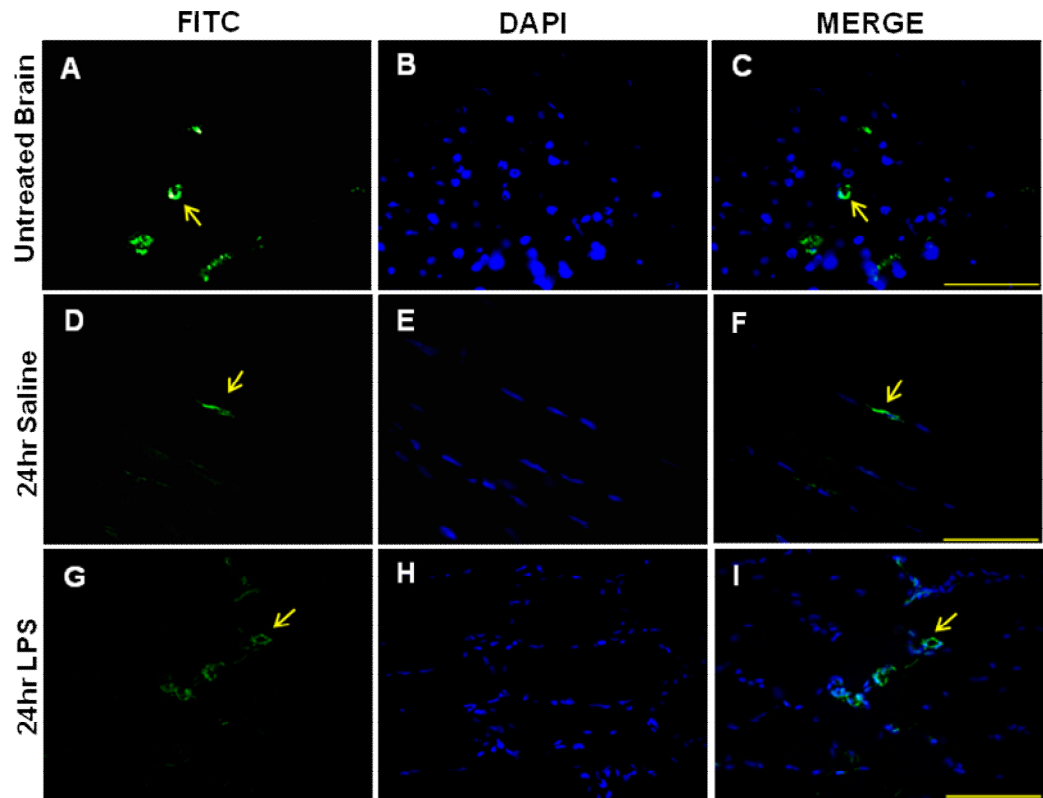


Figure 4.10: Representative photomicrographs of Iba1⁺ microglia and macrophages in untreated adult rat brain (A-C), Saline (D-F) and LPS-treated (G-I) gastrocnemius muscle. 10µm cryosections were stained against Iba1 for 72h and visualised via immunofluorescence. Scale bars; 100µm



4.4.3 TNF- α /macrophage co-localisation

TNF- α is a myokine expressed by myocytes in skeletal muscle (Li 2003); we assessed the distribution of TNF- α expression in gastrocnemius muscle, because it showed a higher magnitude of TNF- α mRNA expression compared to the EDL, to determine the predominant source of secretion. As expected, the saline treated samples showed some TNF- α^+ signals but were of lower intensity compared to LPS counterparts (figure 4.11). TNF- α was distributed in sporadic patches on the LPS treated samples, the majority of expression was localised to macrophages (*arrowed*) and myocytes with some freely dispersed TNF- α^+ granules around endomysial and perimysial connective tissue. Interestingly, some TNF- α expression was seen in 24hr saline treated samples although mostly localised to degenerating muscle fibres (*arrowhead*).

Sections were incubated with TNF- α and Iba1 simultaneously to confirm the presence of TNF- α expressing microglia/macrophages (figure 4.12). Of 22 random Iba1⁺ macrophages counted on cross sections of 24hr LPS treated gastrocnemius muscle, only about 13 cells (~60%) were also positive for TNF- α . However, there were plenty of free floating TNF- α^+ granules in close proximity to Iba1⁺ cells; confirming that most of macrophages secrete TNF- α . In contrast, corresponding control sections showed only ~15% Iba1⁺ macrophages also positive for TNF- α (two cells were positive for both out of thirteen counted).

Figure 4.11: Representative high magnification photomicrographs of TNF- α expression in Saline and LPS treated rat gastrocnemius muscle. 10 μ m frozen cross sections were stained against TNF- α and visualised via immunofluorescence. **A-C:** 2h saline, **D-F:** 2h LPS, **G-J:** 24h saline, **K-N:** 24h LPS. Positive signals are localised to degenerating fibres (*arrowheads*) and macrophages (*arrows*). **J, N** are composite images at a higher magnification. Scale bars: A-C, G-I, K-M = 100 μ m. D-F, J, N = 50 μ m.

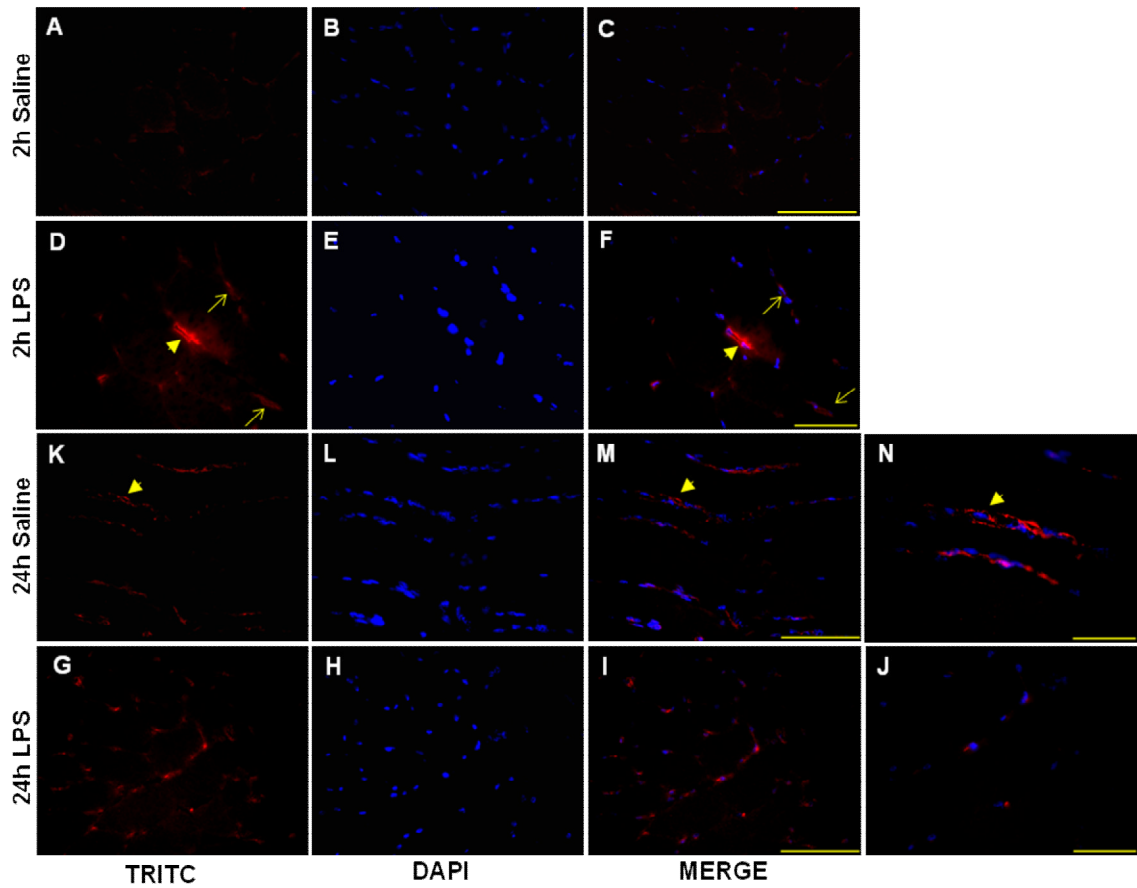
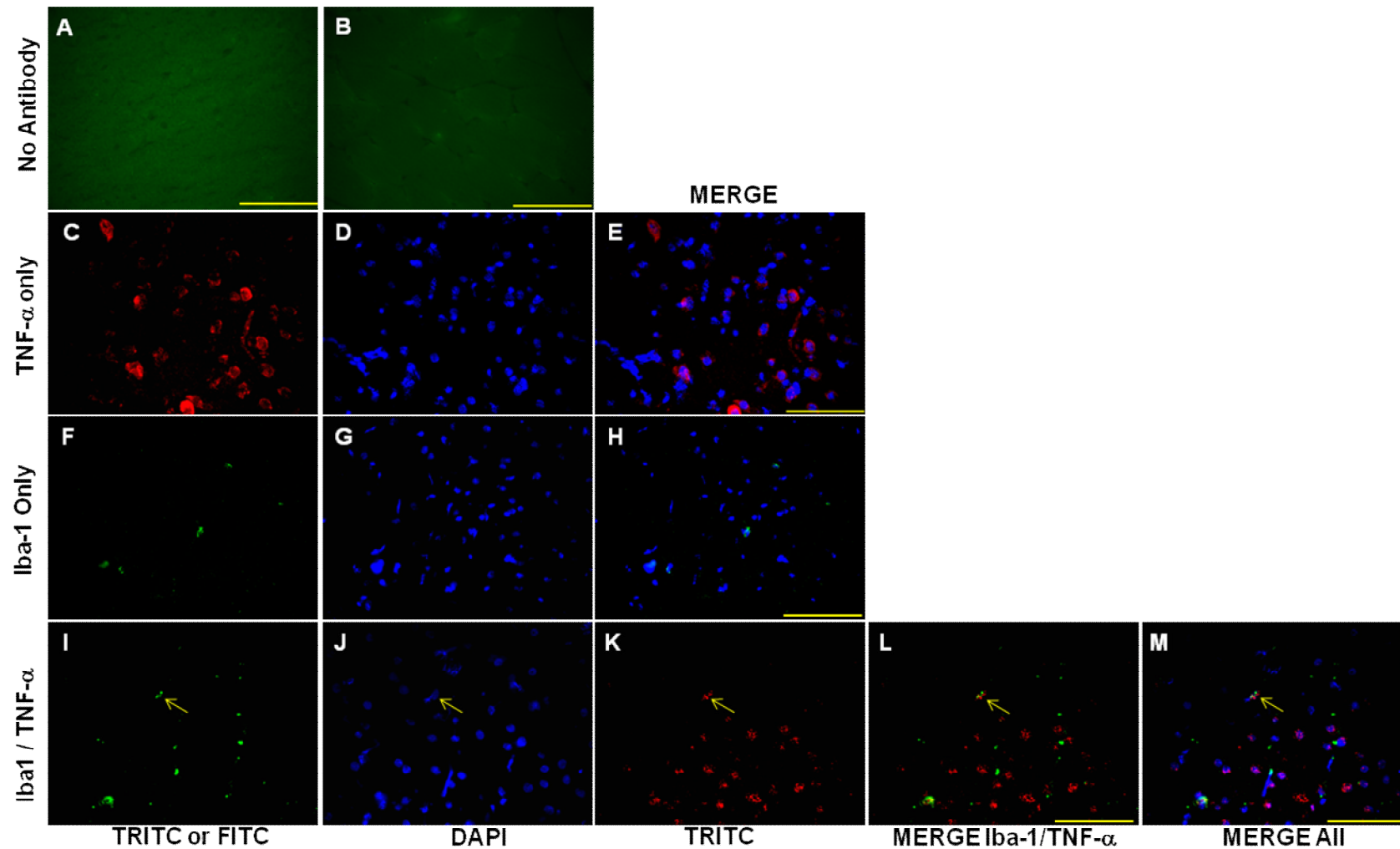
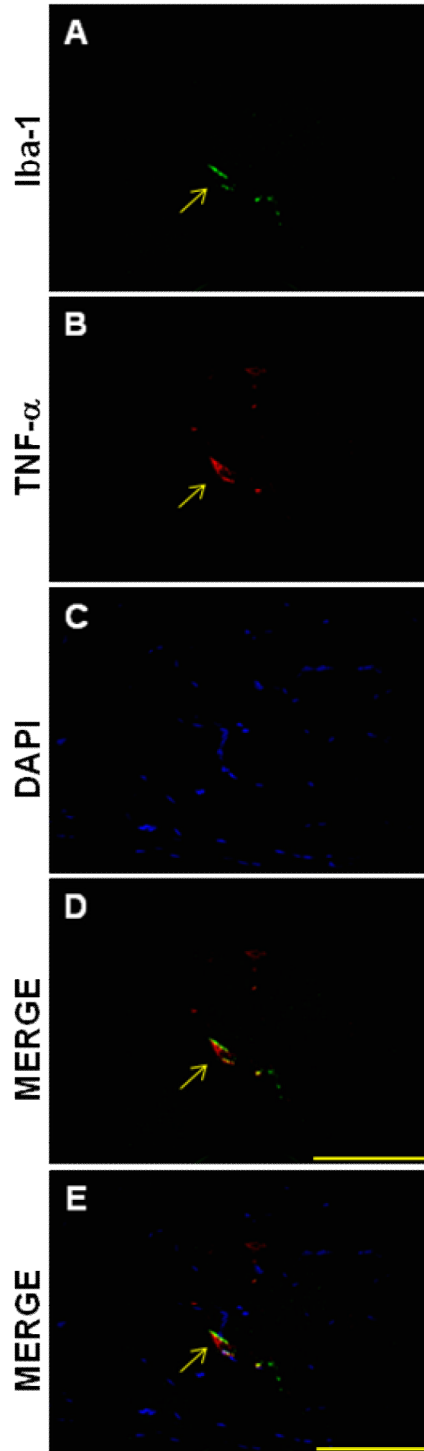


Figure 4.12: TNF- α expression is localised to Iba1⁺ i) microglia and ii) macrophages in untreated adult rat brain and LPS treated gastrocnemius. i) A-B: brain and gastrocnemius no primary antibody control respectively. 10 μ m frozen cross sections were stained against Iba1, TNF- α or both and visualised via immunofluorescence. Some microglia/macrophages are positive for both antibodies (*arrowed*). Scale bars; 100 μ m

1) Untreated Adult Rat Brain (microglia)



ii) LPS-treated Rat Gastrocnemius (macrophages)



4.4.4 Myogenic Regulatory Factors (MRFs)

The mRNA and protein expression patterns of early markers (pax7, myoD, ki-67), late markers (myogenin) and a negative regulator (myostatin) of satellite cell were measured following LPS administration.

LPS infusion differentially suppressed pax7 in the EDL and gastrocnemius muscles (figure 4.13); pax7 mRNA was suppressed after 6hr of administration and stayed reduced after 24hr in the EDL. Pax7 protein demonstrated a tendency toward decreased expression after 6 and 24hr in the EDL. The gastrocnemius muscle displayed an earlier suppression of pax7 mRNA and protein; there was a tendency toward decreased pax7 as early as 2hr after continuous infusion ($p \sim 0.13$ and $p \sim 0.15$; mRNA and protein, respectively). Pax7 mRNA and protein expression was still low after 6hr in the gastrocnemius, but there was a tendency toward a return to basal levels after 24 hr.

MyoD also displayed a similar time dependent response to LPS administration; myoD mRNA and protein was differentially suppressed in both muscles, with the gastrocnemius showing an earlier, more dramatic decrease compared to the EDL (figure 4.14). However, unlike pax7, myoD was still lower relative to control after 24hr, in both muscles. Taken together, these results suggest the gastrocnemius is more sensitive to LPS-mediated myogenic suppression relative to the EDL.

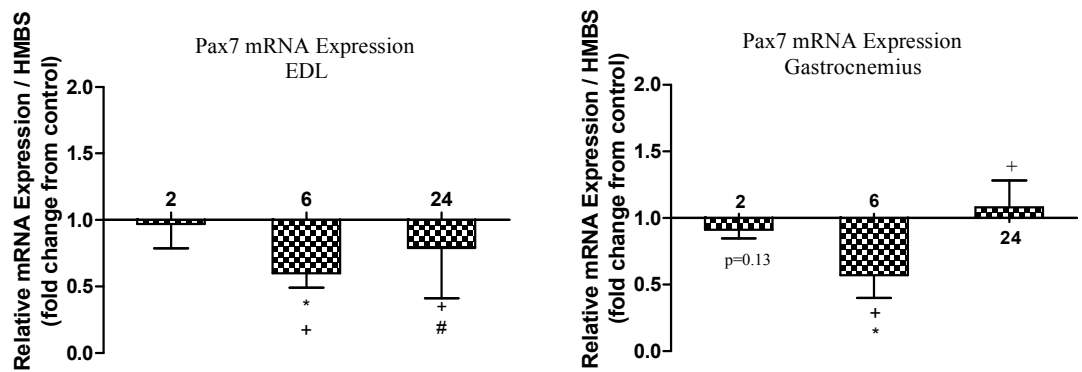
These results were verified by quantitative immunohistochemistry using 3-D stereology as described in chapter 2, section 2.2.6.4 and above in section 4.3.4.4. The total number of pax7⁺ and myoD⁺ satellite cells were estimated per

volume of muscle (figure 4.15). The gastrocnemius was used because it is larger than the EDL muscle and ensured there was sufficient tissue available for cyrosectioning. LPS caused short term changes in the number of pax7⁺ quiescent/proliferating satellite cells. The number of pax7⁺ satellite cells decreased significantly after 2hr and 6hr, but there was a tendency toward a return to baseline levels by 24hr. In contrast, myoD⁺ satellite cells decreased significantly across all time points and similarly to RT-PCR and western blotting data, myoD was still suppressed after 24hr of LPS administration.

Similarly to the Iba-1 data from Western blotting and quantitative IHC reported in section 4.4.2 above, the pax7 and myoD IHC data presented here are also more striking. Heterogeneity of macrophages and satellite cells suggest Western blotting results, which show total relative levels of protein expression, are not representative of quantitative IHC, which show numbers of macrophages and satellite cells expressing Iba-1, pax7 or myoD.

Figure 4.13: Expression of Pax7 a) mRNA and b) protein in EDL and gastrocnemius muscle following 2, 6 or 24hr continuous LPS or saline infusion. a) Relative mRNA expression of saline controls was set at 1; bars denote fold change in mRNA expression from corresponding time matched control with values >1 = increased mRNA expression and <1 = decreased mRNA expression. Values are means \pm S.E.M. b) The densities of ~55kDa pax7 immunoreactive bands were measured by western blotting and representative bands for each group are shown above their corresponding bar. n=4 (2, 6hr) n=6 (24hr). By Kruskal-Wallis 1-way ANOVA: significantly different from corresponding time matched control group: * p<0.05. Significantly different from 2hr LPS treated group: + p<0.05. Significantly different from 6hr LPS treated group: # p<0.05

a) Pax7 mRNA expression



b) Pax7 protein expression

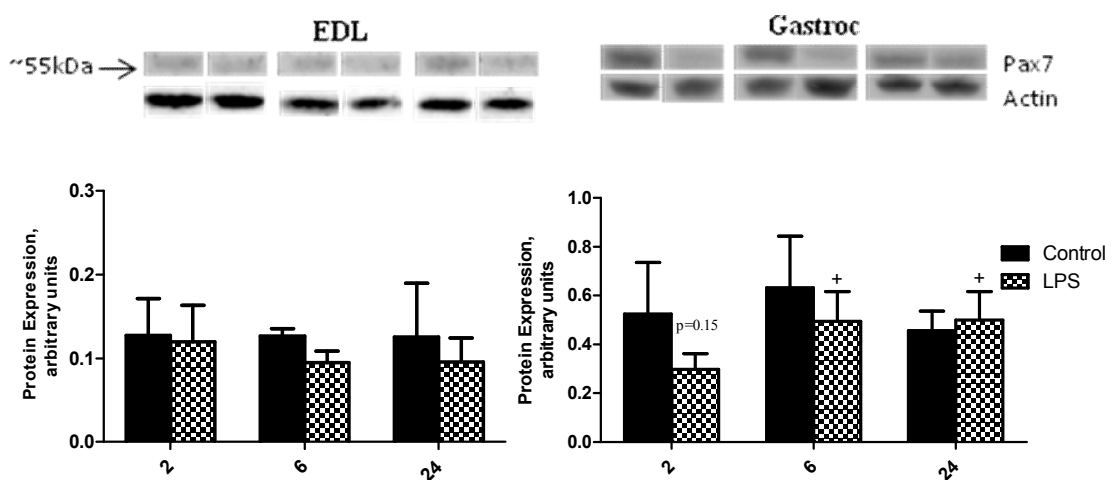
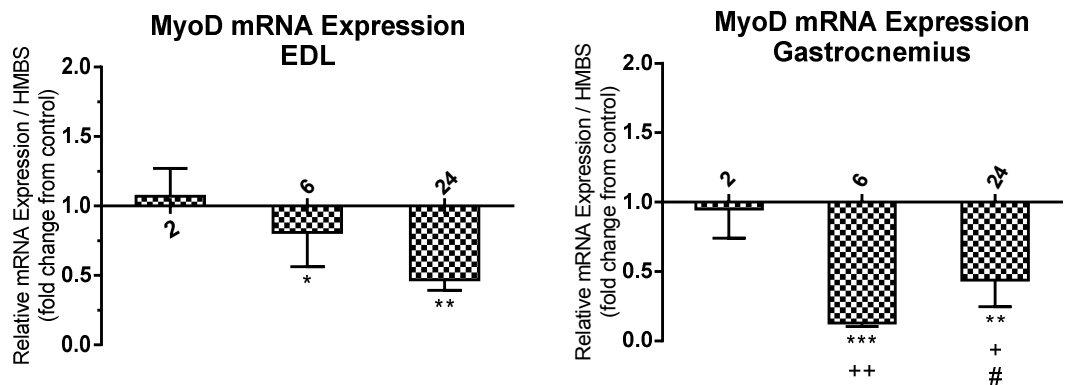


Figure 4.14: Expression of MyoD a) mRNA and b) protein in EDL and gastrocnemius muscle following 2, 6 or 24hr continuous LPS or saline infusion. a) Relative mRNA expression of saline controls was set at 1; bars denote fold change in mRNA expression from corresponding time matched control with values >1 = increased mRNA expression and <1 = decreased mRNA expression. Values are means \pm S.E.M. b) The densities of ~34kDa MyoD immunoreactive bands were measured by western blotting and representative bands for each group are shown above their corresponding bar. n=4 (2, 6hr) n=6 (24hr). By Kruskal-Wallis 1-way ANOVA: significantly different from corresponding time matched control group: *p<0.05, **p<0.005, ***p<0.0005. Significantly different from 2hr LPS treated group: +p<0.05, ++p<0.005. Significantly different from 6hr LPS treated group: #p<0.05

a) *MyoD mRNA expression*



b) *MyoD protein expression*

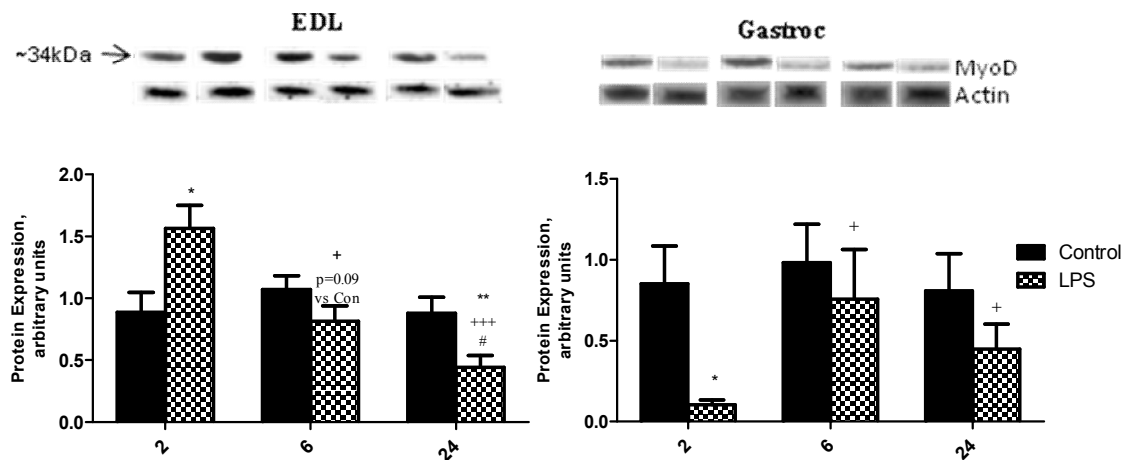
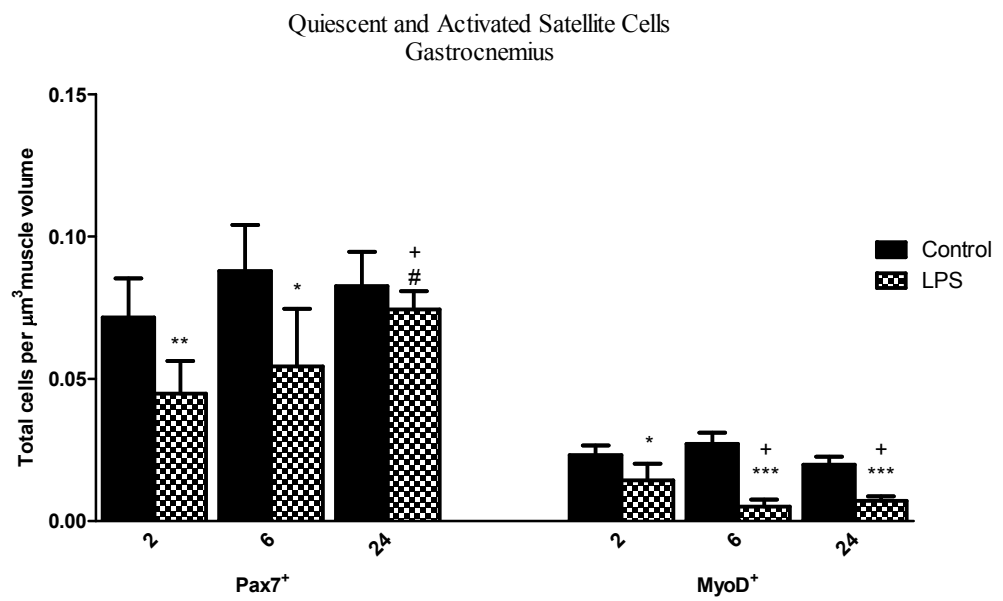


Figure 4.15: The total number of Pax7⁺ quiescent/proliferating and MyoD⁺ activated satellite cells in rat gastrocnemius muscle following 2, 6 or 24hr LPS or saline continuous intravenous infusion. 10µm cryosections were stained against pax7 and myoD via immunohistochemistry. Positive cells were counted by light microscopy and expressed per volume of muscle. Values are means ±S.E.M n=4 (2, 6hr) n=6 (24hr). By 1-way ANOVA: significantly different from corresponding time matched control: * p<0.05, ** p<0.005, *** p<0.0005. Significantly different from 2hr LPS treated muscle: ⁺p<0.05. Significantly different from 6hr LPS treated muscle: [#]p<0.05.



The Ki-67 nuclear antigen is a well known marker of proliferation and although not exclusively expressed in satellite cells, it is increasingly used as a marker for assessing the proliferative potential and activation status of satellite cells (Mackey *et al.* 2009; Snijders *et al.* 2012).

There was a gradual increase in ki-67 mRNA expression in the EDL muscle, peaking after 24hr of LPS (~2.5fold compared to corresponding time-matched control). In contrast, the gastrocnemius showed a gradual decline in ki-67 mRNA: it peaked after 2hr (again ~2.5 fold compared to control) followed by a tendency toward a return to baseline levels after 24hr of LPS infusion (figure 4.16a). This mirrored/reversed expression pattern in both muscles likely represents a delayed response to LPS by the EDL. It appears the gastrocnemius muscle is more sensitive to LPS and responds earlier and quicker to the toxin than the EDL. This is reflected in the pax7 and myoD expression data where the gastrocnemius showed an earlier and more dramatic response to LPS and in the case of pax7 and ki-67, a tendency toward basal levels of expression after 24hr. In addition, TNF- α and IL-6 mRNA was greater in the gastrocnemius.

Ki-67 is a large protein (>340kDa) and often difficult to resolve via Western blotting. We detected the nuclear antigen with a monoclonal and polyclonal antibody using a commercially available proximity ligation assay as described in section 4.3.4.3; it detects the proximity of the two antibodies bound to a single protein target. Ki-67⁺ nuclei were counted on 2hr and 24hr saline and LPS treated EDL muscle cross sections to compare the mRNA and protein expression trends at those time points. Ki-67 protein expression was significantly lower after 2hr but returned to baseline levels after 24hr (figure 4.16b-c)

Figure 4.16a: Ki-67 mRNA expression in EDL and gastrocnemius muscle following 2, 6 or 24hr continuous LPS or saline infusion. Relative mRNA expression of saline controls was set at 1; bars denote fold change in mRNA expression from corresponding time matched control with values >1 = increased mRNA expression and <1 = decreased mRNA expression. Values are means \pm S.E.M. n=4 (2, 6hr) n=6 (24hr). By Kruskal-Wallis 1-way ANOVA: significantly different from corresponding time matched control group: * p<0.05. Significantly different from 2hr LPS treated group: + p<0.05. Significantly different from 6hr LPS treated group: # p<0.05

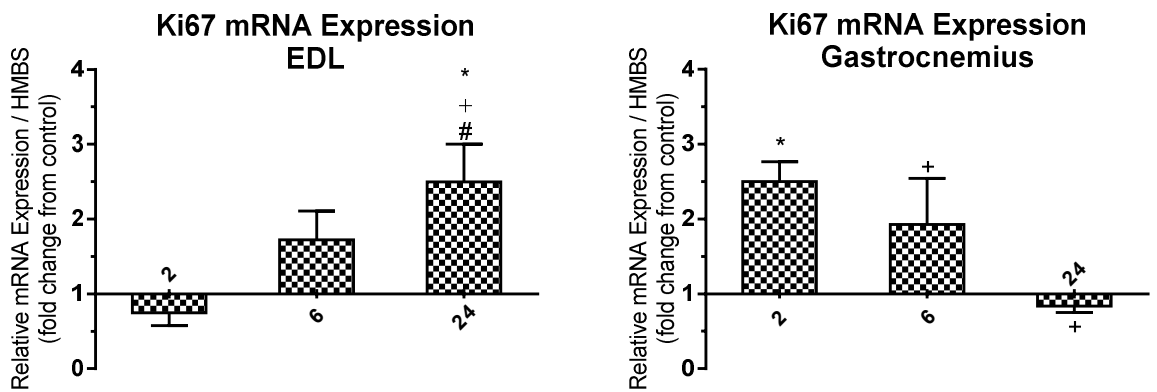


Figure 4.16b. Low and high magnification photomicrographs of Ki67⁺ cells in embryonic tissue (A-B) and 24hr Lipopolysaccharide treated EDL muscle (C-D). 10 μ m cryosections were incubated with a polyclonal and monoclonal antibody against Ki67 simultaneously. The proximity of the two antibodies bound to the same target was determined by Proximity Ligation Assay (PLA). **A,C** are controls with one of the antibodies omitted. Arrowed; Ki67⁺ cell in LPS muscle. Scale bars: A,C = 50 μ m. B,D = 20 μ m

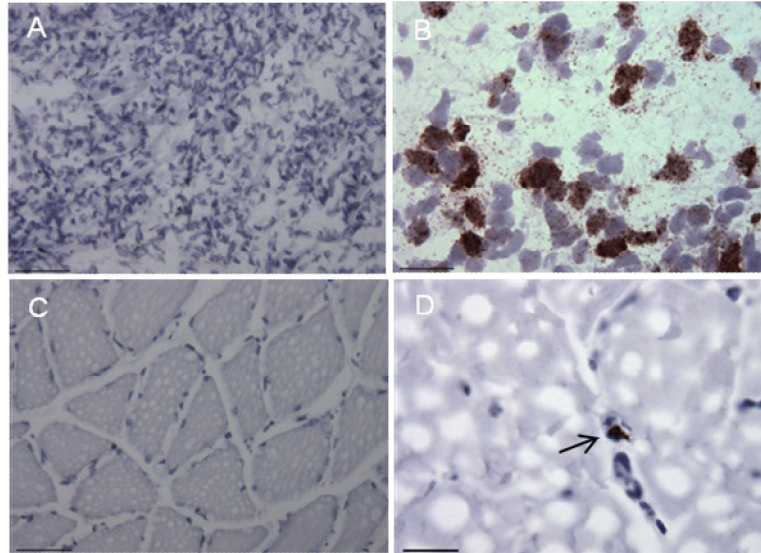
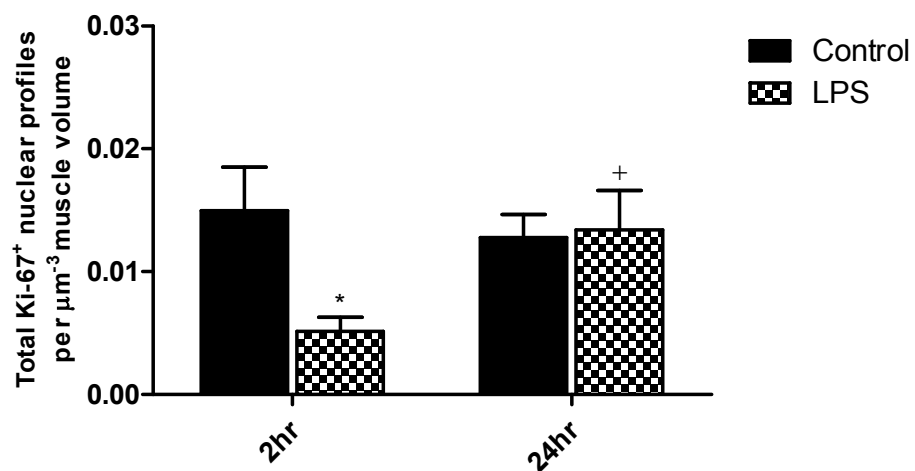


Figure 4.16c: The number of Ki67⁺ nuclei on 2 and 24hr saline and LPS treated rat EDL muscle. Nuclei containing Rolling-cycle Products (RCPs) from Bright-field Proximity Ligation Assay (PLA) for Ki67 were counted by light microscopy and expressed per volume of muscle. Data presented as mean \pm S.E.M. n=4(2hr) n=4(24hr). By Kruskal-Wallis 1-way ANOVA: significantly different from corresponding time-matched control: * p<0.05. Significantly different from 2hr LPS treated muscle: ⁺p<0.05.

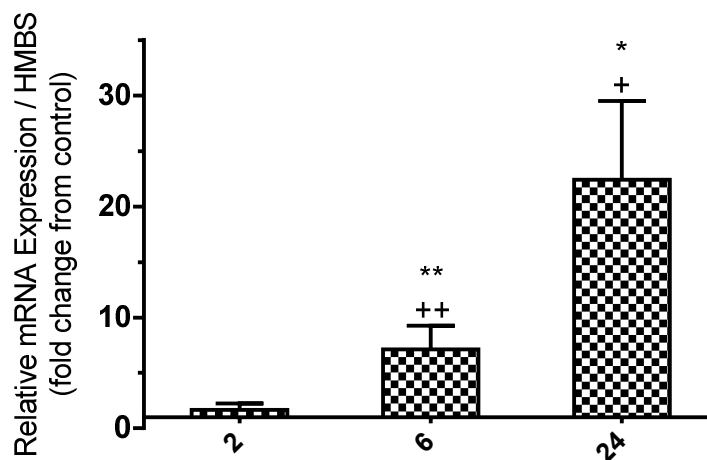


Myogenin is also a well characterised marker for satellite cells and is involved in terminal differentiation of satellite cells (Yablonka-Reuveni and Rivera 1994). Surprisingly, LPS administration significantly increased myogenin mRNA in a time dependent manner (figure 4.17). Myogenin protein also showed a tendency toward increased expression after 24hr. Myogenin protein expression was not measured in the gastrocnemius muscle because myogenin mRNA data from the gastrocnemius (figure 4.18) displayed a similar expression profile to the EDL.

Unlike myoD, which was suppressed at all time points measured, myogenin expression was increased when circulating cytokine levels were at their lowest. It appears sepsis-mediated suppression of myogenesis relies more heavily on the suppression of myoD and that myogenin levels are not influenced as greatly.

Figure 4.17: Expression of Myogenin a) mRNA and b) protein expression in EDL following 2, 6 or 24hr continuous LPS or saline infusion. a) Relative mRNA expression of saline controls was set at 1; bars denote fold change in mRNA expression from corresponding time matched control with values >1 = increased mRNA expression and <1 = decreased mRNA expression. Values are means \pm S.E.M. **b)** The densities of ~ 25 kDa myogenin immunoreactive bands were measured by western blotting and representative bands for each group are shown above their corresponding bar. $n=4$ (2, 6hr) $n=6$ (24hr). Significantly different from corresponding time matched control group: * $p<0.05$, ** $p<.005$. Significantly different from 2hr LPS treated group: + $p<0.05$, ++ $p<0.005$ by 1-way ANOVA.

a) *Myogenin mRNA expression – EDL*



b) *Myogenin protein expression*

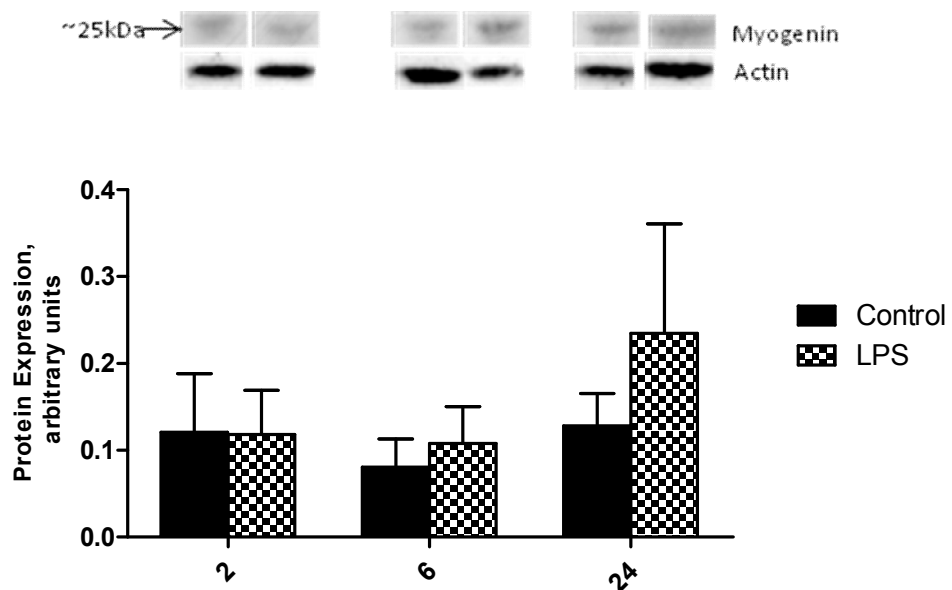
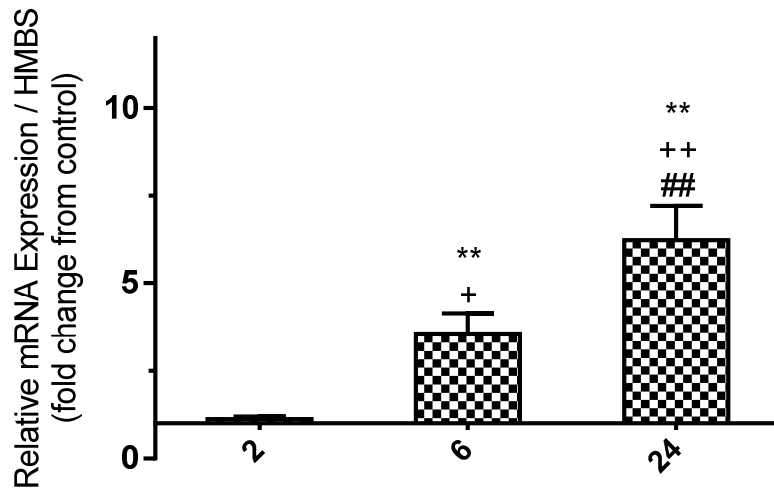


Figure 4.18: Fold changes in Myogenin mRNA expression in Gastrocnemius muscle following 2, 6 or 24hr continuous LPS or saline infusion. Relative mRNA expression of saline controls was set at 1; bars denote fold change in mRNA expression from corresponding time matched control with values >1 = increased mRNA expression and <1 = decreased mRNA expression. Values are means \pm S.E.M. n=4 (2, 6hr) n=6 (24hr). By Kruskal-Wallis 1-way ANOVA: significantly different from corresponding time matched control group: ** p<0.005. Significantly different from 2hr LPS treated group: + p<0.05, ++ p<0.005. Significantly different from 6hr LPS treated group: ## p<0.005

Myogenin mRNA expression – Gastrocnemius



4.4.5. Myostatin

Alterations in skeletal muscle mass are often associated with myostatin dysregulation (reviewed by Elkina *et al.* 2011) and a number of studies have reported an up-regulation of myostatin in conditions characterised by muscle atrophy, such as cancer (Liu *et al.* 2008) and HIV infection (Gonzalez-Cadavid *et al.* 1998). Since sepsis is associated with substantial muscle loss, myostatin mRNA and protein levels were determined to decipher its role (if any) in sepsis-mediated muscle wasting. Myostatin mRNA and protein expression was measured in gastrocnemius and EDL muscle to determine fibre type differences, since fast twitch muscle is reported to display higher susceptibility to atrophy during sepsis (Tiao *et al.* 1997) and endotoxaemia (Murton *et al.* 2009) relative to slow twitch muscles.

Cytosolic and nuclear protein were extracted and quantified by Western blotting, using densitometry, as described in chapter 2, section 2.2.5. We detected four different myostatin migrating bands in muscle cytosolic and nuclear protein fractions (see chapter 3, section 3.3.4). These are reported in the literature as the unprocessed/pro-myostatin (~55kDa), Latency-Associated-Peptide (LAP; ~40kDa), ~26kDa immuno-reactive myostatin (often referred to as a myostatin dimer) and processed/mature (12.5kDa) forms of myostatin (Thomas *et al.* 2000; Anderson *et al.* 2008).

Both the EDL and gastrocnemius muscles displayed an increase in myostatin mRNA followed by a gradual decrease; relative fold changes in mRNA compared to corresponding time matched saline controls were highest after 2hr of LPS infusion and lowest after 24hr (figure 4.19a). Additionally, the

gastrocnemius muscle appeared to be more sensitive to the toxin; the fold changes of myostatin mRNA transcript were greater.

All four species of myostatin were detected in the cytosolic fractions of EDL extracts but only the ~40kDa LAP form was detected in the nuclear fractions. Nevertheless all protein forms followed a similar expression profile to myostatin mRNA; protein levels were either unchanged or highest after 2hr of LPS and lowest after 24hr compared to controls (figure 4.19b). The exception was in the nuclear fraction where the ~40kDa LAP myostatin was increased compared to control after 6hr of infusion but was decreased after 24hr. This increase in nuclear LAP myostatin after 6hr was concomitant with a decrease in cytosolic LAP myostatin within the same time point and likely represents nuclear translocation of myostatin. Indeed, the same phenomenon is observed in the gastrocnemius muscle where a decrease in cytosolic LAP myostatin after 2hr is concomitant with an increase nuclear LAP myostatin within the same time point (figure 4.19c). It suggests this species of myostatin is shuttled to the nuclear compartment in response to LPS.

In contrast to the EDL, we only detected the ~40kDa LAP species of myostatin in the gastrocnemius muscle (figure 4.19c). This is not unexpected as some authors have speculated that myostatin may be regulated differently in different muscle tissue within the same organism (Wehling *et al.* 2000). Whilst the EDL exhibited a gradual decrease in myostatin protein across all time points, remaining tendentially low compared to control after 24 hr, the gastrocnemius showed a tendency toward a return to baseline levels of myostatin protein by 24hr. Protein levels in the cytosolic fraction were significantly low after 2hr and gradually increased whilst the opposite was seen in the nuclear fraction;

myostatin was significantly high after 2hr and gradually decreased. As mentioned above, this likely indicates nuclear translocation of myostatin, especially at the 2hr time point.

Figure 4.19a: Expression of Myostatin mRNA in EDL and gastrocnemius muscle following 2, 6 or 24hr continuous LPS or saline infusion. Relative mRNA expression of saline controls was set at 1; bars denote fold change in mRNA expression from corresponding time matched control with values >1 = increased mRNA expression and <1 = decreased mRNA expression. Values are means \pm S.E.M. n=4 (2, 6hr) n=6 (24hr). By Kruskal-Wallis 1-way ANOVA: significantly different from corresponding time matched control group: * p<0.05. Significantly different from 2hr LPS treated group: + p<0.05. Significantly different from 6hr LPS treated group: # p<0.05

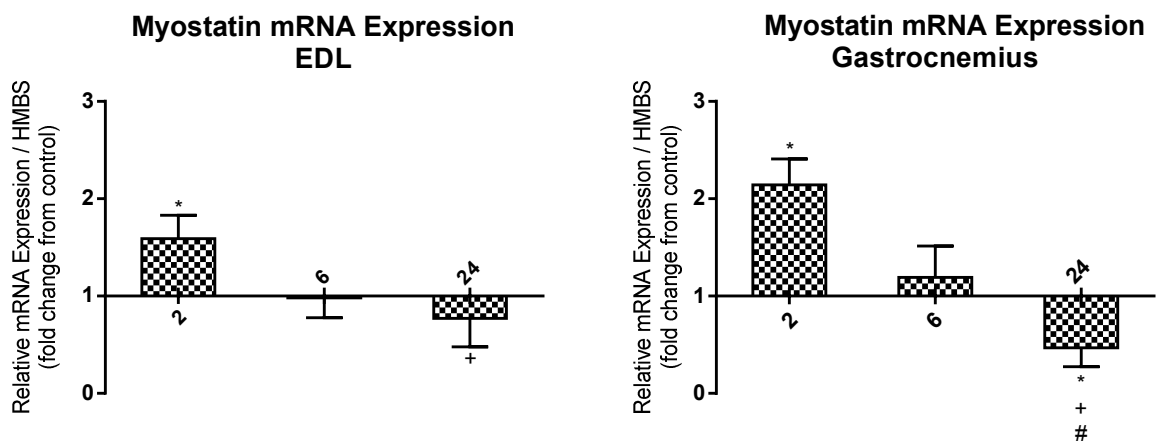


Figure 4.19b: Expression of cytosolic and nuclear Myostatin protein in EDL muscle following 2, 6 or 24hr continuous LPS or saline infusion. Values are means \pm S.E.M. The densities of myostatin immunoreactive bands were measured by western blotting and representative bands for each group are shown above their corresponding bar. n=4 (2, 6hr) n=6 (24hr). By Kruskal-Wallis 1-way ANOVA: significantly different from corresponding time matched control group: * p<0.05, ** p<0.005. Significantly different from 2hr LPS treated group: + p<0.05, ++ p<0.005. Significantly different from 6hr LPS treated group: # p<0.05, ## p<0.005

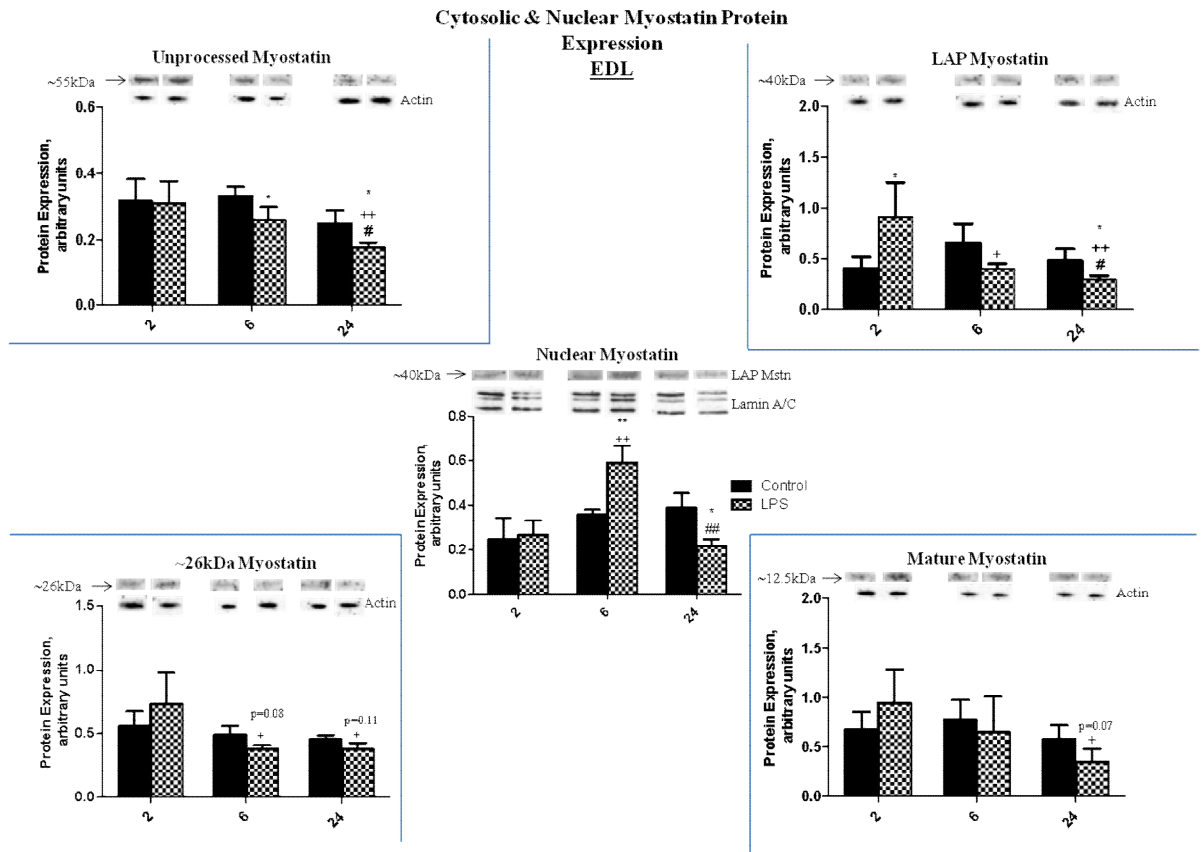
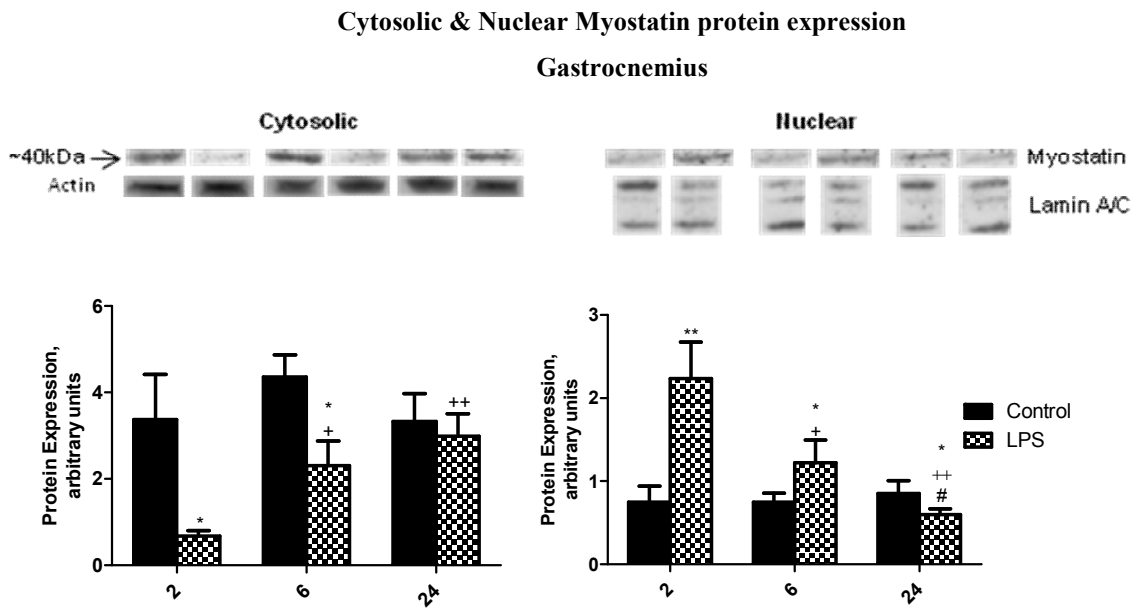


Figure 4.19c: Expression of cytosolic and nuclear Myostatin protein in gastrocnemius muscle following 2, 6 or 24hr continuous LPS or saline infusion. Values are means \pm S.E.M. The densities of \sim 40kDa LAP myostatin immunoreactive bands were measured by western blotting and representative bands for each group are shown above their corresponding bar. n=4 (2, 6hr) n=6 (24hr). By Kruskal-Wallis 1-way ANOVA: significantly different from corresponding time matched control group: * p<0.05, ** p<0.005. Significantly different from 2hr LPS treated group: ⁺ p<0.05, ⁺⁺ p<0.005. Significantly different from 6hr LPS treated group: [#] p<0.05 by 1-way ANOVA



4.5 DISCUSSION

Continuous LPS infusion resulted in the transient elevation of all three inflammatory cytokines in the EDL and gastrocnemius muscles. Whilst LPS caused a modest, time-dependent increase in NF- κ B expression, there were substantial elevations in TNF- α and IL-6, especially the latter. NF- κ B is an important mediator of LPS effects and inflammatory induction (reviewed in Muller *et al.* 1993; Guha and Mackman 2001); therefore it appears pertinent that modest increases in its expression are sufficient to induce considerable increases in its downstream effectors, most notably TNF- α and IL-6. These results are similar to the findings by Waller *et al.* (1995), where in an identical model, an early (1-2hr) elevation in plasma TNF- α was noted. Likewise, Alamdari *et al.* (2008) and Murton *et al.* (2009) observed a similar expression profile for TNF- α and IL-6.

LPS rapidly induces these cytokines and plasma levels peak after 2 hrs but such elevations are transient due to tight regulatory mechanisms and a limited half life. For example, TNF- α is highly unstable with an approximate half-life of 6-7 minutes; it is rapidly degraded after binding and a highly specific radio-iodinated assay for TNF- α developed by Beutler *et al.* (1985b) showed that it is quickly absorbed by the liver, kidney and gastro-intestinal tract to achieve rapid plasma clearance. As a result, additional release of LPS-induced inflammatory cytokines is most dramatic in the initial phase just after the appearance of endotoxin. Consequently, consecutive or continuous administration of LPS to rats show a reduction in effect after initial

administration (Waage 1987) and alterations in signalling are blunted by 24 hours (el-Dwairi *et al.* 1998).

These increases in inflammatory cytokines were partly due to increased muscle macrophage infiltration. Using a well characterised macrophage/microglia specific marker (Iba-1), we demonstrated increased numbers of macrophages in the EDL and gastrocnemius muscles. This was concomitant with increased Iba-1 protein expression and macrophage activation. In addition, approximately 60% of Iba-1 positive macrophages co-localised with TNF- α ; thus confirming that macrophages were a major source of cytokine production in muscle during endotoxaemia. Skeletal muscle recruitment of macrophages is normally a protective phenomenon; they are essential for triggering muscle regeneration following injury via phagocytosis of cellular debris and stimulation of myoblast proliferation (reviewed in Chazaud *et al.* 2009). However, excessive LPS induced macrophage infiltration during endotoxaemia contributes and perpetuates the inflammatory response by increasing macrophage activation, thus increasing the production of inflammatory cytokines, which in turn mediate many of the derangements in muscle homeostasis. Indeed, many of the alterations to muscle homeostasis observed with LPS administration can be replicated with administration of inflammatory cytokines such as TNF- α and interleukins; these changes are likely to be due to a cascade of events such as the induction of nitric oxide synthase triggered by cytokines (Gardiner *et al.* 1998). It is worth noting that macrophages are not the only source of cytokine production in rat skeletal muscle (Borge *et al.* 2009); TNF- α was also produced locally by myocytes during endotoxaemia and likely contributes to the inflammatory milieu.

Transient elevations of inflammatory cytokines in the EDL and gastrocnemius muscles had a direct, time and dose-dependent impact on satellite cell specific markers. At the time points at which cytokine expression was highest (i.e. 2hr), myogenic regulatory factors pax7, myoD and myogenin, were more dramatically altered. High levels of cytokines transiently suppressed the expression of pax7 and the number of pax7⁺ resident satellite cells. Whether the reduction in pax7⁺ satellite cells is due to apoptosis or transient repression of pax7 transcription is undetermined but elevated cytokines, especially TNF- α has been implicated in pax7 dysregulation.

A study by Palacois *et al.* (2010) showed that TNF- α activated p38 α MAPK and promoted polycomb repressive complex silencing of the pax7 promoter. Silencing pax7 allows satellite cell differentiation to proceed as pax7 is known to induce inhibitors of differentiation (Id proteins), which transcriptionally repress the induction of myogenic basic Helix Loop Helix (bHLH) proteins, thus maintaining a state of quiescence (Kumar *et al.* 2009). TNF- α is also implicated in preferential apoptosis of satellite cells, denoted by a steady increase in caspase-8 activity when C2 cells are cultured *in vitro* to mimic muscle wasting (Stewart *et al.* 2004) and the increased susceptibility of satellite cells from old animals to apoptosis compared to young due to raised plasma TNF- α (Jejurikar *et al.* 2006).

Whilst pax7 expression and pax7⁺ satellite cell numbers showed a tendency toward a return to basal levels by 24hr of LPS infusion, myoD expression and myoD⁺ satellite cells remained suppressed relative to control at this time point. It is tempting to speculate that the modest increase in cytokines, observed after

24hr relative to earlier time points sampled, was still sufficient to continuously down-regulate myoD and suppress satellite cell activation. MyoD suppression is frequently implicated as a major patho-mechanism in the development of critical illness myopathy (reviewed by Friedrich 2006). Down-regulation of myoD in inflammatory conditions is thought to occur through TNF- α and NF- κ B dependent mechanisms; TNF- α induced activation of NF- κ B suppressed C2C12 myoblasts and constitutive *in vivo* expression of TNF- α in mouse muscle down-regulated myoD mRNA (Guttridge *et al.* 2000). NF- κ B is able to check satellite cell myogenesis by stimulating cyclin D1 at the level of the promoter, thus maintaining hyperphosphorylated pRb and cell cycle progression (Guttridge *et al.* 1999; Mitin *et al.* 2001). TNF- α and NF- κ B-mediated suppression of satellite cells also results in the loss of myoD protein through increased destabilisation and proteolysis via the ubiquitin proteasome pathway (Langen *et al.* 2004). As well as contributing to muscle wasting, this could have serious consequences for subsequent muscle regeneration, as myoD regulates the expression of myofibrillar proteins and loss of myoD can lead to further down-regulation of myosin (Acharyya *et al.* 2004).

The levels of myogenin were unaltered relative to control at the 2hr time point when cytokine levels were at their highest and were increased after 6hr and 24hr of LPS when circulating cytokines were attenuated. TNF- α also is a known inhibitor of myogenin (Layne and Farmer 1999) but 'physiological' levels added to medium have been shown to stimulate myogenic differentiation via activation of the p38 MAPK pathway, stimulation of Myocyte Enhancer Factor 2C (MEF2C), myogenin, p21 and MHC in C2C12 myoblasts (Chen *et al.* 2007). TNF- α mediated effects on myogenesis assume divergent fates and

its ability to either inhibit or stimulate myogenin is partly concentration and time-dependent. As a result, it is the considered paradigm that TNF- α mediated suppression of myogenesis relies more heavily on the suppression of myoD and myogenin levels only play a minor role (Wieteska-Skrzeczynska *et al.* 2011). Decreased NF- κ B activity is also associated with increased myoblast differentiation (Guttridge *et al.* 1999) and taken together, this likely explains the time-lagged induction of myogenin – expression was highest with reduced cytokines.

As mentioned in section 4.2, the exact role of IL-6 in myogenic regulation during endotoxaemia is not apparent. Whilst clear roles for TNF- α and NF- κ B in the regulation of satellite cell activity in cachectic muscle wasting have been described, that of IL-6 maybe more complicated; a possible function of IL-6 during endotoxaemia is the suppression of TNF- α (Clowes *et al.* 1983) - a protective anti-inflammatory phenomenon that may be necessary for the stimulation of muscle regeneration following atrophy. This is supported, albeit loosely, by its association with *in vivo* protection in cardiac muscle (Smart *et al.* 2006). IL-6 is also thought to play an anti-inflammatory role during exercise (Pedersen *et al.* 2003) and staphylococcal enterotoxaemia (Matthys *et al.* 1995) essentially by inhibiting TNF- α production and negatively regulating acute phase proteins (Tilg *et al.* 1997). However, the most widely accepted paradigm is that IL-6 modulates the inflammatory response and facilitates cachectic muscle wasting; for example, by shortening the half life of long lived proteins through activation of proteolytic pathways (Ebisui *et al.* 1995). However, as much evidence exists for (Ebisui *et al.* 1995; Tsujinaka *et al.* 1996; Haddad *et*

al. 2005) as well as against (Garcia-Martinez *et al.* 1994; Williams *et al.* 1998; Serrano *et al.* 2008) the involvement of IL-6 in muscle wasting.

An elevation in circulating IL-6 is observed in many disease states as well as in the elderly and healthy individuals, especially after intense or pro-longed exercise. Its role within the context of skeletal muscle may be multifunctional; it has disparately been reported to regulate carbohydrate and lipid metabolism, cause muscle atrophy or increase satellite cell proliferation. We found evidence of the latter by using Ki-67, a marker of proliferation to assess the proliferative status of muscle during endotoxaemia. The gastrocnemius muscle displayed high Ki-67 mRNA expression at peak cytokine levels, after 2hrs of LPS; likewise, the EDL displayed a time-lagged increase in Ki-67 mRNA after 24hr of infusion but whether this was directly IL-6 mediated is undetermined. It does however support the notion previously reported by our group that a reduction in the protein-to-DNA ratio (Gamrin *et al.* 1996), an index of net muscle protein mass (i.e. reduced alkaline soluble protein content and increased DNA content) accompanies endotoxaemia in the EDL muscle after 24hr LPS infusion (Crossland *et al.* 2008; Murton *et al.* 2009).

IL-6 is known to promote satellite cell proliferation via activating c-Myc in a STAT3-dependent manner. Thus regulating cell cycle kinetics (through up-regulation of numerous cyclins and down-regulation of p21), which are involved in the G1 cell growth phase (Toth *et al.* 2011). Indeed, an increase in IL-6 protein in satellite cells following muscle damage was concomitant with increased cyclin D1 expression and satellite cell number (McKay *et al.* 2009). Furthermore, IL-6 knockout mice display impaired satellite cell proliferation

and myonuclear accretion in a STAT3-cyclin D1-dependent manner (Serrano et al. 2008). TNF- α also differentially influences satellite cell proliferation (Szalay *et al.* 1997; Layne and Farmer 1999). Satellite cells exposed to inflammatory milieu may be able to proliferate (evident in the gastrocnemius muscle at the 2hr time point for Ki-67 mRNA expression), but not necessarily proceed toward differentiation (evident by myoD suppression in the same muscle at the same time point of sampling). It is possible that fluctuations between high cytokine-low MRF expression and low/basal cytokine-high MRF expression, ultimately tips the balance between satellite cell quiescence, growth or apoptosis.

The expression profile of myostatin, a negative regulator of satellite cell activity, displayed the most congruent evidence of direct cytokine action on muscle homeostasis. Both its mRNA and protein expression were directly correlated with TNF- α , IL-6 and NF- κ B expression; myostatin was up-regulated when these cytokines were at their peak, i.e. 2hr after LPS infusion and the gradual reduction in cytokine elevation was congruent with reduced myostatin. NF- κ B directly influences myostatin regulation by binding to putative NF- κ B responsive elements in the 5' regulatory region of the myostatin promoter (Ma *et al.* 2001). Myostatin is often up-regulated following stress in an extracellular signal-regulated kinase (ERK)-dependent manner (Bish *et al.* 2010), therefore it is not surprising that the initial endotoxin insult and dramatic elevation of inflammatory cytokines resulted in an increase in myostatin mRNA and protein after 2 hours of infusion.

The early increase in myostatin may be responsible for the suppression of the satellite cell markers pax7 and myoD, which were also suppressed by early peak elevations of cytokines after 2hr of LPS. It is likely myostatin had a direct negative effect on satellite cell activity during the early stages of endotoxaemia, and the reductions in pax7 and myoD was one such consequence of cytokine-mediated myostatin up-regulation. Indeed, one of the known downstream targets of myostatin (through smad signalling) is myoD; down-regulation of myoD had been demonstrated during cachexia via TNF- α mediated NF- κ B dependent and independent pathways (Dogra *et al.* 2006; McFarlane *et al.* 2006).

Myostatin also inhibits pax7 expression in an ERK1/2-MAPK-dependent manner and the genetic inactivation or functional antagonism of myostatin resulted in an increase in pax7 expression. Thus increased expression of myostatin negatively influences satellite cell activation, proliferation and self renewal (McFarlane *et al.* 2008). The direct action of myostatin on pax7 and myoD promoter activity (McFarlane *et al.* 2006; McFarlane *et al.* 2008) is supported by its increased nuclear translocation following LPS infusion. Its increased nuclear localization suggests myostatin may play more of a transcriptional role during the early stages of endotoxaemia, to modulate the transcription of genes essential for satellite cell activation, self renewal and differentiation.

The return to basal and reduced expression of myostatin after 6 and 24 hr of LPS respectively, saw a return to basal levels of pax7 expression whilst myoD remained low. In addition to the myostatin mediated suppression of myoD,

other factors such as TNF- α and NF- κ B also directly contribute to its mRNA destabilisation and protein degradation (Guttridge *et al.* 2000; Langen *et al.* 2004); as a result, the attenuation of myostatin signalling is insufficient to return myoD to basal levels of expression. As mentioned above, such an inhibition could have serious consequences for subsequent muscle growth and repair following inflammation-associated muscle wasting; the work of Langen *et al.* (2004) showed that TNF- α mediated suppression of myoD (through NF- κ B signalling) inhibited myogenic differentiation, interfered with muscle regeneration and contributed to muscle wasting. The same authors also found that in a murine model of chronic pulmonary inflammation, muscle wasting (indicated by decreased body weight) and elevated inflammatory cytokines were concomitant with attenuated satellite cell activity and impaired muscle regeneration (Langen *et al.* 2006).

Finally, a consistent observation throughout this study was the differential response of the fast twitch EDL and mixed fibre type gastrocnemius muscle to LPS infusion. As mentioned above, the gastrocnemius was more sensitive to LPS and this likely reflects its higher degree of vascularisation compared to the EDL. Capillary architecture is muscle specific; slow fibres being more oxidative, tend to have higher capillary density than fast fibres which are more glycolytic. The density and distribution of the microvascular supply in different muscles parallels their metabolic demand (Egginton 2011) and the heterogeneity in microvascular supply of different muscles reflect differences in fibre type composition and mechanical load, ultimately to normalise the ratio of oxygen delivery to consumption. Hence, the ratio of capillaries-to-fibre in muscles involved in locomotion increases with the proportion of oxidative

fibres (reviewed by Hudlicka 1985). The gastrocnemius muscle, being of mixed fibre type composition requires greater oxygen delivery compared to the EDL and thus displays increased blood flow (Gray and Renkin 1978), which facilitates increased delivery and removal of endotoxin. As a result, the gastrocnemius muscle responded to the toxin infusion earlier, at a greater magnitude and in some instances (e.g. pax7 expression) showed a tendency toward earlier recovery than the EDL.

In summary, we have described the effects of continuous LPS infusion on the expression profile of three key cytokine markers of systemic inflammation and the resulting impairment of satellite cell activity. Modest increases in cytokine expression help rather than impair the regenerative process and the apparent contradiction to their action on satellite cell inhibition may be explained by the fact that their effects are concentration and time dependent. It is believed satellite cells play a vital role in maintaining muscle homeostasis, modulating the balance between muscle growth and loss. LPS, through its induction of excessive cytokine production, tips that balance such that pathogenic alterations that instigate muscle loss compromise the satellite cell microenvironment and thus satellite cell function; leading to less effective muscle homeostasis, which in turn could have consequences for muscle regeneration or growth following sepsi- induced muscle atrophy.

CHAPTER 5

Results (III)

Co-infusion of low dose dexamethasone is additive to lipopolysaccharide induced myogenic suppression

5.1 SUMMARY

Results from the study presented in chapter 4 suggested a role for LPS-induced elevations in inflammatory cytokines, in the suppression of skeletal muscle myogenesis, via the down-regulation of key satellite cell transcripts such as pax7 and myoD. Strategies aimed at suppressing elevated inflammatory cytokines, such as low dose glucocorticoid therapy, could be beneficial in increasing survival from severe sepsis. Therefore, we examined whether administration of low dose dexamethasone (equivalent to 300µg/kg/day - less than half the dose reported to induce muscle atrophy), would prevent elevations in inflammatory cytokines and thereby reduce LPS-induced myogenic suppression.

Male Sprague-Dawley rats were continuously infused with saline (0.4ml/hr, i.v.), LPS (15 µg/kg/hr), Dex (12.5µg/kg/hr.) or Dex+LPS, intravenously, for 24hr (n=7-8 per group). Animals were terminally anaesthetised and EDL muscles were removed, snap-frozen and stored in liquid nitrogen for analysis of mRNA and protein expression of markers for systemic inflammation and satellite cell myogenesis.

Dex infusion during endotoxaemia caused a reduction in LPS-induced up-regulation of muscle TNF- α , IL-6 and NF- κ B mRNA expression. Dex blunted the LPS-induced increase of the macrophage marker, Iba-1. However, Dex infusion suppressed pax7 and myoD mRNA and protein expression. Dex+LPS co-infusion resulted in an additive effect on satellite cell myogenic suppression, greater than that elicited by either substance alone. Dex caused a reduction in myogenin and blunted the LPS-induced increase in myogenin.

Combined Dex+LPS infusion resulted in additional suppression of myostatin mRNA and protein after 24hr compared to the LPS or Dex only groups.

We concluded that low dose dexamethasone had an anti-inflammatory effect by suppressing transcript levels of inflammatory cytokines and inhibiting muscle macrophage infiltration. However, the suppression of inflammation had consequences for satellite cell myogenesis, which can benefit from modest muscle inflammation (for e.g. during muscle regeneration from injury). Therefore, negative regulation of satellite cells by glucocorticoids could impede their efficacy in the treatment of inflammatory muscle disorders.

5.2 INTRODUCTION

The previous chapter described the effects of lipopolysaccharide (LPS) on satellite cell myogenic activity during the early stage of endotoxaemia. LPS transiently suppressed satellite cell specific markers by modulating inflammatory cytokine expression through the increased recruitment of macrophages (see chapter 4). Glucocorticoids are frequently proposed in the treatment of sepsis and inflammatory muscle myopathies, due to their ability to prevent excessive cytokine production and reduce some of the symptoms associated with systemic inflammatory response syndrome (reviewed by Rhen and Cidlowski 2005). Glucocorticoid-mediated down-regulation of systemic inflammation can restore homeostasis, decrease morbidity and improve survival of septic patients when low to moderate doses are used (reviewed in Meduri *et al.* 2009).

Glucocorticoids are able activate gene transcription of target genes by binding to glucocorticoid receptors in the cytosolic compartment, thereby forming a complex. This translocates to the nucleus and binds to Glucocorticoid Response Elements (GRE) in the promoter of target genes for transcriptional activation (e.g. anti-inflammatory IL-10, IL-10R, TGF- β , etc) and in some instances, transcriptional repression (e.g. pro-inflammatory IL-1, TNF receptors, NF-kB, etc) of specific transcription factors involved in stress related homeostasis (Galon *et al.* 2002). Activation of cytoplasmic glucocorticoid receptors by endogenous (e.g. cortisol from increased adrenocorticotrophic hormone (ACTH) activity and Hypothalamic-Pituitary-Adrenal (HPA) axis stimulation) or exogenous synthetic glucocorticoids (e.g.

dexamethasone) administration limits the inflammatory response by aiding antigen clearing, stimulating cell trafficking and scavenger systems, whilst halting cellular immune responses by inhibiting antigen presentation and T-cell activation.

Glucocorticoids have been shown to have a variety of effects on skeletal muscle growth and metabolism, most notably in inflammatory myopathies such as Duchenne muscular dystrophy (DMD), where long-lasting benefits such as increased muscle strength and function are noted. Since DMD involves repeated cycles of muscle injury and regeneration, these beneficial effects have been attributed to reduced muscle inflammation and the suppression of cytotoxic cells (reviewed by Bogdanovich *et al.* 2004). In addition, glucocorticoids have been reported to stimulate myoblast proliferation and differentiation in culture (Ball and Sanwal 1980; Guerriero and Florini 1980) and daily administration of the glucocorticoid prednisone increased the proliferative activity of satellite cells and demonstrated a protective effect on exercise induced muscle fibre damage in a rodent exercise model (Jacobs *et al.* 1996).

However studies depicting negative effects on skeletal muscle, predominantly muscle catabolism can also be found; for example increased proteolytic activity is observed in many animal and human models where glucocorticoids are administered (reviewed by Tisdale 2007). Furthermore, glucocorticoid levels are elevated in muscle wasting conditions and are associated with the up-regulation of atrogenes *in vivo* and *in vitro* (Cassano *et al.* 2009). The catabolic actions of glucocorticoids on skeletal muscle are thought to occur via stimulation of protein degradative, and suppression of protein synthetic

pathways (reviewed by Schakman *et al.* 2008). As a result, the use of glucocorticoids in the treatment of sepsis has remained contentious and it is currently hypothesised that the diametric effects observed are dependent on the dose, as well as the type of glucocorticoid administered. High doses of dexamethasone (equivalent to 700µg/kg/day or more) are known to cause muscle atrophy in rats (Tiao *et al.* 1996; Zhao *et al.* 2008). This is characterised by large increases in the rate of muscle protein breakdown (Auclair *et al.* 1997; Chrysis and Underwood 1999) and negative regulation of protein synthetic machinery (Shah *et al.* 2000).

However, given the evidence supporting a role for elevated pro-inflammatory cytokines in the aetiology of muscle wasting (reviewed by Spate and Schulze 2004), strategies aimed at suppressing increases in pro-inflammatory cytokines without compromising muscle recovery could be beneficial in the treatment of sepsis. Previous work done by our group demonstrated that a low dose of dexamethasone (equivalent to 300µg/kg/day) is sufficient for suppressing pro-inflammatory cytokine mRNA levels without producing the catabolic effects associated with higher doses of glucocorticoids (Crossland *et al.* 2010).

Therefore the aims of this study were two-fold; to examine the effects of low dose dexamethasone on satellite cell activity, when administered continuously for 24 hours and its influence on cytokine mediated myogenic suppression when administered one hour before and during LPS infusion.

5.3 METHODS

5.3.1 Animals and tissue collection

All animal work was carried out as described in section chapter 2, section 2.1.3. Briefly, Male Sprague-Dawley rats (380-480g; Charles River) were anaesthetised with fetanyl citrate (300µg/kg; i.p., Janssen-Cilag) and medetomidine (300µg/kg; i.p., Domitor, Pfizer) and implanted with intravenous catheters for administration of substances. Under anaesthesia, animals were fitted with a harness to allow unrestricted movement. Anaesthesia was reversed with atipamezole (1mg/kg; s.c., Antisedan, Pfizer), analgesia was provided (buprenorphine; 0.03 mg/kg, s.c., Vetergesic; Alstoe Animal Health) and animals were left to recover for 24 hours (with access to food and water) before the commencement of experiments. The venous line was connected to an infusion pump via a fluid filled swivel, which maintained a continuous intravenous infusion of sterile heparinised saline (15U/ml) at 0.4ml/hr to maintain catheter patency.

Following catheterization, prepared rats were assigned to one of four groups (n=7-8 per group) and received a continuous intravenous infusions of sterile isotonic saline (0.4ml/hr) as control, LPS (15µg/kg/hr; *E. coli*, serotype 0127:B8, Sigma Aldrich), Dex (12.5µg/kg/hr; Sigma Aldrich) or Dex+LPS simultaneously. Dex was administered for 1hr before and throughout the 24hr infusion. After 24hr, animals were terminally anaesthetised (sodium pentobarbital (inactin); 80 mg/kg, i.v.) and the EDL muscle was freeze

clamped and removed. Muscles were immediately snap-frozen and stored in liquid nitrogen for subsequent analyses.

5.3.2 mRNA measurements (real-time PCR)

Real time PCR was carried out as described in section chapter 2, section 2.2.1 and chapter 4, section 4.3.2 for the transcripts listed in table 5.1. All Taqman primer/probe sets were obtained from Applied Biosystems. Reactions were carried out in an ABI Prism 7000 sequence detection system in duplicate; each well contained 2µl cDNA template, 12.5µl PCR master mix and 1.25µl primer/probe mix in a 25µl reaction volume, the latter of which had final concentrations of 900nM for each primer and 250nM for the Taqman probe. Relative quantification of gene expression between control and treated groups was calculated using the $2^{-\Delta\Delta C_t}$ method. The saline control group was given a value of 1 and fold changes in mRNA expression of treated groups were calculated relative to the control group. Thus values >1 or <1 indicate an increase or decrease in mRNA expression from control respectively.

5.3.3 Protein Measurements (Western Blotting)

Protein extraction and western blotting was carried out as previously described in chapter 2, section 2.2.5 and chapters 3-4, to determine protein expression of the targets listed in table 5.2

Table 5.1: Catalogue and Unigene Numbers for Taqman Primer/Probes sets

Gene	Catalogue Number	Unigene Number
HMBS	Rn00565886_m1	Rn.11080
TNF-a	Rn00562055_m1	Rn.2275
IL-6	Rn00561420_m1	Rn.9873
NFkB1	Rn01399583_m1	Rn.2411
Pax7	Rn00834076_m1	Rn.226327
MyoD1	Rn00598571_m1	Rn.9493
Myogenin	Rn00567418_m1	Rn.9465
Myostatin	Rn00569683_m1	Rn.44460

Table 5.2: Primary and secondary antibodies used in the Western blotting protocol.

Primary Antibody	Supplier	Dilution
Goat Anti-TNFα pAb	R&D Systems Mineapolis, USA	1:500
Goat Anti-IL-6 pAb	R&D Systems Mineapolis, USA	1:500
Rabbit Anti-NFκB p105/p50 [E381] mAb	Abcam Cambridge UK	1:2500
Rabbit Anti-Iba1 pAb	Wako Osaka, Japan	1:500
Mouse Anti-Pax7 mAb	DSHB Iowa City, IA, USA	1:500
Rabbit Anti-MyoD (C-20) pAb	Santa Cruz Biotechnology Santa Cruz, CA, USA	1:500
Mouse Anti-Myogenin mAb	DSHB Iowa City, IA, USA	1:500
Rabbit Anti-Myostatin, Near C-terminus pAb	Millipore Billerica, MA, USA	1:250

Secondary Antibody	Supplier	Dilution
Rabbit Anti-Goat Immunoglobulins/HRP pAb	Dako Glostrup, Denmark	1:2000
Swine Anti-Rabbit Immunoglobuline/HRP pAb	Dako Glostrup, Denmark	1:2000
Rabbit Anti-Mouse Immunoglobulins/HRP pAb	Dako Glostrup, Denmark	1:2000

5.3.4 Statistical Analyses

As reported in the previous study, not all data obtained were consistent with a Gaussian distribution; slight deviations from the Gaussian ideal (i.e., skewness of data) were noted in frequency distribution plots of some data sets. Therefore, a non parametric statistical test was used - the Kruskal-Wallis one-way analysis of variance (ANOVA), followed by the Dunn's multiple comparison test to compare differences between saline control and treatment (e.g., Saline vs Dex) and between different treated groups (LPS vs Dex). All data are presented as the mean \pm standard error of the mean (S.E.M) and significance was accepted at the 5% level ($p < 0.05$).

5.4 RESULTS

5.4.1 Cytokines

As reported in chapter 4, 24hr of LPS infusion elevated TNF- α mRNA expression but there was a decrease in protein relative to saline control, which likely represents increased proteolytic processing of the ~26kDa membrane bound protein by TACE enzymes. Dex infusion significantly decreased TNF- α mRNA expression and a co-infusion of Dex 1hr before and during LPS infusion prevented LPS induced elevation in TNF- α mRNA (figure 5.1).

Although Dex suppressed LPS mediated increase in TNF- α mRNA, it did not significantly alter its protein expression compared to saline control.

Dexamethasone infusion significantly reduced IL-6 mRNA compared to saline control and blunted LPS-induced increase in IL-6 mRNA expression, when both substances were co-administered. However, infusion of either substance did not significantly alter IL-6 protein expression (figure 5.2).

LPS infusion resulted in a tendency toward an increase in NF- κ B mRNA expression, which was significantly reduced by Dex infusion relative to saline control. Co-infusion of both substances attenuated the LPS-mediated increase in NF- κ B mRNA (figure 5.3). No significant changes were detected in NF- κ B p105 protein expression but the p50 subunit protein expression showed a tendency toward an increase after LPS infusion ($p \sim 0.18$ vs. saline). Dex infusion alone elicited no significant change on p50 protein relative to control.

Dexamethasone suppression of NF- κ B is thought to occur at the mRNA transcriptional level, via two main mechanisms; activated glucocorticoid receptors bind to GREs and up-regulate I κ B gene expression, thereby increasing the levels of the NF- κ B inhibitor and allowing increased cytoplasmic retention (Scheinman *et al.* 1995). Another principal mechanism of suppression occurs via ligand-bound glucocorticoid receptors, which interact directly with cytosolic NF- κ B subunits (e.g. p65), and down-regulate their trans-activation potential without affecting DNA binding capability (Ray and Prefontaine 1994).

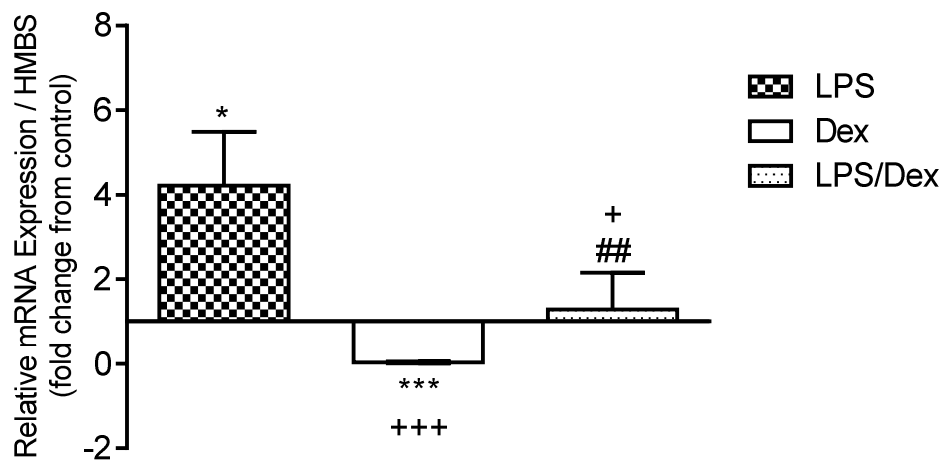
Co-infusion of LPS and Dex caused an increase in p50 protein expression. This suggests dexamethasone suppressed NF- κ B mRNA transcription but had limited influence on its protein pool. LPS increased NF- κ B mRNA and protein synthesis (also see chapter 4, section 4.4.1) but it appears that dexamethasone, whilst able to regulate further protein synthesis by suppressing mRNA transcription, did not negatively regulate the NF- κ B protein pool.

As discussed in the last chapter, some of the changes in cytokine expression can be attributed to muscle macrophage infiltration. We measured the protein expression of the macrophage marker Iba-1 in saline and treated samples, to determine the magnitude of infiltration based on the expression of Iba-1 protein by Western blotting. There was a slight increase ($p \sim 0.08$) in Iba-1 protein expression in LPS treated samples (figure 5.4). Dex infusion caused a significant reduction in Iba-1 protein relative to saline control and blunted Iba-1 expression in LPS+Dex treated samples. It appears that the immune

suppressing actions of dexamethasone may also have an effect on macrophages.

Figure 5.1: Expression of Tumour TNF- α a) mRNA and b) protein expression in EDL muscle following 24hr continuous intravenous infusions of either saline, LPS, Dex or both (Dex/LPS). a) Relative mRNA expression of saline controls was set at 1; bars denote fold change in mRNA expression from saline control with values >1 = increased mRNA expression and <1 = decreased mRNA expression. Values are means \pm S.E.M. b) The densities of \sim 26kDa TNF- α immunoreactive bands were measured by western blotting and representative bands for each treatment group are shown above their corresponding bar. n=7-8 per group. By Kruskal-Wallis 1-way ANOVA: significantly different from saline group: * $p<0.05$, * $p<0.0005$. Significantly different from LPS-treated group: + $p<0.05$, +++ $p<0.0005$. Significantly different from Dex-treated group: ## $p<0.005$.**

a) *TNF- α mRNA expression*



b) *TNF- α protein expression*

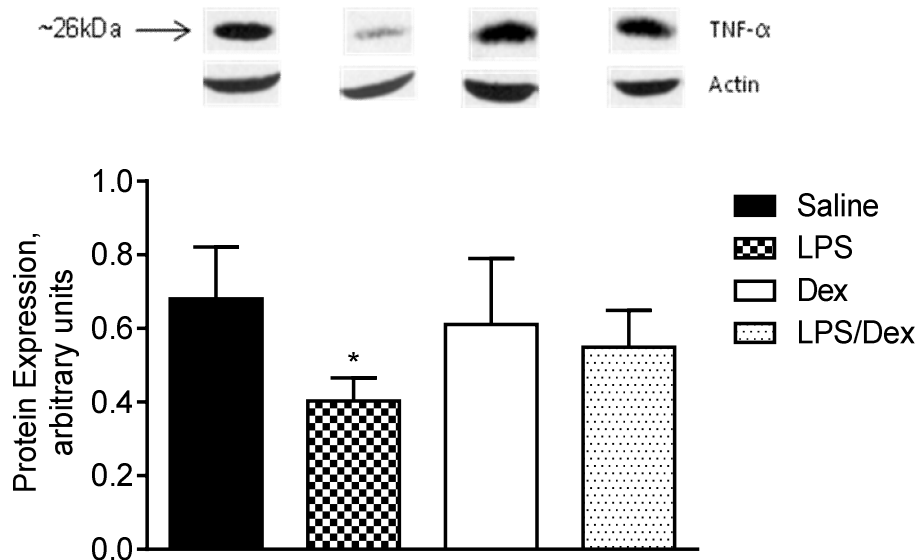
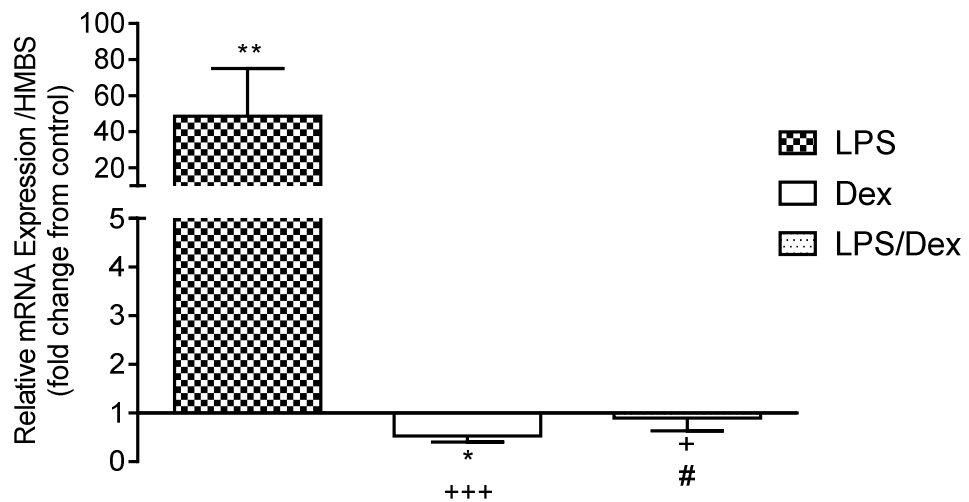


Figure 5.2: Expression of IL-6 a) mRNA and b) protein EDL muscle following 24hr continuous intravenous infusion of either saline, LPS, Dex or both (Dex/LPS). a) Relative mRNA expression of saline controls was set at 1; bars denote fold change in mRNA expression from saline control with values >1 = increased mRNA expression and <1 = decreased mRNA expression. Values are means \pm S.E.M. b) The densities of ~24kDa IL-6 immunoreactive bands were measured by western blotting and representative bands for each treatment group are shown above their corresponding bar. n=7-8 per group. By Kruskal-Wallis 1-way ANOVA: significantly different from saline group: * p<0.05, ** p<0.005. Significantly different from LPS-treated group: + p<0.05, +++ p<0.0005. Significantly different from Dex-treated group: # p<0.05.

a) *IL-6 mRNA expression*



b) *IL-6 protein expression*

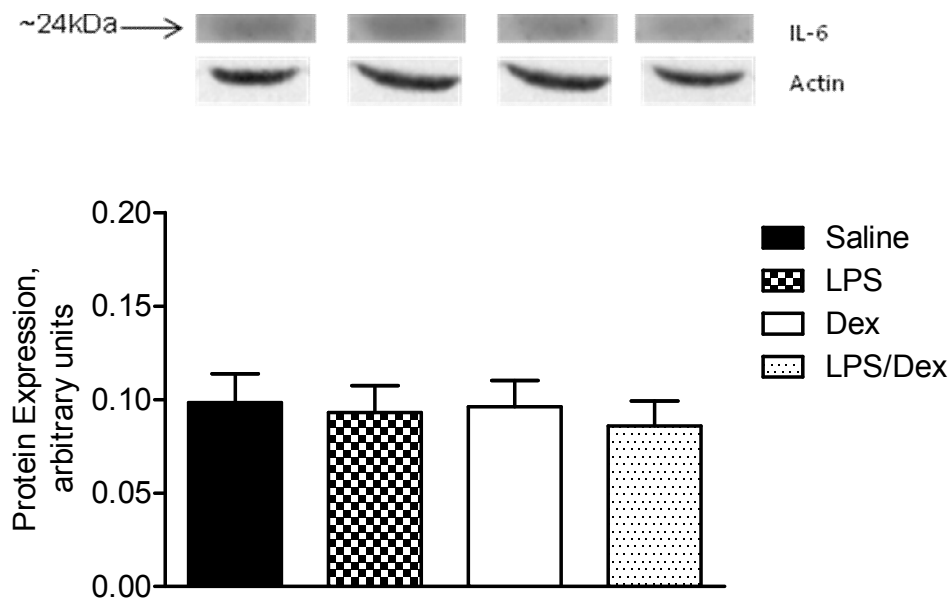
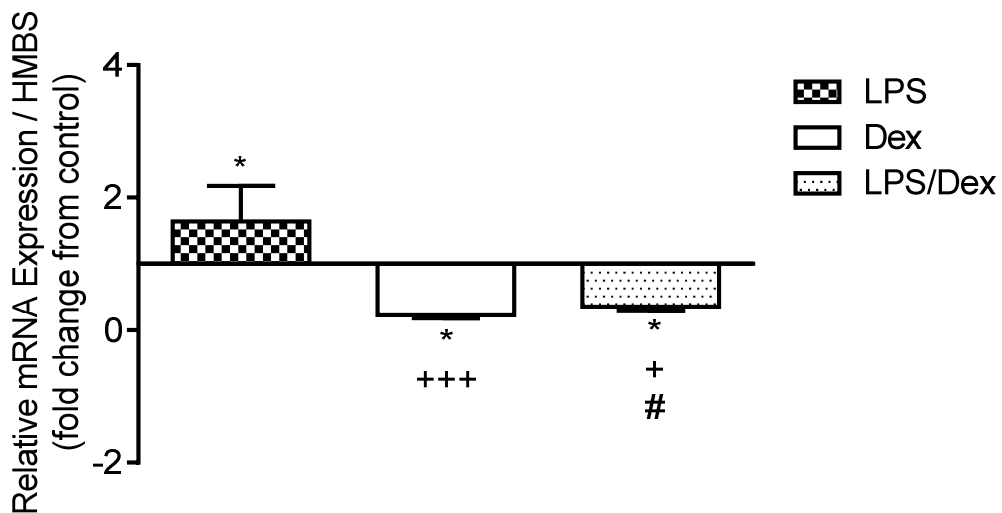


Figure 5.3: Expression of NF κ B a) mRNA and b) protein in EDL muscle following 24hr continuous intravenous infusion of either saline, LPS, Dex or both (Dex/LPS). a) Relative mRNA expression of saline controls was set at 1; bars denote fold change in mRNA expression from saline control with values >1 = increased mRNA expression and <1 = decreased mRNA expression. Values are means \pm S.E.M. b) The densities of ~ 105 kDa and ~ 50 kDa NF- κ B immunoreactive bands were measured by western blotting and representative bands for each treatment group are shown above their corresponding bar. n=7-8 per group. By Kruskal-Wallis 1-way ANOVA: significantly different from saline group: * $p < 0.05$. Significantly different from LPS-treated group: + $p < 0.05$, +++ $p < 0.0005$. Significantly different from Dex-treated group: # $p < 0.05$.

a) *NF κ B mRNA expression*



b) *NF κ B protein expression*

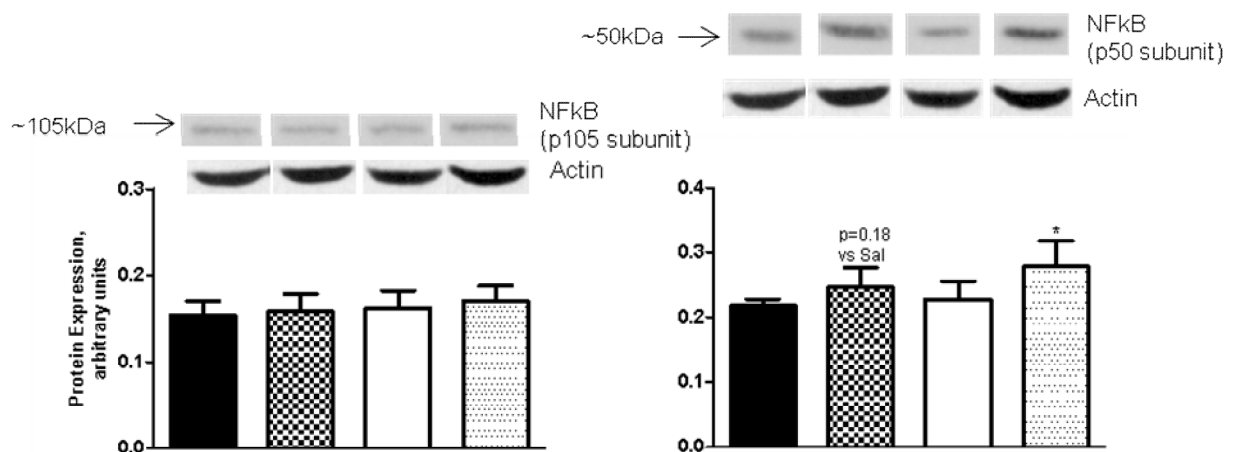
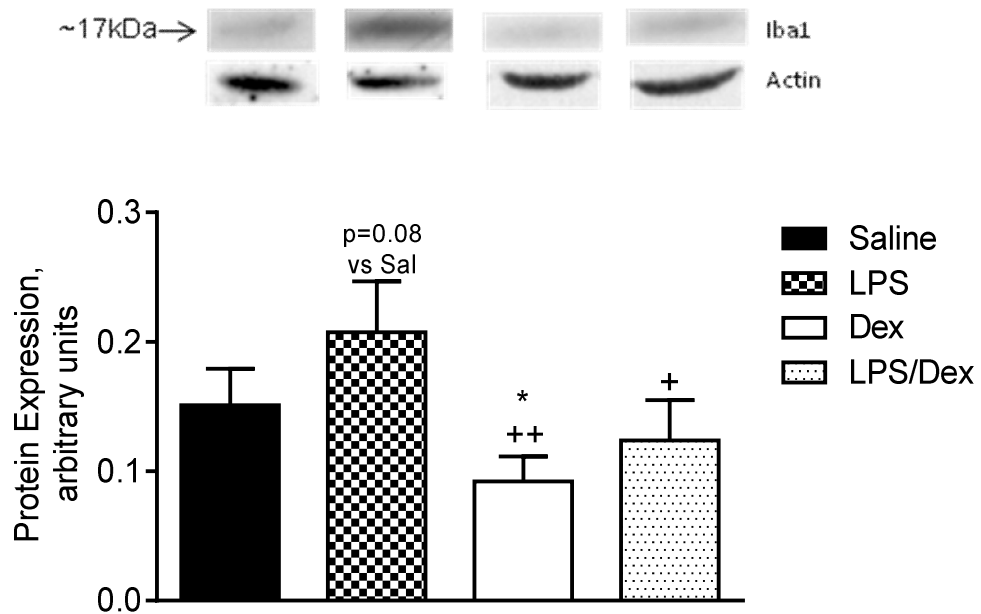


Figure 5.4: Expression of Iba-1 protein in EDL muscle following 24hr continuous intravenous infusion of either saline, LPS, Dex or both simultaneously (Dex/LPS). Values are means \pm S.E.M. The densities of \sim 17kDa Iba1 immunoreactive bands were measured by western blotting and representative bands for each treatment group are shown above their corresponding bar. n=7-8 per group. By Kruskal-Wallis 1-way ANOVA: significantly different from saline group: * p<0.05. Significantly different from LPS-treated group: + p<0.05, ++ p<0.005.



5.4.2 Myogenic Regulatory Factors (MRFs)

Continuous LPS infusion for 24hr tendentially reduced pax7 mRNA expression (figure 5.5). Dex also significantly suppressed pax7 mRNA and co-infusion of both demonstrated an additive effect; the combination of both substances suppressed pax7 mRNA more than either alone. This decrease in mRNA was replicated in pax7 protein expression, which showed a tendency toward decreased protein expression relative to saline control across all three treated groups.

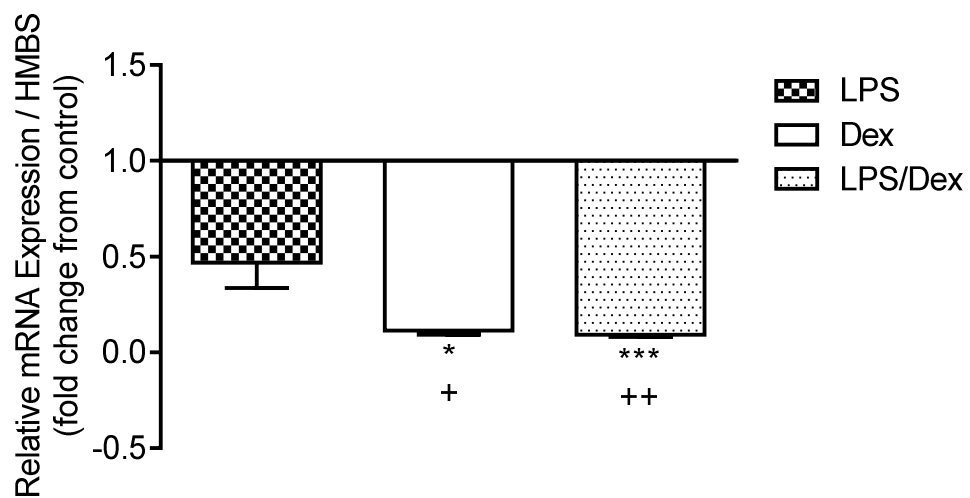
Likewise, myoD mRNA was significantly reduced by LPS, Dex and LPS+Dex administration (figure 5.6). Dex had a greater suppressive effect on myoD than LPS and co-infusion of both did not alter LPS or Dex-induced myoD suppression. The protein expression followed a similar pattern to its mRNA; myoD protein was significantly lower in the treated groups relative to saline control. Interestingly, while myoD protein was reduced to similar levels in LPS and Dex treated samples; co-infusion of both substances caused a further reduction in myoD protein, thus further demonstrating the additive effect described above.

Myogenin mRNA expression was significantly increased in the LPS group compared to control (figure 5.7). The Dex group showed a significant reduction in myogenin mRNA, which was not significantly altered by co-administration with LPS, although there was a tendency toward basal levels of myogenin mRNA expression. The protein expression showed a similar trend; there was a tendency toward increased myogenin protein in the LPS group. The Dex and Dex+LPS treated groups showed significant reductions in myogenin

protein compared to the saline group. Co-administration of Dex with LPS did not improve Dex-induced suppression of myogenin protein expression.

Figure 5.5: Expression of Pax7 a) mRNA and b) protein in EDL muscle following 24hr continuous intravenous infusion of either saline, LPS, Dex or both (Dex/LPS). a) Relative mRNA expression of saline controls was set at 1; bars denote fold change in mRNA expression from saline control with values >1 = increased mRNA expression and <1 = decreased mRNA expression. Values are means \pm S.E.M. b) The densities of ~55kDa pax7 immunoreactive bands were measured by western blotting and representative bands for each treatment group are shown above their corresponding bar. n=7-8 per group. By Kruskal-Wallis 1-way ANOVA: significantly different from saline group: *** p<0.0005. Significantly different from LPS-treated group: + p<0.05, ++ p<0.005.

a) *Pax7 mRNA expression*



a) *Pax7 protein expression*

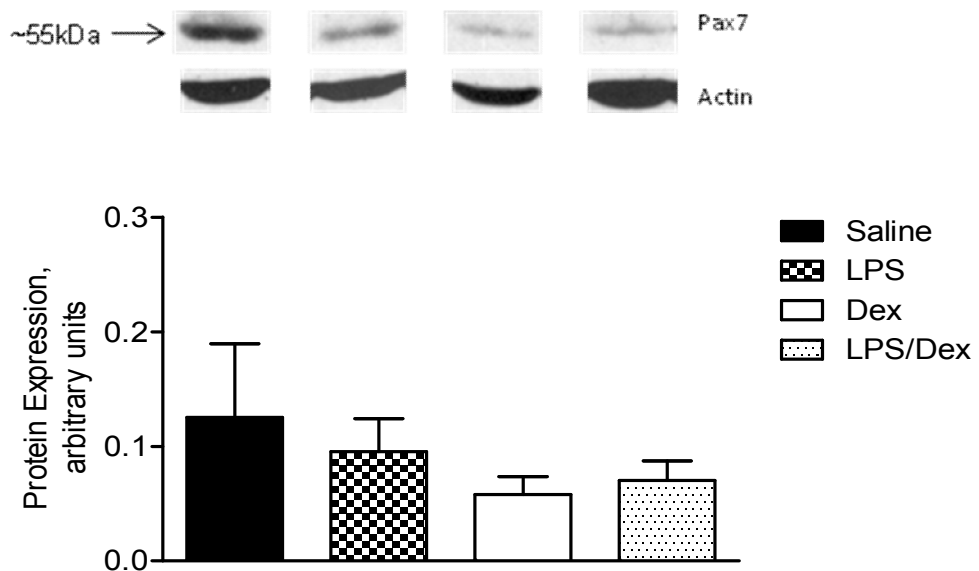
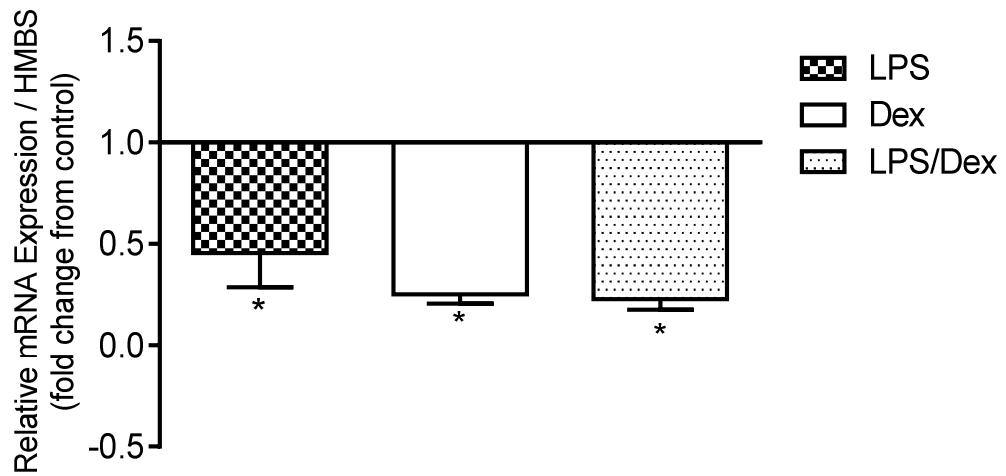


Figure 5.6: Expression of MyoD a) mRNA and b) protein EDL muscle following 24hr continuous intravenous infusion of either saline, LPS, Dex or both (Dex/LPS). a) Relative mRNA expression of saline controls was set at 1; bars denote fold change in mRNA expression from saline control with values >1 = increased mRNA expression and <1 = decreased mRNA expression. Values are means \pm S.E.M. b) The densities of ~34kDa MyoD immunoreactive bands were measured by western blotting and representative bands for each treatment group are shown above their corresponding bar. n=7-8 per group. By Kruskal-Wallis 1-way ANOVA: significantly different from saline group: * p<0.05, ** p<0.005.

a) *MyoD mRNA expression*



b) *MyoD protein expression*

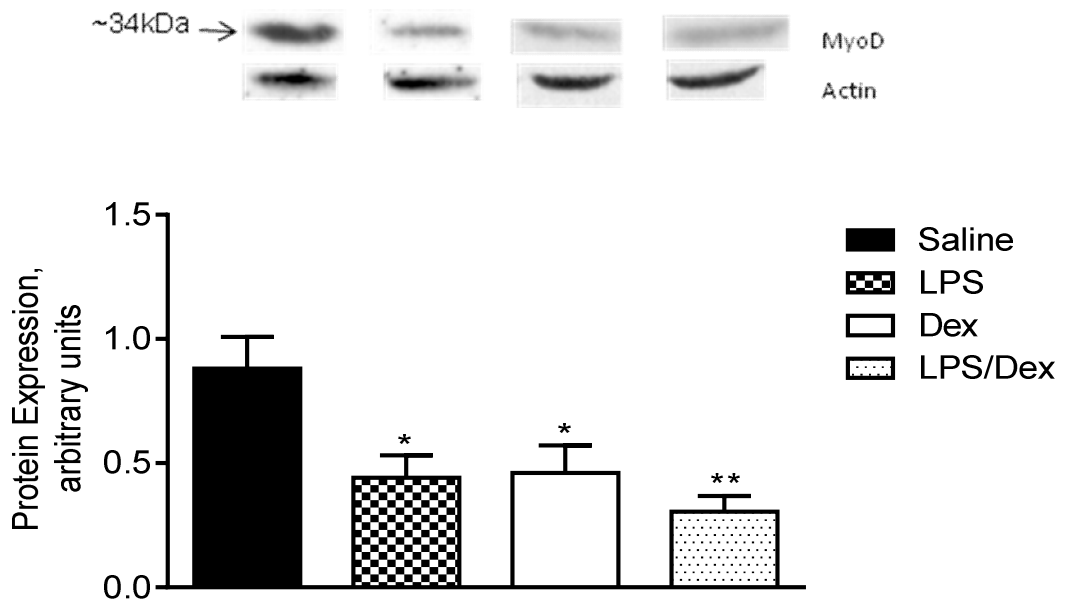
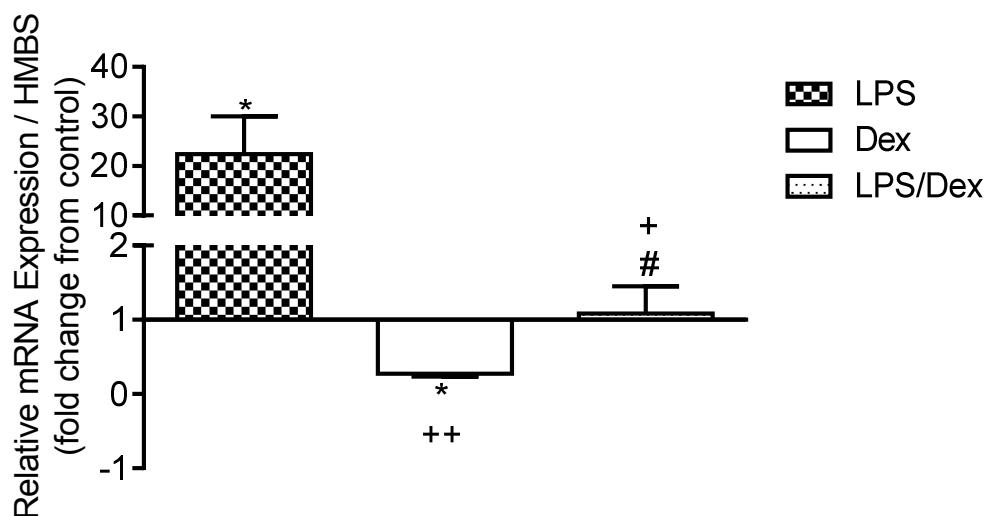
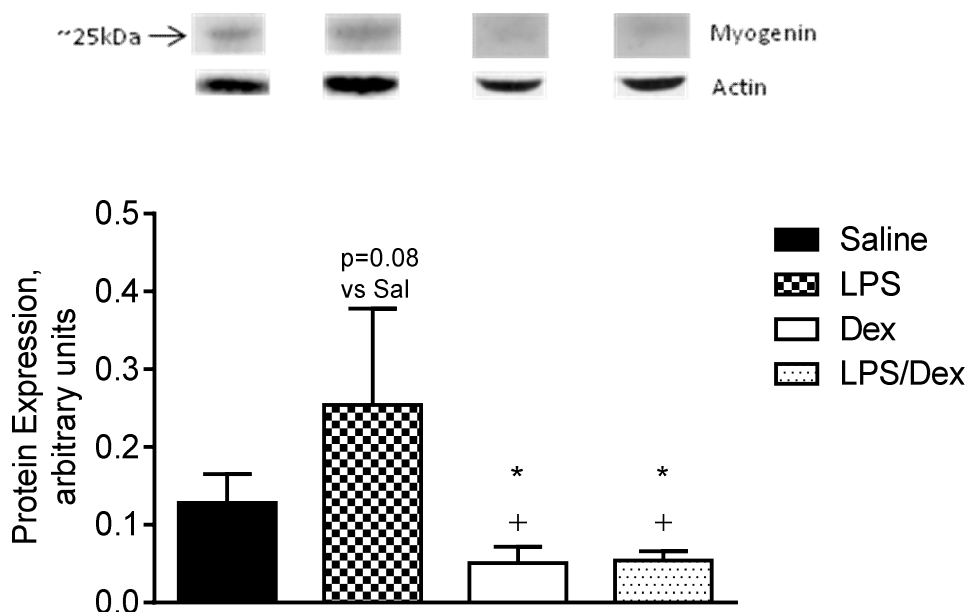


Figure 5.7: Expression of Myogenin a) mRNA and b) protein EDL muscle following 24hr continuous intravenous infusion of either saline, LPS, Dex or both (Dex/LPS). a) Relative mRNA expression of saline controls was set at 1; bars denote fold change in mRNA expression from saline control with values >1 = increased mRNA expression and <1 = decreased mRNA expression. Values are means \pm S.E.M. b) The densities of \sim 25kDa MyoD immunoreactive bands were measured by western blotting and representative bands for each treatment group are shown above their corresponding bar. n=7-8 per group. By Kruskal-Wallis 1-way ANOVA: significantly different from saline group: * p<0.05. Significantly different from LPS-treated group: + p<0.05, ++ p<0.005. Significantly different from Dex-treated group: # p<0.05.

a) *Myogenin protein expression*



b) *Myogenin protein expression*



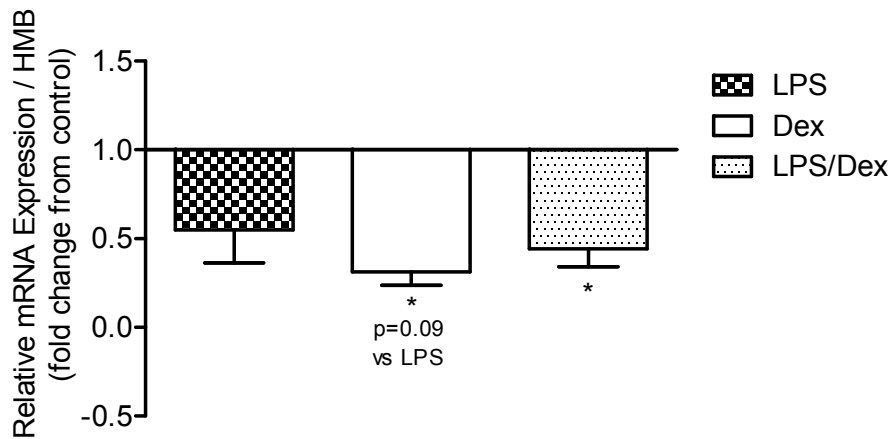
5.4.3 Myostatin

There was a tendency toward a reduction in myostatin mRNA expression in response to LPS infusion (figure 5.8). Dex significantly reduced myostatin mRNA relative to saline control. Simultaneous Dex+LPS-infusion also suppressed myostatin mRNA; although mRNA expression trended toward LPS only levels of suppression. The magnitude of mRNA suppression was greater in the Dex group, which suggests myostatin mRNA is perhaps more affected by dexamethasone relative to LPS, at the doses administered.

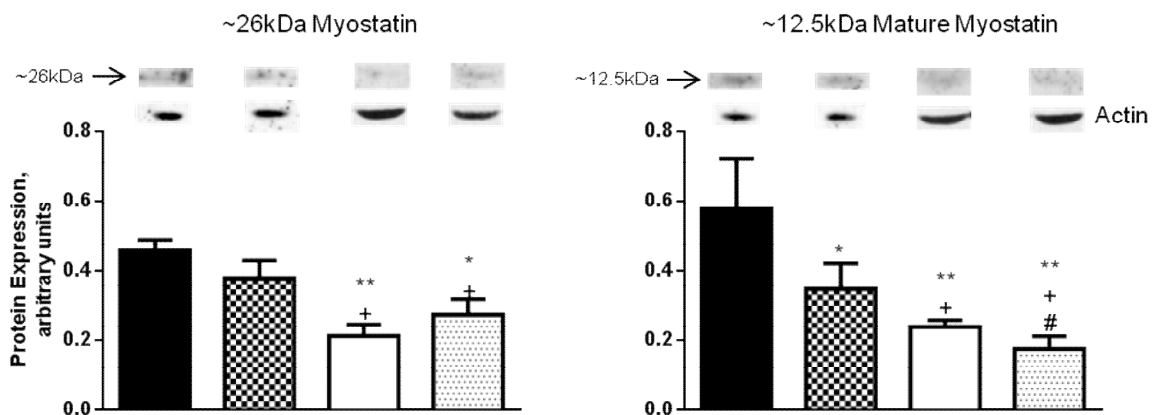
We detected the ~26kDa and ~12.5kDa immuno-reactive forms of myostatin protein in crude cytosolic fractions by Western blotting. We did not detect any immuno-reactive myostatin bands in Dex or LPS+Dex treated nuclear fractions (after 30 minutes exposure), so results shown represent myostatin expression in cytosolic protein fractions only (figure 5.8b). LPS caused a reduction in both forms of myostatin protein; similarly to myostatin mRNA, Dex infusion caused a greater suppression of both forms of myostatin protein, relative to LPS-only group. Co-infusion of LPS and Dex elicited a statistically significant reduction in the ~26kDa myostatin protein expression relative to the saline group, which trended toward LPS-only levels relative to Dex alone infusion. In contrast, there was a steep graded reduction in the ~12.5kDa myostatin protein expression across all three experimental groups, with the lowest reduction in the co-infused group. Co-infusion of both LPS and Dex demonstrated an additive effect on mature myostatin protein expression, which appeared to be independent of the pattern of mRNA and ~26kDa protein expression.

Figure 5.8: Expression of Myostatin a) mRNA and b) protein EDL muscle following 24hr continuous intravenous infusion of either saline, LPS, Dex or both (Dex/LPS). **a)** Relative mRNA expression of saline controls was set at 1; bars denote fold change in mRNA expression relative to saline control with values >1 = increased mRNA expression and <1 = decreased mRNA expression. Values are means \pm S.E.M. **b)** The densities of ~ 26 kDa and ~ 12.5 kDa myostatin immunoreactive bands were measured by western blotting and representative bands for each treatment group are shown above their corresponding bar. $n=7-8$ per group. By Kruskal-Wallis 1-way ANOVA; significantly different from Saline group: * $p<0.05$, ** $p<0.005$. Significantly different from LPS-treated group: $^{\dagger}p<0.05$. Significantly different from Dex-treated group: $^{\#}p<0.05$.

a) Myostatin mRNA expression



b) Myostatin protein expression



5.5 DISCUSSION

Results from the study presented in chapter 4 suggested a role for LPS-induced elevations in inflammatory cytokines, in the suppression of skeletal muscle myogenesis, via the down-regulation of essential satellite cell markers such as pax7 and myoD. Strategies aimed at suppressing elevated inflammatory cytokines, such as low doses of glucocorticoid therapy are beneficial in increasing survival from severe sepsis (reviewed by Annane 2001). Therefore we examined whether the administration of low dose dexamethasone (equivalent to 300µg/kg/day - less than half the dose reported to induce muscle atrophy) prevents elevations in inflammatory cytokines and thereby improve LPS-induced myogenic suppression.

Dexamethasone infusion during endotoxaemia significantly suppressed LPS-induced elevations in TNF- α , IL-6 and NF- κ B mRNA expression in the EDL muscle. These results are consistent with an anti-inflammatory systemic effect, similar to that reported by Crossland *et al.* (2010) and Gardiner *et al.* (1996). The inhibition of NF- κ B at the transcriptional level is pivotal for inflammatory suppression, as NF- κ B signalling mediates the production and further release of many inflammatory cytokines including TNF- α and IL-6 (Muller *et al.* 1993; Guha and Mackman 2001). Dexamethasone did not induce significant alterations in local muscle TNF- α and IL-6 protein expression; it is unlikely the dose of dexamethasone administered, whilst able to significantly suppress local muscle cytokine mRNA expression, is not sufficiently high enough, for suppressing cytokine expression at the protein level. This is supported in a study by Myers *et al.* (2003), where the infusion of a much higher dose of

dexamethasone in swine (equivalent to 1200 μ g/kg/day) was sufficient to significantly suppress LPS-induced increases in plasma TNF- α and IL-6. Another potential reason for the discordance between cytokine RNA and protein levels could be that dexamethasone has limited effects on active cytokine protein. Indeed, dexamethasone inhibits TNF- α at the transcriptional and post-transcriptional level but it is incapable of inhibiting it once TNF- α biosynthesis is initiated (Beutler *et al.* 1986). The authors also noted dexamethasone suppression of endotoxin-induced TNF- α mRNA was not complete and very low levels of mRNA expression could still be detected. A combination of diminished, but not completely ablated mRNA expression, and protein resistance to glucocorticoid therapy could explain the limited effects of dexamethasone on cytokine protein expression.

This inability of low dose dexamethasone to significantly down-regulate the cytokine protein pool likely accounts for the increased NF- κ B p50 protein in LPS/Dex treated samples relative to saline control. Complete antagonism between glucocorticoids and active NF- κ B may not be universal; the glucocorticoid receptor escaped antagonism by NF- κ B and showed normal processing and transcriptional activities in L6 muscle cells in a study by Dekelbab *et al.* (2007). In short, dexamethasone did not have an effect on NF- κ B p50 protein subunit expression when administered alone and therefore had limited influence on the LPS-induced increase when administered one hour before and during LPS infusion. The increase in NF- κ B p50 subunit in LPS/Dex samples suggest NF- κ B protein may be up-regulated by other

mechanisms other than alterations its mRNA pool, for example, vesicular storage and release.

However, dexamethasone reduced the protein expression of the macrophage marker Iba-1 and blunted its LPS-induced increase. Glucocorticoids exert anti-inflammatory action by negatively regulating circulating mononuclear cells; prednisolone decreased muscle macrophages by about 50% in the soleus and quadriceps muscles of mdx mice, by down-regulating cellular adhesion molecules that are required for inflammatory cell infiltration (Wehling-Henricks *et al.* 2004). Likewise, Leibovich and Ross (1975), showed that the recruitment of macrophages and monocytes to sites of inflammation is impaired by hydrocortisone treatment in guinea pigs. It is believed the rapid, marked decrease in circulating mononuclear cells following steroid treatment is likely due to rapid sequestration of macrophages rather than a direct lytic effect (Thompson and van Furth 1970). Glucocorticoids inhibit macrophages motility (Gell and Hinde 1953), by altering the tissue environment and permeability (through down-regulation of cellular adhesion molecules), which may in turn, interfere with movement of cells to sites of inflammation. Our results suggest dexamethasone interferes with local cytokine production and release by suppressing Iba-1 protein expression, a key component for macrophage membrane ruffling/motility and phagocytosis of infectious particles. Thus, the degree of macrophage infiltration in EDL muscle in response to LPS was attenuated by Dex co-infusion.

Continuous LPS infusion suppressed the satellite cell markers pax7 and myoD and co-infusion with dexamethasone did not improve LPS-induced suppression of these markers. In fact, co-administration of Dex/LPS appeared to have an

additive effect on pax7 and myoD suppression. It appears that the dose of dexamethasone administered, whilst capable of inhibiting the transcription of inflammatory cytokines, did not improve cytokine mediated suppression of satellite cell markers. Whether the suppression of satellite cell markers is a direct consequence of inflammatory suppression (as TNF- α and IL-6 also have beneficial dose-dependent effects on satellite cell proliferation and differentiation (Li 2003; Serrano *et al.* 2008)), is undetermined. However, prostaglandins synthesised from arachidonic acid, in response to cytokine signalling (reviewed by Funk 2001) have been shown to stimulate muscle growth and satellite cell activity (Horsley and Pavlath 2003; Bondesen *et al.* 2006). This was blunted by the administration of anti-inflammatory drugs, which inhibit cyclooxygenase (COX) enzymes (Mendias *et al.* 2004; Soltow *et al.* 2006). Prostaglandins regulate muscle growth by altering the rate of muscle protein turnover (Rodemann and Goldberg 1982), through modulation of protein synthesis and degradation (Palmer 1990; Vandeburgh *et al.* 1990). Consistent with this is an impairment of satellite cells and myotubes *in vivo*, when prostaglandin signalling pathway is dysregulated, for example by COX2 genetic deletion (Shen *et al.* 2006).

The anti-inflammatory actions of dexamethasone include suppression of prostaglandin synthesis and release, by inhibition of plasma membrane phospholipase A2, an enzyme which hydrolyses the bonds releasing arachidonic acid for prostaglandin synthesis (Blackwell *et al.* 1980; Hirata *et al.* 1980). Dexamethasone-induced alterations in prostaglandin synthesis are associated with the inhibition of muscle protein synthesis (Reeds and Palmer 1984). Furthermore, inhibition of prostaglandin synthesis is known to reduce

myoD expression in rat muscle (Monda *et al.* 2009). The authors found that administration of the COX inhibiting drug, keftoprofen elicited a very large decrease in MyoD⁺/M-Cadherin⁺ cells in functionally overloaded soleus muscles. Administration of the synthetic glucocorticoid prednisolone to rats for eight weeks also reduced the number of mechanically activated myoD⁺ satellite cells, an effect which was rescued with nitric oxide donor supplementation (Better *et al.* 2008). The authors described a role for glucocorticoid-mediated inhibition of nitric oxide production (a primary signal for satellite cell activation and myoblast fusion), in glucocorticoid-induced satellite cell dysfunction. Also, exposure of cultured myotubes to glucocorticoids induced a rapid degradation of myoD protein, through increased expression of components of the ubiquitin-proteasome system such as E3 ligases MAFbx/MuRF1 and N-terminal ubiquitination of myoD, which facilitated its subsequent degradation (Sun *et al.* 2008). Indeed, high doses of dexamethasone (>700µg/kg/day) rapidly up-regulate the E3 ubiquitin ligase MAFbx (Zhao *et al.* 2008), which interacts with myoD via an LXXLL sequence motif and promotes its degradation (Tintignac *et al.* 2005).

Likewise, local infusion of the COX1/2-inhibiting-NSAID (Non-Steroidal Anti-inflammatory Drug), indomethacin suppressed the exercise-induced increase in pax7⁺ satellite cells in human vastus lateralis muscle (Mikkelsen *et al.* 2009). Clearly satellite cells require correctly balanced inflammatory signalling (for a review see, Smith *et al.* 2008), as an excessive elevation of inflammatory mediators or inflammatory suppression can compromise muscle homeostasis. Our results support this contention, as demonstrated by the

additional suppression of myoD and pax7 expression when LPS and dexamethasone were co-administered, compared to either alone.

Dexamethasone infusion suppressed myogenin expression at the mRNA and protein level and blunted its LPS mediated increase. Dexamethasone is known to reduce the differentiation capacity of cultured C2C12 myoblasts, by dose-dependently suppressing myogenin mRNA expression (te Pas *et al.* 2000). Dex-mediated down-regulation of myogenin is thought to occur indirectly, via Dex-induced increase in MAFbx expression, which interacts directly with myogenin (likely via a similar LXXLL sequence motif as with myoD) and promotes proteasomal degradation (Jogo *et al.* 2009). Furthermore, MAFbx overexpression resulted in myogenin protein reduction, an effect blunted by administration of the proteasome inhibitor MG-132 or MAFbx siRNA silencing. Inhibition of MRFs is likely a primary mechanism by which glucocorticoids mediate muscle catabolic effects. A study by Bruscoli *et al.* (2010) also found that dexamethasone stimulates a Glucocorticoid-Induced-Leucine-Zipper (GILZ), which reduces myotube formation in culture, by inhibiting myoD and myogenin, an effect exacerbated or dampened by GILZ overexpression or RNA silencing, respectively.

Twenty-four hours of LPS and dexamethasone infusion reduced myostatin mRNA and protein expression, when administered either independently or both simultaneously. In chapter 4, we showed that myostatin is increased during the initial stages of endotoxin insult, followed by a return to basal and a subsequent reduction in expression, relative to control. This expression trend was congruent with the elevation in inflammatory cytokines TNF- α , IL-6 and NF- κ B, which were at their highest levels of expression following the initial toxin

insult (after 2hr of LPS) and gradually declined by 24hr. Possible explanations for the reduction in myostatin after 24hr of LPS infusion likely include attenuation of inflammatory signalling, or myostatin negative feedback control. Indeed, this reduction in myostatin mRNA and protein after 24hr of LPS infusion is similar to that reported by Smith *et al.* (2011), who found that myostatin mRNA was significantly reduced in rats 16hr after induction of sepsis by cecal ligation and puncture. The same authors found that administration of dexamethasone also suppressed myostatin mRNA expression; this supports our contention, that myostatin expression is increased in response to elevated inflammatory cytokine signalling and dexamethasone induced suppression of these cytokines likely attenuates the increased myostatin expression.

The reduction in myostatin expression after 24hr of LPS contrasts with previous studies suggesting that conditions depicting muscle atrophy such as cancer, HIV infection, burn injury or ageing are associated with myostatin up-regulation (Gonzalez-Cadavid *et al.* 1998; Lang *et al.* 2001; Baumann *et al.* 2003; Liu *et al.* 2008). As mentioned in chapter 3, sections 3.3.4 and 3.5, although increased expression of myostatin mRNA or protein activity has been noted in these muscle wasting conditions, conflicting results have also been reported. Studies by Carlson *et al.* (1999), Sakuma *et al.* (2000) and Wehling *et al.* (2000), report a lack of correlation between muscle regulation and myostatin expression. For example the study by Baumann *et al.* (2003), found that myostatin mRNA was significantly reduced, rather than increased in aged rats despite a ~50% reduction in gastrocnemius muscle mass. It is tempting to speculate that the tight mechanisms regulating myostatin expression (for

example, myostatin is naturally inhibited by its own pro-peptide) facilitate negative feedback and that perhaps, an increase or decrease in myostatin is dependent on tissue sampling time. This is supported by our results presented in chapter 4 (see section 4.4.5), where an early increase in myostatin is noted after 2 and 6hr of LPS infusion but attenuated by 24 hr.

The reduction in myostatin mRNA and protein following dexamethasone treatment was lower than that elicited by LPS alone. This is similar to the findings of Song *et al.* (2011), where administration of dexamethasone to broiler chickens for 3 days resulted in significantly decreased myostatin mRNA expression. Myostatin was also suppressed by glucocorticoid treatment in fish (Rodgers *et al.* 2003; Weber *et al.* 2005). This contrasts with studies by Ma *et al.* (2003) and Lang *et al.* (2001), in which dexamethasone treatment resulted in myostatin mRNA up-regulation. The 5' regulatory region of the myostatin gene contains putative GREs (Ma *et al.* 2001), so glucocorticoids likely regulate myostatin expression directly. Further evidence of myostatin regulation by glucocorticoids was presented by Lang *et al.* (2001) and Gilson *et al.* (2007), who found that pre-treatment with a glucocorticoid receptor antagonist, prevented glucocorticoid-mediated increase in myostatin mRNA and myostatin gene deletion prevented dexamethasone-induced muscle atrophy.

However, the apparent contradiction to our results may be explained by the dexamethasone dosage used; dexamethasone dose dependently increased myostatin promoter activity *in vitro* (Ma *et al.* 2001) and the studies by Gilson *et al.* (2007), Lang *et al.* (2001) and Ma *et al.* (2003), used much higher doses of dexamethasone (ranging from 600-1200µg/kg/day) compared to the present

study (300 µg/kg/day). Intriguingly, a study by Carraro *et al.* (2009) found that the myostatin gene was down-regulated when very low, sub-therapeutic doses of dexamethasone (equivalent to 1.6µg/kg/day) were administered to cattle; notably a much lower dose than that used in the present study, but it appears the ability of ligand bound glucocorticoid receptors to trans-activate or repress GREs on the myostatin promoter may be dependent (in part) on the concentration of the ligand.

In summary, skeletal muscle regeneration can profit or suffer from an inflammatory process, therefore, administration of anti-inflammatory substances, as a means to combat or reverse inflammatory-mediated muscle wasting, needs to be carefully calibrated. Our results suggest that the administration of a lower dose of dexamethasone (less than half that reported to have catabolic effects on rat skeletal muscle) suppressed LPS-induced transcription of inflammatory cytokines and reduced excessive muscle macrophage infiltration. However, the ablation of such inflammatory signals by dexamethasone implicated consequences for muscle regenerative capacity, because suppressive effects on myogenic regulatory factors were elicited. Pax7, myoD and myogenin have pivotal roles in satellite cell activation, proliferation and differentiation and their down-regulation suggested inhibited satellite cell activity, likely a key mechanism for dexamethasone-induced muscle atrophy. Dysregulation of satellite cell activity introduces a functional deficit in skeletal muscle where-by its ability to adapt to altered load, recover from acute injury or insult, is interrupted or delayed. The negative effects of glucocorticoids on satellite cell activity may supersede their efficacy in the treatment of inflammatory muscle disorders depicting muscle wasting. Despite

their anti-inflammatory actions, the debilitating muscle wasting effects of glucocorticoids and the potential to cause long term muscle repair deficit with prolonged use could hinder therapeutic benefits. Therefore, further elucidation of the mechanisms underlying muscle atrophy and loss of regenerative potential, in response to glucocorticoid treatment, is required in order to fully utilize their net therapeutic potential.

CHAPTER 6

General Discussion

6.1 OVERVIEW OF THESIS

The original aims of this thesis were to assess the activity of skeletal muscle satellite cells (based on the gene expression profiles of specific markers) in rodent models of hypertrophy and atrophy. Satellite cells are known to contribute to muscle hypertrophy (predominantly by nuclear addition) and atrophy (because of an opposing deficit in nuclear supplementation) but their 'activity status' has not been routinely addressed in such studies.

In chapter 3, we examined satellite cell specific signalling events in hypertrophic muscle induced by chronic administration and an anabolic agent – the clenbuterol pro-drug BRL-47262. Eight weeks of daily administration of the drug caused statistically significantly ($p < 0.05$) increases in the mRNA expression of key satellite cell markers pax7 and myoD, accompanied by a tendential increase in protein expression relative to control animals. There was also a significant increase ($p < 0.05$) in myostatin mRNA and protein expression. The mRNA expression of the proliferation marker, ki-67 was also increased compared to control. No significant alterations in the expression of myogenin or the myostatin inhibitor follistatin were noted.

Taken together, these results provide evidence for increased satellite cell activity in hypertrophying muscle. Maintaining increased levels of pax7 and myoD is compatible with continuous activation/proliferation of satellite cells in a state of 'preparedness' for subsequent recruitment into myofibres to maintain nuclear domain size and allow fibre hypertrophy. We interpret the induction of myostatin, with its inhibitory activity towards satellite cell activation, as an antagonistic action in a balanced system which enables increased precision in

the control of myonuclear and satellite cell numbers. Similar roles have recently been attributed to microRNAs, which are thought to level out fluctuations in mRNA transcription (reviewed by Ebert and Sharp 2012). We hypothesised that chronic administration of the pro-drug lead to the stimulation of compensatory pathways, which may include myostatin, and were likely concomitant with a levelling out of muscle growth. Intermittent pro-drug administration coupled with myostatin suppression (e.g., via neutralising antibody) may represent an effective method for preventing or reversing muscle atrophy.

Chapter 4 described the gene expression profiles of satellite cell specific markers in an animal model of sepsis. Muscles from animals continuously infused with the bacterial toxin lipopolysaccharide demonstrate a propensity for muscle wasting due to dysregulation of their protein synthesis/degradation balance and derangements in carbohydrate oxidation and insulin resistance (reviewed in chapter 4, section 4.2). It is thought early events, such as a massive elevation in mediators of systemic inflammation may lead to the induction of cachetic muscle wasting during sepsis. We measured the mRNA/protein expression patterns of key cytokine markers implicated in sepsis and components of the satellite cell myogenic program at three sampling points during the first 24 hours of endotoxaemia.

Continuous LPS infusion caused significant, transient elevations in TNF- α , IL-6 and NF- κ B in the EDL and gastrocnemius muscles, with the most dramatic magnitude of change occurring after 2 hours, an effect which was attenuated by

24 hours. Excessive cytokine expression was attributed to increase macrophage infiltration in the two muscles analysed and TNF- α protein expression was localised to the macrophage infiltrate. LPS-induced up-regulation of inflammatory cytokines demonstrated a time and dose-dependent effect on myogenic markers. Pax7 and myoD mRNA were suppressed by continuous LPS infusion in both muscles, with the protein expression showing a similar trend. Furthermore, quantitative immunohistochemical analyses of pax7⁺ and myoD⁺ satellite cells showed an apparent reduction in number of quiescent and activated satellite cells. Activated myoD⁺ satellite cells were suppressed at all time points whilst pax7⁺ satellite cells showed a tendency to a return to basal levels. It is unknown whether the decrease in satellite cell numbers was a result of apoptosis or a down-regulation of both markers. Accordingly, myostatin was up-regulated at the early sampling time point, when cytokine expression was highest and showed a reduction in expression after 24 hours. It is likely that early up-regulation of myostatin on may have been responsible for pax7 and myoD suppression.

Taken together, these findings suggested that LPS induced transient elevations in inflammatory cytokines, which altered the satellite cell myogenic program. Although some markers (notably pax7) showed a tendency of returning to basal expression relative to control, others (e.g., myoD) remained suppressed throughout all sampling points and it will be interesting to discover what the consequences (if any) are of chronic LPS-mediated suppression of satellite cells. Given the proposed role of satellite cells in muscle homeostasis, it is tempting to speculate their continuous impairment should have consequences for long-term muscle maintenance.

In chapter 5, we examined the effect of continuous infusion of an anti-inflammatory agent, dexamethasone, independently and 1 hour before and during LPS infusion to determine whether suppression of LPS-induced inflammatory cytokines would counter myogenic suppression. Co-infusion of dexamethasone blunted cytokine elevation but had an additive effect on myogenic suppression and did not improve LPS-induced suppression of pax7 or myoD. Since (modest) inflammatory signalling via cytokines such as TNF- α , IL-6 and NF- κ B is beneficial for muscle regeneration under normal physiological conditions, it seems pertinent that the suppression of these factors could impact on satellite cell myogenesis. This was evident by the additive inhibition of pax7 and myoD when LPS and dexamethasone were co-administered.

6.2 CONCLUSIONS

Taken together, the studies described within this thesis emphasise satellites are important for maintenance of muscle homeostasis and their activation / inhibition may determine the magnitude of muscle loss or gain. This was demonstrated by the pattern of pax7 and myoD expression in hypertrophying muscle, where both markers were up-regulated and in atrophying muscle, where they were down-regulated. We believe the down-regulation of these markers in atrophy could have implications for muscle regenerative capacity, especially myoD, whose expression was continuously inhibited across all time-points sampled in septic muscles. Future studies should be directed at examining the effects of chronic infusion of LPS (longer than just 24 hours) to

determine if markers like myoD do stay suppressed. Recent studies by several groups show that pax7 and myoD are essential for satellite cell function and their continuous inhibition introduces aberrant behaviour in satellite cells, ultimately contributing to a muscle regenerative deficit (reviewed by Mansouri *et al.* 1996; Sabourin *et al.* 1999; Cornelison *et al.* 2000; Seale *et al.* 2000). For example, loss of myoD by genetic ablation delays muscle regeneration and myoblasts lacking myoD fail to fuse (Knapp *et al.* 2006). Similarly, loss of pax7 reduces the number of functioning satellite cells in adult muscle (Kuang *et al.* 2006), which displayed reduced growth and marked muscle wasting coupled with a regenerative deficit following muscle injury.

In summary, satellite cells are a major source of compensatory action in skeletal muscle, their activation and subsequent myogenesis represents an auxiliary mechanism by which muscle responds to damaging stimuli; therefore their dysregulation (through the alteration of key myogenic markers or increased apoptosis) results in an alteration in normal function. A recent publication by Bruusgaard *et al.* (2010) highlighted this link between satellite cells and hypertrophy quite well, using an *in vivo* time-course analysis, they showed that increased number of myonuclei is a major cause of hypertrophy in rodents. New myonuclei were added before any discernable increase in muscle fibre size during muscle overload. However, the authors also challenged the concept of “fixed nuclear domain sizes”, which theorises that the increase in muscle size is due to satellite cell related nuclear addition and the selective apoptosis of some myonuclei during atrophy/disuse. The authors observed that newly acquired myonuclei were retained during subsequent denervation-induced muscle atrophy and for a considerable period thereafter. This

protection of some myonuclei from apoptosis could be beneficial for sarcopenia; strength training at an earlier age could improve myonuclear retention since the ability to create new myonuclei in the elderly is impaired.

However, it is possible that dysregulation of satellite cells limits the efficacy of muscle compensatory processes (i.e. satellite cell activation/proliferative or differentiation potential), thereby contributing to the progression of muscle atrophy and myopathy. Failure of satellite cell compensatory action is more prominent in cases of progressive muscle diseases and in old age. It is thought that alteration of the anti-oxidative potential of satellite cells, as a result of increased reactive oxygen species (ROS) accumulated over one's lifetime decreases the regenerative potential of satellite cells in sarcopenia (reviewed by Fulle *et al.* 2005). Reduced muscle regenerative capacity, as a result of reduced number of satellite cells, due to repeated bouts of muscle repair in DMD is also considered a key factor in determining the severity of the dystrophy phenotype. In both ageing and DMD, repeated bouts of regeneration, accumulation of epigenetic mutations in key satellite cell regulatory genes as well as telomere shortening, lead to loss of satellite cell self-renewal activity and impaired myogenicity.

6.3 LIMITATIONS AND FUTURE DIRECTIONS

It would be beneficial to our studies to determine whether the increased pax7 and myoD expression relative to control noted in chapter 3 is consistent with increased numbers of activated/proliferating satellite cells in soleus muscle by

quantitative immunohistochemistry. By use of the Duolink[®] proximity ligation assay, which co-localises complexed protein targets as a single signal visualised by immuno-microscopy, the proportion of activated/proliferating (pax7⁺/myoD⁺) satellite cells could be estimated from the total number of pax7⁺ or myoD⁺ only cells, thus providing an estimate of the degree of activation elicited by BRL-47262. Additionally, localisation of the myostatin mRNA message (for example, by *in-situ* hybridisation) within the same study should have provided an interesting avenue of investigation. We tried this using a modification of the method by Braissant *et al.* (1996) for *in-situ* hybridisation (Tellez 2005; Tellez *et al.* 2006), using specific probes for myostatin, but could not get a clearly interpretable signal. The source of the increased myostatin mRNA expression is unknown, it is undetermined if its expression was global or localised to specific entities, e.g., satellite cells or myofibres. Our studies were also limited by the lack of a sensitive commercial antibody for myostatin. None of the antibodies mentioned within this thesis produced a convincing myostatin signal by immunohistochemistry. Discovery and optimisation of a suitable antibody should enable localisation of myostatin protein expression. Myostatin protein is a secreted protein thought to function in an autocrine/paracrine manner and it would be beneficial to clarify the predominant source of myostatin synthesis.

In chapter 4, we observed a decrease in the number of pax7⁺ and myoD⁺ cells in LPS samples compared to control. This could have been as a result of increased satellite cell apoptosis or of significant down-regulation of pax7 and myoD, below the limit of detection by immunohistochemistry. The

incorporation of a TUNEL (terminal deoxynucleotidyl transferase dUTP nick end labelling) assay, along with measurements for markers of apoptosis (e.g. caspase-3) should clarify whether LPS indeed led to sudden and frequent apoptosis of satellite cells.

LPS is known to induce apoptosis of myonuclei in rat skeletal muscle (Gierer *et al.* 2007) and in rat cardiomyocytes via TNF- α -mediated mechanisms (Comstock *et al.* 1998). However, a frequent finding in studies indicating muscle nuclei loss from atrophy is the lack of distinction between TUNEL-positive myonuclei and TUNEL-positive satellite cells (reviewed by Gundersen and Bruusgaard 2008). Using a ‘flipped sectioning’ technique (described in the appendix), which identifies the same cells spanning across the plane of a series of muscle cross-sections; with roughly one half being in each section, should identify TUNEL-positive nuclei on one section, whilst utilising the adjacent section to identify the other half of these cells using satellite cell specific markers. This should provide an estimate of the proportion of satellite cells undergoing apoptosis.

In chapter 5, dexamethasone infusion was found to suppress pax7, myoD and myogenin expression relative to control. It would enhance our findings to correlate the suppression of these markers with a decrease in the number of pax7⁺, myoD⁺ or myogenin⁺ satellite cells in these muscles by quantitative immunocytochemistry. Unfortunately, muscle samples were shared with group colleagues interested in muscle metabolic derangements and the small nature of the rat EDL muscle meant there were insufficient muscle samples available for cryo-sectioning.

In both chapters 4 and 5, the inflammatory cytokines TNF- α , IL-6 and NF- κ B were implicated in satellite cell impairment; however the exact contribution of them was not examined. The interactions between cytokines and the signalling pathways they regulate paint a very complex picture. With all three cytokines measured reported to contribute to the aetiology of muscle wasting, it would enhance our studies further to outline the specific roles attributed to each, for e.g. via use of cytokine inhibitors or continuous infusion of specific cytokines to measure and compare LPS-mediated and specific cytokine-mediated responses.

METHOD DEVELOPMENT APPENDICES

APPENDIX I

Myostatin Antibody Validation

1. Rationale

Some discrepancies still exist regarding the precise molecular weight of the full length myostatin protein and its processed forms (Mendler *et al.* 2000; Matsakas *et al.* 2006; Smith *et al.* 2011). The consensus from the literature is that the most prominent myostatin bands detected by western blotting migrate at ~52-55kDa (often referred to as myostatin precursor or pro-myostatin), at ~40kDa (referred to as LAP myostatin), at ~26kDa (deemed to be a myostatin dimer) and at ~12.5kDa (which is the fully processed, mature myostatin peptide). However some authors have also reported bands varying between ~15kDa and ~42kDa, using either in-house or commercial antibodies.

Therefore, we carried out a series of preliminary western blotting experiments to determine the specificity of three commercially available antibodies for the various reported forms of myostatin protein; rabbit anti-GDF8 (A300-401A, Bethly Labs, Montgomery, TX, USA), rabbit anti-myostatin near c-terminus (Ab3239, Millipore, Billerica, MA, USA) and goat anti-GDF8 C-20 (sc-6884, Santa Cruz Biotechnology CA, USA). These antibodies have been shown to detect the 12.5kDa fully processed monomeric myostatin peptide (Rios *et al.* 2004; Bish *et al.* 2010), the ~26kDa immuno-reactive myostatin band, suspected to represent a myostatin homodimer (Gonzalez-Cadavid *et al.* 1998; Sakuma *et al.* 2000; Hittel *et al.* 2010), the ~40kDa LAP (McFarlane *et al.* 2005) and the ~55kDa myostatin protein precursor (Taylor *et al.* 2001; Wojcik *et al.* 2005; Chandrasheharan and Martin 2009). All three antibodies were raised against an epitope specific for the C-terminal portion of myostatin, which forms part of the mature fully processed form and the precursor proteins, and thus all antibodies

should be able to detect the unprocessed precursor, myostatin intermediates and the mature peptide.

2. Methods

Anti-myostatin near c-terminus (diluted 1:250 in 5% (w/v) non-fat milk powder in TBS-T), rabbit anti-GDF-8 (1:400 in 5% (w/v) non-fat milk powder in TBS-T) and goat anti-GDF-8 sc-6884 (diluted 1:500 in 5% BSA-TBS) were used as described in chapter 3, section 3.3.3. 100µg of cytosolic and nuclear muscle proteins from untreated adult male Wistar rats were loaded per lane. A recombinant myostatin peptide (100ng/µl, R & D System, Mineapolis, USA), which contains a mixture of pro-peptide and active fragments was used as a positive control.

2.1 Myostatin competitive blocking studies

Antibody specificity was also assessed by pre-incubating with a blocking peptide (GDF-8 blocking peptide, Bethyl Labs) according to the manufacturer's instructions. Briefly, the amount of antibody (by weight) ordinarily required for western blotting was mixed with a 5-fold (by weight) excess of blocking peptide to a total volume of 500µl with 5% non-fat milk in TBS-T blocker. Antibody stock was 1µg/µl, thus 25µg of blocking peptide was added to 5µg of antibody. Studies by Gonzalez-Cadavid (1998) showed that 7ng/µl of blocking peptide was sufficient to block myostatin antibody activity by immunohistochemistry. Solutions were incubated for 2hr at room temperature, made up to 2ml with milk blocker and western blotting was carried out, as above.

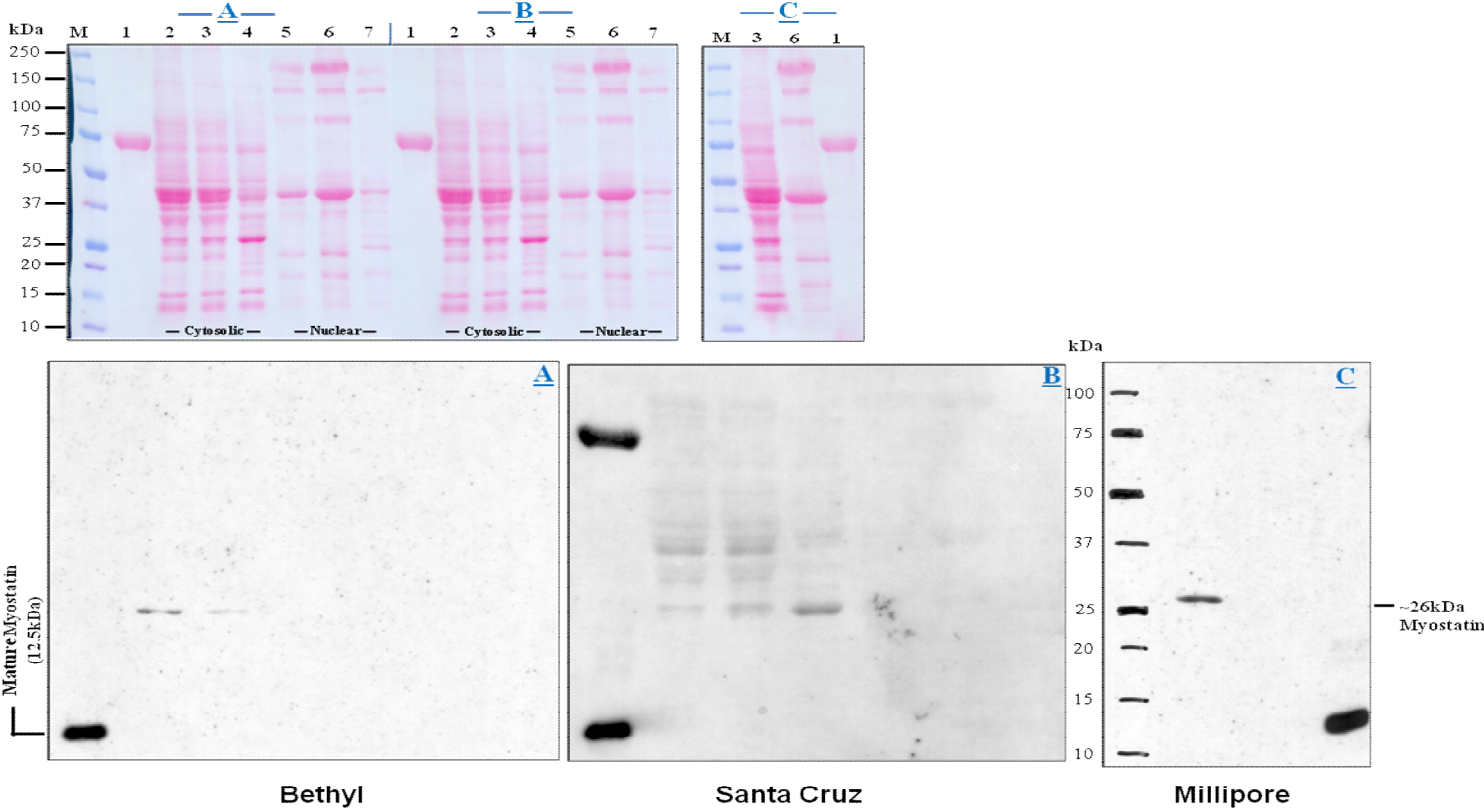
2.2 Minimum myostatin protein concentration for western blotting

To determine the minimum concentration of myostatin that can be detected by western blotting, serial dilutions of a recombinant myostatin peptide (R & D System, Mineapolis, USA) were prepared in reconstitution buffer (4mM HCl containing 0.3% (w/v) BSA) and were loaded onto 5-20% SDS-PAGE, as described above. Untreated adult muscle homogenate (50 μ g) from male Wistar rats was used as a positive control. All three anti-myostatin antibodies were tested to determine their specificity for recombinant myostatin; rabbit anti-GDF-8 (1:400, Bethyl Labs, Montgomery, TX, USA) and goat anti-GDF-8 sc-6884 (diluted 1:400 in 5% BSA-TBS, Santa Cruz Biotechnology, CA, USA).

3. Observations and conclusions

All three antibodies detected the 12.5kDa mature recombinant myostatin peptide positive control and a ~26kDa immunoreactive myostatin protein band (figure 1). The Santa Cruz antibody appears to be less specific as it bound to several other species in the muscle samples in three separate experiments. The natures of these bands are unknown. This antibody also bound to a <75kDa band that was not recognised by the other two; the nature of this band is also unknown although it is tempting to speculate it is the BSA in the reconstitution buffer. It is possible the Santa Cruz antibody may not recognise any myostatin; the fact that the soleus sample in figure 1 contains a more intense protein band about 26kDa by Ponceau staining, which is replicated in the Santa Cruz blot, indicates this antibody may bind to proteins non-specifically. In addition, using Duolink[®]

Figure .1: Myostatin antibody validation by western blotting. The specificity of three commercially available antibodies was tested using muscle homogenate from untreated adult male Wistar rats. *Top*: Ponceau stain to confirm protein transfer and equal loading, *Bottom*: Immunoblots (A-Bethyl α -GDF8, B-Santa Cruz α -GDF8, C-Millipore α -myostatin near C-terminus). Loading order: **M**-marker, **1**-Recombinant myostatin peptide (100ng/ μ l), **2**-EDL cytosolic fraction, **3**-Gastrocnemius cytosolic, **4**-Soleus cytosolic, **5**-EDL nuclear fraction, **6**-Gastrocnemius nuclear, **7**-Soleus nuclear (all at 100 μ g total protein). Blots A+C were exposed to hyperfilm for 5minutes



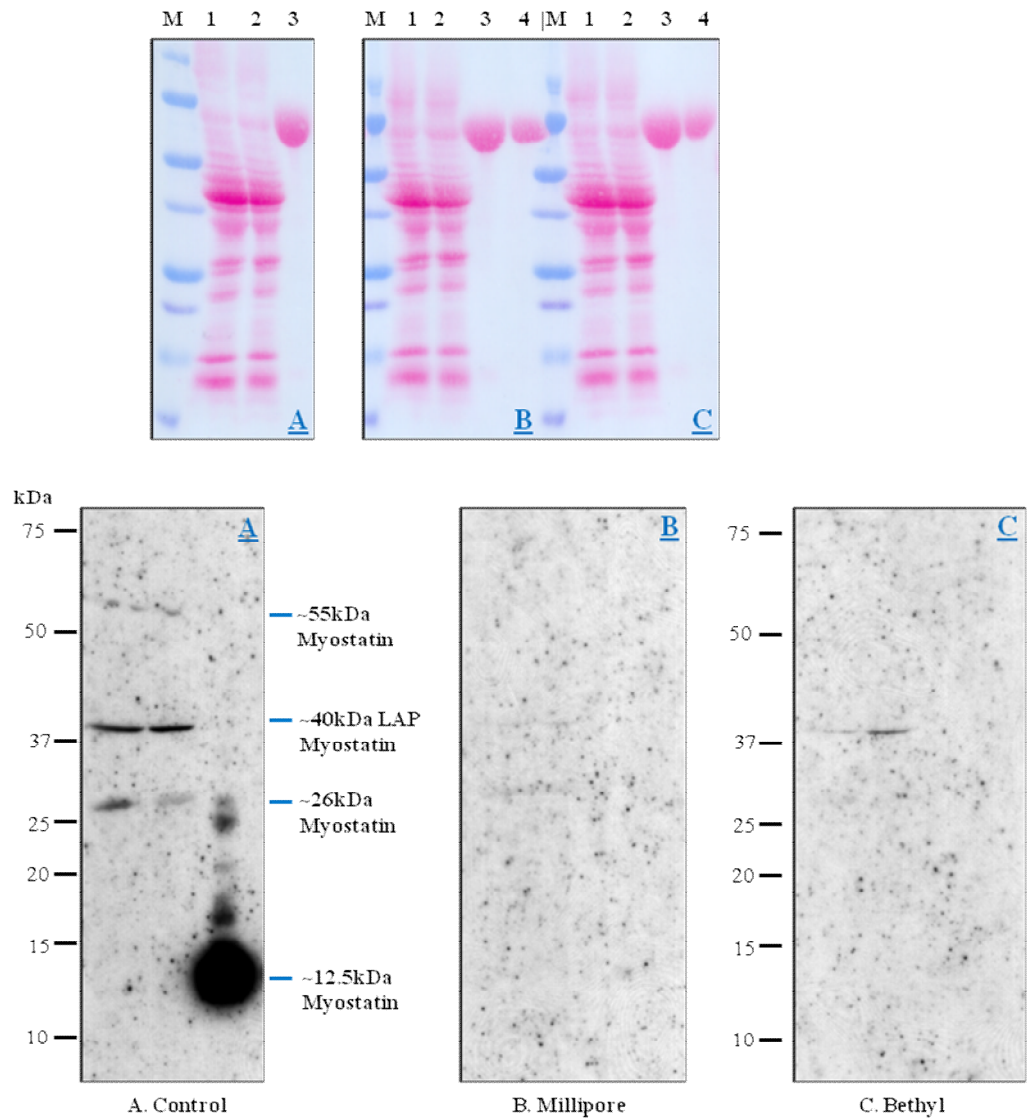
PLA, which increases the specificity of immuno-detection by using two targeted secondary antibodies (see chapter 2, section 2.2.6.3), no bands were detected in that region. We deemed this non-specificity sufficient to eliminate this antibody from further study.

The specificity of the remaining two antibodies was further tested by incubating with an excess of blocking peptide containing portions of the myostatin c-terminal. The blocking peptide completely eliminated the Millipore antibody's ability to recognise any of the myostatin species after long exposure to hyperfilm (>10 minutes), which is usually sufficient to pick up any rare species of myostatin that are on the brink of detection via western blotting (figure 2).

Interestingly, the longer exposure of the control blot to film revealed some rare species of myostatin in the recombinant peptide mix. These are bands of ~17kDa, ~19kDa and ~25kDa previously reported by Lalani *et al.* (2000), Mendler *et al.* (2000) and Baumann *et al.* (2003), respectively. These bands are thought to be rare in skeletal muscle homogenate (Lalani *et al.* 2000) and could represent differentially glycosylated forms of myostatin that are of low abundance, detectable after long exposure to hyperfilm (Gonzalez-Cadavid *et al.* 1998; Rios *et al.* 2004).

The activity of the Bethyl antibody was not completely eliminated by its blocking peptide; the ~40kDa LAP myostatin peptide seen in the control blot could still be detected. It is possible the Bethyl antibody requires a higher concentration of blocking peptide to completely inhibit its activity. In summary, although the blocking peptide eliminated both antibodies' affinity for the recombinant mature myostatin peptide, the Bethyl antibody was more resistant to inhibition by its blocking peptide. Thus we surmised that the Millipore

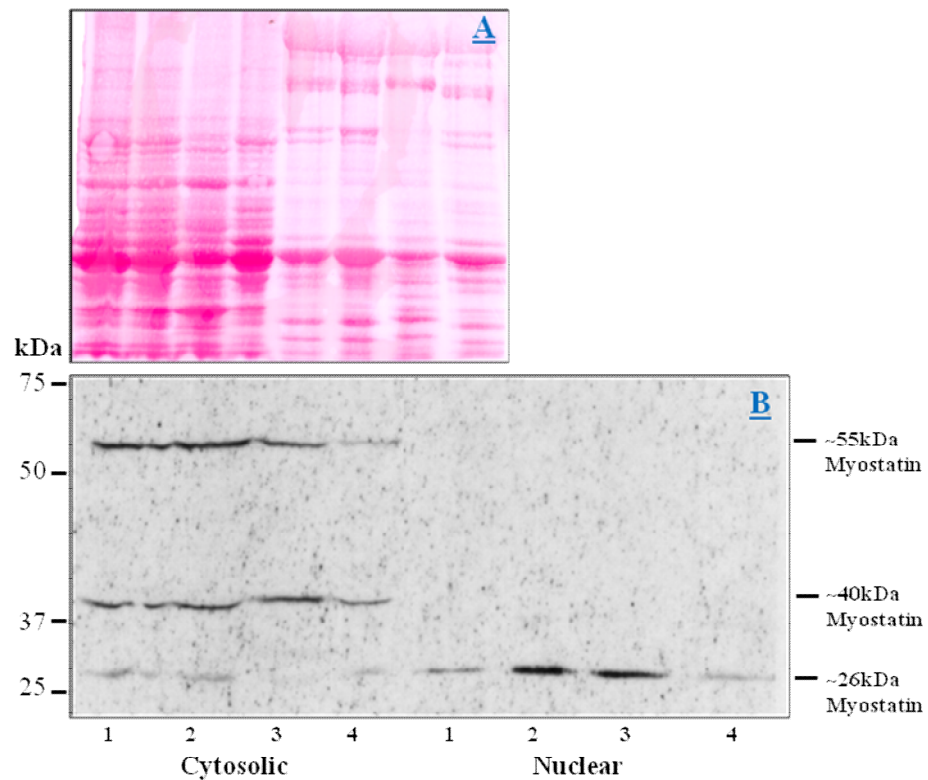
Figure 2: Assessment of Myostatin antibody specificity by competitive blocking and western blotting. The specificity of two commercially available antibodies was tested using muscle homogenate from untreated adult male Wistar rats. *Top*: Ponceau stain to confirm protein transfer and equal loading, *Bottom*: Immunoblots (A-Control (No blocking): Millipore α -myostatin, B-Millipore α -myostatin, C-Bethyl α -myostatin). Loading order: M-marker, 1-Recombinant myostatin peptide (100ng/ μ l), 1-EDL cytosolic fraction, 2-Gastrocnemius cytosolic, 3- Recombinant myostatin peptide (100ng/ μ l), 4- Recombinant myostatin peptide (1ng/ μ l). All blots were exposed to hyperfilm for 10 minutes to enable detection of any protein bands resulting from inefficient antibody blocking.



antibody was more specific and was therefore used to quantify myostatin protein expression in control and treated tissues in our studies (see chapters 3-5).

Some authors such as Wehling *et al.* (2000) have observed a 2kDa difference in myostatin protein in two different types of muscles within the same animal. To rule out such a possibility, we ran a high concentration of total protein (200µg) of cytosolic and nuclear protein fractions from four different skeletal muscles to verify the nature of all the myostatin bands that could be detected using the Millipore antibody (figure 3). Since myostatin protein expression is measured in other muscle types elsewhere in this thesis, it was essential to verify the presence of unprocessed and processed forms within these tissues and rule out any discrepancies regarding molecular size. Three prominent forms of myostatin were detected; pro-myostatin (~55kDa), LAP (~40kDa) and the myostatin dimer (~26kDa), the latter of which was the only species detected in the nuclear fraction. The mature monomeric form was not detected, which confirms reports that active myostatin predominantly exist in its dimeric form in normal adult skeletal muscle. This form of myostatin seemed resistant to the extreme denaturing and reducing conditions used by us (8M Urea) and Gonzalez-Cadavid *et al.* (1998) and Lalani *et al.* (2000), where up to 6M Urea was used.

Figure 3: Myostatin protein detected in cytosolic and nuclear fractions of untreated adult male Wistar rat muscles by western blotting. 200 μ g of protein sample was loaded per lane in the following order: **1-** EDL, **2-** Gastrocnemius, **3-** Soleus, and **4-** Tibialis Anterior. **(A)** Ponceau stain to confirm protein transfer. **(B)** Immunoblot of protein bands present in untreated adult skeletal muscle extracts. Blot was exposed to hyperfilm for 1 minute and developed.



APPENDIX II

Estimating satellite cell size *in situ*

1. Summary

Satellite cell nuclei are between 8 and 12 μ m long in human and rat muscle.

Based on the observation that they're often cut in half on muscle cryo-sections, we reasoned that identifying those cells that are in the cutting plane of two adjacent sections would provide a means of running multiple analysis on the same cell without compromising the cell 'activation status'. In order to be able to use this approach on a series of frozen cross-sections, one needs to establish the proportion of satellite cells that span the cutting plane between a given pair of sections.

Consecutive muscle cross-section pairs were cryo-sectioned, of which the second one was 'flipped' to expose the same cutting surface between the two sections. They were stained using well established satellite cell markers (pax7 or CD56) and imaged. The images of the second (flipped) section were then flipped back in silico, which allowed identification of those nuclei that spanned across the two sections to be counted by light microscopy.

In 8 μ m thick sections of rat muscles, approximately 24% of pax7⁺ satellite cells were identified by position across two consecutive cross-sections. Pax7 is a nuclear antigen, staining with a membrane antigen (CD56/NCAM, a cell-cell recognition glycoprotein) yielded a higher percentage of matched cells across both sections (~36%).

From our observations of the frequency of the same satellite cell spanning the cutting plane of two consecutive cross sections, we devised a mathematical model, which enabled an estimate of the *in-situ* satellite cell size, if the

proportion of satellite cells spanning the cutting plane is known. This could, for example, enable estimation of satellite cell activity status (based on size), following exercise, or in pathological conditions such as DMD or polymyositis, where satellite cell alterations have been reported.

2. Background

As briefly reviewed in Chapter 1, satellite cells are a rare population of progenitor cells in adult skeletal muscle constituting approximately 2-7% of total muscle nuclei within adult muscle (Allbrook *et al.* 1971; Schultz 1974; Schmalbruch and Hellhammer 1976; Halevy *et al.* 2004). The behaviour of satellite cells *in vivo* is poorly understood; it appears that disturbances to the basal lamina (e.g., from exercise-induced myotrauma), activates satellite cells. They subsequently migrate to the source of disturbance using tissue bridges (Watt *et al.* 1987) and participate in repair process, which may include nuclear supplementation or secretion of MRFs.

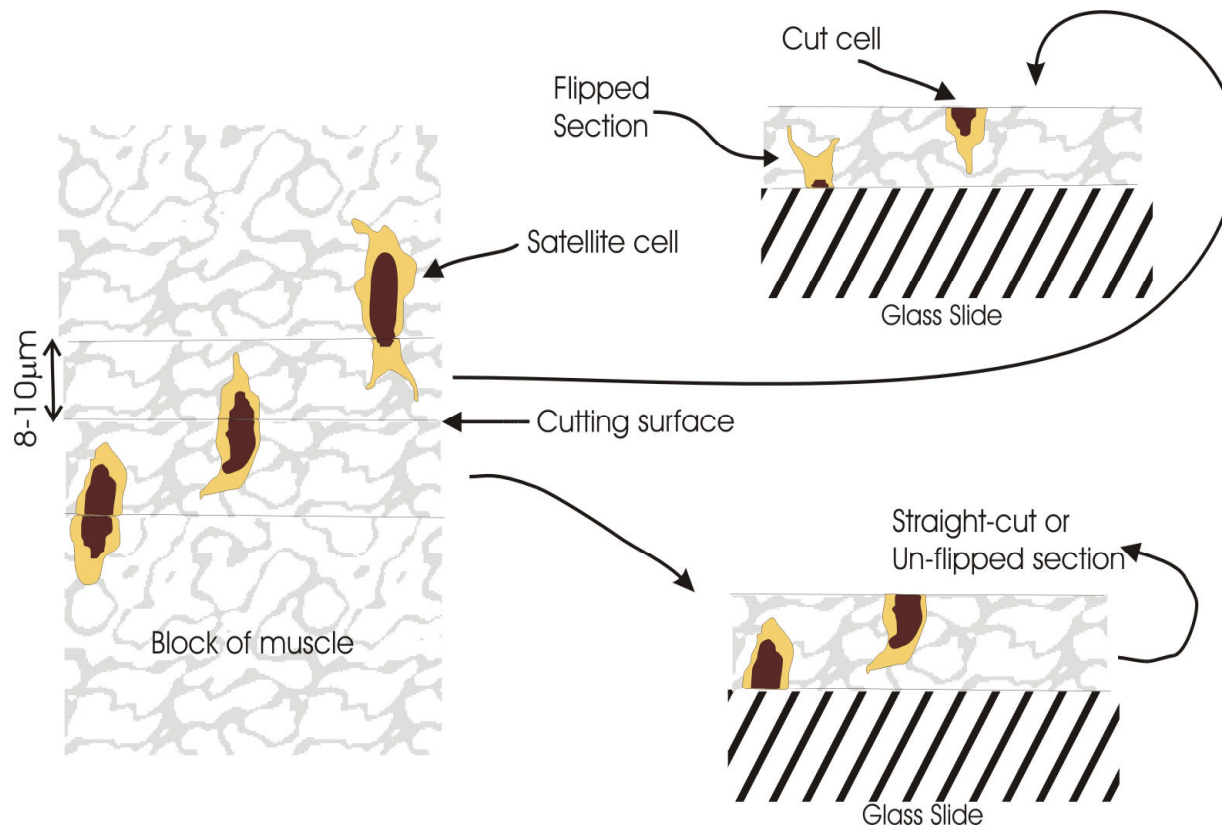
The close association between satellite cells and the basal lamina creates a sense of immediacy between satellite cells and their associated myofibres. This enables satellite cells to function as sensors for muscle mechanical or structural damage. Thus, studying satellite cell activity *in vivo* is quite difficult; isolation of satellite cells disrupts muscle structural integrity, often resulting in activation and alteration of gene expression. As a result, the gene expression profiles of quiescent satellite cells have remained, largely unknown. Therefore, defining the molecular events/mechanisms regulating satellite cell quiescence, under normal physiological conditions and those regulating activation under pathological conditions *in vivo* remains a challenge.

Ultra-structural and immunohistochemical techniques are useful for satellite cell identification, assessing distribution and 'activity status'. However, immunohistochemical approaches are limited by the discovery of satellite cell specific markers and the availability of antibodies. Furthermore, interpretation

of satellite cell specific signalling events derived from crushed muscle extract is made more difficult, since satellite cells represent a relatively small fraction of total tissue volume. With this in mind we sought to explore an alternative method to identify satellite cells in their native environment in the muscle that does not compromise 'activation status'.

Based on the observation that satellite cells are often cut in half in muscle cryo-sections, we reasoned that flipping the second of two adjacent cross-sections, will expose the same cutting surface, and enable the identification of those satellite cells within the cutting plane of two consecutive sections by position (summarised in figure 1), after optically re-flipping images of the second section, such that images of both sections are super-imposable. Thus, satellite cells on one section can be identified by immunohistochemistry using well established satellite cell markers (e.g., pax7 or CD56), whilst utilising the second section as a template. The second section could also be used to determine satellite cell biomarkers with techniques that may be incompatible with the first section. For example, a Duolink[®] PLA assay for rabbit and mouse primary antibodies (as described in chapter 2, section 2.2.6.3), or *in-situ* hybridisation, which requires uncompromised RNA. Another approach could identify satellite cells on the first sections and use the adjacent sections to enrich for satellite cells via laser capture micro-dissection. Theoretically, this should allow multiple molecular analyses to be conducted on the same satellite cell, without compromising its native state. However there is a need to establish the numbers of satellite cells that span the cutting plane of a given pair of sections, i.e., the number of satellite cells that can be identified, using specific markers on both sections.

Fig. 1: Schematic representation of Method. Two consecutive 8-10 μ m muscle sections are cut on the cryostat. The second section is flipped to reveal the same cutting surface as the first. This exposes cut satellite cells for immunohistochemical analysis on the first section and allows the second section to be used as a template for other investigations.



3. Methods

Soleus and TA muscles were obtained from sedentary young female Sprague-Dawley rats (200-250g). Human muscle samples were obtained post-mortem, from the vastus lateralis muscle of a healthy fit 24year old male. Tissue samples were directly frozen in isopentane cooled by liquid nitrogen, then stored at -80°C for later analysis.

Frozen 8-10 μm serial or flipped sections were cut in a cryostat (C1900 microtome, Leica Microsystems, Wetzler, Germany) at -25°C (chamber temperature) and -17°C (chuck temperature). Sections were mounted onto Superfrost® Plus slides (Thermo Fisher, Loughborough, UK) and fixed in 4% Paraformaldehyde (PFA/PBS: 4% (w/v) PFA, 137mM NaCl, 2.7mM KCl, 4.3mM KH_2PO_4 5mM MgCl_2 pH 7.4) for 3 minutes. Sections were washed in tris-buffered saline (TBS; 0.05M Tris, 0.15M NaCl, pH 7.4) for 3 x 5minutes and blocked with 5% normal horse serum (Vector Laboratories, Burlingame, CA, USA). Sections were incubated in primary antibody for 1-2hr at either room temperature (anti-pax7 monoclonal antibody 1:20 – Developmental Studies Hybridoma Bank, Iowa, USA) or at 37°C (anti-CD56 monoclonal antibody 1:30 – BD Biosciences, NJ, USA). Control sections were incubated in blocker only.

Primary antibodies were visualised with Vectastain® anti-mouse kit (biotinylated anti-mouse IgG secondary antibodies 1:300, ABC reagent and DAB substrate kit for peroxidase – Vector Labs). Rat muscle sections were incubated with a rat adsorbed secondary antibody (Vector Labs) to improve signal-to-noise ratio. Optimal antibody dilutions were determined in

preliminary optimisation experiments and DAB staining was controlled visually (minimum, 2 min and maximum, 5 min). Slides were immediately rinsed in double distilled water for at least 5 minutes to stop the reaction, air dried and mounted in glycerol gelatine (Merck, Darmstadt, Germany) for microscopy. Satellite cells were counted with light microscopy and images acquired using a Micropublisher 3.3 RTV digital camera (Q-Imaging, British Columbia, Canada) attached to a Leica DM4000B light microscope.

4. Results

To determine the incidence of a cut satellite cell spanning across two 8µm sections of a pair, adjacent/flipped cross-sections from rat soleus and tibialis anterior muscles were stained with pax7. Section 1 and section 2 (the flipped section) were stained with anti-pax7 antibody only. For human vastus lateralis muscle, 10µm adjacent cross-sections were stained with anti-CD56 only, or pax7 and CD56; i.e. section 1 was stained against pax7 and section 2 against CD56 (see examples in figure 2). CD56, also known as neural cell adhesion molecule (NCAM) is a cell surface glycoprotein involved in cell-cell interaction (Schubert *et al.* 1989). It is expressed in quiescent and activated satellite cells and has been used in a number of human studies to identify and quantify satellite cells (Kadi *et al.* 2004; Mackey *et al.* 2007; O'Reilly *et al.* 2008; Mackey *et al.* 2009).

The number of pax7⁺/pax7⁺ and pax7⁺/CD56⁺ satellite cells identified in the same position across both sections, were counted and expressed as a percentage of the total number of satellite cells identified on both sections (% match). The percentages of matched cells on different muscles, using either one or a combination of both antibodies are presented in figure 3. The numbers of satellite cells matched on adjacently paired sections stained with CD56 only were slightly higher than those stained with CD56/Pax7 or pax7 only.

Figure 2A: Photomicrograph showing CD56⁺ satellite cells identified on adjacent cross-sections of human vastus lateralis muscle. One section (panel A) was flipped to reveal the same cutting surface as the adjacent sections and both stained against CD56. The photomicrographs are mirror images of each other. Arrows indicate those cells that are CD56⁺, with the white ones showing those cut cells present on both sections.

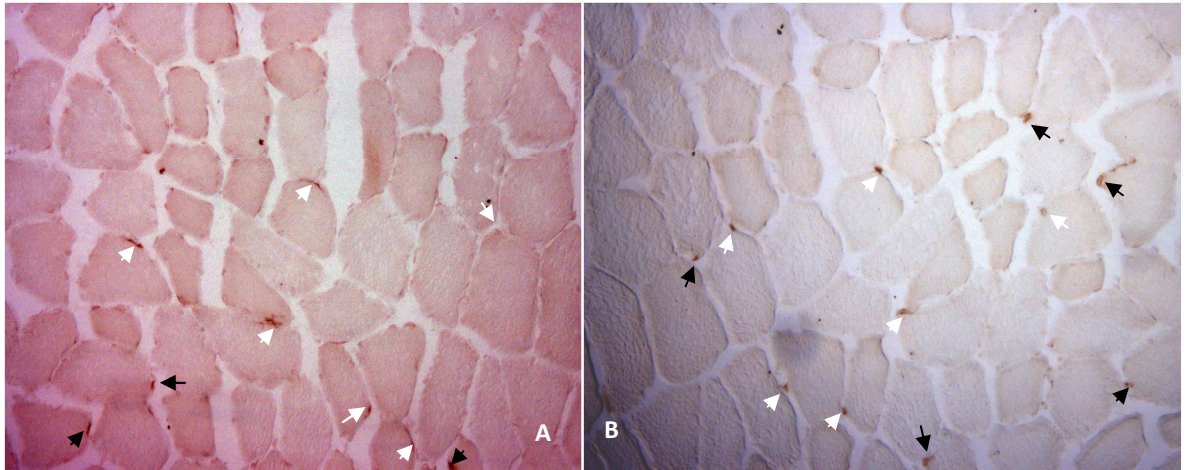


Fig 2B: Pax7⁺ and NCAM⁺ satellite cells identified on adjacent cross-sections of human vastus lateralis muscle. Panel A represents the flipped section, stained against CD56 whilst panel B shows the un-flipped section, which was stained against Pax7⁺. Both images mirror each other and are representative of the entire section. The arrows show those cells that were positive for either antigen in the respective sections; the red arrows show only those cells that are positive on both

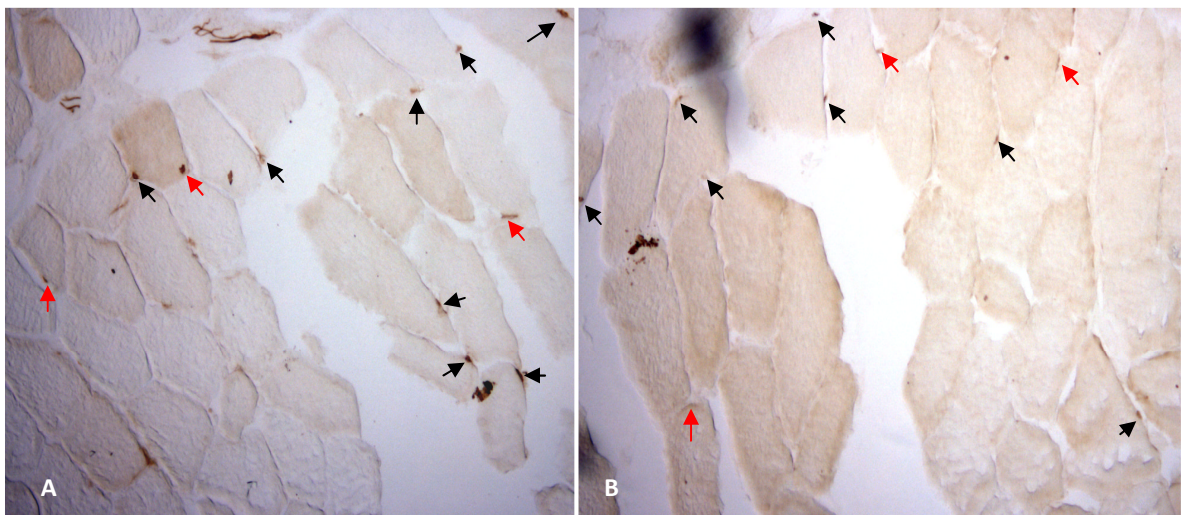
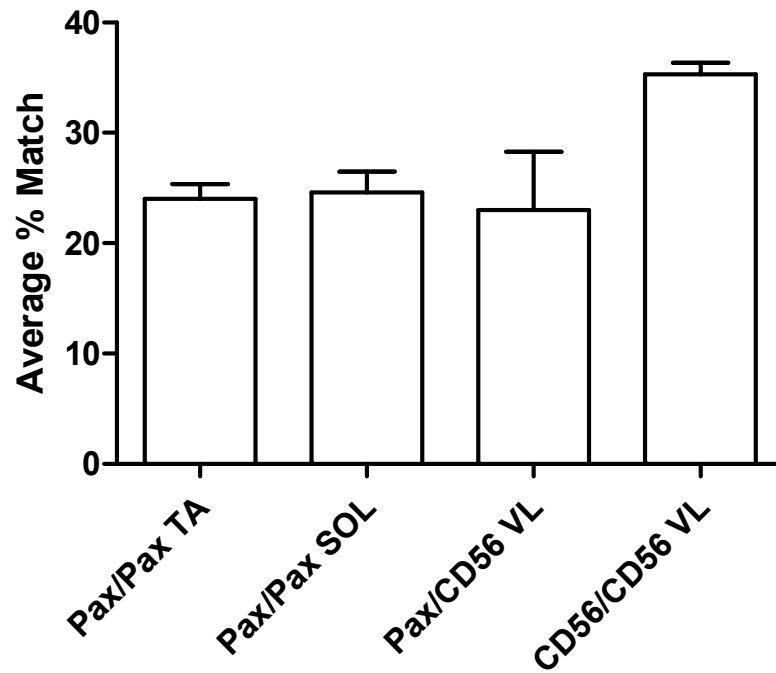


Figure 3: Average % match of satellite cells at the cutting surface of adjacent cross sections of rat and human muscle. Values are means and vertical bars represent S.E.M (n=5). Comparisons between Pax/Pax, Pax/CD56 and CD56/CD56 by 1-way ANOVA: $p=0.04$. Rat muscles: Tibialis Anterior (TA), Soleus (SOL). Human: Vastus Lateralis (VA).



5. Discussion

From observations of the frequency of cut satellite cells spanning across a pair of adjacent cross-sections and published information on satellite cell length (Muir *et al.* 1965; Tome and Fardeau 1986), we devised a mathematical model, to estimate the expected proportion of matched cells given the length of a satellite cell and section thickness (figure 4). The model is consistent with the hypothesis that the proportion of matched cells increases with thinner sections and decreases with thicker sections (see figure 5). The larger the satellite cell, the greater the incidence of it spanning the cutting plane.

Given an average satellite cell length of $8\mu\text{m}$ on $10\mu\text{m}$ thick sections: using $P = a / (2a + 2b) \times 100$, as shown in figure 3, the theoretical proportion of matched cells expected would be $\sim 22\%$. Using the same satellite cell length to calculate the proportion of matched cells on $5\mu\text{m}$ thick sections estimates a 30% match, compared to a $10\mu\text{m}$ section. It appears the hypothesis that the larger the cell or thinner the section, the larger the percentage match, is only valid to a certain extent. This is demonstrated in figure 4; doubling the theoretical satellite cell length or halving the section thickness does not double the percentage match.

Electron microscopy studies on normal, disease-free human and rat muscles have reported the average length of a satellite cell nuclei varies between 8 and $12\mu\text{m}$ (Schmalbruch 1977; Snow 1977b; Snow 1977a; Watkins and Cullen 1988). Using the model and the formula presented in figure 3, the average length of satellite cells in a cross section can be estimated, when the percentage match is known. Reversing the formula should enable estimation of satellite cell length, given:

Figure 4: Schematic diagram of theoretical limitations of the method. The red line depicts the cutting surface with a pair of 8µm sections of interest on either side, one of which is flipped. Assuming a linear distribution of satellite cells in a block of muscle, the proportion of satellite cells spanning across both sections can be estimated using a formula. Based on this model, the theoretical % of identified satellite cells spanning across both sections, P, can be estimated, given a cell length of 8µm and 8µm sections = $8/[(2 \times 8) + (2 \times 8)] = 25\%$, this is close to our observation of ~24% in rat soleus and TA muscles. By reversing the formula to solve for 'a', the satellite cell length can also be estimated.

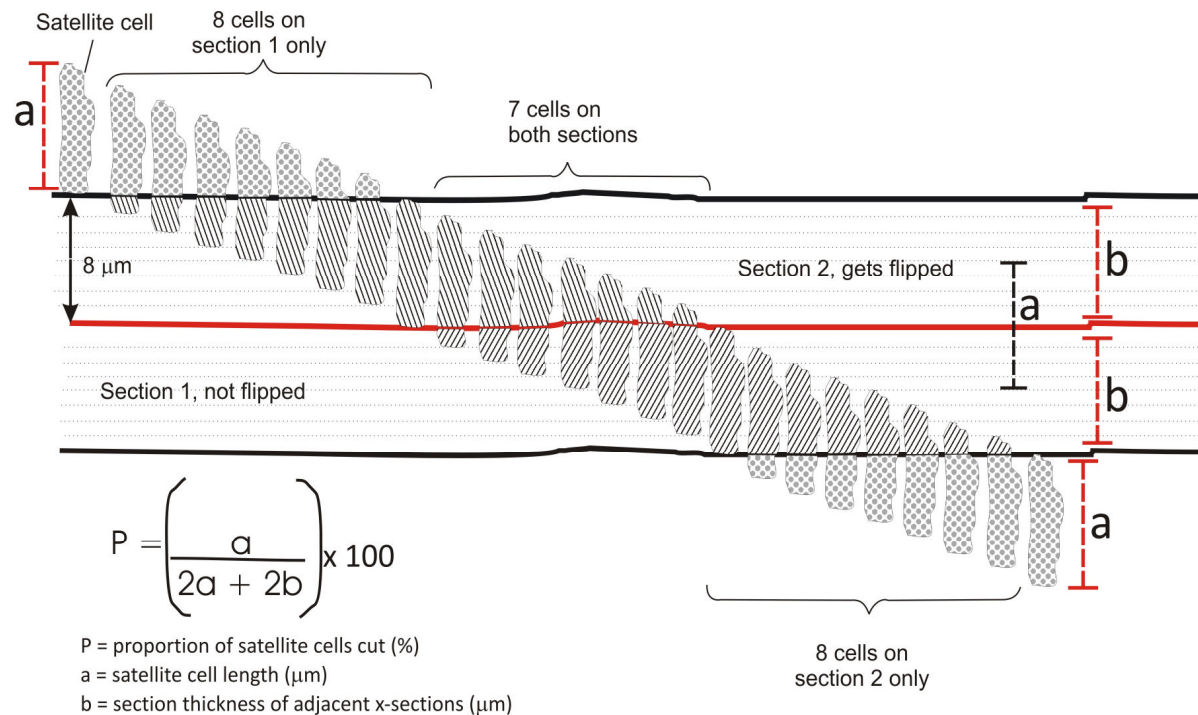
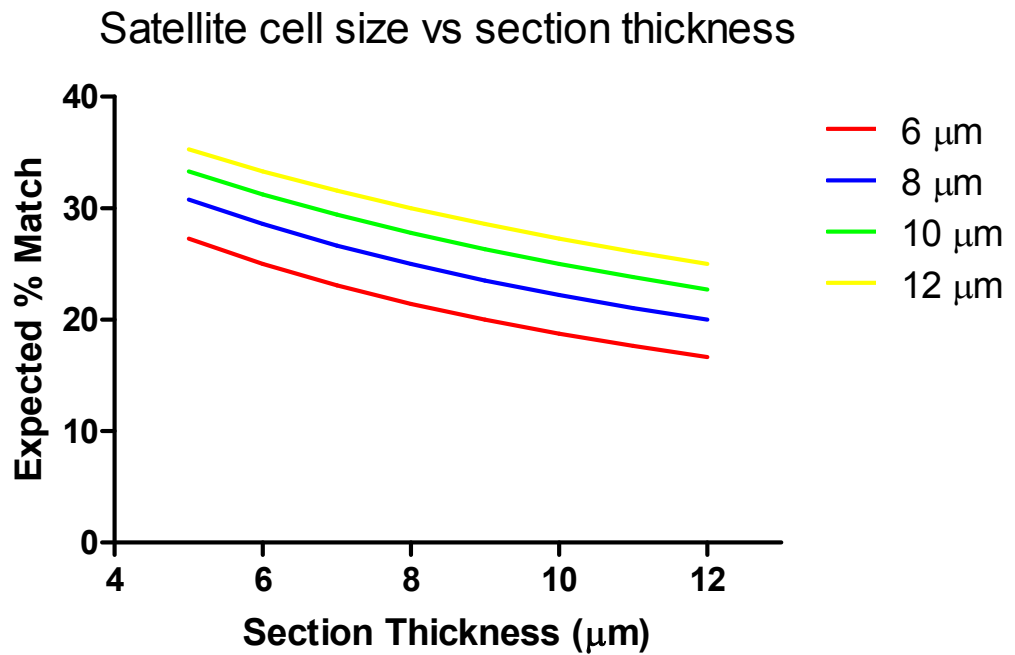


Figure 5: Expected % of satellite cells matched based on theoretical distribution of satellite cells in a muscle. Using the formula $P = a / (2a + 2b) \times 100$, see figure. 3, calculating the theoretical percentage of satellite cells expected given the thickness of cryostat sections and the average satellite cell length, shows a decrease with section thickness and vice versa. The trend favours an increase in % matches with increased satellite cell length.



the proportion of matched cells. For example given, $P \sim 24\%$ on adjacent $8\mu\text{m}$ sections of rat muscle, the average length of a satellite cell, 'a' can be estimated thus

$$P = 24/100 = 0.24$$

$$a = (P \times 2b) / (1-2P)$$

$$\Rightarrow (0.24 \times 16) / (1-0.48) = 7.4\mu\text{m}.$$

This is quite close to published reports of satellite cell nuclear length, which has been found to vary between $8-12\mu\text{m}$. This model could provide a novel approach for quantitative study of satellite cell nuclear changes in muscle disorders, as an alternative to electron microscopy. Pax7 is a nuclear antigen (Gnocchi et al, 2009); hence positive matches show those satellite cells cut at the level of the cell nuclei; a lower frequency than using a membrane antigen such as CD56, which increases the proportion of satellite cell identified spanning the cutting plane, since the probability identifying cut satellite cell cytoplasm is greater compared to the nucleus. This explains the higher proportion of matched cells seen in the CD56-only stained sections. Solving the formula for 'a' as above, using the average proportion of matched cells on CD56 only stained sections ($\sim 36\%$) estimates an average length of $22\mu\text{m}$.

This likely explains the modest numbers of pax7 only satellite cells identified across adjacent cross-sections; since pax7 is confined to the nucleus, in contrast to the membrane staining of CD56, which stains the longer lamellipodia satellite cell extensions. In a satellite cell profile tracing study by Mackey *et al.* (2009), comparisons between pax7 and CD56 stained satellite cells across

multiple consecutive $7\mu\text{m}$ cross sections, showed the same pax7^+ satellite cell could not be seen in more than two consecutive cross-sections, a depth of $14\mu\text{m}$. This was in contrast to CD56^+ satellite cells, which could be traced over 5 consecutive sections, a depth of $35\mu\text{m}$.

Quiescent satellite cells have scant cytoplasm, a high nuclear-to-cytoplasmic ratio with large amounts of heterochromatin relative to activated satellite cells, which undergo cytoplasmic expansion due to increased size and number of organelles (reviewed by Schultz and McCormick 1994). Therefore, the frequency of satellite cells spanning the cutting plane should improve with activated satellite cells.

The mathematical analysis presented show results obtained are close to the theoretical optimum; we sought to identify satellite cells in the cutting plane of two adjacent muscle cross sections, in order to test the feasibility of developing a method, which extracts maximum information from a series of cryo-sections, without compromising satellite cell 'activation status'. In summary, establishment of the proportion of satellite cells spanning the cutting plane facilitated the formulation of a mathematical model, which enabled estimation of satellite cell size, when the proportion of satellite cells on either side of the cutting plane is known. Estimation of satellite cell nuclear and cytoplasmic size, using the model revealed in lengths of $\sim 7\mu\text{m}$ and $\sim 22\mu\text{m}$, respectively – similarly to published reports.

Further development of the model could be useful for estimating satellite cell size in various pathological conditions such as polymyositis, and muscular dystrophies, where satellite cell nuclear alterations are markers of disease

severity (reviewed by Tome and Fardeau 1986; Watkins and Cullen 1988; Park *et al.* 2009). Using this method, a more complete picture of satellite cell 'activity status' could be determined; based on the size and gene expression profile (using established markers) of satellite cells from muscle biopsies, following an exercise regime or drug intervention for example. Future work aimed at developing this method further should compare pax7/pax7 and CD56/CD56 results in the same species (since the CD56 antibody used here was specific for human NCAM). It would also be useful to determine the proportion of that could be identified on the adjacent section when a non-specific satellite cell marker is used such as ki-67. Additionally, it would be beneficial to test the feasibility of the method further, by estimating satellite cell size in different muscles/species, under different conditions (e.g. atrophy, hypertrophy, etc).

REFERENCES

- Aagaard P. (2004). "Making muscles "stronger": exercise, nutrition, drugs." J Musculoskelet Neuronal Interact **4**(2): 165-74.
- Acharyya S., Ladner K.J., Nelsen L.L., Damrauer J., Reiser P.J., Swoap S. and Guttridge D.C. (2004). "Cancer cachexia is regulated by selective targeting of skeletal muscle gene products." J Clin Invest **114**(3): 370-8.
- Alamdari N., Constantin-Teodosiu D., Murton A.J., Gardiner S.M., Bennett T., Layfield R. and Greenhaff P.L. (2008). "Temporal changes in the involvement of pyruvate dehydrogenase complex in muscle lactate accumulation during lipopolysaccharide infusion in rats." J Physiol **586**(6): 1767-75.
- Alberti C., Brun-Buisson C., Burchardi H., Martin C., Goodman S., Artigas A., Sicignano A., Palazzo M., Moreno R., Boulme R., Lepage E. and Le Gall R. (2002). "Epidemiology of sepsis and infection in ICU patients from an international multicentre cohort study." Intensive Care Med **28**(2): 108-21.
- Allbrook D.B., Han M.F. and Hellmuth A.E. (1971). "Population of muscle satellite cells in relation to age and mitotic activity." Pathology **3**(3): 223-43.
- Allen D.L., Roy R.R. and Edgerton V.R. (1999). "Myonuclear domains in muscle adaptation and disease." Muscle Nerve **22**(10): 1350-60.
- Anderson J.E. (2000). "A Role for Nitric Oxide in Muscle Repair: Nitric Oxide-mediated Activation of Muscle Satellite Cells." Mol. Biol. Cell **11**(5): 1859-1874.
- Anderson J.E. and Vargas C. (2003). "Correlated NOS-I[μ] and myf5 expression by satellite cells in mdx mouse muscle regeneration during NOS manipulation and deflazacort treatment." Neuromuscular Disorders **13**(5): 388-396.
- Anderson S.B., Goldberg A.L. and Whitman M. (2008). "Identification of a novel pool of extracellular pro-myostatin in skeletal muscle." J Biol Chem **283**(11): 7027-35.
- Andres V. and Walsh K. (1996). "Myogenin expression, cell cycle withdrawal, and phenotypic differentiation are temporally separable events that precede cell fusion upon myogenesis." J Cell Biol **132**(4): 657-66.
- Annane D. (2001). "Corticosteroids for septic shock." Crit Care Med **29**(7 Suppl): S117-20.
- Appell H.J., Forsberg S. and Hollmann W. (1988). "Satellite cell activation in human skeletal muscle after training: evidence for muscle fiber neof ormation." Int J Sports Med **9**(4): 297-9.

- Armand O., Boutineau A.M., Mauger A., Pautou M.P. and Kiény M. (1983). "Origin of satellite cells in avian skeletal muscles." Arch Anat Microsc Morphol Exp **72**(2): 163-81.
- Auclair D., Garrel D.R., Chaouki Zerouala A. and Ferland L.H. (1997). "Activation of the ubiquitin pathway in rat skeletal muscle by catabolic doses of glucocorticoids." Am J Physiol **272**(3 Pt 1): C1007-16.
- Austin L. and Burgess A.W. (1991). "Stimulation of myoblast proliferation in culture by leukaemia inhibitory factor and other cytokines." J Neurol Sci **101**(2): 193-7.
- Baker D.J. (2004). Effect of Pharmacological Intervention on Skeletal Muscle Composition, Metabolism and Function in the Rat. Biomedical Sciences. Nottingham, University of Nottingham. **PhD thesis**.
- Balagopal P., Schimke J.C., Ades P., Adey D. and Nair K.S. (2001). "Age effect on transcript levels and synthesis rate of muscle MHC and response to resistance exercise." Am J Physiol Endocrinol Metab **280**(2): E203-8.
- Baldwin A.S., Jr. (1996). "The NF-kappa B and I kappa B proteins: new discoveries and insights." Annu Rev Immunol **14**: 649-83.
- Ball E.H. and Sanwal B.D. (1980). "A synergistic effect of glucocorticoids and insulin on the differentiation of myoblasts." J Cell Physiol **102**(1): 27-36.
- Barton-Davis E.R., Shoturma D.I. and Sweeney H.L. (1999). "Contribution of satellite cells to IGF-I induced hypertrophy of skeletal muscle." Acta Physiol Scand **167**(4): 301-5.
- Baumann A.P., Ibebunjo C., Grasser W.A. and Paralkar V.M. (2003). "Myostatin expression in age and denervation-induced skeletal muscle atrophy." J Musculoskelet Neuronal Interact **3**(1): 8-16.
- Beauchamp J.R., Heslop L., Yu D.S.W., Tajbakhsh S., Kelly R.G., Wernig A., Buckingham M.E., Partridge T.A. and Zammit P.S. (2000). "Expression of CD34 and Myf5 Defines the Majority of Quiescent Adult Skeletal Muscle Satellite Cells." J. Cell Biol. **151**(6): 1221-1234.
- Ben-Yair R., Kahane N. and Kalcheim C. (2003). "Coherent development of dermomyotome and dermis from the entire mediolateral extent of the dorsal somite." Development **130**(18): 4325-4336.
- Benson D.W., Foley-Nelson T., Chance W.T., Zhang F.S., James J.H. and Fischer J.E. (1991). "Decreased myofibrillar protein breakdown following treatment with clenbuterol." J Surg Res **50**(1): 1-5.
- Bettors J.L., Long J.H., Howe K.S., Braith R.W., Soltow Q.A., Lira V.A. and Criswell D.S. (2008). "Nitric oxide reverses prednisolone-induced inactivation of muscle satellite cells." Muscle Nerve **37**(2): 203-9.

- Beutler B., Krochin N., Milsark I.W., Luedke C. and Cerami A. (1986). "Control of cachectin (tumor necrosis factor) synthesis: mechanisms of endotoxin resistance." Science **232**(4753): 977-80.
- Beutler B., Mahoney J., Le Trang N., Pekala P. and Cerami A. (1985a). "Purification of cachectin, a lipoprotein lipase-suppressing hormone secreted by endotoxin-induced RAW 264.7 cells." J Exp Med **161**(5): 984-95.
- Beutler B.A., Milsark I.W. and Cerami A. (1985b). "Cachectin/tumor necrosis factor: production, distribution, and metabolic fate in vivo." J Immunol **135**(6): 3972-7.
- Bhasin S., Calof O.M., Storer T.W., Lee M.L., Mazer N.A., Jasuja R., Montori V.M., Gao W.Q. and Dalton J.T. (2006). "Drug Insight: testosterone and selective androgen receptor modulators as anabolic therapies for chronic illness and aging." Nature Clinical Practice Endocrinology & Metabolism **2**(3): 146-159.
- Bish L.T., Morine K.J., Sleeper M.M. and Sweeney H.L. (2010). "Myostatin is upregulated following stress in an Erk-dependent manner and negatively regulates cardiomyocyte growth in culture and in a mouse model." PLoS ONE **5**(4): e10230.
- Black R.A. (2002). "Tumor necrosis factor-alpha converting enzyme." Int J Biochem Cell Biol **34**(1): 1-5.
- Blackwell G.J., Carnuccio R., Di Rosa M., Flower R.J., Parente L. and Persico P. (1980). "Macro cortin: a polypeptide causing the anti-phospholipase effect of glucocorticoids." Nature **287**(5778): 147-9.
- Blough E., Dineen B. and Esser K. (1999). "Extraction of nuclear proteins from striated muscle tissue." Biotechniques **26**(2): 202-4, 206.
- Bogdanovich S., Perkins K.J., Krag T.O. and Khurana T.S. (2004). "Therapeutics for Duchenne muscular dystrophy: current approaches and future directions." J Mol Med (Berl) **82**(2): 102-15.
- Bondesen B.A., Mills S.T. and Pavlath G.K. (2006). "The COX-2 pathway regulates growth of atrophied muscle via multiple mechanisms." Am J Physiol Cell Physiol **290**(6): C1651-9.
- Bone R.C., Balk R.A., Cerra F.B., Dellinger R.P., Fein A.M., Knaus W.A., Schein R.M. and Sibbald W.J. (1992). "Definitions for sepsis and organ failure and guidelines for the use of innovative therapies in sepsis. The ACCP/SCCM Consensus Conference Committee. American College of Chest Physicians/Society of Critical Care Medicine." Chest **101**(6): 1644-55.
- Brack A.S., Bildsoe H. and Hughes S.M. (2005). "Evidence that satellite cell decrement contributes to preferential decline in nuclear number from

- large fibres during murine age-related muscle atrophy." J Cell Sci **118**(Pt 20): 4813-21.
- Brack A.S., Conboy M.J., Roy S., Lee M., Kuo C.J., Keller C. and Rando T.A. (2007). "Increased Wnt signaling during aging alters muscle stem cell fate and increases fibrosis." Science **317**(5839): 807-10.
- Bradley L., Yaworsky P.J. and Walsh F.S. (2008). "Myostatin as a therapeutic target for musculoskeletal disease." Cell Mol Life Sci **65**(14): 2119-24.
- Braissant O., Foufelle F., Scotto C., Dauca M. and Wahli W. (1996). "Differential expression of peroxisome proliferator-activated receptors (PPARs): tissue distribution of PPAR-alpha, -beta, and -gamma in the adult rat." Endocrinology **137**(1): 354-66.
- Briguet A., Courdier-Fruh I., Foster M., Meier T. and Magyar J.P. (2004). "Histological parameters for the quantitative assessment of muscular dystrophy in the mdx-mouse." Neuromuscul Disord **14**(10): 675-82.
- Bruscoli S., Donato V., Velardi E., Di Sante M., Migliorati G., Donato R. and Riccardi C. (2010). "Glucocorticoid-induced leucine zipper (GILZ) and long GILZ inhibit myogenic differentiation and mediate anti-myogenic effects of glucocorticoids." J Biol Chem **285**(14): 10385-96.
- Brunnsgaard H., Pedersen M. and Pedersen B.K. (2001). "Aging and proinflammatory cytokines." Curr Opin Hematol **8**(3): 131-6.
- Bruusgaard J.C., Johansen I.B., Egnér I.M., Rana Z.A. and Gundersen K. (2010). "Myonuclei acquired by overload exercise precede hypertrophy and are not lost on detraining." Proc Natl Acad Sci U S A **107**(34): 15111-6.
- Cantini M., Massimino M.L., Rapizzi E., Rossini K., Catani C., Dalla Libera L. and Carraro U. (1995). "Human satellite cell proliferation in vitro is regulated by autocrine secretion of IL-6 stimulated by a soluble factor(s) released by activated monocytes." Biochem Biophys Res Commun **216**(1): 49-53.
- Cao Y., Zhao Z., Gruszczynska-Biegala J. and Zolkiewska A. (2003). "Role of Metalloprotease Disintegrin ADAM12 in Determination of Quiescent Reserve Cells during Myogenic Differentiation In Vitro." Mol. Cell. Biol. **23**(19): 6725-6738.
- Carlson B.M. and Faulkner J.A. (1989). "Muscle transplantation between young and old rats: age of host determines recovery." Am J Physiol **256**(6 Pt 1): C1262-6.
- Carlson C.J., Booth F.W. and Gordon S.E. (1999). "Skeletal muscle myostatin mRNA expression is fiber-type specific and increases during hindlimb unloading." Am J Physiol **277**(2 Pt 2): R601-6.

- Carraro L., Ferraresso S., Cardazzo B., Romualdi C., Montesissa C., Gottardo F., Patarnello T., Castagnaro M. and Bargelloni L. (2009). "Expression profiling of skeletal muscle in young bulls treated with steroidal growth promoters." Physiol Genomics **38**(2): 138-48.
- Casey L.C., Balk R.A. and Bone R.C. (1993). "Plasma cytokine and endotoxin levels correlate with survival in patients with the sepsis syndrome." Ann Intern Med **119**(8): 771-8.
- Cassano M., Quattrocchi M., Crippa S., Perini I., Ronzoni F. and Sampaolesi M. (2009). "Cellular mechanisms and local progenitor activation to regulate skeletal muscle mass." J Muscle Res Cell Motil **30**(7-8): 243-53.
- Champion D.R. (1984). "The muscle satellite cell: a review." Int Rev Cytol **87**: 225-251.
- Chandrasheharan K. and Martin P.T. (2009). "Embryonic overexpression of Galgt2 inhibits skeletal muscle growth via activation of myostatin signaling." Muscle Nerve **39**(1): 25-41.
- Charge S.B.P. and Rudnicki M.A. (2004). "Cellular and Molecular Regulation of Muscle Regeneration." Physiol. Rev. **84**(1): 209-238.
- Chazaud B., Brigitte M., Yacoub-Youssef H., Arnold L., Gherardi R., Sonnet C., Lafuste P. and Chretien F. (2009). "Dual and beneficial roles of macrophages during skeletal muscle regeneration." Exerc Sport Sci Rev **37**(1): 18-22.
- Chen S.E., Jin B. and Li Y.P. (2007). "TNF-alpha regulates myogenesis and muscle regeneration by activating p38 MAPK." Am J Physiol Cell Physiol **292**(5): C1660-71.
- Chi N. and Epstein J.A. (2002). "Getting your Pax straight: Pax proteins in development and disease." Trends Genet **18**(1): 41-7.
- Chretien S., Dubart A., Beaupain D., Raich N., Grandchamp B., Rosa J., Goossens M. and Romeo P.H. (1988). "Alternative transcription and splicing of the human porphobilinogen deaminase gene result either in tissue-specific or in housekeeping expression." Proc Natl Acad Sci U S A **85**(1): 6-10.
- Christ B., Jacob H.J. and Jacob M. (1974). "[Origin of wing musculature. Experimental studies on quail and chick embryos]." Experientia **30**(12): 1446-9.
- Chrysis D. and Underwood L.E. (1999). "Regulation of components of the ubiquitin system by insulin-like growth factor I and growth hormone in skeletal muscle of rats made catabolic with dexamethasone." Endocrinology **140**(12): 5635-41.

- Clowes G.H., Jr., George B.C., Villee C.A., Jr. and Saravis C.A. (1983). "Muscle proteolysis induced by a circulating peptide in patients with sepsis or trauma." N Engl J Med **308**(10): 545-52.
- Cohen J. (2002). "The immunopathogenesis of sepsis." Nature **420**(6917): 885-91.
- Comstock K.L., Krown K.A., Page M.T., Martin D., Ho P., Pedraza M., Castro E.N., Nakajima N., Glembotski C.C., Quintana P.J. and Sabbadini R.A. (1998). "LPS-induced TNF-alpha release from and apoptosis in rat cardiomyocytes: obligatory role for CD14 in mediating the LPS response." J Mol Cell Cardiol **30**(12): 2761-75.
- Conboy I.M., Conboy M.J., Wagers A.J., Girma E.R., Weissman I.L. and Rando T.A. (2005). "Rejuvenation of aged progenitor cells by exposure to a young systemic environment." Nature **433**(7027): 760-4.
- Conboy I.M. and Rando T.A. (2002). "The Regulation of Notch Signaling Controls Satellite Cell Activation and Cell Fate Determination in Postnatal Myogenesis." Developmental Cell **3**(3): 397-409.
- Cooper R.N., Tajbakhsh S., Mouly V., Cossu G., Buckingham M. and Butler-Browne G.S. (1999). "In vivo satellite cell activation via Myf5 and MyoD in regenerating mouse skeletal muscle." J Cell Sci **112**(17): 2895-2901.
- Cornelison D.D., Olwin B.B., Rudnicki M.A. and Wold B.J. (2000). "MyoD(-/-) satellite cells in single-fiber culture are differentiation defective and MRF4 deficient." Dev Biol **224**(2): 122-37.
- Cornelison D.D.W. and Wold B.J. (1997). "Single-Cell Analysis of Regulatory Gene Expression in Quiescent and Activated Mouse Skeletal Muscle Satellite Cells." Developmental Biology **191**(2): 270-283.
- Cossu G., Eusebi F., Grassi F. and Wanke E. (1987). "Acetylcholine receptor channels are present in undifferentiated satellite cells but not in embryonic myoblasts in culture." Dev Biol **123**(1): 43-50.
- Criswell D.S., Powers S.K. and Herb R.A. (1996). "Clenbuterol-induced fiber type transition in the soleus of adult rats." Eur J Appl Physiol Occup Physiol **74**(5): 391-6.
- Crossland H., Constantin-Teodosiu D., Gardiner S.M., Constantin D. and Greenhaff P.L. (2008). "A potential role for Akt/FOXO signalling in both protein loss and the impairment of muscle carbohydrate oxidation during sepsis in rodent skeletal muscle." J Physiol **586**(Pt 22): 5589-600.
- Crossland H., Constantin-Teodosiu D., Greenhaff P.L. and Gardiner S.M. (2010). "Low-dose dexamethasone prevents endotoxaemia-induced muscle protein loss and impairment of carbohydrate oxidation in rat skeletal muscle." J Physiol **588**(Pt 8): 1333-47.

- D'Agostino R.B. and Stephens M.A. (1986). Goodness of Fit Techniques, Dekker.
- Dangott B., Schultz E. and Mozdziak P.E. (2000). "Dietary creatine monohydrate supplementation increases satellite cell mitotic activity during compensatory hypertrophy." Int J Sports Med **21**(1): 13-6.
- Darr K.C. and Schultz E. (1989). "Hindlimb suspension suppresses muscle growth and satellite cell proliferation." J Appl Physiol **67**(5): 1827-34.
- Day K., Shefer G., Richardson J.B., Enikolopov G. and Yablonka-Reuveni Z. (2007). "Nestin-GFP reporter expression defines the quiescent state of skeletal muscle satellite cells." Dev Biol **304**(1): 246-59.
- Day K., Shefer G., Shearer A. and Yablonka-Reuveni Z. (2010). "The depletion of skeletal muscle satellite cells with age is concomitant with reduced capacity of single progenitors to produce reserve progeny." Dev Biol **340**(2): 330-43.
- De Angelis L., Berghella L., Coletta M., Lattanzi L., Zanchi M., Gabriella C.M., Ponzetto C. and Cossu G. (1999). "Skeletal Myogenic Progenitors Originating from Embryonic Dorsal Aorta Coexpress Endothelial and Myogenic Markers and Contribute to Postnatal Muscle Growth and Regeneration." J. Cell Biol. **147**(4): 869-878.
- Dedkov E.I., Kostrominova T.Y., Borisov A.B. and Carlson B.M. (2003). "MyoD and myogenin protein expression in skeletal muscles of senile rats." Cell Tissue Res **311**(3): 401-16.
- Degens H. (2007). "Age-related skeletal muscle dysfunction: causes and mechanisms." J Musculoskelet Neuronal Interact **7**(3): 246-52.
- Degens H. (2009). "The role of systemic inflammation in age-related muscle weakness and wasting." Scand J Med Sci Sports **4**: 4.
- Dekelbab B.H., Witchel S.F. and DeFranco D.B. (2007). "TNF-alpha and glucocorticoid receptor interaction in L6 muscle cells: a cooperative downregulation of myosin heavy chain." Steroids **72**(9-10): 705-12.
- Delday M.I. and Maltin C.A. (1997). "Clenbuterol increases the expression of myogenin but not myoD in immobilized rat muscles." Am J Physiol **272**(5 Pt 1): E941-4.
- Delfini M., Hirsinger E., Pourquie O. and Duprez D. (2000). "Delta 1-activated notch inhibits muscle differentiation without affecting Myf5 and Pax3 expression in chick limb myogenesis." Development **127**(23): 5213-5224.
- Dhawan J. and Rando T.A. (2005). "Stem cells in postnatal myogenesis: molecular mechanisms of satellite cell quiescence, activation and replenishment." Trends in Cell Biology **15**(12): 666-673.

- Dodd S.L., Powers S.K., Vrabas I.S., Criswell D., Stetson S. and Hussain R. (1996). "Effects of clenbuterol on contractile and biochemical properties of skeletal muscle." Med Sci Sports Exerc **28**(6): 669-76.
- Dogra C., Changotra H., Mohan S. and Kumar A. (2006). "Tumor necrosis factor-like weak inducer of apoptosis inhibits skeletal myogenesis through sustained activation of nuclear factor-kappaB and degradation of MyoD protein." J Biol Chem **281**(15): 10327-36.
- Doyle A., Zhang G., Abdel Fattah E.A., Eissa N.T. and Li Y.P. (2011). "Toll-like receptor 4 mediates lipopolysaccharide-induced muscle catabolism via coordinate activation of ubiquitin-proteasome and autophagy-lysosome pathways." Faseb J **25**(1): 99-110.
- Dreyfus P.A., Chretien F., Chazaud B., Kirova Y., Caramelle P., Garcia L., Butler-Browne G. and Gherardi R.K. (2004). "Adult Bone Marrow-Derived Stem Cells in Muscle Connective Tissue and Satellite Cell Niches." Am J Pathol **164**(3): 773-779.
- Dutta C., Hadley E.C. and Lexell J. (1997). "Sarcopenia and physical performance in old age: overview." Muscle Nerve Suppl **5**(9): S5-9.
- Ebert M.S. and Sharp P.A. (2012). "Roles for MicroRNAs in Conferring Robustness to Biological Processes." Cell **149**(3): 515-24.
- Ebisui C., Tsujinaka T., Morimoto T., Kan K., Iijima S., Yano M., Kominami E., Tanaka K. and Monden M. (1995). "Interleukin-6 induces proteolysis by activating intracellular proteases (cathepsins B and L, proteasome) in C2C12 myotubes." Clin Sci (Lond) **89**(4): 431-9.
- Egginton S. (2011). "Physiological factors influencing capillary growth." Acta Physiol (Oxf) **202**(3): 225-39.
- el-Dwairi Q., Comtois A., Guo Y. and Hussain S.N. (1998). "Endotoxin-induced skeletal muscle contractile dysfunction: contribution of nitric oxide synthases." Am J Physiol **274**(3 Pt 1): C770-9.
- Elkina Y., von Haehling S., Anker S.D. and Springer J. (2011). "The role of myostatin in muscle wasting: an overview." J Cachexia Sarcopenia Muscle **2**(3): 143-151.
- Emery P.W., Rothwell N.J., Stock M.J. and Winter P.D. (1984). "Chronic effects of beta 2-adrenergic agonists on body composition and protein synthesis in the rat." Biosci Rep **4**(1): 83-91.
- Fink L., Stahl U., Ermert L., Kummer W., Seeger W. and Bohle R.M. (1999). "Rat porphobilinogen deaminase gene: a pseudogene-free internal standard for laser-assisted cell picking." Biotechniques **26**(3): 510-6.
- Finnie J.W., Cai Z., Manavis J., Helps S. and Blumbergs P.C. (2010). "Microglial activation as a measure of stress in mouse brains exposed

- acutely (60 minutes) and long-term (2 years) to mobile telephone radiofrequency fields." Pathology **42**(2): 151-4.
- Fiorotto M.L., Schwartz R.J. and Delaughter M.C. (2003). "Persistent IGF-I overexpression in skeletal muscle transiently enhances DNA accretion and growth." Faseb J **17**(1): 59-60.
- Florini J.R. and Magri K.A. (1989). "Effects of growth factors on myogenic differentiation." Am J Physiol **256**(4 Pt 1): C701-11.
- Foulstone E.J., Huser C., Crown A.L., Holly J.M. and Stewart C.E. (2004). "Differential signalling mechanisms predisposing primary human skeletal muscle cells to altered proliferation and differentiation: roles of IGF-I and TNFalpha." Exp Cell Res **294**(1): 223-35.
- Friedrich O. (2006). "Critical illness myopathy: what is happening?" Curr Opin Clin Nutr Metab Care **9**(4): 403-9.
- Frost R.A., Nystrom G.J. and Lang C.H. (2004). "Lipopolysaccharide stimulates nitric oxide synthase-2 expression in murine skeletal muscle and C(2)C(12) myoblasts via Toll-like receptor-4 and c-Jun NH(2)-terminal kinase pathways." Am J Physiol Cell Physiol **287**(6): C1605-15.
- Frost R.A., Nystrom G.J. and Lang C.H. (2006). "Multiple Toll-like receptor ligands induce an IL-6 transcriptional response in skeletal myocytes." Am J Physiol Regul Integr Comp Physiol **290**(3): R773-84.
- Fukada S.-i., Uezumi A., Ikemoto M., Masuda S., Segawa M., Tanimura N., Yamamoto H., Miyagoe-Suzuki Y. and Takeda S.i. (2007). "Molecular Signature of Quiescent Satellite Cells in Adult Skeletal Muscle." Stem Cells **25**(10): 2448-2459.
- Fulle S., Belia S. and Di Tano G. (2005). "Sarcopenia is more than a muscular deficit." Arch Ital Biol **143**(3-4): 229-34.
- Funk C.D. (2001). "Prostaglandins and leukotrienes: advances in eicosanoid biology." Science **294**(5548): 1871-5.
- Gallucci S., Provenzano C., Mazzarelli P., Scuderi F. and Bartoccioni E. (1998). "Myoblasts produce IL-6 in response to inflammatory stimuli." Int Immunol **10**(3): 267-73.
- Galon J., Franchimont D., Hiroi N., Frey G., Boettner A., Ehrhart-Bornstein M., O'Shea J.J., Chrousos G.P. and Bornstein S.R. (2002). "Gene profiling reveals unknown enhancing and suppressive actions of glucocorticoids on immune cells." Faseb J **16**(1): 61-71.
- Gamrin L., Essen P., Forsberg A.M., Hultman E. and Wernerman J. (1996). "A descriptive study of skeletal muscle metabolism in critically ill patients: free amino acids, energy-rich phosphates, protein, nucleic acids, fat, water, and electrolytes." Crit Care Med **24**(4): 575-83.

- Garcia-Martinez C., Lopez-Soriano F.J. and Argiles J.M. (1994). "Interleukin-6 does not activate protein breakdown in rat skeletal muscle." Cancer Lett **76**(1): 1-4.
- Gardiner S.M. and Bennett T. (1988). "Regional hemodynamic responses to adrenoceptor antagonism in conscious rats." Am J Physiol **255**(4 Pt 2): H813-24.
- Gardiner S.M., Kemp P.A., March J.E. and Bennett T. (1995). "Cardiac and regional haemodynamics, inducible nitric oxide synthase (NOS) activity, and the effects of NOS inhibitors in conscious, endotoxaemic rats." Br J Pharmacol **116**(3): 2005-16.
- Gardiner S.M., Kemp P.A., March J.E. and Bennett T. (1996). "Effects of dexamethasone and SB 209670 on the regional haemodynamic responses to lipopolysaccharide in conscious rats." Br J Pharmacol **118**(1): 141-9.
- Gardiner S.M., Kemp P.A., March J.E., Woolley J. and Bennett T. (1998). "The influence of antibodies to TNF-alpha and IL-1beta on haemodynamic responses to the cytokines, and to lipopolysaccharide, in conscious rats." Br J Pharmacol **125**(7): 1543-50.
- Gell P.G. and Hinde I.T. (1953). "The effect of cortisone on macrophage activity in mice." Br J Exp Pathol **34**(3): 273-5.
- Gibala M.J. (2000). "Nutritional supplementation and resistance exercise: what is the evidence for enhanced skeletal muscle hypertrophy?" Can J Appl Physiol **25**(6): 524-35.
- Gibson M.C. and Schultz E. (1982). "The distribution of satellite cells and their relationship to specific fiber types in soleus and extensor digitorum longus muscles." The Anatomical Record **202**(3): 329-337.
- Gierer P., Hoffmann J.N., Mahr F., Menger M.D., Mittlmeier T., Gradl G. and Vollmar B. (2007). "Activated protein C reduces tissue hypoxia, inflammation, and apoptosis in traumatized skeletal muscle during endotoxemia." Crit Care Med **35**(8): 1966-71.
- Gilson H., Schakman O., Combaret L., Lause P., Grobet L., Attaix D., Ketelslegers J.M. and Thissen J.P. (2007). "Myostatin gene deletion prevents glucocorticoid-induced muscle atrophy." Endocrinology **148**(1): 452-60.
- Gilson H., Schakman O., Kalista S., Lause P., Tsuchida K. and Thissen J.P. (2009). "Follistatin induces muscle hypertrophy through satellite cell proliferation and inhibition of both myostatin and activin." Am J Physiol Endocrinol Metab **297**(1): E157-64.
- Girgenrath S., Song K. and Whittemore L.A. (2005). "Loss of myostatin expression alters fiber-type distribution and expression of myosin heavy

- chain isoforms in slow- and fast-type skeletal muscle." Muscle Nerve **31**(1): 34-40.
- Glass D.J. (2005). "Skeletal muscle hypertrophy and atrophy signaling pathways." Int J Biochem Cell Biol **37**(10): 1974-84.
- Gnocchi V.F., White R.B., Ono Y., Ellis J.A. and Zammit P.S. (2009). "Further characterisation of the molecular signature of quiescent and activated mouse muscle satellite cells." PLoS ONE **4**(4): e5205.
- Gonzalez-Cadavid N.F., Taylor W.E., Yarasheski K., Sinha-Hikim I., Ma K., Ezzat S., Shen R., Lalani R., Asa S., Mamita M., Nair G., Arver S. and Bhasin S. (1998). "Organization of the human myostatin gene and expression in healthy men and HIV-infected men with muscle wasting." Proc Natl Acad Sci U S A **95**(25): 14938-43.
- Grant A.L., Helferich W.G., Merkel R.A. and Bergen W.G. (1990). "Effects of phenethanolamines and propranolol on the proliferation of cultured chick breast muscle satellite cells." J Anim Sci **68**(3): 652-8.
- Gray S.D. and Renkin E.M. (1978). "Microvascular supply in relation to fiber metabolic type in mixed skeletal muscles on rabbits." Microvasc Res **16**(3): 406-25.
- Grifone R., Laclef C., Spitz F., Lopez S., Demignon J., Guidotti J.E., Kawakami K., Xu P.X., Kelly R., Petrof B.J., Daegelen D., Concordet J.P. and Maire P. (2004). "Six1 and Eya1 expression can reprogram adult muscle from the slow-twitch phenotype into the fast-twitch phenotype." Mol Cell Biol **24**(14): 6253-67.
- Grobet L., Martin L.J., Poncelet D., Pirottin D., Brouwers B., Riquet J., Schoeberlein A., Dunner S., Menissier F., Massabanda J., Fries R., Hanset R. and Georges M. (1997). "A deletion in the bovine myostatin gene causes the double-muscled phenotype in cattle." Nat Genet **17**(1): 71-4.
- Guerriero V., Jr. and Florini J.R. (1980). "Dexamethasone effects on myoblast proliferation and differentiation." Endocrinology **106**(4): 1198-202.
- Guha M. and Mackman N. (2001). "LPS induction of gene expression in human monocytes." Cell Signal **13**(2): 85-94.
- Gundersen K. and Bruusgaard J.C. (2008). "Nuclear domains during muscle atrophy: nuclei lost or paradigm lost?" J Physiol **586**(Pt 11): 2675-81.
- Guttridge D.C., Albanese C., Reuther J.Y., Pestell R.G. and Baldwin A.S., Jr. (1999). "NF-kappaB controls cell growth and differentiation through transcriptional regulation of cyclin D1." Mol Cell Biol **19**(8): 5785-99.
- Guttridge D.C., Mayo M.W., Madrid L.V., Wang C.Y. and Baldwin A.S., Jr. (2000). "NF-kappaB-induced loss of MyoD messenger RNA: possible role in muscle decay and cachexia." Science **289**(5488): 2363-6.

- Haddad F., Zaldivar F., Cooper D.M. and Adams G.R. (2005). "IL-6-induced skeletal muscle atrophy." J Appl Physiol **98**(3): 911-917.
- Halevy O., Piestun Y., Allouh M.Z., Rosser B.W.C., Rinkevich Y., Reshef R., Rozenboim I., Wleklinski-Lee M. and Yablonka-Reuveni Z. (2004). "Pattern of Pax7 expression during myogenesis in the posthatch chicken establishes a model for satellite cell differentiation and renewal." Developmental Dynamics **231**(3): 489-502.
- Handschin C., Chin S., Li P., Liu F., Maratos-Flier E., Lebrasseur N.K., Yan Z. and Spiegelman B.M. (2007). "Skeletal muscle fiber-type switching, exercise intolerance, and myopathy in PGC-1alpha muscle-specific knock-out animals." J Biol Chem **282**(41): 30014-21.
- Hartley R.S., Bandman E. and Yablonka-Reuveni Z. (1992). "Skeletal muscle satellite cells appear during late chicken embryogenesis." Dev Biol **153**(2): 206-16.
- Hasselgren P.O., Menconi M.J., Fareed M.U., Yang H., Wei W. and Evenson A. (2005). "Novel aspects on the regulation of muscle wasting in sepsis." Int J Biochem Cell Biol **37**(10): 2156-68.
- Hawke T.J. and Garry D.J. (2001). "Myogenic satellite cells: physiology to molecular biology." J Appl Physiol **91**(2): 534-551.
- Hirata F., Toyoshima S., Axelrod J. and Waxdal M.J. (1980). "Phospholipid methylation: a biochemical signal modulating lymphocyte mitogenesis." Proc Natl Acad Sci U S A **77**(2): 862-5.
- Hittel D.S., Axelson M., Sarna N., Shearer J., Huffman K.M. and Kraus W.E. (2010). "Myostatin decreases with aerobic exercise and associates with insulin resistance." Med Sci Sports Exerc **42**(11): 2023-9.
- Holterman C.E. and Rudnicki M.A. (2005). "Molecular regulation of satellite cell function." Seminars in Cell & Developmental Biology **16**(4-5): 575-584.
- Horsley V. and Pavlath G.K. (2003). "Prostaglandin F2(alpha) stimulates growth of skeletal muscle cells via an NFATC2-dependent pathway." J Cell Biol **161**(1): 111-8.
- Hu P., Zhang K.M., Wright L.D., Spratt J.A. and Briggs F.N. (1997). "Correlations between MyoD, myogenin, SERCA1, SERCA2 and phospholamban transcripts during transformation of type-II to type-I skeletal muscle fibers." Pflugers Arch **434**(2): 209-11.
- Huang Z., Chen X. and Chen D. (2011). "Myostatin: a novel insight into its role in metabolism, signal pathways, and expression regulation." Cell Signal **23**(9): 1441-6.
- Hudlicka O. (1985). "Development and adaptability of microvasculature in skeletal muscle." J Exp Biol **115**: 215-28.

- Hughes S.M. (2004). "Muscle differentiation: a gene for slow muscle?" Curr Biol **14**(4): R156-7.
- Hughes S.M., Chi M.M., Lowry O.H. and Gundersen K. (1999). "Myogenin induces a shift of enzyme activity from glycolytic to oxidative metabolism in muscles of transgenic mice." J Cell Biol **145**(3): 633-42.
- Hughes S.M., Cho M., Karsch-Mizrachi I., Travis M., Silberstein L., Leinwand L.A. and Blau H.M. (1993a). "Three slow myosin heavy chains sequentially expressed in developing mammalian skeletal muscle." Dev Biol **158**(1): 183-99.
- Hughes S.M., Koishi K., Rudnicki M. and Maggs A.M. (1997). "MyoD protein is differentially accumulated in fast and slow skeletal muscle fibres and required for normal fibre type balance in rodents." Mech Dev **61**(1-2): 151-63.
- Hughes S.M., Taylor J.M., Tapscott S.J., Gurley C.M., Carter W.J. and Peterson C.A. (1993b). "Selective accumulation of MyoD and myogenin mRNAs in fast and slow adult skeletal muscle is controlled by innervation and hormones." Development **118**(4): 1137-47.
- Imai Y., Iyata I., Ito D., Ohsawa K. and Kohsaka S. (1996). "A novel gene *iba1* in the major histocompatibility complex class III region encoding an EF hand protein expressed in a monocytic lineage." Biochem Biophys Res Commun **224**(3): 855-62.
- Irintchev A., Zeschnigk M., Starzinski-Powitz A. and Wernig A. (1994). "Expression pattern of M-cadherin in normal, denervated, and regenerating mouse muscles." Developmental Dynamics **199**(4): 326-337.
- Jacobi J. (2002). "Pathophysiology of sepsis." Am J Health Syst Pharm **59** Suppl 1(59): S3-8.
- Jacobs-El J., Zhou M.Y. and Russell B. (1995). "MRF4, Myf-5, and myogenin mRNAs in the adaptive responses of mature rat muscle." Am J Physiol **268**(4 Pt 1): C1045-52.
- Jacobs S.C., Bootsma A.L., Willems P.W., Bar P.R. and Wokke J.H. (1996). "Prednisone can protect against exercise-induced muscle damage." J Neurol **243**(5): 410-6.
- Janssen I., Heymsfield S.B., Wang Z.M. and Ross R. (2000). "Skeletal muscle mass and distribution in 468 men and women aged 18-88 yr." J Appl Physiol **89**(1): 81-8.
- Jarosch R. (2000). "Muscle force arises by actin filament rotation and torque in the Z-filaments." Biochem Biophys Res Commun **270**(3): 677-82.
- Jejurikar S.S., Henkelman E.A., Cederna P.S., Marcelo C.L., Urbanek M.G. and Kuzon W.M., Jr. (2006). "Aging increases the susceptibility of

- skeletal muscle derived satellite cells to apoptosis." Exp Gerontol **41**(9): 828-36.
- Jogo M., Shiraishi S. and Tamura T.A. (2009). "Identification of MAFbx as a myogenin-engaged F-box protein in SCF ubiquitin ligase." FEBS Lett **583**(17): 2715-9.
- Jones S.W., Baker D.J., Gardiner S.M., Bennett T., Timmons J.A. and Greenhaff P.L. (2004). "The effect of the beta2-adrenoceptor agonist prodrug BRL-47672 on cardiovascular function, skeletal muscle myosin heavy chain, and MyoD expression in the rat." J Pharmacol Exp Ther **311**(3): 1225-31.
- Joubert Y. and Tobin C. (1995). "Testosterone Treatment Results in Quiescent Satellite Cells Being Activated and Recruited into Cell Cycle in Rat Levator Ani Muscle." Developmental Biology **169**(1): 286-294.
- Jouliia-Ekaza D. and Cabello G. (2006). "Myostatin regulation of muscle development: molecular basis, natural mutations, physiopathological aspects." Exp Cell Res **312**(13): 2401-14.
- Kadi F., Charifi N., Denis C., Lexell J., Andersen J.L., Schjerling P., Olsen S. and Kjaer M. (2005). "The behaviour of satellite cells in response to exercise: what have we learned from human studies?" Pflugers Arch **451**(2): 319-27.
- Kadi F., Schjerling P., Andersen L.L., Charifi N., Madsen J.L., Christensen L.R. and Andersen J.L. (2004). "The effects of heavy resistance training and detraining on satellite cells in human skeletal muscles." Journal of Physiology-London **558**(3): 1005-1012.
- Kambadur R., Sharma M., Smith T.P. and Bass J.J. (1997). "Mutations in myostatin (GDF8) in double-muscled Belgian Blue and Piedmontese cattle." Genome Res **7**(9): 910-6.
- Katz B. (1961). "The Terminations of the Afferent Nerve Fibre in the Muscle Spindle of the Frog." Philosophical Transactions of the Royal Society of London. Series B, Biological Sciences **243**(703): 221-240.
- Kelly R., Alonso S., Tajbakhsh S., Cossu G. and Buckingham M. (1995). "Myosin light chain 3F regulatory sequences confer regionalized cardiac and skeletal muscle expression in transgenic mice." J Cell Biol **129**(2): 383-96.
- Kim K.H., Kim Y.S. and Yang J. (2011). "The muscle-hypertrophic effect of clenbuterol is additive to the hypertrophic effect of myostatin suppression." Muscle Nerve **43**(5): 700-7.
- Kim M.S., Fielitz J., McAnally J., Shelton J.M., Lemon D.D., McKinsey T.A., Richardson J.A., Bassel-Duby R. and Olson E.N. (2008). "Protein kinase D1 stimulates MEF2 activity in skeletal muscle and enhances muscle performance." Mol Cell Biol **28**(11): 3600-9.

- Kim Y.S., Sainz R.D., Summers R.J. and Molenaar P. (1992). "Cimaterol reduces beta-adrenergic receptor density in rat skeletal muscles." J Anim Sci **70**(1): 115-22.
- Kissel J.T., McDermott M.P., Mendell J.R., King W.M., Pandya S., Griggs R.C. and Tawil R. (2001). "Randomized, double-blind, placebo-controlled trial of albuterol in facioscapulohumeral dystrophy." Neurology **57**(8): 1434-40.
- Kitzmann M., Vandromme M., Schaeffer V., Carnac G., Labbe J.C., Lamb N. and Fernandez A. (1999). "cdk1- and cdk2-mediated phosphorylation of MyoD Ser200 in growing C2 myoblasts: role in modulating MyoD half-life and myogenic activity." Mol Cell Biol **19**(4): 3167-76.
- Knapp J.R., Davie J.K., Myer A., Meadows E., Olson E.N. and Klein W.H. (2006). "Loss of myogenin in postnatal life leads to normal skeletal muscle but reduced body size." Development **133**(4): 601-10.
- Kocamis H. and Killefer J. (2002). "Myostatin expression and possible functions in animal muscle growth." Domest Anim Endocrinol **23**(4): 447-54.
- Kriegler M., Perez C., DeFay K., Albert I. and Lu S.D. (1988). "A novel form of TNF/cachectin is a cell surface cytotoxic transmembrane protein: ramifications for the complex physiology of TNF." Cell **53**(1): 45-53.
- Kuang S., Charge S.B., Seale P., Huh M. and Rudnicki M.A. (2006). "Distinct roles for Pax7 and Pax3 in adult regenerative myogenesis." J Cell Biol **172**(1): 103-13.
- Kumar D., Shadrach J.L., Wagers A.J. and Lassar A.B. (2009). "Id3 is a direct transcriptional target of Pax7 in quiescent satellite cells." Mol Biol Cell **20**(14): 3170-7.
- Kuschel R., Yablonka-Reuveni Z. and Bornemann A. (1999). "Satellite cells on isolated myofibers from normal and denervated adult rat muscle." J Histochem Cytochem **47**(11): 1375-84.
- Lalani R., Bhasin S., Byhower F., Tarnuzzer R., Grant M., Shen R., Asa S., Ezzat S. and Gonzalez-Cadavid N.F. (2000). "Myostatin and insulin-like growth factor-I and -II expression in the muscle of rats exposed to the microgravity environment of the NeuroLab space shuttle flight." J Endocrinol **167**(3): 417-28.
- Lang C.H., Dobrescu C. and Meszaros K. (1990). "Insulin-mediated glucose uptake by individual tissues during sepsis." Metabolism **39**(10): 1096-107.
- Lang C.H., Frost R.A. and Vary T.C. (2007). "Regulation of muscle protein synthesis during sepsis and inflammation." Am J Physiol Endocrinol Metab **293**(2): E453-9.

- Lang C.H., Silvis C., Nystrom G. and Frost R.A. (2001). "Regulation of Myostatin by Glucocorticoids After Thermal Injury." FASEB J.: 00-0849fje.
- Langen R.C., Schols A.M., Kelders M.C., van der Velden J.L., Wouters E.F. and Janssen-Heininger Y.M. (2006). "Muscle wasting and impaired muscle regeneration in a murine model of chronic pulmonary inflammation." Am J Respir Cell Mol Biol **35**(6): 689-96.
- Langen R.C., Van Der Velden J.L., Schols A.M., Kelders M.C., Wouters E.F. and Janssen-Heininger Y.M. (2004). "Tumor necrosis factor-alpha inhibits myogenic differentiation through MyoD protein destabilization." Faseb J **18**(2): 227-37.
- Langley B., Thomas M., Bishop A., Sharma M., Gilmour S. and Kambadur R. (2002). "Myostatin inhibits myoblast differentiation by down-regulating MyoD expression." J Biol Chem **277**(51): 49831-40.
- Larsson L., Li X., Teresi A. and Salviati G. (1994). "Effects of thyroid hormone on fast- and slow-twitch skeletal muscles in young and old rats." J Physiol **481** (Pt 1)(Pt 1): 149-61.
- Layne M.D. and Farmer S.R. (1999). "Tumor necrosis factor-alpha and basic fibroblast growth factor differentially inhibit the insulin-like growth factor-I induced expression of myogenin in C2C12 myoblasts." Exp Cell Res **249**(1): 177-87.
- Le Douarin N. and Barq G. (1969). "[Use of Japanese quail cells as "biological markers" in experimental embryology]." C R Acad Sci Hebd Seances Acad Sci D **269**(16): 1543-6.
- Lecker S.H., Solomon V., Mitch W.E. and Goldberg A.L. (1999). "Muscle protein breakdown and the critical role of the ubiquitin-proteasome pathway in normal and disease states." J Nutr **129**(1S Suppl): 227S-237S.
- Lee S.J. and McPherron A.C. (2001). "Regulation of myostatin activity and muscle growth." Proc Natl Acad Sci U S A **98**(16): 9306-11.
- Legerlotz K. and Smith H.K. (2008). "Role of MyoD in denervated, disused, and exercised muscle." Muscle Nerve **38**(3): 1087-100.
- Leibovich S.J. and Ross R. (1975). "The role of the macrophage in wound repair. A study with hydrocortisone and antimacrophage serum." Am J Pathol **78**(1): 71-100.
- Lescaudron L., Peltekian E., Fontaine-Perus J., Paulin D., Zampieri M., Garcia L. and Parrish E. (1999). "Blood borne macrophages are essential for the triggering of muscle regeneration following muscle transplant." Neuromuscular Disorders **9**(2): 72-80.

- Li H., Malhotra S. and Kumar A. (2008). "Nuclear factor-kappa B signaling in skeletal muscle atrophy." J Mol Med (Berl) **86**(10): 1113-26.
- Li Y.P. (2003). "TNF-alpha is a mitogen in skeletal muscle." Am J Physiol Cell Physiol **285**(2): C370-6.
- Li Y.P. and Schwartz R.J. (2001). "TNF-alpha regulates early differentiation of C2C12 myoblasts in an autocrine fashion." Faseb J **15**(8): 1413-5.
- Lightfoot A., McArdle A. and Griffiths R.D. (2009). "Muscle in defense." Crit Care Med **37**(10 Suppl): S384-90.
- Liu C.M., Yang Z., Liu C.W., Wang R., Tien P., Dale R. and Sun L.Q. (2008). "Myostatin antisense RNA-mediated muscle growth in normal and cancer cachexia mice." Gene Ther **15**(3): 155-60.
- Llovera M., Lopez-Soriano F.J. and Argiles J.M. (1993). "Effects of tumor necrosis factor-alpha on muscle-protein turnover in female Wistar rats." J Natl Cancer Inst **85**(16): 1334-9.
- Lohse M.J. (1993). "Molecular mechanisms of membrane receptor desensitization." Biochim Biophys Acta **1179**(2): 171-88.
- Lowry O.H., Rosebrough N.J., Farr A.L. and Randall R.J. (1951). "Protein measurement with the Folin phenol reagent." J Biol Chem **193**(1): 265-75.
- Lu D.X., Huang S.K. and Carlson B.M. (1997). "Electron microscopic study of long-term denervated rat skeletal muscle." Anat Rec **248**(3): 355-65.
- Lu Y.C., Yeh W.C. and Ohashi P.S. (2008). "LPS/TLR4 signal transduction pathway." Cytokine **42**(2): 145-51.
- Lynch G.S. and Ryall J.G. (2008). "Role of beta-adrenoceptor signaling in skeletal muscle: implications for muscle wasting and disease." Physiol Rev **88**(2): 729-67.
- Ma K., Mallidis C., Artaza J., Taylor W., Gonzalez-Cadavid N. and Bhasin S. (2001). "Characterization of 5'-regulatory region of human myostatin gene: regulation by dexamethasone in vitro." Am J Physiol Endocrinol Metab **281**(6): E1128-1136.
- Ma K., Mallidis C., Bhasin S., Mahabadi V., Artaza J., Gonzalez-Cadavid N., Arias J. and Salehian B. (2003). "Glucocorticoid-induced skeletal muscle atrophy is associated with upregulation of myostatin gene expression." Am J Physiol Endocrinol Metab **285**(2): E363-71.
- Mackey A.L., Kjaer M., Charifi N., Henriksson J., Bojsen-Moller J., Holm L. and Kadi F. (2009). "Assessment of satellite cell number and activity status in human skeletal muscle biopsies." Muscle Nerve **40**(3): 455-65.

- Mackey A.L., Kjaer M., Dandanell S., Mikkelsen K.H., Holm L., Dossing S., Kadi F., Koskinen S.O., Jensen C.H., Schroder H.D. and Langberg H. (2007). "The influence of anti-inflammatory medication on exercise-induced myogenic precursor cell responses in humans." J Appl Physiol **103**(2): 425-31.
- Maltin C.A. and Delday M.I. (1992). "Satellite cells in innervated and denervated muscles treated with clenbuterol." Muscle Nerve **15**(8): 919-25.
- Mansouri A., Stoykova A., Torres M. and Gruss P. (1996). "Dysgenesis of cephalic neural crest derivatives in Pax7^{-/-} mutant mice." Development **122**(3): 831-8.
- Marimuthu K., Murton A.J. and Greenhaff P.L. (2011). "Mechanisms regulating muscle mass during disuse atrophy and rehabilitation in humans." J Appl Physiol **110**(2): 555-60.
- Marzetti E., Privitera G., Simili V., Wohlgemuth S.E., Aulisa L., Pahor M. and Leeuwenburgh C. (2010). "Multiple pathways to the same end: mechanisms of myonuclear apoptosis in sarcopenia of aging." ScientificWorldJournal **10**: 340-9.
- Matsakas A., Bozzo C., Cacciani N., Caliaro F., Reggiani C., Mascarello F. and Patruno M. (2006). "Effect of swimming on myostatin expression in white and red gastrocnemius muscle and in cardiac muscle of rats." Exp Physiol **91**(6): 983-94.
- Matthys P., Mitera T., Heremans H., Van Damme J. and Billiau A. (1995). "Anti-gamma interferon and anti-interleukin-6 antibodies affect staphylococcal enterotoxin B-induced weight loss, hypoglycemia, and cytokine release in D-galactosamine-sensitized and unsensitized mice." Infect Immun **63**(4): 1158-64.
- Mauro A. (1961). "Satellite Cell of Skeletal Muscle Fibers." J. Cell Biol. **9**(2): 493-495.
- Mayhew T.M., Pharaoh A., Austin A. and Fagan D.G. (1997). "Stereological estimates of nuclear number in human ventricular cardiomyocytes before and after birth obtained using physical disectors." J Anat **191** (Pt 1)(Pt 1): 107-15.
- McCroskery S., Thomas M., Maxwell L., Sharma M. and Kambadur R. (2003). "Myostatin negatively regulates satellite cell activation and self-renewal." J. Cell Biol. **162**(6): 1135-1147.
- McCroskery S., Thomas M., Platt L., Hennebry A., Nishimura T., McLeay L., Sharma M. and Kambadur R. (2005). "Improved muscle healing through enhanced regeneration and reduced fibrosis in myostatin-null mice." J Cell Sci **118**(Pt 15): 3531-41.

- McElligott M.A., Barreto A., Jr. and Chaung L.Y. (1989). "Effect of continuous and intermittent clenbuterol feeding on rat growth rate and muscle." Comp Biochem Physiol C **92**(1): 135-8.
- McFarlane C., Hennebry A., Thomas M., Plummer E., Ling N., Sharma M. and Kambadur R. (2008). "Myostatin signals through Pax7 to regulate satellite cell self-renewal." Exp Cell Res **314**(2): 317-29.
- McFarlane C., Langley B., Thomas M., Hennebry A., Plummer E., Nicholas G., McMahon C., Sharma M. and Kambadur R. (2005). "Proteolytic processing of myostatin is auto-regulated during myogenesis." Dev Biol **283**(1): 58-69.
- McFarlane C., Plummer E., Thomas M., Hennebry A., Ashby M., Ling N., Smith H., Sharma M. and Kambadur R. (2006). "Myostatin induces cachexia by activating the ubiquitin proteolytic system through an NF-kappa B-independent, FoxO1-dependent mechanism." Journal of Cellular Physiology **209**(2): 501-514.
- McKay B.R., De Lisio M., Johnston A.P., O'Reilly C.E., Phillips S.M., Tarnopolsky M.A. and Parise G. (2009). "Association of interleukin-6 signalling with the muscle stem cell response following muscle-lengthening contractions in humans." PLoS ONE **4**(6): e6027.
- McMahon C.D., Popovic L., Oldham J.M., Jeanplong F., Smith H.K., Kambadur R., Sharma M., Maxwell L. and Bass J.J. (2003). "Myostatin-deficient mice lose more skeletal muscle mass than wild-type controls during hindlimb suspension." Am J Physiol Endocrinol Metab **285**(1): E82-7.
- McMillan D.N., Noble B.S. and Maltin C.A. (1992). "The effect of the beta-adrenergic agonist clenbuterol on growth and protein metabolism in rat muscle cell cultures." J Anim Sci **70**(10): 3014-23.
- McPherron A.C., Lawler A.M. and Lee S.J. (1997). "Regulation of skeletal muscle mass in mice by a new TGF-beta superfamily member." Nature **387**(6628): 83-90.
- Meduri G.U., Annane D., Chrousos G.P., Marik P.E. and Sinclair S.E. (2009). "Activation and regulation of systemic inflammation in ARDS: rationale for prolonged glucocorticoid therapy." Chest **136**(6): 1631-43.
- Mendias C.L., Tatsumi R. and Allen R.E. (2004). "Role of cyclooxygenase-1 and -2 in satellite cell proliferation, differentiation, and fusion." Muscle Nerve **30**(4): 497-500.
- Mendler L., Zador E., Ver Heyen M., Dux L. and Wuytack F. (2000). "Myostatin levels in regenerating rat muscles and in myogenic cell cultures." J Muscle Res Cell Motil **21**(6): 551-63.

- Mignone J.L., Kukekov V., Chiang A.S., Steindler D. and Enikolopov G. (2004). "Neural stem and progenitor cells in nestin-GFP transgenic mice." J Comp Neurol **469**(3): 311-24.
- Mikkelsen U.R., Langberg H., Helmark I.C., Skovgaard D., Andersen L.L., Kjaer M. and Mackey A.L. (2009). "Local NSAID infusion inhibits satellite cell proliferation in human skeletal muscle after eccentric exercise." J Appl Physiol **107**(5): 1600-11.
- Miller J.B., Schaefer L. and Dominov J.A. (1999). "Seeking muscle stem cells." Curr Top Dev Biol **43**: 191-219.
- Mitin N., Kudla A.J., Konieczny S.F. and Taparowsky E.J. (2001). "Differential effects of Ras signaling through NFkappaB on skeletal myogenesis." Oncogene **20**(11): 1276-86.
- Monda M., Vicidomini C., Viggiano A., Sampaolo S., Di Iorio G., Viggiano E. and De Luca B. (2009). "Inhibition of prostaglandin synthesis reduces the induction of MyoD expression in rat soleus muscle." J Muscle Res Cell Motil **30**(3-4): 139-44.
- Moore N.G., Pegg G.G. and Sillence M.N. (1994). "Anabolic effects of the beta 2-adrenoceptor agonist salmeterol are dependent on route of administration." Am J Physiol **267**(3 Pt 1): E475-84.
- Moresi V., Williams A.H., Meadows E., Flynn J.M., Potthoff M.J., McAnally J., Shelton J.M., Baks J., Klein W.H., Richardson J.A., Bassel-Duby R. and Olson E.N. (2010). "Myogenin and class II HDACs control neurogenic muscle atrophy by inducing E3 ubiquitin ligases." Cell **143**(1): 35-45.
- Moss F.P. and Leblond C.P. (1971). "Satellite cells as the source of nuclei in muscles of growing rats." The Anatomical Record **170**(4): 421-435.
- Mozdziak P.E., Greaser M.L. and Schultz E. (1998). "Myogenin, MyoD, and myosin expression after pharmacologically and surgically induced hypertrophy." J Appl Physiol **84**(4): 1359-64.
- Mozdziak P.E., Pulvermacher P.M. and Schultz E. (2000). "Unloading of juvenile muscle results in a reduced muscle size 9 wk after reloading." J Appl Physiol **88**(1): 158-64.
- Muhlfeld C., Nyengaard J.R. and Mayhew T.M. (2009). "A review of state-of-the-art stereology for better quantitative 3D morphology in cardiac research." Cardiovasc Pathol **19**(2): 65-82.
- Muir A.R., Kanji A.H. and Allbrook D. (1965). "The structure of the satellite cells in skeletal muscle." J Anat **99**(Pt 3): 435-44.
- Muller J.M., Ziegler-Heitbrock H.W. and Baeuerle P.A. (1993). "Nuclear factor kappa B, a mediator of lipopolysaccharide effects." Immunobiology **187**(3-5): 233-56.

- Murton A.J. (2007). Mechanisms Modulating Muscle Mass During Endotoxaemia. Biomedical Sciences. Nottingham, The University of Nottingham. **PhD thesis**.
- Murton A.J., Alamdari N., Gardiner S.M., Constantin-Teodosiu D., Layfield R., Bennett T. and Greenhaff P.L. (2009). "Effects of endotoxaemia on protein metabolism in rat fast-twitch skeletal muscle and myocardium." PLoS ONE **4**(9): e6945.
- Musaro A., McCullagh K., Paul A., Houghton L., Dobrowolny G., Molinaro M., Barton E.R., Sweeney H.L. and Rosenthal N. (2001). "Localized Igf-1 transgene expression sustains hypertrophy and regeneration in senescent skeletal muscle." Nat Genet **27**(2): 195-200.
- Myers M.J., Farrell D.E., Palmer D.C. and Post L.O. (2003). "Inflammatory mediator production in swine following endotoxin challenge with or without co-administration of dexamethasone." Int Immunopharmacol **3**(4): 571-9.
- Nagata Y., Kobayashi H., Umeda M., Ohta N., Kawashima S., Zammit P.S. and Matsuda R. (2006). "Sphingomyelin Levels in the Plasma Membrane Correlate with the Activation State of Muscle Satellite Cells." J. Histochem. Cytochem. **54**(4): 375-384.
- Narici M.V. and de Boer M.D. (2011). "Disuse of the musculo-skeletal system in space and on earth." Eur J Appl Physiol **111**(3): 403-20.
- Nathan C.F. (1987). "Secretory products of macrophages." J Clin Invest **79**(2): 319-26.
- Nofziger D., Miyamoto A., Lyons K.M. and Weinmaster G. (1999). "Notch signaling imposes two distinct blocks in the differentiation of C2C12 myoblasts." Development **126**(8): 1689-1702.
- O'Reilly C., McKay B., Phillips S., Tarnopolsky M. and Parise G. (2008). "Hepatocyte growth factor (HGF) and the satellite cell response following muscle lengthening contractions in humans." Muscle & Nerve **38**(5): 1434-1442.
- Oh M., Rybkin, II, Copeland V., Czubyrt M.P., Shelton J.M., van Rooij E., Richardson J.A., Hill J.A., De Windt L.J., Bassel-Duby R., Olson E.N. and Rothermel B.A. (2005). "Calcineurin is necessary for the maintenance but not embryonic development of slow muscle fibers." Mol Cell Biol **25**(15): 6629-38.
- Ohsawa K., Imai Y., Kanazawa H., Sasaki Y. and Kohsaka S. (2000). "Involvement of Iba1 in membrane ruffling and phagocytosis of macrophages/microglia." J Cell Sci **113** (Pt 17)(Pt 17): 3073-84.
- Olguin H.C. and Olwin B.B. (2004). "Pax-7 up-regulation inhibits myogenesis and cell cycle progression in satellite cells: a potential mechanism for self-renewal." Dev Biol **275**(2): 375-88.

- Olsen S., Aagaard P., Kadi F., Tufekovic G., Verney J., Olesen J.L., Suetta C. and Kjaer M. (2006). "Creatine supplementation augments the increase in satellite cell and myonuclei number in human skeletal muscle induced by strength training (vol 573, pg 525, 2006)." Journal of Physiology-London **575**(3): 971-971.
- Ordahl C.P. and Le Douarin N.M. (1992). "Two myogenic lineages within the developing somite." Development **114**(2): 339-53.
- Palacios D., Mozzetta C., Consalvi S., Caretti G., Saccone V., Proserpio V., Marquez V.E., Valente S., Mai A., Forcales S.V., Sartorelli V. and Puri P.L. (2010). "TNF/p38alpha/polycomb signaling to Pax7 locus in satellite cells links inflammation to the epigenetic control of muscle regeneration." Cell Stem Cell **7**(4): 455-69.
- Paldi A. (2003). "Stochastic gene expression during cell differentiation: order from disorder?" Cell Mol Life Sci **60**(9): 1775-8.
- Palmer R.M. (1990). "Prostaglandins and the control of muscle protein synthesis and degradation." Prostaglandins Leukot Essent Fatty Acids **39**(2): 95-104.
- Paludan S.R. (2000). "Synergistic action of pro-inflammatory agents: cellular and molecular aspects." J Leukoc Biol **67**(1): 18-25.
- Park Y.E., Hayashi Y.K., Goto K., Komaki H., Hayashi Y., Inuzuka T., Noguchi S., Nonaka I. and Nishino I. (2009). "Nuclear changes in skeletal muscle extend to satellite cells in autosomal dominant Emery-Dreifuss muscular dystrophy/limb-girdle muscular dystrophy 1B." Neuromuscul Disord **19**(1): 29-36.
- Parrillo J.E. (1993). "Pathogenetic mechanisms of septic shock." N Engl J Med **328**(20): 1471-7.
- Pedersen B.K., Steensberg A., Fischer C., Keller C., Keller P., Plomgaard P., Febbraio M. and Saltin B. (2003). "Searching for the exercise factor: is IL-6 a candidate?" J Muscle Res Cell Motil **24**(2-3): 113-9.
- Poli-de-Figueiredo L.F., Garrido A.G., Nakagawa N. and Sannomiya P. (2008). "Experimental models of sepsis and their clinical relevance." Shock **30** **Suppl 1**: 53-9.
- Rajab P., Fox J., Riaz S., Tomlinson D., Ball D. and Greenhaff P.L. (2000). "Skeletal muscle myosin heavy chain isoforms and energy metabolism after clenbuterol treatment in the rat." Am J Physiol Regul Integr Comp Physiol **279**(3): R1076-81.
- Ray A. and Prefontaine K.E. (1994). "Physical association and functional antagonism between the p65 subunit of transcription factor NF-kappa B and the glucocorticoid receptor." Proc Natl Acad Sci U S A **91**(2): 752-6.

- Reeds P.J., Hay S.M., Dorward P.M. and Palmer R.M. (1988). "The effect of beta-agonists and antagonists on muscle growth and body composition of young rats (*Rattus* sp.)." Comp Biochem Physiol C **89**(2): 337-41.
- Reeds P.J., Hay S.M., Dorwood P.M. and Palmer R.M. (1986). "Stimulation of muscle growth by clenbuterol: lack of effect on muscle protein biosynthesis." Br J Nutr **56**(1): 249-58.
- Reeds P.J. and Palmer R.M. (1984). "Changes in prostaglandin release associated with inhibition of muscle protein synthesis by dexamethasone." Biochem J **219**(3): 953-7.
- Rhen T. and Cidlowski J.A. (2005). "Antiinflammatory action of glucocorticoids--new mechanisms for old drugs." N Engl J Med **353**(16): 1711-23.
- Rios R., Fernandez-Nocelos S., Carneiro I., Arce V.M. and Devesa J. (2004). "Differential response to exogenous and endogenous myostatin in myoblasts suggests that myostatin acts as an autocrine factor in vivo." Endocrinology **145**(6): 2795-803.
- Roberts P. and McGeachie J.K. (1992). "The effects of clenbuterol on satellite cell activation and the regeneration of skeletal muscle: an autoradiographic and morphometric study of whole muscle transplants in mice." J Anat **180 (Pt 1)**(Pt 1): 57-65.
- Rodemann H.P. and Goldberg A.L. (1982). "Arachidonic acid, prostaglandin E2 and F2 alpha influence rates of protein turnover in skeletal and cardiac muscle." J Biol Chem **257**(4): 1632-8.
- Rodgers B.D., Weber G.M., Kelley K.M. and Levine M.A. (2003). "Prolonged fasting and cortisol reduce myostatin mRNA levels in tilapia larvae; short-term fasting elevates." Am J Physiol Regul Integr Comp Physiol **284**(5): R1277-86.
- Rosenblatt J.D. and Parry D.J. (1992). "Gamma irradiation prevents compensatory hypertrophy of overloaded mouse extensor digitorum longus muscle." J Appl Physiol **73**(6): 2538-43.
- Rosenblatt J.D. and Parry D.J. (1993). "Adaptation of rat extensor digitorum longus muscle to gamma irradiation and overload." Pflugers Arch **423**(3-4): 255-64.
- Rosenblatt J.D., Yong D. and Parry D.J. (1994). "Satellite cell activity is required for hypertrophy of overloaded adult rat muscle." Muscle Nerve **17**(6): 608-13.
- Roth S.M., Martel G.F., Ivey F.M., Lemmer J.T., Tracy B.L., Metter E.J., Hurley B.F. and Rogers M.A. (2001). "Skeletal Muscle Satellite Cell Characteristics in Young and Older Men and Women After Heavy Resistance Strength Training." J Gerontol A Biol Sci Med Sci **56**(6): B240-247.

- Rothwell N.J., Stock M.J. and Sudera D.K. (1987). "Changes in tissue blood flow and beta-receptor density of skeletal muscle in rats treated with the beta2-adrenoceptor agonist clenbuterol." Br J Pharmacol **90**(3): 601-7.
- Ryall J.G. and Lynch G.S. (2008). "The potential and the pitfalls of beta-adrenoceptor agonists for the management of skeletal muscle wasting." Pharmacol Ther **120**(3): 219-32.
- Ryall J.G., Plant D.R., Gregorevic P., Sillence M.N. and Lynch G.S. (2004). "Beta 2-agonist administration reverses muscle wasting and improves muscle function in aged rats." J Physiol **555**(Pt 1): 175-88.
- Sabourin L.A., Girgis-Gabardo A., Seale P., Asakura A. and Rudnicki M.A. (1999). "Reduced differentiation potential of primary MyoD^{-/-} myogenic cells derived from adult skeletal muscle." J Cell Biol **144**(4): 631-43.
- Sakuma K., Watanabe K., Sano M., Uramoto I. and Totsuka T. (2000). "Differential adaptation of growth and differentiation factor 8/myostatin, fibroblast growth factor 6 and leukemia inhibitory factor in overloaded, regenerating and denervated rat muscles." Biochim Biophys Acta **1497**(1): 77-88.
- Schakman O., Gilson H. and Thissen J.P. (2008). "Mechanisms of glucocorticoid-induced myopathy." J Endocrinol **197**(1): 1-10.
- Scheinman R.I., Cogswell P.C., Lofquist A.K. and Baldwin A.S., Jr. (1995). "Role of transcriptional activation of I kappa B alpha in mediation of immunosuppression by glucocorticoids." Science **270**(5234): 283-6.
- Schmalbruch H. (1977). "Regeneration of soleus muscles of rat autografted in toto as studied by electron microscopy." Cell Tissue Res **177**(2): 159-80.
- Schmalbruch H. (1978). "Satellite cells of rat muscles as studied by freeze-fracturing." Anat Rec **191**(3): 371-6.
- Schmalbruch H. and Hellhammer U. (1976). "The number of satellite cells in normal human muscle." The Anatomical Record **185**(3): 279-287.
- Schmalbruch H. and Hellhammer U. (1977). "The number of nuclei in adult rat muscles with special reference to satellite cells." The Anatomical Record **189**(2): 169-175.
- Schoenfeld B.J. (2010). "The mechanisms of muscle hypertrophy and their application to resistance training." J Strength Cond Res **24**(10): 2857-72.
- Schubert W., Zimmermann K., Cramer M. and Starzinski-Powitz A. (1989). "Lymphocyte antigen Leu-19 as a molecular marker of regeneration in human skeletal muscle." Proc Natl Acad Sci U S A **86**(1): 307-11.

- Schultz E. (1974). "A quantitative study of the satellite cell population in postnatal mouse lumbrical muscle." Anat Rec **180**(4): 589-95.
- Schultz E. (1976). "Fine structure of satellite cells in growing skeletal muscle." American Journal of Anatomy **147**(1): 49-69.
- Schultz E. (1989). "Satellite cell behavior during skeletal muscle growth and regeneration." Med Sci Sports Exerc **21**(5 Suppl): S181-6.
- Schultz E. and McCormick K.M. (1994). "Skeletal muscle satellite cells." Rev Physiol Biochem Pharmacol **123**: 213-57.
- Scuderi F., Mannella F., Marino M., Provenzano C. and Bartoccioni E. (2006). "IL-6-deficient mice show impaired inflammatory response in a model of myosin-induced experimental myositis." J Neuroimmunol **176**(1-2): 9-15.
- Seale P., Ishibashi J., Scime A. and Rudnicki M.A. (2004). "Pax7 is necessary and sufficient for the myogenic specification of CD45⁺:Sca1⁺ stem cells from injured muscle." PLoS Biol **2**(5): E130.
- Seale P., Sabourin L.A., Girgis-Gabardo A., Mansouri A., Gruss P. and Rudnicki M.A. (2000). "Pax7 Is Required for the Specification of Myogenic Satellite Cells." Cell **102**(6): 777-786.
- Serrano A.L., Baeza-Raja B., Perdiguero E., Jardi M. and Munoz-Canoves P. (2008). "Interleukin-6 is an essential regulator of satellite cell-mediated skeletal muscle hypertrophy." Cell Metab **7**(1): 33-44.
- Shah O.J., Kimball S.R. and Jefferson L.S. (2000). "Acute attenuation of translation initiation and protein synthesis by glucocorticoids in skeletal muscle." Am J Physiol Endocrinol Metab **278**(1): E76-82.
- Shappell N.W., Feil V.J., Smith D.J., Larsen G.L. and McFarland D.C. (2000). "Response of C2C12 mouse and turkey skeletal muscle cells to the beta-adrenergic agonist ractopamine." J Anim Sci **78**(3): 699-708.
- Shen W., Prisk V., Li Y., Foster W. and Huard J. (2006). "Inhibited skeletal muscle healing in cyclooxygenase-2 gene-deficient mice: the role of PGE2 and PGF2alpha." J Appl Physiol **101**(4): 1215-21.
- Sieck G.C. and Regnier M. (2001). "Invited Review: plasticity and energetic demands of contraction in skeletal and cardiac muscle." J Appl Physiol **90**(3): 1158-64.
- Sillence M.N., Matthews M.L., Moore N.G. and Reich M.M. (1995). "Effects of BRL-47672 on growth, beta 2-adrenoceptors, and adenylyl cyclase activation in female rats." Am J Physiol **268**(1 Pt 1): E159-67.
- Sinha-Hikim I., Roth S.M., Lee M.I. and Bhasin S. (2003). "Testosterone-induced muscle hypertrophy is associated with an increase in satellite

- cell number in healthy, young men." Am J Physiol Endocrinol Metab **285**(1): E197-205.
- Sinha-Hikim I., Taylor W.E., Gonzalez-Cadavid N.F., Zheng W. and Bhasin S. (2004). "Androgen Receptor in Human Skeletal Muscle and Cultured Muscle Satellite Cells: Up-Regulation by Androgen Treatment." J Clin Endocrinol Metab **89**(10): 5245-5255.
- Smart N., Mojet M.H., Latchman D.S., Marber M.S., Duchon M.R. and Heads R.J. (2006). "IL-6 induces PI 3-kinase and nitric oxide-dependent protection and preserves mitochondrial function in cardiomyocytes." Cardiovasc Res **69**(1): 164-77.
- Smith C., Kruger M.J., Smith R.M. and Myburgh K.H. (2008). "The inflammatory response to skeletal muscle injury: illuminating complexities." Sports Med **38**(11): 947-69.
- Smith I.J., Aversa Z., Alamdari N., Petkova V. and Hasselgren P.O. (2011). "Sepsis downregulates myostatin mRNA levels without altering myostatin protein levels in skeletal muscle." J Cell Biochem **111**(4): 1059-73.
- Snijders T., Verdijk L.B., Beelen M., McKay B.R., Parise G., Kadi F. and van Loon L.J. (2012). "A single bout of exercise activates skeletal muscle satellite cells during subsequent overnight recovery." Exp Physiol **2012**: 10.
- Snow M.H. (1977a). "The effects of aging on satellite cells in skeletal muscles of mice and rats." Cell Tissue Res **185**(3): 399-408.
- Snow M.H. (1977b). "Myogenic cell formation in regenerating rat skeletal muscle injured by mincing. I. A fine structural study." Anat Rec **188**(2): 181-99.
- Soltow Q.A., Betters J.L., Sellman J.E., Lira V.A., Long J.H. and Criswell D.S. (2006). "Ibuprofen inhibits skeletal muscle hypertrophy in rats." Med Sci Sports Exerc **38**(5): 840-6.
- Song Z.G., Zhang X.H., Zhu L.X., Jiao H.C. and Lin H. (2011). "Dexamethasone alters the expression of genes related to the growth of skeletal muscle in chickens (*Gallus gallus domesticus*)." J Mol Endocrinol **46**(3): 217-25.
- Spate U. and Schulze P.C. (2004). "Proinflammatory cytokines and skeletal muscle." Curr Opin Clin Nutr Metab Care **7**(3): 265-9.
- Stanton L.W. (2001). "Methods to profile gene expression." Trends Cardiovasc Med **11**(2): 49-54.
- Steelman C.A., Recknor J.C., Nettleton D. and Reecy J.M. (2006). "Transcriptional profiling of myostatin-knockout mice implicates Wnt

- signaling in postnatal skeletal muscle growth and hypertrophy." Faseb J **20**(3): 580-2.
- Stewart C.E., Newcomb P.V. and Holly J.M. (2004). "Multifaceted roles of TNF-alpha in myoblast destruction: a multitude of signal transduction pathways." J Cell Physiol **198**(2): 237-47.
- Strachan J. (2012). Expression and interactions of the ubiquitin receptor ZNF216. Biomedical Sciences. Nottingham, University of Nottingham. **PhD thesis**.
- Sun L., Trausch-Azar J.S., Muglia L.J. and Schwartz A.L. (2008). "Glucocorticoids differentially regulate degradation of MyoD and Id1 by N-terminal ubiquitination to promote muscle protein catabolism." Proc Natl Acad Sci U S A **105**(9): 3339-44.
- Szalay K., Razga Z. and Duda E. (1997). "TNF inhibits myogenesis and downregulates the expression of myogenic regulatory factors myoD and myogenin." Eur J Cell Biol **74**(4): 391-8.
- Tajbakhsh S., Bober E., Babinet C., Pournin S., Arnold H. and Buckingham M. (1996). "Gene targeting the myf-5 locus with nlacZ reveals expression of this myogenic factor in mature skeletal muscle fibres as well as early embryonic muscle." Dev Dyn **206**(3): 291-300.
- Talmadge R.J. (2000). "Myosin heavy chain isoform expression following reduced neuromuscular activity: potential regulatory mechanisms." Muscle Nerve **23**(5): 661-79.
- Tatsumi R., Anderson J.E., Nevoret C.J., Halevy O. and Allen R.E. (1998). "HGF/SF Is Present in Normal Adult Skeletal Muscle and Is Capable of Activating Satellite Cells." Developmental Biology **194**(1): 114-128.
- Taylor W.E., Bhasin S., Artaza J., Byhower F., Azam M., Willard D.H., Jr., Kull F.C., Jr. and Gonzalez-Cadavid N. (2001). "Myostatin inhibits cell proliferation and protein synthesis in C2C12 muscle cells." Am J Physiol Endocrinol Metab **280**(2): E221-8.
- te Pas M.F., de Jong P.R. and Verburg F.J. (2000). "Glucocorticoid inhibition of C2C12 proliferation rate and differentiation capacity in relation to mRNA levels of the MRF gene family." Mol Biol Rep **27**(2): 87-98.
- Tellez J.O. (2005). Molecular mapping of the rabbit sinoatrial node. Biomedical Sciences. Leeds, University of Leeds. **PhD thesis**.
- Tellez J.O., Dobrzynski H., Greener I.D., Graham G.M., Laing E., Honjo H., Hubbard S.J., Boyett M.R. and Billeter R. (2006). "Differential expression of ion channel transcripts in atrial muscle and sinoatrial node in rabbit." Circ Res **99**(12): 1384-93.

- Temm-Grove C.J., Wert D., Thompson V.F., Allen R.E. and Goll D.E. (1999). "Microinjection of calpastatin inhibits fusion in myoblasts." Exp Cell Res **247**(1): 293-303.
- Termin A. and Pette D. (1992). "Changes in myosin heavy-chain isoform synthesis of chronically stimulated rat fast-twitch muscle." Eur J Biochem **204**(2): 569-73.
- Thevenaz P. and Unser M. (2007). "User-friendly semiautomated assembly of accurate image mosaics in microscopy." Microsc Res Tech **70**(2): 135-46.
- Thomas M., Langley B., Berry C., Sharma M., Kirk S., Bass J. and Kambadur R. (2000). "Myostatin, a negative regulator of muscle growth, functions by inhibiting myoblast proliferation." J Biol Chem **275**(51): 40235-43.
- Thompson J. and van Furth R. (1970). "The effect of glucocorticosteroids on the kinetics of mononuclear phagocytes." J Exp Med **131**(3): 429-42.
- Tiao G., Fagan J., Roegner V., Lieberman M., Wang J.J., Fischer J.E. and Hasselgren P.O. (1996). "Energy-ubiquitin-dependent muscle proteolysis during sepsis in rats is regulated by glucocorticoids." J Clin Invest **97**(2): 339-48.
- Tiao G., Lieberman M., Fischer J.E. and Hasselgren P.O. (1997). "Intracellular regulation of protein degradation during sepsis is different in fast- and slow-twitch muscle." Am J Physiol **272**(3 Pt 2): R849-56.
- Tilg H., Dinarello C.A. and Mier J.W. (1997). "IL-6 and APPs: anti-inflammatory and immunosuppressive mediators." Immunol Today **18**(9): 428-32.
- Tintignac L.A., Lagirand J., Batonnet S., Sirri V., Leibovitch M.P. and Leibovitch S.A. (2005). "Degradation of MyoD mediated by the SCF (MAFbx) ubiquitin ligase." J Biol Chem **280**(4): 2847-56.
- Tisdale M.J. (2007). "Is there a common mechanism linking muscle wasting in various disease types?" Curr Opin Support Palliat Care **1**(4): 287-92.
- Toigo M. and Boutellier U. (2006). "New fundamental resistance exercise determinants of molecular and cellular muscle adaptations." Eur J Appl Physiol **97**(6): 643-63.
- Tome F.M. and Fardeau M. (1986). "Nuclear changes in muscle disorders." Methods Achiev Exp Pathol **12**: 261-96.
- Toth K.G., McKay B.R., De Lisio M., Little J.P., Tarnopolsky M.A. and Parise G. (2011). "IL-6 induced STAT3 signalling is associated with the proliferation of human muscle satellite cells following acute muscle damage." PLoS ONE **6**(3): e17392.

- Tracey K.J. and Cerami A. (1993). "Tumor necrosis factor, other cytokines and disease." Annu Rev Cell Biol **9**: 317-43.
- Tracey K.J., Morgello S., Koplin B., Fahey T.J., 3rd, Fox J., Aledo A., Manogue K.R. and Cerami A. (1990). "Metabolic effects of cachectin/tumor necrosis factor are modified by site of production. Cachectin/tumor necrosis factor-secreting tumor in skeletal muscle induces chronic cachexia, while implantation in brain induces predominantly acute anorexia." J Clin Invest **86**(6): 2014-24.
- Tsujinaka T., Fujita J., Ebisui C., Yano M., Kominami E., Suzuki K., Tanaka K., Katsume A., Ohsugi Y., Shiozaki H. and Monden M. (1996). "Interleukin 6 receptor antibody inhibits muscle atrophy and modulates proteolytic systems in interleukin 6 transgenic mice." J Clin Invest **97**(1): 244-9.
- Tzahor E., Kempf H., Mootosamy R.C., Poon A.C., Abzhanov A., Tabin C.J., Dietrich S. and Lassar A.B. (2003). "Antagonists of Wnt and BMP signaling promote the formation of vertebrate head muscle." Genes Dev. **17**(24): 3087-3099.
- Vandenburgh H.H., Hatfaludy S., Sohar I. and Shansky J. (1990). "Stretch-induced prostaglandins and protein turnover in cultured skeletal muscle." Am J Physiol **259**(2 Pt 1): C232-40.
- Vary T.C., Jurasinski C.V., Karinch A.M. and Kimball S.R. (1994). "Regulation of eukaryotic initiation factor-2 expression during sepsis." Am J Physiol **266**(2 Pt 1): E193-201.
- Vary T.C. and Kimball S.R. (1992). "Sepsis-induced changes in protein synthesis: differential effects on fast- and slow-twitch muscles." Am J Physiol **262**(6 Pt 1): C1513-9.
- Viguie C.A., Lu D.X., Huang S.K., Rengen H. and Carlson B.M. (1997). "Quantitative study of the effects of long-term denervation on the extensor digitorum longus muscle of the rat." Anat Rec **248**(3): 346-54.
- Vinciguerra M., Musaro A. and Rosenthal N. (2010). "Regulation of muscle atrophy in aging and disease." Adv Exp Med Biol **694**: 211-33.
- Voisin L., Breuille D., Combaret L., Pouyet C., Taillandier D., Aurousseau E., Obled C. and Attaix D. (1996). "Muscle wasting in a rat model of long-lasting sepsis results from the activation of lysosomal, Ca²⁺-activated, and ubiquitin-proteasome proteolytic pathways." J Clin Invest **97**(7): 1610-7.
- Volonte D., Liu Y. and Galbiati F. (2004). "The modulation of caveolin-1 expression controls satellite cell activation during muscle repair." FASEB J.: 04-2215fje.

- Voytik S.L., Przyborski M., Badylak S.F. and Konieczny S.F. (1993). "Differential expression of muscle regulatory factor genes in normal and denervated adult rat hindlimb muscles." Dev Dyn **198**(3): 214-24.
- Waage A. (1987). "Production and clearance of tumor necrosis factor in rats exposed to endotoxin and dexamethasone." Clin Immunol Immunopathol **45**(3): 348-55.
- Waller J., Gardiner S.M., Jose J. and Bennett T. (1995). "Lack of effect of TNF antibodies on the cardiovascular sequelae of lipopolysaccharide infusion in conscious rats." Br J Pharmacol **116**(5): 2487-95.
- Wanek L.J. and Snow M.H. (2000). "Activity-induced fiber regeneration in rat soleus muscle." Anat Rec **258**(2): 176-85.
- Watkins S.C. and Cullen M.J. (1988). "A quantitative study of myonuclear and satellite cell nuclear size in Duchenne's muscular dystrophy, polymyositis and normal human skeletal muscle." The Anatomical Record **222**(1): 6-11.
- Watt D.J., Morgan J.E., Clifford M.A. and Partridge T.A. (1987). "The movement of muscle precursor cells between adjacent regenerating muscles in the mouse." Anat Embryol (Berl) **175**(4): 527-36.
- Weber T.E., Small B.C. and Bosworth B.G. (2005). "Lipopolysaccharide regulates myostatin and MyoD independently of an increase in plasma cortisol in channel catfish (*Ictalurus punctatus*)." Domest Anim Endocrinol **28**(1): 64-73.
- Wehling-Henricks M., Lee J.J. and Tidball J.G. (2004). "Prednisolone decreases cellular adhesion molecules required for inflammatory cell infiltration in dystrophin-deficient skeletal muscle." Neuromuscul Disord **14**(8-9): 483-90.
- Wehling M., Cai B. and Tidball J.G. (2000). "Modulation of myostatin expression during modified muscle use." FASEB J. **14**(1): 103-110.
- Wehling M., Spencer M.J. and Tidball J.G. (2001). "A nitric oxide synthase transgene ameliorates muscular dystrophy in mdx mice." J. Cell Biol. **155**(1): 123-132.
- Welle S., Burgess K., Thornton C.A. and Tawil R. (2009). "Relation between extent of myostatin depletion and muscle growth in mature mice." Am J Physiol Endocrinol Metab **297**(4): E935-40.
- Wieteska-Skrzeczynska W., Grzelkowska-Kowalczyk K., Tokarska J. and Grabiec K. (2011). "Growth factor and cytokine interactions in myogenesis. Part I. The effect of TNF-alpha and IFN-gamma on IGF-I-dependent differentiation in mouse C2C12 myogenic cells." Pol J Vet Sci **14**(3): 417-24.

- Williams A., Wang J.J., Wang L., Sun X., Fischer J.E. and Hasselgren P.O. (1998). "Sepsis in mice stimulates muscle proteolysis in the absence of IL-6." Am J Physiol **275**(6 Pt 2): R1983-91.
- Wirenfeldt M., Clare R., Tung S., Bottini A., Mathern G.W. and Vinters H.V. (2009). "Increased activation of Iba1+ microglia in pediatric epilepsy patients with Rasmussen's encephalitis compared with cortical dysplasia and tuberous sclerosis complex." Neurobiol Dis **34**(3): 432-40.
- Wojcik S., Engel W.K., McFerrin J. and Askanas V. (2005). "Myostatin is increased and complexes with amyloid-beta within sporadic inclusion-body myositis muscle fibers." Acta Neuropathol **110**(2): 173-7.
- Wokke J.H., Van den Oord C.J., Leppink G.J. and Jennekens F.G. (1989). "Perisynaptic satellite cells in human external intercostal muscle: a quantitative and qualitative study." Anat Rec **223**(2): 174-80.
- Wozniak A.C., Kong J., Bock E., Pilipowicz O. and Anderson J.E. (2005). "Signaling satellite-cell activation in skeletal muscle: Markers, models, stretch, and potential alternate pathways." Muscle & Nerve **31**(3): 283-300.
- Yablonka-Reuveni Z. (2011). "The skeletal muscle satellite cell: still young and fascinating at 50." J Histochem Cytochem **59**(12): 1041-59.
- Yablonka-Reuveni Z. and Rivera A.J. (1994). "Temporal expression of regulatory and structural muscle proteins during myogenesis of satellite cells on isolated adult rat fibers." Developmental Biology **164**(2): 588-603.
- Young R.B., Moriarity D.M., McGee C.E., Farrar W.R. and Richter H.E. (1990). "Protein metabolism in chicken muscle cell cultures treated with cimaterol." J Anim Sci **68**(4): 1158-69.
- Yusuf I. and Fruman D.A. (2003). "Regulation of quiescence in lymphocytes." Trends in Immunology **24**(7): 380-386.
- Zammit P.S., Golding J.P., Nagata Y., Hudon V., Partridge T.A. and Beauchamp J.R. (2004). "Muscle satellite cells adopt divergent fates: a mechanism for self-renewal?" J. Cell Biol. **166**(3): 347-357.
- Zammit P.S., Partridge T.A. and Yablonka-Reuveni Z. (2006). "The Skeletal Muscle Satellite Cell: The Stem Cell That Came in From the Cold." J. Histochem. Cytochem. **54**(11): 1177-1191.
- Zeman R.J., Ludemann R., Easton T.G. and Etlinger J.D. (1988). "Slow to fast alterations in skeletal muscle fibers caused by clenbuterol, a beta 2-receptor agonist." Am J Physiol **254**(6 Pt 1): E726-32.
- Zhao W., Pan J., Zhao Z., Wu Y., Bauman W.A. and Cardozo C.P. (2008). "Testosterone protects against dexamethasone-induced muscle atrophy,

protein degradation and MAFbx upregulation." J Steroid Biochem Mol Biol **110**(1-2): 125-9.

Zimmers T.A., Davies M.V., Koniaris L.G., Haynes P., Esquela A.F., Tomkinson K.N., McPherron A.C., Wolfman N.M. and Lee S.J. (2002). "Induction of cachexia in mice by systemically administered myostatin." Science **296**(5572): 1486-8.